

**EFFECT OF ARSENIC ON THE DENITRIFICATION PROCESS  
IN THE PRESENCE OF NATURALLY-PRODUCED  
VOLATILE FATTY ACIDS  
AND  
ARSENIC REMOVAL BY NEW ZEALAND IRON SAND (NZIS)**

---

A thesis submitted in partial fulfilment  
of the requirements for the Degree of  
Doctor of Philosophy  
in Civil Engineering  
in the University of Canterbury

by

**Sudan Raj Panthi**

Department of Civil and Natural Resources Engineering

University of Canterbury

2009

---

## **ACKNOWLEDGEMENTS**

I would firstly like to express my sincere gratitude to my Supervisor, Dr David G. Wareham, Associate Professor, Department of Civil and Natural Resources Engineering for his extensive help, constant guidance and coherent effort in terms of regular advice and encouragement throughout this research. His excellent ideas helped me to formulate the research and carry out the work in a smooth way. In particular, I am deeply indebted to him for providing his outstanding help with respect to thesis writing, especially, his promptness in returning my drafts. His prudence in reviewing my writing was superb. I am equally impressed by his kindness towards my daily life concerns and his keen interest in my family situation. Sincere thanks are also due to Associate Professor, Dr Mark Milke for his help in fulfilling the important role of my associate-supervisor. He has provided very large support especially at the time of Dr. Wareham's absence.

It is my great pleasure to express my special thanks to the technical staff, Peter McGuigan and David MacPherson in the Department of Civil and Natural Resources Engineering. I had excellent technical support from Peter McGuigan throughout my entire experimental work while Dave Macpherson was very helpful with all kinds of problems I experienced in the Environmental Engineering Laboratory.

This research was sponsored by a research grant from the Department of Civil and Natural Resources Engineering, University of Canterbury, which is gratefully acknowledged. Valuable thank is given to NZAID (New Zealand Agency for International Development) for providing a New Zealand Development Scholarship (NZDS) allowing me to study at the University of Canterbury and making this research possible. The International Student Support Office, especially Dr Sarah Beaven helped me a great deal in the management of my scholarship as well as some of my family difficulties while staying in New Zealand.

Finally, thanks to my family-members and friends who have made significant contribution in supporting my study. Heartfelt thanks goes to my wife Namrata, daughters Sukriti and Prakriti and son Prasun for their understanding, support and love during every moment of this research work.

# TABLE OF CONTENTS

<b>ACKNOWLEDGEMENTS .....</b>	<b>II</b>
<b>TABLE OF CONTENTS .....</b>	<b>III</b>
<b>LIST OF FIGURES .....</b>	<b>VIII</b>
<b>LIST OF TABLES .....</b>	<b>X</b>
<b>LIST OF TABLES .....</b>	<b>X</b>
<b>ABSTRACT .....</b>	<b>XI</b>
<b>1 INTRODUCTION .....</b>	<b>1</b>
<b>2 BACKGROUND LITERATURE REVIEW .....</b>	<b>2</b>
<b>2.1 Arsenic Pollution .....</b>	<b>2</b>
2.1.1 Introduction .....	2
2.1.2 Speciation and Mobility of Arsenic .....	3
2.1.3 Toxicity of Arsenic .....	5
2.1.4 Removal of Arsenic from Water .....	6
2.1.5 New Zealand Iron Sand (NZIS) .....	8
<b>2.2 Nitrogen in the Water Environment .....</b>	<b>11</b>
2.2.1 Introduction .....	11
2.2.2 Nitrogen Pollution and Its Effect .....	12
<b>2.3 Nitrification .....</b>	<b>13</b>
<b>2.4 Denitrification .....</b>	<b>14</b>
2.4.1 Microbiology .....	15
2.4.2 Stoichiometry .....	16
<b>2.5 Factors Affecting Denitrification .....</b>	<b>17</b>
2.5.1 Carbon Source .....	18

2.5.2	Dissolved Oxygen .....	19
2.5.3	Alkalinity, pH and Temperature.....	20
2.5.4	Heavy Metals.....	21
<b>2.6</b>	<b>Sequencing Batch Reactor (SBR).....</b>	<b>22</b>
2.6.1	Introduction .....	22
2.6.2	Controlling Parameters for an SBR.....	23
2.6.2.1	Dissolved Oxygen (DO) .....	23
2.6.2.2	Solid Retention Time (SRT) and C/N Ratio.....	24
<b>2.7</b>	<b>Anaerobic Digestion.....</b>	<b>25</b>
2.7.1	Introduction .....	25
2.7.2	VFA Production in an Acid Phase Digester .....	27
2.7.2.1	VFAs from Monosaccharides (MS).....	27
2.7.2.2	VFAs from Amino Acids (AA).....	28
2.7.2.3	Acetate from Long Chain Fatty Acids (LCFA) and Other VFAs.....	28
2.7.3	Factors Affecting Performance.....	29
<b>2.8</b>	<b>Research Objectives.....</b>	<b>31</b>
<b>3</b>	<b>MATERIAL AND METHODS FOR DENITRIFICATION TESTS .....</b>	<b>33</b>
<b>3.1</b>	<b>Experimental Set-up and Operation.....</b>	<b>33</b>
3.1.1	Sequencing Batch Reactor (SBR) .....	34
3.1.1.1	Hardware .....	34
3.1.1.2	Feeding Methodology.....	35
3.1.1.3	Reactor Operation and Control.....	36
3.1.2	Anaerobic Digester.....	38
3.1.2.1	Hardware .....	38
3.1.2.2	Feeding Methodology and Digester Inoculation .....	39
3.1.3	Denitrification Batch Test Reactors .....	41
3.1.3.1	Preparation of Biomass.....	42
3.1.3.2	Feeding Methodology.....	42
3.1.3.3	Preparation of Stock Solutions .....	43
3.1.3.4	Selection of Concentration of Various Parameters.....	43
<b>3.2</b>	<b>Sampling and Analytical Methods .....</b>	<b>47</b>
3.2.1	Arsenic .....	49

3.2.2	Nitrate and Nitrogenous Parameters.....	50
3.2.2.1	Nitrate .....	50
3.2.2.2	Ammonia .....	51
3.2.2.3	Nitrite.....	52
3.2.3	COD .....	52
3.2.3.1	Preparation of COD Reagents .....	52
3.2.4	VFAs .....	53
3.2.5	TOC.....	54
3.2.6	Alkalinity.....	55
3.2.7	pH.....	55
3.2.8	Dissolved Oxygen (DO).....	56
3.2.9	TSS and VSS.....	56
3.2.10	Total Solids (TS) and Total Volatile Solids (TVS).....	56
3.2.11	Sludge Volume Index (SVI) .....	57
<b>4</b>	<b>MATERIAL AND METHODS FOR ADSORPTION TESTS .....</b>	<b>58</b>
<b>4.1</b>	<b>Adsorbents.....</b>	<b>58</b>
4.1.1	Physical Chemical Properties .....	58
4.1.2	Sieve Analysis .....	59
<b>4.2</b>	<b>Analytical Methods.....</b>	<b>59</b>
<b>4.3</b>	<b>Adsorption Experiments .....</b>	<b>60</b>
4.3.1	Batch Experiments .....	60
4.3.2	Column Experiments.....	61
<b>5</b>	<b>DENITRIFICATION STUDIES, RESULTS AND DISCUSSIONS.....</b>	<b>62</b>
<b>5.1</b>	<b>Start-up and Preliminary Operation .....</b>	<b>62</b>
5.1.1	SBR .....	62
5.1.1.1	Dissolved Oxygen (DO) in SBR.....	62
5.1.1.2	MLSS and SVI in SBR.....	63
5.1.1.3	Track Studies .....	65
5.1.2	Anaerobic Digester.....	67
5.1.2.1	General Characterisation of Feed Solution and Effluent .....	67
5.1.2.2	VFAs Production and Speciation.....	69

5.1.2.3	Particulate Organic Carbon Solubilization .....	71
5.1.2.4	VFA Production Rate .....	74
5.1.2.5	Gas Production .....	75
5.1.3	Selection of C/N Ratio for Denitrification Batch Tests.....	76
5.1.4	Reaction of Nitrate with Arsenic.....	79
5.1.5	Alkalinity Production during Denitrification .....	80
<b>5.2</b>	<b>Effect of Arsenite (As (III)) on the Denitrification Rates .....</b>	<b>82</b>
5.2.1	Track Studies of Nitrate and COD .....	82
5.2.2	Computation of Denitrification Rates (Arsenite) .....	91
5.2.3	Kinetic Equation of the Effect of Arsenite on Denitrification.....	93
<b>5.3</b>	<b>Effect of Arsenate (As (V)) on the Denitrification Rate .....</b>	<b>96</b>
5.3.1	Track Studies of Nitrate and COD .....	96
5.3.2	Computation of Denitrification Rates (Arsenate).....	103
5.3.3	Kinetic Equation of the Effect of Arsenate on Denitrification .....	105
<b>5.4</b>	<b>Removal of Arsenite during the Denitrification Batch Tests.....</b>	<b>109</b>
5.4.1	Removal Efficiency .....	109
5.4.2	Removal Isotherms.....	111
<b>5.5</b>	<b>Removal of Arsenate during the Denitrification Batch Tests .....</b>	<b>113</b>
5.5.1	Removal Efficiency .....	113
5.5.2	Removal Isotherms.....	114
<b>5.6</b>	<b>Removal Mechanism of Arsenic .....</b>	<b>115</b>
<b>6</b>	<b>ARSENIC ADSORPTION, RESULTS AND DISCUSSION.....</b>	<b>117</b>
<b>6.1</b>	<b>Scanning Electron Microscopy (SEM) Analysis .....</b>	<b>117</b>
<b>6.2</b>	<b>Batch Studies.....</b>	<b>119</b>
6.2.1	Effect of pH.....	119
6.2.2	Effect of Contact Time (Kinetics of Arsenic Adsorption) .....	123
6.2.3	Effect of Initial Arsenic Concentration (Adsorption Isotherms).....	125
<b>6.3</b>	<b>Column Study.....</b>	<b>130</b>
<b>7</b>	<b>CONCLUSIONS AND RECOMMENDATIONS.....</b>	<b>132</b>

<b>7.1</b>	<b>Conclusions.....</b>	<b>132</b>
7.1.1	Conclusions from Denitrification Studies (Section 5).....	132
7.1.2	Conclusion from Arsenic Adsorption (Section 6).....	135
<b>7.2</b>	<b>Recommendations.....</b>	<b>137</b>
<b>REFERENCES.....</b>		<b>140</b>
<b>APPENDIX.....</b>		<b>176</b>
<b>Appendix A: Calibration Curves.....</b>		<b>176</b>
<b>Appendix B: Experiment Data.....</b>		<b>182</b>
<b>Appendix C: Images and Photos.....</b>		<b>188</b>

## LIST OF FIGURES

Figure 2-1. The Eh–pH diagram for arsenic at 25°C and 101.3 kPa .....	4
Figure 2-2. Iron sands beaches in Western North Island, New Zealand .....	9
Figure 2-3. Chemical composition of NZIS .....	10
Figure 2-4. Different pathways of an anaerobic digestion system .....	26
Figure 3-1. Schematic diagram of different physical system used in the research .....	33
Figure 3-2. Schematic diagram of SBR and Control System .....	34
Figure 3-3. Degradation of COD in wastewater during the storage .....	36
Figure 3-4. Cyclic operation of SBR .....	37
Figure 3-5. Schematic diagram of anaerobic digester .....	38
Figure 3-6. Schematic diagram of a denitrification batch test reactor .....	41
Figure 3-7. Arsenic generator and absorber assembly .....	49
Figure 4-1. Sieve analysis result of New Zealand Iron Sand (NZIS). .....	59
Figure 4-2. Schematic diagram of column experiments .....	61
Figure 5-1. Typical DO profile in the SBR system .....	62
Figure 5-2. MLSS (a) and SVI (b) profile in the SBR.....	64
Figure 5-3. Typical track study of COD, NO <sub>3</sub> <sup>-</sup> -N, and NH <sub>4</sub> <sup>+</sup> -N in the SBR.....	66
Figure 5-4. Profiles of VFAs (a) total expressed as HAc, (b) speciation expressed in concentration and (c) speciation expressed in percentage. ....	70
Figure 5-5. Track study of NO <sub>3</sub> <sup>-</sup> - N during C/N optimisation test .....	78
Figure 5-6. Nitrate consumption during the reaction with arsenite .....	80
Figure 5-7. Track study of NO <sub>3</sub> <sup>-</sup> -N (a) and COD (b) in Run 1. ....	83
Figure 5-8. Track study of NO <sub>3</sub> <sup>-</sup> -N (a) and COD (b) for Run 2.....	85
Figure 5-9. Track study of NO <sub>3</sub> <sup>-</sup> -N (a) and COD (b) for Run 3.....	87
Figure 5-10. Track study of NO <sub>3</sub> <sup>-</sup> -N (a) and COD (b) for Run 4.....	88
Figure 5-11. Track study of NO <sub>3</sub> <sup>-</sup> -N (a) and COD (b) for Run 5.....	90
Figure 5-12. Decreasing denitrification rate with increasing arsenite concentration.....	92
Figure 5-13. Model testing and evaluation of an equation .....	95
Figure 5-14. Track study of NO <sub>3</sub> <sup>-</sup> -N (a) and COD (b) for Run 6.....	97
Figure 5-15. Track study of NO <sub>3</sub> <sup>-</sup> -N (a) and COD (b) for Run 7.....	99
Figure 5-16. Track study of NO <sub>3</sub> <sup>-</sup> -N (a) and COD (b) for Run 8.....	101
Figure 5-17. Track study of NO <sub>3</sub> <sup>-</sup> -N (a) and COD (b) for Run 9.....	103
Figure 5-18. Decreasing denitrification rate with increasing arsenate concentration.....	105
Figure 5-19. Model testing and evaluation of an equation on arsenate .....	106



Figure 5-20. Model testing and evaluation of equation for two different ranges of arsenate concentrations (a) As(V) = 0 to 100 mg/L, (b) As (V) = 100 to 2,000 mg/L. ....	107
Figure 5-21. Track study of arsenite during the denitrification batch tests .....	109
Figure 5-22. Effect of the concentration of MLSS on arsenite removal.....	110
Figure 5-23. Langmuir plot for arsenite removal at different MLSS concentration.....	112
Figure 5-24. Effect of the concentration of MLSS on arsenate removal .....	113
Figure 5-25. Langmuir plot for arsenate removal at different MLSS concentration .....	114
Figure 5-26. Concentrations of arsenite after a contact time of 24 h .....	115
Figure 6-1. SEM Images of ISNZ (a) without adsorbed arsenic, (b) with As (III) (c) and As (V) adsorption during batch tests.....	118
Figure 6-2. Effect of pH on (a) As (III) and (b) As (V) adsorption on NZIS .....	120
Figure 6-3. Effect of pH on As(III) and As(V) adsorption on NZIS at a contact time of 144 h....	120
Figure 6-4. Effect of contact time on (a) As (III) and (b) As (V) adsorption .....	124
Figure 6-5. Linearized Langmuir plot for (a) As (III) and (b) As (V) .....	126
Figure 6-6. Linearized Freundlich plot for (a) As (III) and (b) As (V) .....	127
Figure 6-7. Development of As concentration in the effluent of the NZIS column-filter . ....	130

## LIST OF TABLES

Table 2-1: Countries affected by arsenic contamination .....	3
Table 2-2: Biological nitrate reduction.....	14
Table 2-3: Key denitrification relationships .....	16
Table 2-4: Summary of denitrification rate for various organic carbon sources .....	18
Table 2-5: VFAs production from MS .....	27
Table 2-6: VFAs production from different kind of amino acids.....	28
Table 2-7. Oxidation of LCFAs to acetic acids .....	29
Table 3-1: Mean values of some major constituents of influent wastewater of the SBR .....	35
Table 3-2: Initial concentrations of arsenic and other reactants (as per added).....	45
Table 3-3: Arsenic removal tests with different concentrations of MLSS .....	46
Table 3-4: Physical / chemical parameters monitored during the experiments .....	47
Table 4-1: Common physical and chemical properties of NZIS .....	58
Table 4-2: Batch tests with different concentration of arsenic .....	60
Table 5-1: Major parameters in the influent and effluent of the anaerobic digester.....	67
Table 5-2: Typical VFAs composition distributions for fermentation effluents.....	71
Table 5-3: Anaerobic digester particulate organic carbon solubilisation .....	72
Table 5-4: Specific VFA production rate.....	74
Table 5-5: COD and VFA concentration conversion factors.....	75
Table 5-6: Specific denitrification rate for different C/N ratios .....	77
Table 5-7: Estimation of an average theoretical alkalinity production rate .....	81
Table 5-8: Alkalinity production rate; a comparison between theoretical and practical values .....	81
Table 5-9: Specific denitrification rate computed in the denitrification batch tests (As (III)) .....	91
Table 5-10: Specific denitrification rate computed in the denitrification batch tests (As (V)).....	104
Table 6-1: Correlation coefficients and adsorption isotherms parameters.....	128
Table 6-2: Comparison of maximum arsenic adsorption capacity on natural adsorbents .....	129

## ABSTRACT

This thesis is comprised of two phases; the first phase concerns the effect of arsenic on the denitrification process in the presence of naturally-produced volatile fatty acids (VFAs); while the second phase evaluates the arsenic removal efficiency of New Zealand Iron Sand (NZIS) by adsorption.

To accomplish the first phase of the study, VFAs were first produced naturally in an acid-phase anaerobic digester by using commercially-available soy flour. Secondly, a denitrifying biomass was cultivated in a sequencing batch reactor (SBR) using domestic wastewater as a feed solution. Finally, a series of biological denitrification batch tests were conducted in the presence of different concentrations of arsenic and nitrate.

As mentioned, the VFAs were generated from an anaerobic digester using 40 g/L soy solution as a synthetic feed. The digester was operated at a solids retention time (SRT) and hydraulic retention time (HRT) of 10 days. The pH of the digester was measured to be 4.7 to 4.9 while the mean temperature was  $31 \pm 4$  °C; however, both these parameters were not controlled. In the effluent of the digester, a mean VFA concentration of  $5,997 \pm 538$  mg/L as acetic acid was achieved with acid speciation results of acetic (33 %), propionic (29 %), butyric (21 %), iso-valeric (5%) and n-valeric acid (12 %). The specific VFA production rate was estimated to be 0.028 mg VFA as acetic acid/mg VSS per day. The effluent sCOD was measured to be 14,800 mg/L (27.9 % of the total COD), as compared to 9,450 mg/L (16.8 % of total COD) in the influent of the digester. Thus, the COD solubilization increased by 11.1 % during digestion yielding a specific COD solubilization rate of 0.025 mg sCOD/mg VSS per day. The extent of the digestion process converting the substrate from particulate to soluble form was also evaluated via the specific TOC solubilization rate (0.008 mg TOC/mg VSS per day), and VSS reduction percentage ( $17.7 \pm 1.8$  %).

A denitrifying biomass was developed successfully in an SBR fed with domestic sewage (100 % denitrification was achieved for the influent concentration of sCOD =  $285 \pm 45$  mg/L and  $\text{NH}_4^+\text{-N} = 32.5 \pm 3.5$  mg/L). A mean mixed liquor suspended solids (MLSS) of  $3,007 \pm 724$  mg/L and a mean SRT of  $20.7 \pm 4.4$  days were measured during the period of

the research. The settleability of the SBR sludge was excellent evidenced by a low sludge volume index (SVI) measured to be between 50-120 mL/g (with a mean value of  $87 \pm 33$  mL/g) resulting in a very low effluent solids concentration (in many cases less than 20 mg/L).

Several preliminary tests were conducted to estimate the right dosage of VFAs (digester effluent), nitrates and arsenic to be added and to confirm the occurrence of denitrification in an appropriate time frame of 4-6 h. From these tests, an optimum C/N ratio was observed to be somewhere between 2 to 4, somewhat higher than all the theoretical C/N ratios required for a complete denitrification using the four major VFAs identified in the digester effluent. During the denitrification batch tests, it was also observed that some  $\text{NO}_3^-$ -N was removed instantaneously by reacting with As (III) ( $\text{As}_2\text{O}_3$ ); while an increase in alkalinity of around 5.60 mg as  $\text{CaCO}_3$  produced per mg  $\text{NO}_3^-$ -N reduction was also observed. This latter number was very close to the theoretical value of alkalinity production (i.e. 5.41 mg as  $\text{CaCO}_3$  per mg  $\text{NO}_3^-$ -N).

The effect of arsenic on the denitrification process was evaluated by observing the specific denitrification rate in series of denitrification batch tests (with different concentrations of arsenic). Results from the denitrification batch tests showed that there was a clear effect for both As (III) and As (V) on denitrification. In particular, the specific denitrification rate fell from 0.37 to 0.01 g  $\text{NO}_3^-$ -N /g VSS per day as the concentration of As (III) increased from 0 to 50 mg/L. In contrast, there was comparatively less effect for As (V); i.e. only a 37 % decrease in the specific denitrification rate (from 0.34 g  $\text{NO}_3^-$ -N /g VSS per day to 0.23 g  $\text{NO}_3^-$ -N /g VSS per day) when the initial arsenic concentration increased from 0 to a very high level of 2,000 mg/L. The effects of both the As (III) and As (V) forms of inorganic arsenic on the denitrification rate were further quantified by constructing exponential equation models. It was suspected that the effect of As (III) on denitrification was more substantial than the effect of As (V) because of the former's toxicity to microbes.

Finally, the fate of arsenic was tracked by examining bacterial uptake. During the normal denitrification batch tests (i.e. designed for evaluation of the effect of arsenic on denitrification), no significant arsenic removal was observed. However, additional batch

tests with a comparatively low concentration of biomass revealed that the denitrifying biomass removed 1.35  $\mu\text{g As (III) /g dry biomass}$  and 2.10  $\mu\text{g As (V) /g dry biomass}$ .

In the second phase of this research, a series of arsenic adsorption batch tests as well as a column test were performed to examine the arsenic (As (III) and As (V)) removal efficiency of NZIS from an arsenic-contaminated water. The kinetics and isotherms for adsorption were analysed in addition to studying the effect of pH during the batch tests. Breakthrough characteristics for both As (III) and As (V) were studied to appraise the effectiveness of NZIS treating an arsenic contaminated water.

Batch tests were performed with different concentrations of arsenic as well as at different pH conditions. A maximum adsorption of As (III) of approximately 90 % occurred at a pH of 7.5, while the As (V) adsorption reached its maximum value of 97.6 % at a very low pH value of 3. Both Langmuir and Freundlich Models were tested and found to fit with  $R^2$  values of more than 0.92 in all cases. From the Langmuir adsorption model, the maximum adsorption capacity of NZIS for As (III) was estimated to be 1,250  $\mu\text{g/g}$ , significantly higher (about three times) than for As (V) of 500  $\mu\text{g/g}$ . In column tests, arsenic-contaminated water with total As concentration of 400  $\mu\text{g/L}$  (in either form of As) were treated and a pore volume (PV) of 700 and 300 yielded a total arsenic level less than the WHO guideline value of 10  $\mu\text{g/L}$  for As (III) and As (V) respectively; while, the breakthrough occurred after a throughput of approximately 3,000 PV of As (III) and 2,700 PV of As (V) with an average flow rate of approximately 1.0 mL/min.

# 1 INTRODUCTION

Several studies have indicated a growing concern about the level of arsenic contamination in the environment (Bagla and Kaiser, 1996; Ahmed, 2003a). For example, arsenic contamination of ground water has long been identified as a public health concern in different parts of the world (Ng, et al., 2003), most severely in Bangladesh and India (Chakraborti, et al., 2002; Spallholz, et al., 2004). Based on research into health impacts of arsenic (ranging from skin lesions to cancer), many international agencies have identified inorganic arsenic as a carcinogen (IARC, 1987; IPCS, 2001). Research focusing on arsenic removal technologies include very small scale (low-cost household level technologies) (Murcott, 2001; Ahmed, 2003c) as well as large-scale, in situ applications in the field (Appelo, et al., 1999; Welch, et al., 2008).

Nitrogen in water bodies is also another large problem (Fraser and Chilvers, 1980; Fan and Steinberg, 1996; Smith, et al., 1999) with nitrate ( $\text{NO}_3^-$ ) having two major adverse effects. Firstly, even a relatively low concentration of  $\text{NO}_3^-$  in drinking water can pose health risks, particularly for infants, as it diminishes the capacity of blood to transport and transfer oxygen (Sadeq, et al., 2008). Secondly,  $\text{NO}_3^-$  acts as a nutrient source for algae and other aquatic plants and, particularly in stagnant water bodies (e.g. lakes and estuaries); it creates an ecological imbalance by growing excessive algal blooms (eutrophication). This is a serious problem in which the water body could eventually silt up (USEPA, 1973).

These two problems have been coupled in the first part of this research by an investigation into the effect of arsenic on the denitrification process (i.e. the removal of  $\text{NO}_3^-$ ). In order to study this phenomenon, a denitrifying biomass was cultivated in a sequencing batch reactor (SBR) which was grown on volatile fatty acids (VFAs) that had been generated from an anaerobic digester. Correspondingly, the literature review (Section 2) will discuss arsenic and nitrogen pollution (denitrification in particular), SBR and anaerobic digester in some detail. In the second part of this research, naturally-available New Zealand Iron Sand (NZIS) (an iron-rich sand found in the west coast of North Island, New Zealand) will be tested for its arsenic removal capacity by adsorption.

## **2 BACKGROUND LITERATURE REVIEW**

### **2.1 Arsenic Pollution**

#### **2.1.1 Introduction**

Heavy metals, natural components of the Earth's crust, cannot be degraded or destroyed, and many are known to be toxic to all living organisms as well as influencing the activity of microbial communities (Tyler, 1981). To a small extent, some heavy metals enter the human body via food, drinking water and air and may be used to maintain metabolic functions. However, at higher concentrations they can lead to severe health problems. Normally heavy metals are considered to be dangerous because of their tendency to accumulate in living organisms. This is called bioaccumulation and is a phenomenon where the concentration in an organism builds up over a period of time to a much higher concentration of that chemical in the environment. Arsenic, one such heavy metal, is best known for its toxic properties and occurs widely in nature including soil, air, and water. In addition, its concentration may increase because of human-activities such as mining and smelting, pesticide usage, wood treatment, and coal-burning (Bumbla and Keefer, 1994).

Arsenic has been a major public health concern in many countries around the world, such as Bangladesh, India, Nepal, Taiwan, Vietnam, Argentina, China, USA, and Mexico (Table 2-1). For example, in the region of the Ganges Delta, ground water, in which naturally occurring arsenic has been mobilized from the sediments, has put millions of people at risk; while thousands have developed “arsenicosis” (i.e. symptoms of chronic arsenic poisoning occurs as a result of long term arsenic exposure through drinking water and /or ingesting arsenic contaminated food) (Bagla and Kaiser, 1996; Nriagu, 2002). The World Health Organization (WHO, 2006) in 1993 and the United States Environmental Protection Agency (USEPA, 2001) in 2001 reduced the limit of arsenic in drinking water to 0.01 mg/L from an earlier value of 0.05 mg/L.

**Table 2-1:** Countries affected by arsenic contamination and their maximum permissible limits for drinking water

Country	Affected Population (million)	Arsenic concentration range (µg/L)	Guideline Value for drinking water (µg/L)	References
Argentina	2	<1-5300	50	(Bundschuh, et al., 2004)
Bangladesh	50	<1 - 4700	50	(Ahmad, 2001; Ahmed, 2003a)
Cambodia - Vietnam (Mekong Delta )	0.5-1	1- 1610	n/a	(Berg, et al., 2007; Buschmann, et al., 2007)
Chile (North)	0.5	Up to 860	50	(Caceres, et al., 2005)
China (XinJiang, Inner Mongolia, Jilin, and Ningxia)	14.5	Up to 2400	50	(Wang, et al., 1993; An, et al., 1997; Guo, et al., 2001; Sun, et al., 2004)
Hungary	0.22	10-176	10	(Sancha and Castro, 2001)
India (West Bengal)	1	<10 - 3900	50	(Chakraborti, et al., 2001; Chakraborti, et al., 2002)
Mexico	0.4	10-4100	50	(Sancha and Castro, 2001)
Nepal	0.46-0.75	Up to 600	50	(Panthi, et al., 2006)
Taiwan	0.2	10-1820	10	(Tseng, 1977)
USA	Unknown	1-3050	10	(Welch, et al., 1988)
Vietnam (Red River Delta)	10	1-3050	10	(Berg, et al., 2007)

n/a = not available

### 2.1.2 Speciation and Mobility of Arsenic

Arsenic exists in the environment in both the organic and inorganic forms and in four different oxidation states (-III, 0, III and V). In natural waters, arsenic is mostly found in the inorganic form as oxy-anions of trivalent arsenite (As (III)) or pentavalent arsenate (As (V)). Both redox potential (Eh) and pH impose important controls on arsenic speciation in the natural environment (Ferguson and Gavis, 1972). Figure 2-1 shows the Eh–pH diagram for inorganic arsenic compounds at a temperature of 25°C and standard atmospheric pressure. In a natural surface water (pH ranging from 5 to 9) where As (V) is more common, the predominant species of arsenic are  $\text{H}_2\text{AsO}_4^-$  (at low pHs) and  $\text{HAsO}_4^{2-}$  (at high pHs) (Baeyens, et al., 2007).



On the other hand, anaerobic groundwater at a normal pH range of 4 to 9 has  $\text{H}_3\text{AsO}_3$  as the predominant form of arsenic and it contains arsenic in the As (III) state (Guo, et al., 2003; Berg, et al., 2007).

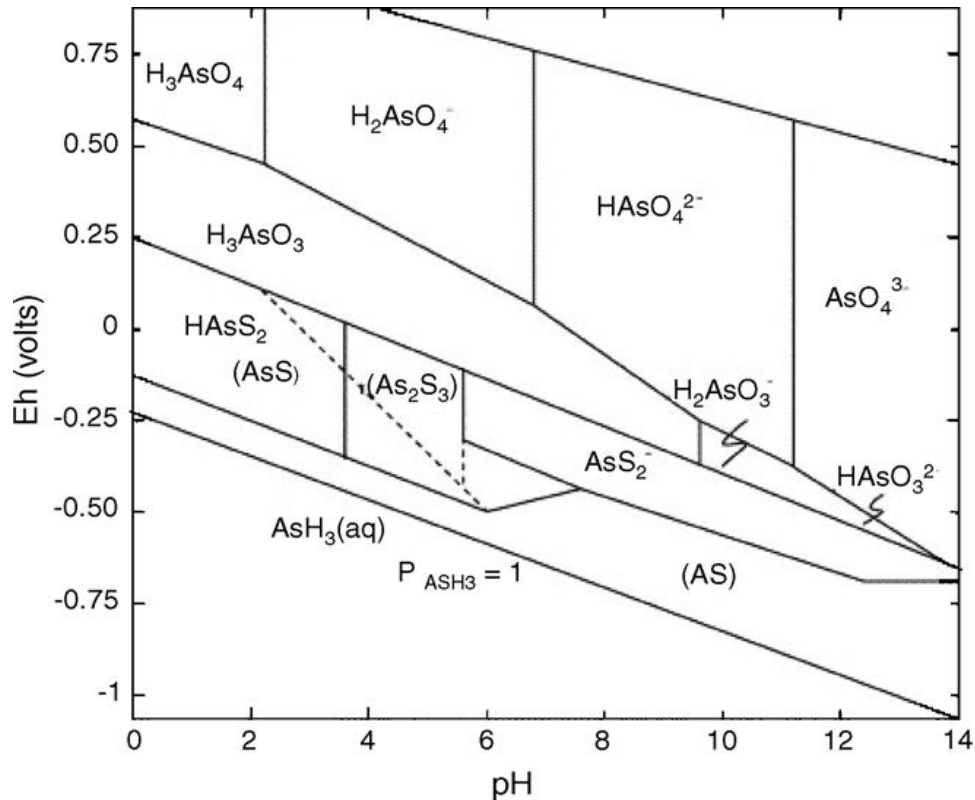


**Figure 2-1.** The Eh–pH diagram for arsenic at 25°C and 101.3 kPa (from Wang and Mulligan, 2006)

Although the dynamics between the different states of arsenic can be achieved by purely chemical means, microorganisms can also mediate a diversity of arsenic–based reactions including reduction, oxidation, and methylation (Cullen, et al., 1994; Santini, et al., 2001; Craig and Cook, 2004). Some researchers (Senn and Hemond, 2002; Oremland and Stolz, 2003; Oremland, et al., 2004) have focused on the biological cycling of arsenic in the environment, mainly in soil and water. However, very limited work has been done on the transformation of arsenic from one to form another, as well as on the effect of arsenic on microorganisms. In addition, the solubility of arsenic compounds is normally very limited under neutral and acidic conditions (Ferguson and Gavis, 1972). Under very strong reducing conditions, arsine ( $\text{AsH}_3$ ) gas and elemental arsenic (As) are formed; but again, only rarely if ever in the natural environment (Wang and Mulligan, 2006).

### 2.1.3 Toxicity of Arsenic

Arsenic is toxic to both plants and animals and inorganic arsenic is a proven carcinogen in humans (Ng, 2005). The toxicity of arsenic to human health is related to its concentration in food or water, cumulative exposure to arsenic and health issues including nutrition and genetic predisposition to its effects of the recipient. Hence the symptoms and signs of chronic arsenic poisoning (arsenicosis) appear to differ between individuals, population groups and geographic areas. Thus there is no universal definition of the disease caused by arsenic; however, the effect may include skin lesions, respiratory problems, multiple internal organ damage and subsequent cancers (Smith, et al., 1992). Depending on the individual, normally it may take 5 to 15 years for the symptoms to appear when continuous exposure occurs at an arsenic concentration of around 20 µg/L (AusAID, 2004). On the other hand, a wide range of arsenic toxicity has been reported that depends on the form and speciation of arsenic. Many researchers have reported that inorganic arsenic is more toxic than the organic form (Goessler and Kuehnelt, 2002; Meharg and Hartley-Whitaker, 2002; Ng, 2005) and that the As (III) form is more toxic compared to the As (V) form (NRC, 1999; ATSDR, 2001). The oral LD50 (i.e. the dose amount of a toxic substance required to kill 50 % of a tested population) for inorganic arsenic ranges from 15-293 mg (As) / kg and 11-150 mg (As) / kg body weight in rats and other laboratory animals respectively (Done and Peart, 1971; Ng, 2005).

It is also noted that the toxicity of As (III) is related to its high affinity for the sulfhydryl groups of bio-molecules such as glutathione, lipoic acids and cysteinyl residues of many enzyme (Korte and Fernando, 1991; Aposhian and Aposhian, 2006). The formation of As (III)-sulphur bonds results in various effects by inhibiting the activities of those enzymes (Lin, et al., 2001; Schuliga, et al., 2002; Chang, et al., 2003). On the other hand, it is considered that As (V) does not directly bind to sulfhydryl groups to cause such toxic effects (Suzuki, et al., 2008).

Furthermore, the toxicity of arsenic decreases with increasing methylation (Hughes, 2002), although, Vega, et al., (2001) have reported that the As (V) form of monomethyl arsenic acids and dimethyl arsenic acids (DMA) can be more toxic

than the As (V) form of inorganic arsenic. It has also been claimed that methylation of inorganic arsenic can generate more reactive and toxic organic arsenical species (Shen, et al., 2006). Evidently, more research in this area is needed before drawing a firm conclusion about the toxicity of different species of arsenic; for the moment, however, it is reasonable to suggest that the transformation of arsenic from one state to another is just as important as its removal.

#### **2.1.4 Removal of Arsenic from Water**

Several technologies have been proposed to remove arsenic from waters. These include coagulation, precipitation, co-precipitation, filtration, ion exchange, lime softening, reverse osmosis, electro-dialysis and adsorption on a suitable adsorbent (Jekel, 1994; Kartinen Jr and Martin, 1995; Zouboulis and Katsoyiannis, 2002; Mohan and Pittman, 2007). The oxidation state of arsenic critically affects its mobility in natural systems as well as the removal efficiency in a treatment process (Raven, et al., 1998; Su and Puls, 2001). As (V) generally exhibits a low mobility in natural systems due to its existence in anionic form. This means it is easily retained on mineral surfaces by adsorption as a metal hydroxide (Pichler, et al., 1999). On the other hand, the non-ionic species of As (III) is more mobile; hence, it is more difficult to remove As (III) as compared to As (V) in natural waters by simple adsorption and precipitation processes (Borho and Wilderer, 1996; Subramanian, et al., 1997; Meng, et al., 2000). It is not surprising therefore that many methods for As (III) oxidation have been suggested as a pre-treatment step to reduce toxicity and promote immobilization. For example, As (III) can be oxidized to As (V) by  $O_2$  and/or  $O_3$  (Kim and Nriagu, 2000),  $H_2O_2$  (Pettine, et al., 1999), synthetic  $MnO_2$  (Manning, et al., 2002; Tournassat, et al., 2002), UV/iron (Hug, et al., 2001; Kocar and Inskeep, 2003), and  $TiO_2$ /UV (Yang, et al., 1999; Lee and Choi, 2002). Although these methods are effective in oxidizing As (III), some of these may cause several problems such as the formation of by-products, large volumes of residue (Driehaus, et al., 1995) and significantly high operational costs (Kim and Nriagu, 2000). Hence, in recent years, attention has been given to adsorption by the adsorbents that can remove As (III) without preoxidation to As (V) (Pierce and

Moore, 1982; Wilkie and Hering, 1996; Raven, et al., 1998; Sun and Doner, 1998; Zeng, 2003; Guo, et al., 2007a).

Various review-papers on recent technologies (Mondal, et al., 2006; Choong, et al., 2007; Mohan and Pittman, 2007) suggest that removal of arsenic from drinking water is most common and suitable by adsorption. Mohan and Pittman (2007) have provided an excellent overview of the adsorption capacities of both available and developed sorbents used for arsenic removal together with traditional remediation methods. Adsorption of arsenic by activated carbon has been studied in detail and the problem of regeneration of the spent adsorbent has been noted, in addition to a comparatively low arsenic removal capacity (Chuang, et al., 2005; Gu, et al., 2005). Several other adsorbents such as activated alumina, ion-exchange resins, sand, silica, clays, iron, iron compounds, and organic polymers have equal or greater efficiency than activated carbon for removal of arsenic (Goldberg and Johnston, 2001; Mohan, et al., 2007). Activated alumina requires low pH and oxidation of As (III) for efficient As removal (Lin and Wu, 2001; Singh and Pant, 2004). Ion-exchange resins are less pH dependent, but other common constituents of natural waters such as sulfates and nitrates reduce the efficiency (Bacocchi, et al., 2005) of the adsorbent. In general, clays, sand, and silica are relatively less efficient than most other adsorbents (Manning and Goldberg, 1997; Goldberg, 2002).

Iron and iron-based compounds (IBCs) are considered to have a high affinity for dissolved arsenic; and apparently are observed to be the best material to remove arsenic by adsorption. Several authors (Wilkie and Hering, 1996; Manning and Goldberg, 1997; Manning, et al., 1998) have reported very high capacities for arsenic adsorption by a different type of IBC. In particular, elementary iron (Lackovic, et al., 2000; Su and Puls, 2001), granular iron hydroxides and ferrihydrites (Pavan, et al., 1998; Thirunavukkarasu, et al., 2001; Driehaus and Dupont, 2005) have been studied and are considered to be the most effective IBC for the removal of arsenic from water. Due to the effectiveness of IBCs, many other materials that have comparatively low arsenic removal capacity are being iron-modified. For example, comparatively better results have been observed with iron-modified activated carbon and iron-coated sand than either unmodified activated

carbon (Chen, et al., 2007a; Zhang, et al., 2007; Muniz, et al., 2009) or just plain sand (Benjamin, et al., 1996; Gupta, et al., 2005).

It seems then, that many kinds of IBCs are emerging as treatment materials for removal of arsenic. One advantage of IBCs is that they have strong affinities for arsenic at neutral pH, hence no pH adjustment is needed (Mohan, et al., 2007). Also many IBCs are equally effective in removing both As (III) and As (V) and/or remove As (III) alone very effectively (Raven, et al., 1998; Altundogan, et al., 2002; Lenoble, et al., 2002; Guo, et al., 2007b). One drawback of IBCs is that many of them are synthetically-prepared which is often a very complicated process. Thus, New Zealand Iron-Sand (NZIS), a type of naturally-available sand that is ubiquitous in many coastal parts of the North Island of New Zealand will be tested for the removal of arsenic during this research work.

### **2.1.5 New Zealand Iron Sand (NZIS)**

Iron sand is a type of sand with heavy concentrations of iron (Fe). It is typically dark grey or blackish in colour. Beachfronts containing iron sands are common around the world and New Zealand's iron sand onshore deposits are the most extensive and the most concentrated in the world (Wikipedia, 2008). A typical iron content in beach sands is 20-25 % iron by weight. Many countries have been studied with respect to iron sand being a potential source of iron, but few (eg. Canada, Iceland, Costa Rica, Japan, Indonesia, Malaysia, Hong Kong, China and the Philippines) are exploited for their commercial value, and then, only to a limited extent (Ozdemir and Dunlop, 2003; Cruz-Sanchez, et al., 2004; Baratoux, 2005).

NZIS is a black, heavy, magnetic iron ore which originates as crystals within volcanic rocks before being transported to the coast by rivers. In the North Island of New Zealand, it occurs in the darker rocks of the Taranaki volcanoes and the lighter-coloured rocks of the Taupo volcanic zone. As the rock is eroded, rivers carry the grains of titanomagnetite to the coast. Ocean currents then move the minerals along the coastline, and the action of wind and waves concentrates them in dark-coloured sands on the sea floor, on beaches and in dunes. The iron sand

deposits of the North Island's west coast extend from South Kaipara and Muriwai (north of Auckland) to over 300 miles southwards to the Whangaehu River (south of Wanganui) (Figure 2-2) (Wylde and Marshall, 1999).



**Figure 2-2.** Iron sands beaches in Western North Island, New Zealand (from Teara, 2008)

The main iron mineral in the iron sand is (titano)magnetite ( $\text{Fe}_{3-x}\text{Ti}_x\text{O}_4$  ( $0 \leq x \leq 1$ )), (Ozdemir and Dunlop, 2003). As indicated by the formula, the compound contains the elements titanium, iron, and oxygen. While the iron sands are generally rich in iron (mainly magnetite ( $\text{Fe}_3\text{O}_4$ )), they also contain other valuable minerals such as titanium oxide ( $\text{TiO}_2$ ) and vanadium oxide ( $\text{V}_2\text{O}_5$ ). Depending upon the oxygen concentration in the original magma, titanohematite intergrowths may occur as well. Inclusions and free particles of apatite, plagioclase feldspars, pyroxene and the spinel group lamellae account for the presence of aluminium oxide ( $\text{Al}_2\text{O}_3$ ), silica

(SiO<sub>2</sub>), magnesium oxide (MgO), calcium oxide (CaO) and Phosphorus (P) in the iron sand (TTR, 2008). A typical chemical composition for NZIS is shown in Figure 2-3.

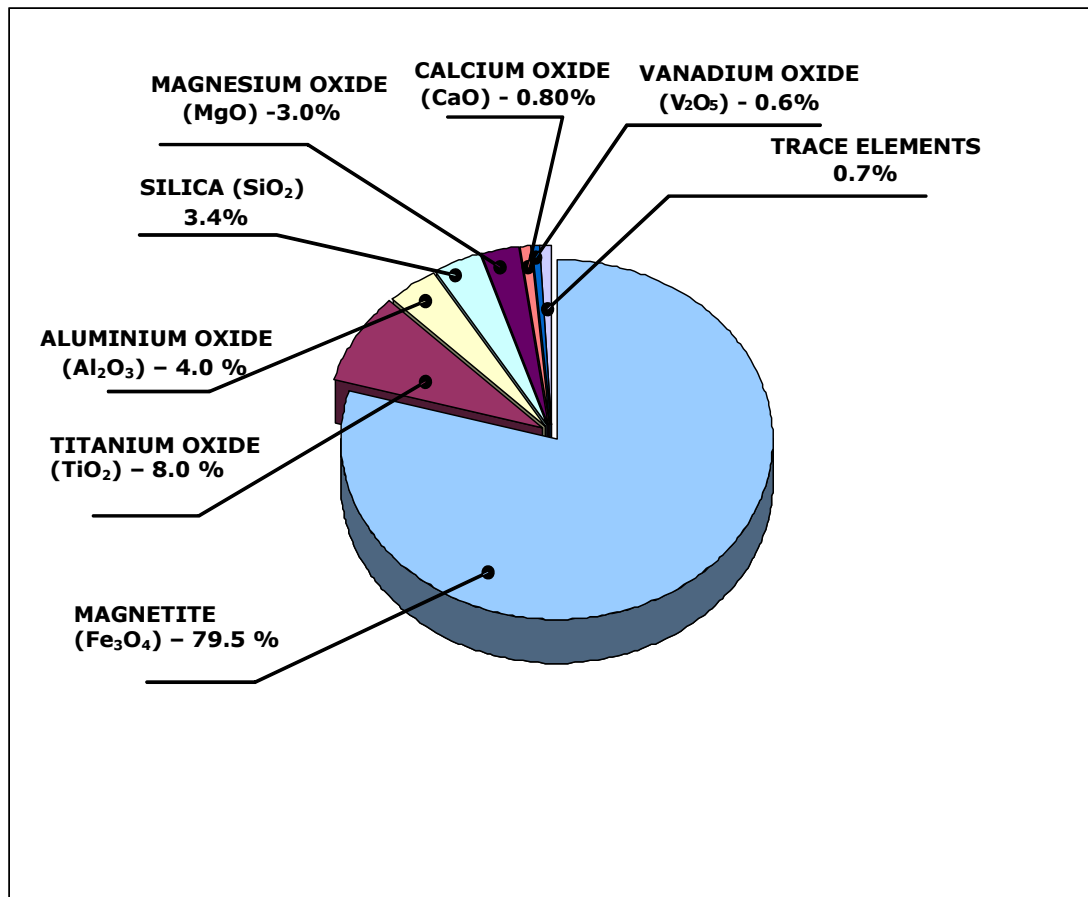


**Figure 2-3.** Chemical composition of NZIS (from Wylde and Marshall, 1999)

More than 20 iron sand deposits (including some river banks) have been investigated in New Zealand and the estimate is that the 5 billion tonnes of sand contain nearly 1440 million tonnes of iron sand as titanomagnetite and 8.4 million tonnes as ilmenite (a weakly magnetic titanium-iron oxide) minerals (NZMIA, 2008). These resources would keep the existing scale of operation going for several hundred years. Sediments sampled at the rivers mouths of the Mokau, Awakino and Patea rivers have a very high content of iron sands (~98 %) which have a very high concentration of iron (typically 57 % Fe in weight).

## 2.2 Nitrogen in the Water Environment

### 2.2.1 Introduction

Nitrogen enters the water environment from both natural and anthropogenic sources. Precipitation, dustfall, non-urban runoff and biological fixation are known natural sources while other sources derived from human activities include municipal and industrial wastewaters, urban runoff drainage from agricultural activities and leachate from landfills and septic tanks (USEPA, 1993). Nitrogen compounds in animal and plant waste are associated with protein and nucleic acids, and these are termed organic nitrogen. As a result of the decomposition of organic nitrogen, ammonia-nitrogen is formed. Ammonia-nitrogen exists either as the ammonia ( $\text{NH}_3\text{-N}$ ) or ammonium ion ( $\text{NH}_4^+\text{-N}$ ) form depending upon the pH and temperature; however very little  $\text{NH}_3\text{-N}$  exist at pH levels less than 9 (Metcalf and Eddy, 1991). Other key forms of nitrogen that are of interest to this research are nitrite-nitrogen ( $\text{NO}_2^-\text{-N}$ ), nitrate-nitrogen ( $\text{NO}_3^-\text{-N}$ ) and nitrogen gas ( $\text{N}_2$ ). Typically, an untreated domestic sewage contains 20-85 mg/L of total nitrogen, which is comprised of approximately 60 %  $\text{NH}_4^+\text{-N}$ , 40 % organic-nitrogen and a very small quantities of  $\text{NO}_3^-\text{-N}$  (USEPA, 1993). Primary and secondary treatment facilities do not remove nitrogen from wastewater; hence, unless nitrification occurs ammonia is the major form of nitrogen. An effluent from a treatment plant may have a variety of nitrogen levels, depending on the type of treatment applied. For example effluent from a typical wastewater treatment plant that is a conventional activated sludge process may contain nitrogen levels of 15-35 mg/L total nitrogen (USEPA, 1993). This may eventually contaminate the water body where it is discharged.

On the other hand, many forms of nitrogen are used for agricultural purposes such as fertilizers. Unused or excessive amounts of nitrogen can accumulate in the form of nitrogen minerals ( $\text{NH}_4^+$  and  $\text{NO}_3^-$ ) within the crop root zone (Follett, 1989); which, may then leach out of the soil and eventually contaminate ground water and surface water supplies.



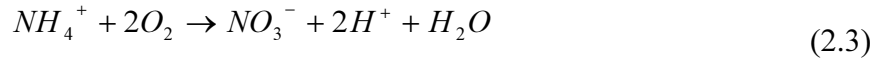
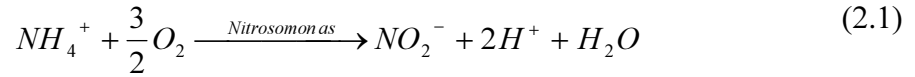
### 2.2.2 Nitrogen Pollution and Its Effect

Excessive accumulation of various forms of nitrogen in surface and ground waters can lead to adverse ecological and human health effects. A very small level of  $\text{NH}_3\text{-N}$  (0.01 mg/L) is toxic to fish and other aquatic life (USEPA, 1973). Most nitrogen which enters the environment is eventually oxidized to  $\text{NO}_3^-\text{-N}$ , which may be used as a nutrient by plants. Excess quantities of nitrogen in any form can contribute to eutrophication, which is excessive plant growth and/or algae “blooms” resulting from over fertilization of the water bodies particularly those which are stationary. Eutrophication can result in deterioration in the appearance of previously clear waters, odour problems from decomposing plant growth, and a lower DO level, which can adversely effect the respiration of other aquatic lives (USEPA, 1973). Nitrate nitrogen itself is also the causative agent of methemoglobinemia, a disease primarily affecting infants and often known as “blue baby syndrome”. High intakes of  $\text{NO}_3^-$  and its subsequent reduction to  $\text{NO}_2^-$  leads to the formation of methemoglobin, a derivative of hemoglobin that cannot bind oxygen because the iron component of the haemoglobin has been oxidized from the ferrous ( $\text{Fe}^{2+}$ ) to the ferric ( $\text{Fe}^{3+}$ ) state (Shuval and Gruener, 1977; Sadeq, et al., 2008). In this way, nitrogen discharges may constitute a direct public health hazard in some circumstances.

In summary, for the sake of the water environment and public health,  $\text{NO}_3^-$  should be removed. One way to do this is through the nitrification-denitrification process.

## 2.3 Nitrification

Nitrification is a two-step biological conversion of  $\text{NH}_4^+$  to  $\text{NO}_2^-$  and to  $\text{NO}_3^-$  under aerobic conditions. Traditionally, two separate genera of bacteria (*Nitrosomonas* and *Nitrobacter*) are involved in the conversion of  $\text{NH}_4^+$  to  $\text{NO}_2^-$  and  $\text{NO}_3^-$  as indicated in Equations (2.1) and (2.2).



The reaction in Equation (2.2) depends upon the rate at which the reaction in Equation (2.1) proceeds. It is conjectured that the transformation of  $\text{NH}_4^+$  to  $\text{NO}_2^-$  by *Nitrosomonas* and the oxidation of  $\text{NO}_2^-$  to  $\text{NO}_3^-$  by *Nitrobacter* may be taken as first order with respect to the  $\text{NH}_4^+$  and  $\text{NO}_2^-$  concentrations respectively (Boon, et al., 1962); and that the specific rates of the reactions are proportional to the biomass densities of the relevant organisms. Normally natural water contains little nitrite; and if produced, it is thermodynamically unstable because of its biologically-mediated transformation into  $\text{NO}_3^-$  (Alexander, 2005). The organisms responsible for nitrification do not oxidise carbon. They are autotrophs and use  $\text{CO}_2$  as a carbon source. For their cellular growth and maintenance they obtain energy from reactions (2.1) and (2.2). In the above reactions, only oxygen can serve as the electron acceptor, so an aerobic environment is the necessary condition for nitrification to proceed.

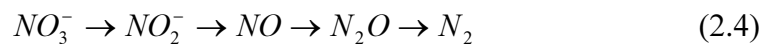
## 2.4 Denitrification

Biological  $\text{NO}_3^-$  removal is conducted by a wide variety of organisms by either assimilatory or dissimilatory pathways (Table 2-2) (van Rijn and Barak, 1998).

**Table 2-2:** Biological nitrate reduction\*

Process	Regulator(s)	Organisms
<b>Assimilatory</b>		
Nitrate reduction to ammonia ( $\text{NO}_3^- \rightarrow \text{NO}_2^- \rightarrow \text{NH}_4^+$ )	$\text{NH}_4^+$	Plants, fungi, algae, bacteria
<b>Dissimilatory</b>		
Nitrate reduction to ammonia ( $\text{NO}_3^- \rightarrow \text{NO}_2^- \rightarrow \text{NH}_4^+$ )	$\text{O}_2$ , Carbon/Nitrogen(C/N)	Anaerobic and facultative anaerobic bacteria
Denitrification ( $\text{NO}_3^- \rightarrow \text{NO}_2^- \rightarrow \text{NO} \rightarrow \text{N}_2\text{O} \rightarrow \text{N}_2$ )	$\text{O}_2$ , C/N	Facultative anaerobic bacteria

Assimilatory  $\text{NO}_3^-$  reduction takes place under both aerobic and anaerobic conditions, and involves the reduction of  $\text{NO}_3^-$  to  $\text{NH}_4^+$  for use in cell synthesis. This does not normally occur if the  $\text{NH}_4^+$  present in the water is sufficient to meet growth requirements. On the other hand during the denitrification process,  $\text{NO}_3^-$  act as terminal electron acceptor and microorganisms reduce it to  $\text{NO}_2^-$  and then to nitric oxide (NO) to nitrous oxide ( $\text{N}_2\text{O}$ ) and finally to nitrogen gas ( $\text{N}_2$ ) (Eq.2.4).



Denitrification is accomplished by chemoheterotrophic, bacteria that obtain energy from chemical reactions involving organic carbon material under anoxic conditions (i.e. when the dissolved oxygen conditions are very low but not necessarily zero), with the dissolved oxygen conditions < 2 % saturation (Kiff, 1972).

\* From van Rijn and Barak, 1998

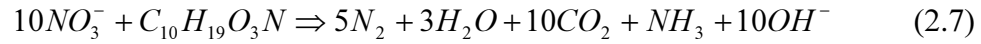
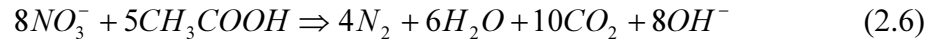
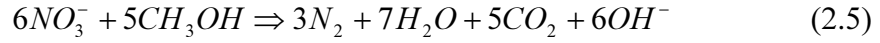
### 2.4.1 Microbiology

A number of bacterial species that naturally occur in the activated sludge system are capable of denitrification. For example, *Achromobacter*, *Acinetobacter*, *Bacillus*, *Micrococcus*, *Pseudomonas* and *Spirillus* are among the heterotrophs, whereas *Paracoccus* can grow as autotrophs as well and use a wide range of carbon sources (Randall, et al., 1992). All the denitrifiers are facultative aerobes, which means that they shift to  $\text{NO}_3^-$  or  $\text{NO}_2^-$  respiration when  $\text{O}_2$  becomes limiting (Rittmann and McCarty, 2001). Thus in wastewater engineering, denitrification describes the use of  $\text{NO}_2^-$  or  $\text{NO}_3^-$  by facultative anaerobes (denitrifying bacteria) to degrade the organic carbon or BOD present in the wastewater. Because of their great metabolic diversity, denitrifiers are commonly found in soils, sediments, surface-waters, ground-waters, and wastewater treatment plants (Arslan-Alaton, et al., 2008). It has been estimated that 80 % of the bacteria found in an activated sludge system are facultative anaerobes and can participate in the denitrification process (Gerardi, 2002).

Heterotrophs use both molecular-oxygen and  $\text{NO}_3^-$  as a terminal electron acceptor when they oxidize organic compounds. Thus, oxygen is not required for denitrifying bacteria in the denitrification reaction, but, when present, it is preferentially used as a terminal electron acceptor. In both cases, the same series of enzymatic reactions take place but the key difference between oxygen respiration and denitrification results from a single enzyme, nitrate reductase, produced in the absence of oxygen and that completes the electron transport process required for  $\text{NO}_3^-$  dissimilation. For this reason, some facultative bacteria are able to switch easily from using oxygen to  $\text{NO}_3^-$  as electron acceptors in the oxidation of organic compounds in a single sludge process. In addition, as these organisms utilise protons in the reduction of  $\text{NO}_3^-$ , denitrification helps the wastewater to keep alkaline compared with the acidity produced during nitrification. Denitrifiers are heterotrophic bacteria and thus are much more energetic and efficient than the nitrifiers and thus their yield and growth rates are also higher (Tiedje, 1982).

### 2.4.2 Stoichiometry

The stoichiometric equations for denitrification depend on the substrate (carbon source). For example, the energy equations using methanol, acetic acid, and wastewater as the carbon source can be written as in Equations (2.5) to (2.7) (USEPA, 1993).



The hydroxide ion formed during denitrification will react with  $CO_2$  in the water to create bicarbonate ions according to the following equation:



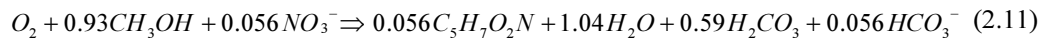
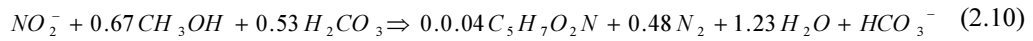
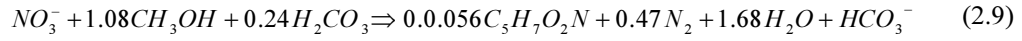
Each of these carbon substrates has several theoretical relationships with denitrification. For example, equation 2.5 states that 1.91 g of methanol (2.86 g when expressed as COD) is required and a theoretical bicarbonate alkalinity of 3.57 g alkalinity as  $CaCO_3$  is produced per g of  $NO_3^-$ -N reduced to  $N_2$ -N (Table 2-3).

**Table 2-3: Key denitrification relationships**

Parameters	Co-efficient	Unit
Methanol consumed	1.91	g- methanol/g $NO_3^-$ -N
Oxygen demand consumed	2.86	g- methanol/g $NO_3^-$ -N
Alkalinity generated	3.57	g- alkalinity (as $CaCO_3$ ) /g $NO_3^-$ -N

In addition to providing energy for the reduction of  $NO_3^-$ , the substrate is used to create new biomass. As a result, more carbon substrate is required than is theoretically calculated. The amount of new biomass generated and the portion used

for denitrification are specific to each substrate and evaluated only by conducting experiments. For example, using methanol as a substrate the stoichiometry with biosynthesis can be presented as in Equations (2.9) to (2.11) (USEPA, 1993):



Equation 2.9 suggests 2.47 g of CH<sub>3</sub>OH is required to reduce 1 g of NO<sub>3</sub><sup>-</sup>-N. Some additional CH<sub>3</sub>OH may also require if any NO<sub>2</sub><sup>-</sup>-N and/or O<sub>2</sub> are present (Equations 2.10 and 2.11). Where, equation 2.11 shows heterotrophic consumption of NO<sub>3</sub><sup>-</sup> in the presence of O<sub>2</sub>. From these equations the overall requirement for methanol can be calculated and given as:

$$\text{Methanol requirement (mg/L)} = 2.47 (\text{NO}_3^- \text{-N}) + 1.53 (\text{NO}_2^- \text{-N}) + 0.93 \text{ DO} \quad (2.12)$$

In the similar way the generation of alkalinity may be higher than the theoretical value (3.57 g- alkalinity (as CaCO<sub>3</sub>) /g NO<sub>3</sub><sup>-</sup>-N) depending upon the presence of NO<sub>2</sub><sup>-</sup>-N and oxygen. Stoichiometric equations with the corresponding carbon requirements and theoretical alkalinity productions for the primary VFAs used in this research (acetic, propionic, butyric and valeric acids) have been calculated in Sections 5.1.3 and 5.1.5.

## 2.5 Factors Affecting Denitrification

There are several environmental and operational factors that strongly influence the denitrification rate. These factors include the concentrations of substrate, NO<sub>3</sub><sup>-</sup>, presence of oxygen, population of denitrifying bacteria, pH, alkalinity, temperature and redox potential. In addition, the presence of heavy metals is another factor influencing denitrification. Several of these are discussed in the following sections.

### 2.5.1 Carbon Source

The most important factor to be considered in denitrification is the type of organic carbon-source and its concentration. Although the wastewater itself contains many suitable sources of carbon, this is inadequate in treated effluents, thus in two stage treatment systems a supplementary carbon source must be provided.

Heterotrophic denitrifiers exhibit an affinity for a wide range of organic substrates; however, most of the research (Akunna, et al., 1993; Constantin and Fick, 1997; Thalasso, et al., 1997; Bickers and Oostrom, 2000) addressed exogenous electron donors (carbon sources). In addition, they investigated simple compounds which can be purchased in bulk quantity (e.g. methanol, acetate, glucose, ethanol, and a few others). Because methanol has been relatively inexpensive historically, it gained widespread use and a very large database has been created (Akunna, et al., 1993; Thalasso, et al., 1997; Gomez, et al., 2000). However as prices increased, effective and inexpensive alternatives have been intensively studied as shown in Table 2-4.

**Table 2-4:** Summary of denitrification rate for various organic carbon sources

<b>Organic carbon sources</b>	<b>Denitrification rate (g NO<sub>3</sub><sup>-</sup>-N/g-VSS per day)</b>	<b>References</b>
Methanol	0.289	(Xu, 1996)
Acetate	0.016-0.603	(Xu, 1996; Li, 2001)
Propionate	0.008-0.362	(Xu, 1996; Li, 2001)
Butyrate	0.519	(Xu, 1996)
Valerate	0.487	(Xu, 1996)
Mixed VFA	0.36-0.754	(Fass, et al., 1994; Xu, 1996)
VFA effluent	0.22	(Hatziconstantinou, et al., 1996)
	0.28	(Pavan, et al., 1998)
	0.054	(Llabres, et al., 1999)
	0.011	(Elefsiniotis, et al., 2004)
	0.57	(Aesoy and Odegaard, 1994)

The denitrification rates presented are not directly comparable, since many different environmental conditions and experimental set-ups have been applied in these studies. Using VFAs at a given temperature, Elefsiniotis and Li (2006) showed that, the specific denitrification rate appeared to depend on the initial nitrogen concentration, while the specific carbon consumption rate was a function of the initial carbon content. They also claimed a C/N (carbon to  $\text{NO}_3^-$ -N ) ratio of 2.0 was sufficient for complete denitrification at all temperatures and types of carbon investigated.

However, the C/N ratio required for a complete  $\text{NO}_3^-$  reduction to  $\text{N}_2$  by denitrifying bacteria depends upon the nature of the carbon source and the bacterial species (Payne, 1973). By using aliphatic C-sources like methanol and acetic acid, the minimum C/N ratio required for complete denitrification ranges from 0.9 to 2.0 which is significantly lower than the requirements for the aromatic carbon sources like benzoic acid, which is about 3.0 to 3.6 (Her and Huang, 1995).

### **2.5.2 Dissolved Oxygen (DO)**

Since, denitrifiers are facultative bacteria that energetically prefer oxygen instead of  $\text{NO}_3^-$  as the terminal electron acceptor, the concentration of DO controls whether or not facultative aerobes respire with  $\text{NO}_3^-$ . Research has found that denitrification can occur when the DO concentration is well above zero (Rittmann and Langeland, 1985); however, very low concentrations of the electron donor or too high concentrations of DO can lead to accumulation of denitrification intermediates:  $\text{NO}_2^-$ , NO, and  $\text{N}_2\text{O}$  (Rittmann and McCarty, 2001). The latter two are greenhouse gases whose release should be avoided. In addition, oxygen suppresses production of a critical enzyme in the electron transport system required for denitrification (Stouthamer, 1988). Use of oxygen as electron acceptor also yields more free energy; therefore oxygen respiration is more favoured when both are present. Tiedje (1988) suggested a threshold level of oxygen as low as 0.2 mg/L, below which there is no or very little denitrification. On the other hand, simultaneous nitrification and denitrification (SND) has been reported in activated sludge with DO concentration



as high as 3 mg/L, although the rate was less than 25 % of the anoxic rate (Munch, et al., 1996). Several researchers (Robertson and Kuenen, 1984; Robertson, et al., 1988; Bell, et al., 1990; Patureau, et al., 1994) have focused their research on the mechanism of aerobic denitrification during an SND system and reported the occurrence of simultaneous nitrification in the outer region in contact with bulk water DO while denitrification in the anoxic zone existed in the inner region of the activated sludge flocs (Li and Ganczarczyk, 1986; Holman, 2004).

### **2.5.3 Alkalinity, pH and Temperature**

As Equation (2.9) shows, during denitrification, carbonic acid is converted to bicarbonate and there is a net production of alkalinity. The production of alkalinity will raise the pH of the system if high concentrations of  $\text{NO}_3^-$  are to be removed (USEPA, 1993); however, nitrification in a combined system offset some of the loss of the alkalinity. Various studies (Prakasam and Loehr, 1972; Arvin and Kristensen, 1982; Flora, et al., 1993; Thomas, et al., 1994; Glass and Silverstein, 1998; Ghafari, et al., 2009) suggest a pH between 7 and 8 is the optimum for a denitrification process; however, it varies depending on bacterial types and wastewater components. In general, for any given temperature, the highest biological reaction rates occur within the pH range of 7.0 and 7.5 and pH values outside the optimal range of 7 to 8 can lead to accumulation of intermediates (Glass and Silverstein, 1998). According to Delwiche (1956), the hydrogen ion concentration affects both the rate of denitrification and the product distribution of the reactions. He noticed the optimum pH for denitrification somewhere between 7.0 and 8.2;  $\text{N}_2$  was the end product of denitrification above pH 7.3, while increasing level of  $\text{N}_2\text{O}$  was observed below this pH level.

Like other biological reactions, temperature affects both the microbial growth rate and nitrogen removal rate. Temperature generally exerts a stronger effect below 15 °C than above it (Rittmann and McCarty, 2001; Carrera, et al., 2003). In particular, Elefsiniotis and Li (2006) explored the effect of temperature on denitrification using VFAs as a carbon source and found that a temperature change from 10 to 20 °C exerted a larger effect on both the specific denitrification and carbon consumption

rates than a temperature increase from 20 to 30 °C. In other research (Delwiche, 1956), the maximum specific denitrification rate was observed at 27 °C when batch tests were performed at different temperatures using particular culture of *Pseudomonas Denitrificans*.

#### **2.5.4 Heavy Metals**

Heavy metals are known to influence the activity of soil microbial communities, altering the conformation of enzymes, blocking essential functional groups or by exchanging with essential metal ions (Tyler, 1981). Numerous studies have demonstrated that heavy metals affect soil respiration, soil biomass, N-mineralization and nitrification, while only a few studies (Bardgett, et al., 1994; Gumaelius, et al., 1996; Sakadevan, et al., 1999; Holtan-Hartwig, et al., 2002; Vasquez-Murrieta, et al., 2006) have focussed on the influence of heavy metals on denitrification and these have indicated that denitrification might be inhibited by heavy metals. Most research has been done in soil and less effort has been directed toward wastewater denitrification in the presence of heavy metals.

## 2.6 Sequencing Batch Reactor (SBR)

### 2.6.1 Introduction

The major contaminants in wastewater can be broadly classified into three categories; organic carbon (chemical oxygen demand (COD)), nutrients such as nitrogen and phosphorus and suspended solids (organic or inorganic). To remove these contaminants, micro-organisms play an essential role in a wastewater treatment system. In general, three types of overall processes (aerobic, anaerobic or photosynthetic) are distinguished in a waste treatment system based on the environment where the process takes place (IETC, 2008). Under aerobic conditions, micro-organisms utilise oxygen to oxidise organic substances to obtain energy for maintenance, mobility and the synthesis of cellular material. Under anaerobic/anoxic conditions, the micro-organisms utilise  $\text{NO}_3^-$ , sulphate ( $\text{SO}_4^{2-}$ ) and other hydrogen acceptors to obtain energy for the synthesis of cellular material from organic substances (e.g. denitrification). Photosynthetic organisms use  $\text{CO}_2$  as a carbon source, inorganic nutrients as sources of phosphate and nitrogen and utilise light energy to drive the conversion process.

In a wastewater treatment system, because of the different metabolisms of the micro-organisms involved in the removal of different type of contaminants, a conventional continuous-flow activated sludge system uses a multi-tank or multi-zone tank system where the activities of different groups of micro-organisms are promoted in different tanks. In an SBR however, the biomass is subjected to changing conditions, such as substrate feast and famine as well as alternating aerobic and anaerobic periods. For many years now, an SBR has been regarded as a viable alternative to the continuous-flow activated sludge process for the removal of COD, nitrogen and phosphorus (Irvine and Busch, 1979; Silverstein and Schroeder, 1983; Arora, et al., 1985; Irvine, et al., 1987). Although there are a number of variants, the operational cycle of a SBR is typically comprised of four discrete sequential periods, namely fill, react, settle and decant (Metcalf and Eddy, 1991). These sequential periods can be individually manipulated to achieve various treatment objectives. For example, when biological nutrient removal is desired, the steps in the react cycle are adjusted to provide anaerobic, anoxic and aerobic phases

in a certain number and sequence (Umble and Ketchum, 1997; Qin, et al., 2005). An SBR process has many advantages over the continuous flow activated sludge system including reduction in operating costs and space, improvement in nitrogen and phosphorus removal as well as less sludge bulking (Wilderer, et al., 2001); however, due to process complexity, several operational parameters affect the nutrient removal performance of the SBR.

## **2.6.2 Controlling Parameters for an SBR**

### **2.6.2.1 Dissolved Oxygen (DO)**

A proper duration for both aerobic and anoxic phases in an SBR is necessary for good nitrification and denitrification to occur. For example, it might take substantial time for the oxygen to drop to zero if the oxygen concentration is too high in the aerobic phase, which might lead to incomplete denitrification (Holman and Wareham, 2005). Similarly, nitrifiers are only able to function under aerobic conditions and consequently, the DO concentration in the bulk liquid can have a significant effect on the growth rate of the nitrifiers. Painter (1977) found the DO concentration for nitrification should be higher than 2.0 mg/L for nitrification to occur without oxygen being the rate limiting factor to the process. Another researcher (Li and Irvin, 2007) reported that with DO levels of 1.0 mg/L, the nitrification process was incomplete giving effluent concentration of  $\text{NH}_4^+$  more than 13 mg/L; and, when they increased the DO level to more than 5.0 mg/L (during the aerobic phase), nitrification was complete but effluent  $\text{NO}_3^-$  was measured at more than 2.0 mg/L due to incomplete denitrification. It is also reported that the nitrification process ceased at residual DO concentration of less than 0.2 mg/L (Bliss and Barnes, 1986). In addition, the DO level plays a role in the settleability of the sludge in an SBR. For example, at low DO concentrations (0.5–2.0 mg/L) in a SBR sludge is produced with poorer settling properties and higher turbidities as compared to effluents with higher DO concentrations (2.0–5.0 mg/L) (Wilén and Balmer, 1999).

#### **2.6.2.2 Solids Retention Time (SRT) and C/N Ratio**

Nitrifying bacteria include species that do not grow as quickly as other bacteria that oxidize organic material (Watson, et al., 1989; Rittmann and McCarty, 2001). Kargi and Uygur (2002) studied nutrient removal performance of an SBR at different SRTs and reported the highest removal efficiency (COD, TKN and TP) at an SRT of 10 days with a slightly lower removal efficiency at 15 days. Some researchers (Moussa, et al., 2005; Rene, et al., 2008) have reported that COD and nitrogen removal rates increase with higher SRTs; as for example, Moussa et al. (2005), who found that increasing the SRT increased the biomass concentration, with the nitrification rate reaching a saturation point at a 40 day SRT. Kos (1998) suggested that a nitrifying process can occur even at very low SRTs (7 to 10 days) during winter temperature (10 °C), instead of the 13 to 18 days used for conventional nitrification. In addition, a higher level of effluent-suspended solids is observed at lower SRTs, than that at higher SRTs (Liao, et al., 2006).

The type of carbon source and the C/N ratio largely affect the nitrogen removal performance in an SBR (Monteith, et al., 1980; Skrinde and Bhagat, 1982). Depending upon the operating conditions, different C/N ratios have been recommended to improve the performance of an SBR. A C/N ratio of 10.0 produced the best performance in an SBR in terms of the maximum nitrogen and carbon removal from a wastewater (Fontenot, et al., 2007), while a COD/NH<sub>4</sub><sup>+</sup>-N ratio of 11.1 achieved complete removal of NH<sub>4</sub><sup>+</sup>-N and COD in another SBR (Chiu, et al., 2007). Some researchers (Bernet, et al., 1996; Obaja, et al., 2005) have reported that a C/N ratio of 1.7 is enough to get complete denitrification. The denitrification rate is also influenced by the chemical structure and the molecular weight of the substrate used as carbon source. By using an aromatic carbon source like benzoic acid, the minimum C/N ratio required for complete denitrification ranged from 3.0 to 3.6 which is significantly higher than the requirement for the aliphatic C-sources like methanol and acetic acid, which is about 0.9 to 2.0 (Her and Huang, 1995). In particular, Her and Huang (1995) found an optimum C/N ratio range of 3.0 to 3.6 for benzoic acid while methanol had comparatively a larger upper range of 0.9 to 5.0 for 100 % denitrification to occur. In addition, they observed carbon breakthrough at C/N ratios of approximately 15.0 (for both C-sources).

## 2.7 Anaerobic Digestion

### 2.7.1 Introduction

In an anaerobic digestion system, a group of anaerobic bacteria decompose organic matter into methane ( $\text{CH}_4$ ), carbon dioxide ( $\text{CO}_2$ ), and nutrient-rich sludge. The advantages of this system over conventional aerobic systems are a low energy requirement for operation, a low initial investment cost, low sludge production and a considerable ( $> 2$  log) removal of pathogenic microorganisms (Horan, et al., 2004; Cooney, et al., 2007). In addition,  $\text{CH}_4$  is a biogas which can be used as a clean renewable energy source.

The multistep nature of an anaerobic digestion operation is depicted in Figure 2-4. It shows that there are four basic steps in an anaerobic digestion system; these are hydrolysis, acidogenesis, acetogenesis and methanogenesis. Hydrolysis and acidogenesis are carried out by a complex consortium of bacteria. Several of them degrade organic polymers such as carbohydrates, proteins and lipids by the means of extracellular enzymes. The resulting monosaccharides (MS) and amino acids (AA) are taken up by bacteria and fermented to produce organic acids such as lactate, succinate, pyruvate, valerate, butyrate, propionate, acetate as well as alcohol (e.g. ethanol), sulphide,  $\text{NH}_3$ ,  $\text{H}_2$  and  $\text{CO}_2$  (Horiuchi, et al., 2002). Acetogenic bacteria then convert these resulting organic acids into acetic acid, along with additional ammonia, hydrogen, and  $\text{CO}_2$ . Finally, methanogenesis converts these products to  $\text{CH}_4$  and  $\text{CO}_2$  (Marty, 1984).

Because of the different metabolic characteristics and growth rates of acidogenic and methanogenic bacteria, two-phase digestion systems have been studied to separate out the acid and  $\text{CH}_4$  forming phases (Cohen, et al., 1979; Bull, et al., 1984; Torpey, et al., 1984; Ghosh, 1987). This phase separation is mostly done by physical separation (e.g. membrane barriers or reactors in series) (Ghosh and Pohland, 1974; Ghosh, 1987; Bhattacharya, et al., 1996). In each of these separate reactors, optimal environmental conditions for each group of bacteria can be targeted which may result in higher conversion rates and increase the overall performance of the process.

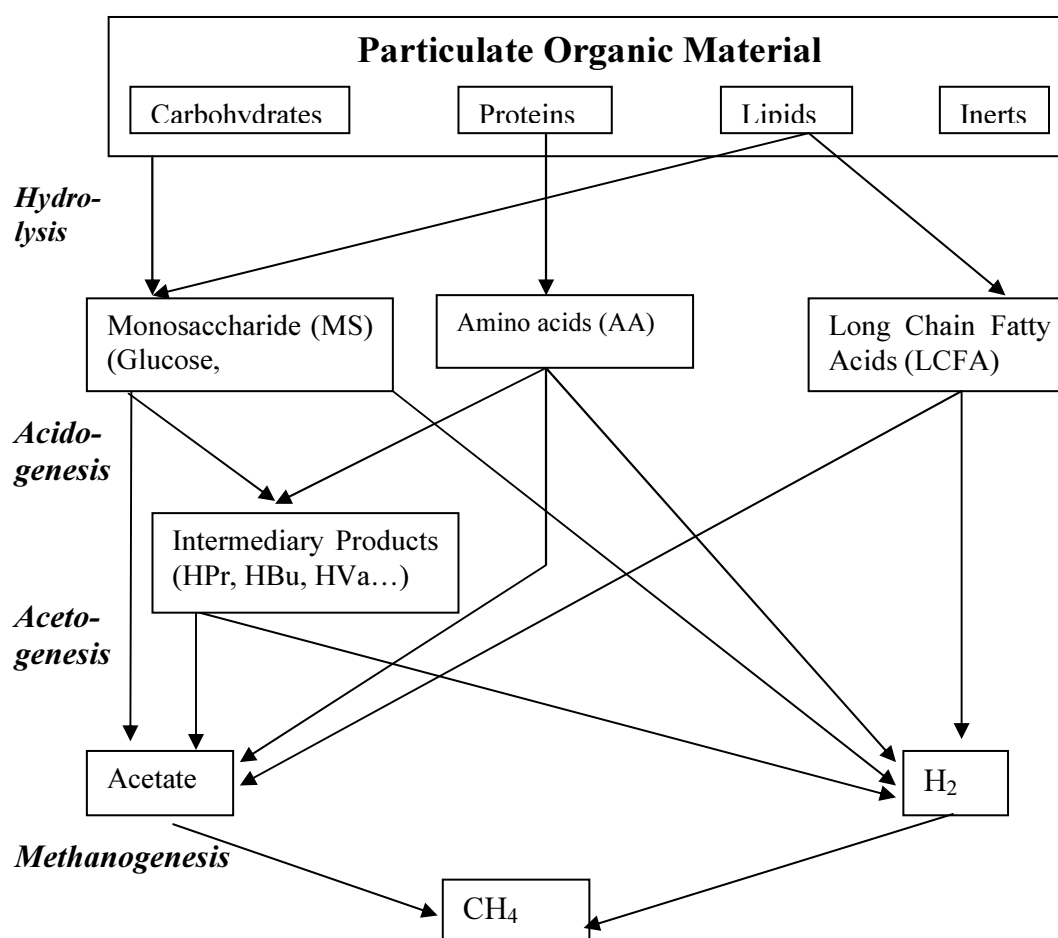


**Figure 2-4.** Different pathways of an anaerobic digestion system (from IWA, 2002)

Several researchers on anaerobic digestion (Verrier, et al., 1987; Chanakya, et al., 1992; Bhattacharya, et al., 1996) have focused on the rate-limiting, methanogenic phase, as it is the energy yielding phase. On the other hand, in wastewater treatment applications, the soluble organic products of acidogenic activity (VFAs and other organic acids) can be used as an external carbon source for microorganisms carrying out other processes, such as biological phosphorus or nitrogen removal (Elefsiniotis and Oldham, 1994b; Raynal, et al., 1998). The presence of VFAs in the influent to a biological nutrient removal (BNR) facility can significantly improve the phosphorus or nitrogen removal efficiency of the process (Danesh and Oleszkiewicz, 1997; Elefsiniotis, et al., 2004; Akin and Ugurlu, 2005). For this purpose, incrementing the VFA concentrations in an influent wastewater entering a BNR plant has been practiced in various ways; for example by addition of synthetic VFAs such as sodium acetate (Bouzas et al., 2002) and by adding starch-rich industrial wastewater

to a domestic wastewater (Banerjee, et al., 1999). Much research has been done to improve acidogenesis of complex substrates (i.e. production of VFAs) through the optimization of operational parameters (Eastman and Ferguson, 1981; Hanaki, et al., 1987; Dinopoulou, et al., 1988; Elefsiniotis and Oldham, 1994a) or through pre-treatment methods to enhance solubilisation (Stucky and McCarty, 1978; Haug, et al., 1983; Li and Noike, 1992).

## 2.7.2 VFA Production in an Acid Phase Digester

Many food processing industrial wastewaters rich in carbohydrates can be easily digested to produce natural VFAs (Kwong and Fang, 1997; Elefsiniotis, et al., 2005). Generally acetic, propionic and butyric acids are the three major VFAs produced in an acid-phase digestion system; however, iso-butyric, valeric and iso-valeric acids are also produced in small amounts. Although VFA production is a very complex process involving many kinds of microorganisms, some reactions are listed below (Table 2-5, 2-6, and 2-7.) representing the stoichiometry of the production of different type of VFAs from MS, AA and long chain fatty acids (LCFA).

### 2.7.2.1 VFAs from Monosaccharides (MS)

**Table 2-5:** VFAs production from MS

Product	Source	Reaction
Acetate	Glucose	$C_6H_{12}O_6 + 2H_2O \rightarrow 2CH_3COOH + 2CO_2 + 4H_2$
Propionate	Glucose	$C_6H_{12}O_6 + 4(H) \rightarrow 2CH_3CH_2COOH + 2H_2O$
Acetate + Propionate	Glucose	$3C_6H_{12}O_6 \rightarrow 4CH_3CH_2COOH + 2CH_3COOH + 2CO_2 + 2H_2O$
Butyrate	Glucose	$C_6H_{12}O_6 \rightarrow 2CH_3CH_2CH_2COOH + 2CO_2 + 2H_2$
Lactate	Glucose	$C_6H_{12}O_6 \rightarrow 2CH_3CHOHCOOH$



When the substrate is either more oxidized or more reduced than glucose, there will be corresponding shift in the products (Moat and Foster, 1988).

### 2.7.2.2 VFAs from Amino Acids (AA)

**Table 2-6:** VFAs production from different kind of amino acids

Product	Source	Reaction
Acetate	AA (alanine)	$CH_3CHNH_2COOH + 2H_2O \rightarrow CH_3COOH + CO_2 + NH_3 + 4H$
VFA (common)	AA (common)	$RCH_2NH_2COOH + 2H_2O \rightarrow RCOOH + CO_2 + NH_3 + 4H$
Propionic + Butyric	Threonine	$3CH_3CHOHCHNH_2COOH + H_2O \rightarrow CH_3CH_2CH_2COOH + 2CH_3CH_2COOH + 2CO_2 + 3NH_3$
Iso-valerate	Leucine	$(CH_3)_2CHCH_2CHNH_2COOH + 2H_2O \rightarrow (CH_3)_2CHCH_2COOH + CO_2 + NH_3 + 4H$

The anaerobic degradation of amino acids involves oxidation reduction reactions between one or more amino acids or nitrogenous compounds derived from amino acids (Barker, 1981).

### 2.7.2.3 Acetate from Long Chain Fatty Acids (LCFA) and Other VFAs

Degradation of LCFAs to acetate is an oxidation step, with no internal electron acceptor. Therefore the organisms oxidising the organic acids are required to utilise an additional electron acceptor such as the hydrogen ion or  $CO_2$  to produce hydrogen gas or formate respectively (IWA, 2002). Occurrence of any reaction depends on the standard Gibbs free energy of the particular reaction. Normally, a reaction would not have taken place if its standard Gibbs free energy is positive. However, whether reactions occur or not in practice is determined by substrate and product concentrations (Wang, et al., 1999). For example, most of the reactions listed above are considered thermodynamically non-feasible because of their positive standard Gibbs free energy. The conjugation of these reactions with a  $CH_4$

producing reaction ( $4H_2 + CO_2 \rightarrow CH_4 + 2H_2O$ ), which has a very high negative standard Gibbs free energy (-135.6 KJ) enables them to become thermodynamically feasible.

**Table 2-7.** Oxidation of LCFAs to acetic acids

Source	Reaction
Palmitate	$CH_3(CH_2)_{14}COOH + 14H_2O \rightarrow 8CH_3COOH + 14H_2$
Benzoic acid	$C_6H_5COOH + 6H_2O \rightarrow 3CH_3COOH + 3H_2 + CO_2$
Propionate	$CH_3CH_2COOH + 2H_2O \rightarrow CH_3COOH + 3H_2 + CO_2$
Butyrate	$CH_3CH_2CH_2COOH + 2H_2O \rightarrow 2CH_3COOH + 2H_2$
Petanoic acid	$CH_3CH_2CH_2CH_2COOH + 2H_2O \rightarrow$ $CH_3COOH + CH_3CH_2COOH + 2H_2$

### 2.7.3 Factors Affecting Performance

Acidogens normally grow more quickly than methanogens and are much hardier organisms, able to survive a broad range of temperature (Eckenfelder and Santhanam, 1981). Hence, many studies on acid-phase anaerobic digestion have been done at room temperature (Elefsiniotis et al. 1996; Chen et al. 2007b; Wu et al. 2009). Recently, Feng et al. (2009) observed that a temperature increase from 10 to 30 °C accelerated waste activated sludge hydrolysis and VFA production was found to increase from 590 mg COD/L to 1590 mg COD /L, when an experiment was carried out at a 12 d SRT. No significant increase however in VFA production was observed at a temperature above 30 °C. During anaerobic digestion an increase in the production of VFAs with increasing temperature has also been observed by many other researchers (Banerjee et al 1998; Maharaj and Elefsiniotis, 2001).

A number of studies (Zoetemeyer, et al., 1982; Fang and Liu, 2002; Yu and Fang, 2003) have been carried out on the effect of pH on acidogenesis of wastewaters and found that the optimal pH for acidogenesis varies between 5.5 and 7.0 with waste composition. Additionally, it has been observed that fermentative microorganisms can function in a wide range of pH (4.0 to 8.5); however at the lower pH ranges, the

main products are acetic and butyric acid, while acetic and propionic are produced at comparatively higher pH ranges (Hwang, et al., 2004).

A longer SRT allows not only more time for the growth of microorganisms but also extends the reaction time. If an ideal anaerobic system operated for a full period of digestion i.e. SRT at 30-60 days (Appels, et al., 2008),  $\text{CH}_4$  is the end product. Hence, to maintain the anaerobic biological activity in the acid-digestion phase and to avoid conversion to  $\text{CH}_4$ , the SRT must be short enough (several days), depending on the wastewater source (Elefsiniotis and Oldham, 1994b). Banister and Pretorius (1998) observed that acid fermentation proceeded rapidly at retention times of less than 6 days with primary sludge, with reduced VFA yields at 10 days. Hence, it can be presumed that any digester operated with an SRT 10 days or less is in the acidogenesis phase (Figure 2-4), does not produce  $\text{CH}_4$  per se, but produces acetic acid (HAc) along with some other VFAs (e.g. propionic acid (HPr), butyric acid (HBu) and valeric acid (HVa) etc).

The HRT controls the contact time between the feed sources that affect the amount and type of substrate being used by the bacteria. Hence a short HRT will not provide sufficient contact time for VFA production; thus, 12 to 18 hours is needed to enable contact time between the bacteria and the compound (Danesh and Oleszkiewicz, 1997; Ndon and Dague, 1997). In an experiment with primary sludge (Elefsiniotis and Oldham, 1994b), both VFA production and COD solubilization increased significantly with increasing HRT up to 12 h: however, it dropped to lower amounts at longer HRTs.

Finally, the loading rate plays a vital role in solubilization and the production of VFA in an anaerobic digester. If the loading rate is too high, VFAs will build up, and gas production drops (Hawkes, et al., 1978). The acid-phase step of anaerobic digestion is generally characterized by very low gas generation, mostly in the form of  $\text{CO}_2$  and  $\text{H}_2$ , which are the by-products of many pathways followed for substrate metabolism (Elefsiniotis and Oldham, 1994b). An upper limit of  $6.4 \text{ kg VS/m}^3$  per day loading rate has been suggested (Grady and Lim, 1980) using sewage sludge ; while a more practical value range is between  $0.27$  and  $2.76 \text{ kg VS/m}^3$  per d (Gray, 2004).

## 2.8 Research Objectives

Several reports have demonstrated the effect of heavy metals (including arsenic) on the microbial community in a soil environment (Bradley and Chapelle, 1993; Sakadevan, et al., 1999; Labbe, et al., 2003). No information however appears to be readily available with respect to the effect of arsenic on the denitrification process in a wastewater treatment system. This effect may depend upon the external carbon source used for the denitrification reaction. The general aim of this research is therefore to investigate the effect of arsenic on the denitrification process when naturally-produced VFAs are used as an external carbon source. The research will provide some information with respect to specific denitrification rates and arsenic removal rates. Secondly, much research has been directed towards finding an ideal adsorbent to remove arsenic from contaminated water (Raven, et al., 1998; Mondal, et al., 2006; Mohan, et al., 2007). It is noted that iron and iron-based compounds (IBC) have a high affinity for both As (III) and As (V) as laid out in Section 2.1.4. Hence, NZIS, an iron ore from New Zealand's iron industry, will be investigated with respect to its arsenic removal capacity.

This research has two overall objectives: the first is to evaluate the effect of arsenic on the denitrification process and the second is to examine the arsenic removal efficiency of NZIS. To achieve these objectives, the experimental work was carried out with the following specific goals:

- Develop a lab scale SBR system to remove carbon and nitrogen from a domestic wastewater and generate a stable biomass suited for use in denitrification batch tests.
- Develop a semi-continuous acid-phase anaerobic digester that can produce a stable concentration of VFAs.
- Assess the performance of the acid-phase anaerobic digester via the VFA production rate.

- Investigate the  $\text{NO}_3^-$  reduction, VFA carbon utilization and arsenic removal profiles during denitrification batch tests.
- Evaluate the effect of both As (III) and As (V) on the denitrification process and compare the level of toxicity of these arsenic species on the biomass.
- Construct a numerical relationship between the initial concentration of arsenic (either As (III) or As (V)) and the specific denitrification rate under a particular environmental condition using the naturally produced VFAs as a carbon source in the denitrification process.
- Explore the arsenic removal efficiency of the denitrifying biomass during the batch tests and speculate on the general mechanism of arsenic removal.
- Observe the effect of pH on arsenic (both As (III) and As (V)) removal by adsorption on NZIS.
- Test different adsorption models for arsenic adsorption on NZIS and calculate the maximum adsorption capacity of the NZIS to remove both species of arsenic (As (III) and As (V)).
- Produce a breakthrough curve of NZIS in a column experiment and investigate the potential of using NZIS in removing As (III) and As (V) from arsenic contaminated waters.

### 3 MATERIAL AND METHODS FOR DENITRIFICATION TESTS

#### 3.1 Experimental Set-up and Operation

The experimental equipment used in the denitrification section of this research consisted of three physical systems as shown in Figure 3-1. The first system was an SBR which was fed domestic wastewater and operated under different sequential oxygen tensions in order to cultivate a denitrifying biomass. The second system was an anaerobic digester without recycle which generated VFAs from a soy flour influent feed solution.

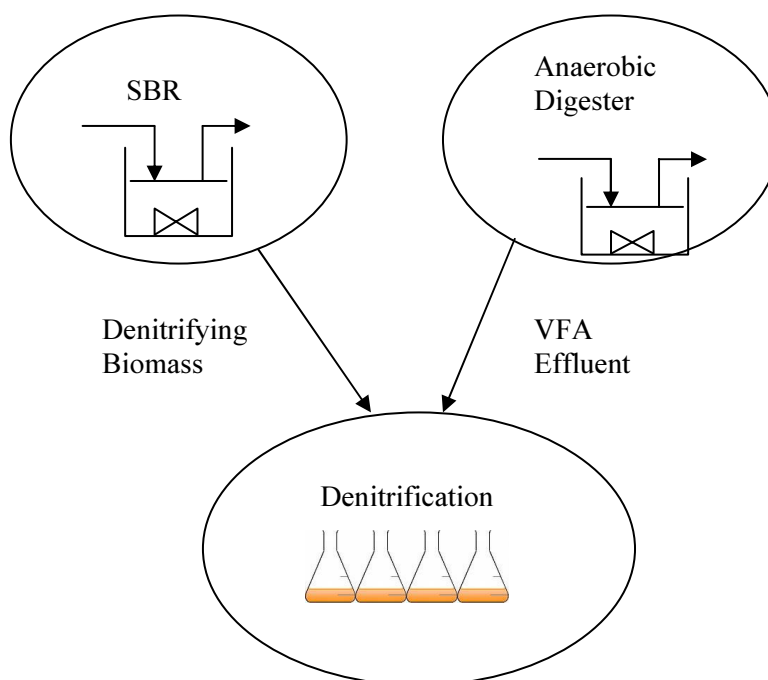


**Figure 3-1.** Schematic diagram of different physical system used in the research

The final system consisted of a series of batch reactors used to study the effects of arsenic on the denitrification process. This system received denitrifying biomass from the first system (i.e. the SBR), VFA-rich effluent from the second system (i.e. the digester) and incremental loadings of As and  $\text{NO}_3^-$ -N concentrations to match suitable C/N ratios, ranging from 2.5 to 3.5. These ratios were obtained from a C/N ratio optimization tests (Section 5.1.3).

### 3.1.1 Sequencing Batch Reactor (SBR)

#### 3.1.1.1 Hardware

A 25 L stainless steel cylinder was used as an SBR such that the working volume was 21 L. The size of the reactor was based upon the cycle lengths of the SBR (5 to 8 hrs) and the quantity of feed that could be stored in a 450 L freezer. The entire operating system was controlled by an automated control system that could run continuously even when no operator was present. The microprocessor control system was composed of two key elements, a central control box and a personal computer (PC) connected to the SBR.

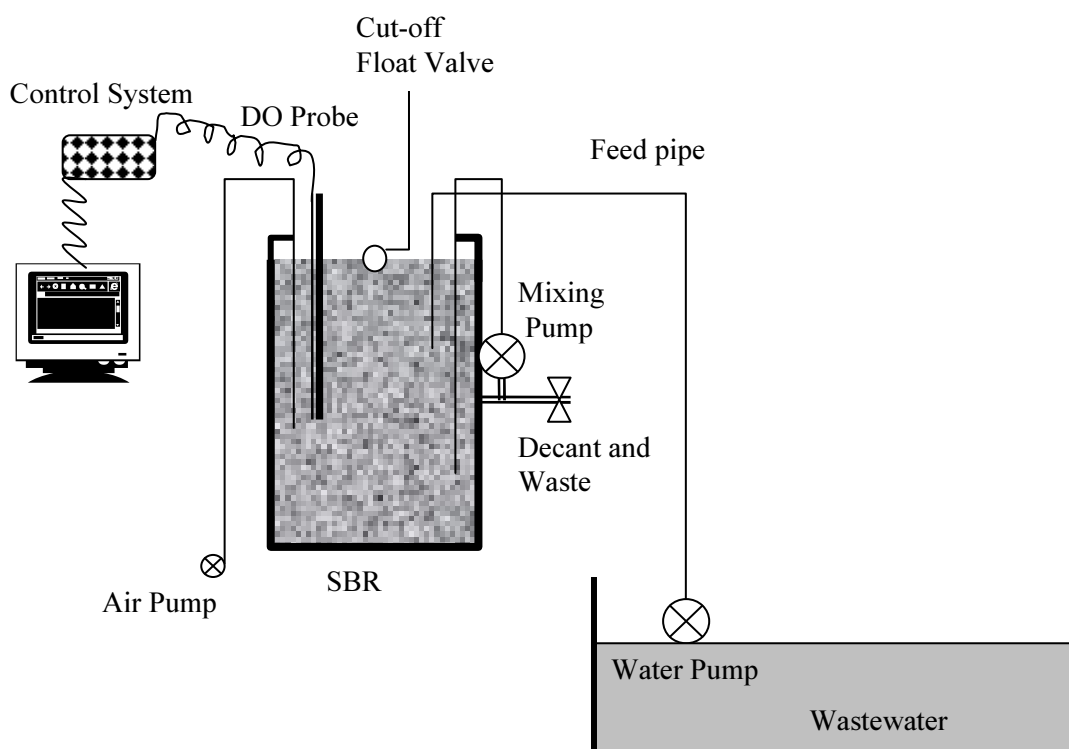


**Figure 3-2.** Schematic diagram of SBR and Control System

The PC ran a software-based process control package with a graphical user interface built specifically for this type of research using the Lab View software by National Instruments. Automated decanting was provided by two solenoid valves fitted to side-mounted ports while the supply of air to the system was provided on an on/off

basis using an air solenoid valve. A schematic of the SBR and the process control system is shown in Figure 3-2.

### 3.1.1.2 Feeding Methodology

The SBR, once seeded with 5 litres of about 10,000 mg/L activated sludge collected from the Christchurch City Wastewater Treatment Plant (CCWTP), was fed with wastewater collected from the same plant located at Bromley, Christchurch, New Zealand. The feed was collected once a week or as per requirements and stored in a modified freezer at 4 °C. The feed composition is shown in Table 3-1.

**Table 3-1:** Mean values of some major constituents of influent wastewater of the SBR

Constituent of Wastewater	Mean Value
COD <sub>Total</sub>	560 ± 118 mg/L
COD <sub>Soluble</sub>	285 ± 45 mg/L
Total organic carbon (TOC)	92 ± 14 mg/L
Total suspended solids (TSS)	150 ± 70 mg/L
Ammonia Nitrogen (NH <sub>4</sub> <sup>+</sup> -N)	32.5 ± 3.5 mg/L
Nitrate Nitrogen (NO <sub>3</sub> <sup>-</sup> -N)	4.8 ± 0.3 mg/L
pH	6.5 to 7.0
Alkalinity (as CaCO <sub>3</sub> )	200 ± 11 mg/L
VFAs (as HAc)	negligible

The large variation in the concentration of COD and other parameters of the feed were not only because of the different collection dates, but also caused by the period of storage. That is, during storage of the wastewater, some degradation of the organic carbon was observed. The pattern of degradation was tracked and a rate of degradation of 10 mg/L of sCOD per day was found as shown in Figure 3-3. However, the COD/N ratio to the SBR was maintained at a ratio of more than 7/1



for all track studies by adding COD-rich effluent from the anaerobic digester. The amount of such effluent was calculated by knowing the COD of the digester effluent (about 15,000 mg/L) and both CODs, required and existing, of the wastewater. Normally the required sCOD of the wastewater was considered to be 300 mg/L.

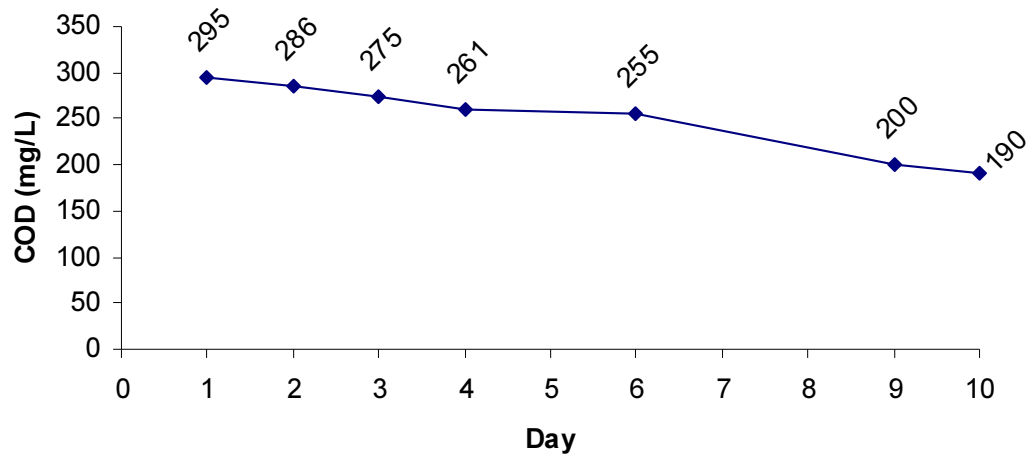


**Figure 3-3.** Degradation of COD in wastewater during the storage

### 3.1.1.3 Reactor Operation and Control

Since the SBR process was carried out in a single tank, it served both as a biological reactor and a settling tank. The total working volume of the reactor was 21 L and consisted of a stationary volume  $V_0$  (10.5 L), and an active volume  $V_F$  (10.5 L), which corresponded to the volume of wastewater that was filled and discharged in every cycle (Figure 3-4). In accordance with the character and the concentration of the sludge in the reactor, the volume of the settled sludge ( $V_S$ ) changed in a daily basis.

The SBR was operated with a 7 h 40 min cycle, consisting of a fill time of 5 min, an anoxic period of 1 h 30 min, an aerobic period 5 h 30 min, a settling time of 30 min and a decanting time of 5 min. During the filling period, at the beginning of a cycle, 10.5 L of wastewater from the freezer was pumped in to the reactor within 5 min.

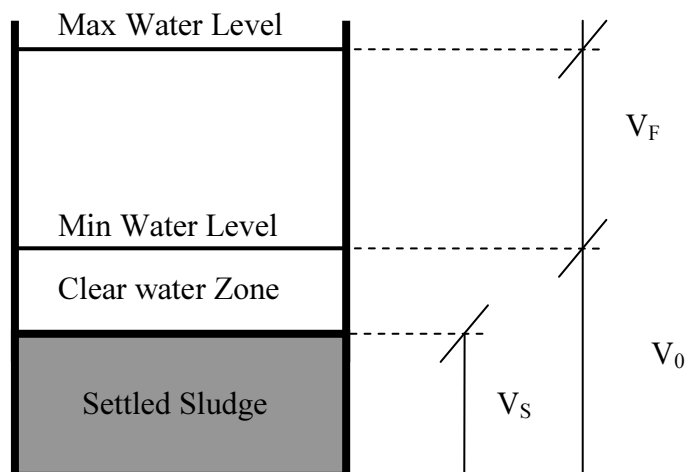


**Figure 3-4.** Cyclic operation of SBR

An external re-circulating pump (2E-38N, Little Giant) was used to mix the contents of the SBR while another pumped the wastewater from the freezer. In addition, one pump was used to mix the sewage in the freezer just before feeding. These pumps were thermally-protected dual purpose, oil-filled pumps, manufactured by Little Giant Co, Oklahoma City, USA. To make up the final working volume of 21 L in the reactor, a floating valve was fixed and operated automatically. The total reaction time of the SBR was 7 h, combining both anoxic (1 h 30-min) and aerobic (5 h 30-min) reactions. After the aerobic reaction, the content was allowed to settle for 30-mins followed by a decantation of 10.5 L clear supernatant. The decantation was made with in the last 5 min of the cycle and this maintained an HRT of 15 h 20 min. Air was supplied to the reactor only for the aerobic period. Dissolved oxygen in the reactor was recorded online.

The concentration of the mixed liquor suspended solids (MLSS) and the sludge volume index (SVI) was measured every day during the entire period of the operation. A target MLSS concentration was fixed at 3,000 mg/L and controlled by changing the volume of the wasting sludge. In normal periods, about 1 L/day of sludge was wasted to yield an SRT of 20 d. The wasted biomass was stored in a refrigerator (at 4 °C) for subsequent use in the denitrification batch tests. The SVI measured was used to examine the settleability of the sludge. The pH in the system

was recorded but not controlled and found to be mostly between 6.5 and 7.0. The system was operated at a normal room temperature ( $20 \pm 2$  °C) of the laboratory. During the operation of the SBR, a few track studies on COD,  $\text{NO}_3^-$ -N, and  $\text{NH}_4^+$ -N were performed. From such studies, removal of the COD and the changing pattern of the concentration of  $\text{NO}_3^-$ -N, and  $\text{NH}_4^+$ -N were observed and the performance of the reactor was inspected. Details of the results of such studies are presented in Section 5.1.1.3.

### 3.1.2 Anaerobic Digester

#### 3.1.2.1 Hardware

VFAs were produced in a bench-scale anaerobic digester in the laboratory. The schematic diagram of the digester is shown in Figure 3-5. The digester consisted of a 25-L stainless steel cylinder with a height of 40 cm and an external diameter of 30 cm. The cylinder contained a liquid of volume 20 L as the working volume. A steel lid fixed with a grease and rubber seal allowed the system to operate under anaerobic conditions.

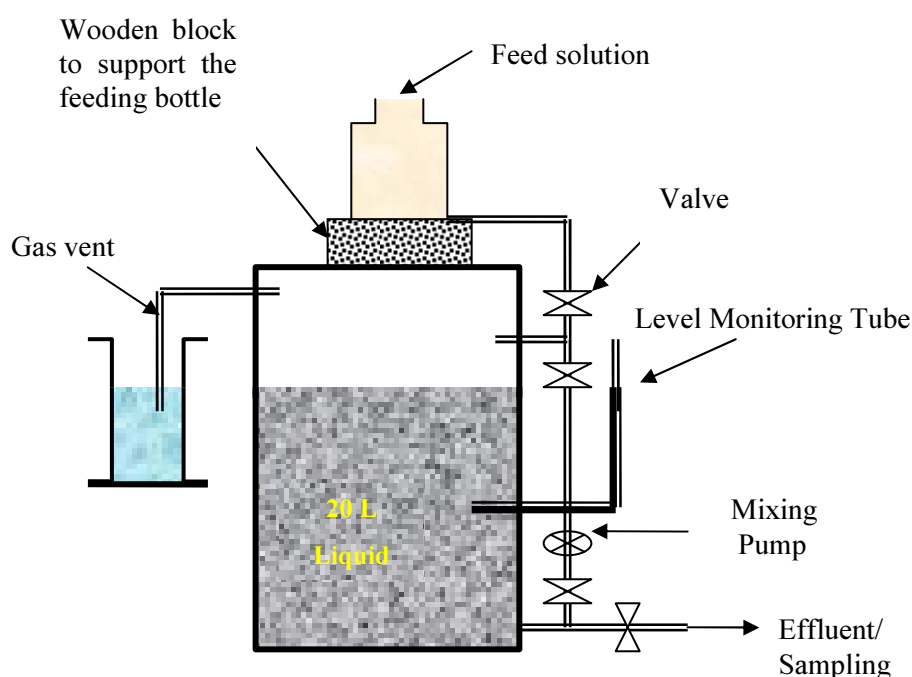


**Figure 3-5.** Schematic diagram of anaerobic digester

An external pump was fitted to mix the digester contents continuously throughout the entire period of the operation. The pump was calibrated to have a flow rate of approximately 8 L/min. Mixed liquor flowed out of the bottom port (outlet) of the digester and returned back into the system through the top port (inlet). A valve was fixed on the bottom port to allow the contents to be sampled and which could be used to drain the digester if needed. In addition a vent pipe from the top port was fixed to release the gases produced inside the digester, which prevented the development of too much pressure in the headspace. Gas produced was first released into a beaker of water. A transparent tube was fixed and mounted vertically to monitor the volume (level) of the contents inside the digester.

### **3.1.2.2 Feeding Methodology and Digester Inoculation**

The synthetic feed was a full-fat, enzyme-active soy flour purchased from the Weston Milling Co. Ltd, Christchurch, New Zealand. The biochemical composition of the soy flour was assumed to contain approximately 36 % protein, 30 % carbohydrate, 18 % fat as well as isoflavones, minerals, amino acids and vitamins (MacDonald, et al., 2005; Answer.com, 2008; USDA, 2008). In this research, 40 g/L of soy flour solution was added, which was similar to the soy concentration previously used to obtain a VFAs concentration of 5,000 mg/L as HAc or more (He, 2006). Before feeding, this solution was prepared by adding 80 g of soy flour into 2 L tap water and stirring for 24 h. The total and soluble CODs of the feed solution were measured to be  $56,200 \pm 2,500$  mg/L and  $9,450 \pm 150$  mg/L respectively. This yielded a COD soluble fraction of about 17 %. Similarly the total organic carbon (TOC) found in the solution was  $3,600 \pm 252$  mg/L. The concentration of VFAs measured in the influent soy flour solution was relatively small ( $< 400$  mg/L as HAc). To provide the initial biomass, the digester was seeded with 10 L of digested sludge (TSS concentration 23,000 mg/L) obtained from another anaerobic digester that was operating in the lab. After seeding, the liquid volume of the new digester was made to exactly 20 L by adding 10 L of 40 g/L soy flour solution. The pump was switched on and closely monitored for the first 2 to 4 hours and any blockages developed in the system were removed manually by disconnecting the valves and fittings. After a complete inspection of the system, the lid of the digester was sealed by compression against greased rubber washers and using bolts all round.

Each day, 2 L of the soy flour solution was added through the top port of the digester while at the same time 2 L of digester contents was wasted through the wasting outlet, at the bottom of the digester. The external mixing pump was stopped prior to feeding and wasting, and then restarted immediately afterwards. The 2 L daily feeding and wasting regime of the 20 L liquid volume yielded a digester SRT and HRT of 10 days. On the basis of previous studies (Elefsiniotis, et al., 1996; He, 2006; Kim, et al., 2006; Appels, et al., 2008), the SRT/HRT chosen was capable of generating a considerable quantity of VFAs.

During the start-up of the digester, samples were taken every day and analysed for total COD and sCOD. Initially CODs (soluble and total) were found to be very low, in the range of 2,000 to 3,000 mg/L and 6,000 to 8,000 mg/L respectively. The sCOD in the effluent was measured every day for about three months and found to be increasing daily until a plateau was reached of 15,000 mg/L. Once this stable level of sCOD was reached, the digester was considered to be in a fully developed phase and samples were analysed for additional parameters. In the first few months, the digester was sampled daily and then every week until the end of the study. Samples were normally analysed for pH, total solids (TS), volatile solids (VS), total suspended solids (TSS), volatile suspended solids (VSS), COD and VFAs. Apart from these, alkalinity, TOC,  $\text{NO}_3^-$  - N, and  $\text{NH}_4^+$  -N were analysed occasionally. The results of these analysis and the details concerning the production of the VFAs is reported in Section 5.1.2 (Results and Discussions).

The digester was ostensibly operated at a room temperature of  $20 \pm 2$  °C; however, during the digestion process, the temperature of the liquor inside the digester was raised to  $31 \pm 4$  °C; which lies in the mesophilic range (25 to 38 °C) of digestion (Gray, 2004). Since, as mentioned, acidogens are not as sensitive to temperature changes as methanogens (Yu and Fang, 2003), this research did not focus on finding the optimum temperature with respect to process performance. Both diurnal and seasonal temperature changes were deemed insignificant with respect to the degree of acidification and VFA production. However, the range of temperature of the digester was found to be similar to the optimum temperature for VFAs production as reported by Feng et al. (2009).

### 3.1.3 Denitrification Batch Test Reactors

Once denitrifying biomass in the first system (the SBR) and the VFAs from the second system (i.e., the digester) was ready, the third system (the denitrification batch tests) were started. Each test was conducted in a 5-L Erlenmeyer flask reactor as shown in Figure 3-6. An air tight rubber stopper capped the flask to make the system anoxic. A long sampling tube, passing through the stopper and extending to the bottom of the reactor was fixed into the system. At the time of sampling, a 40 mL syringe could be attached to the top of the tube and used to draw out the sample from the reactor. All the tests were carried out at ambient temperature ( $20 \pm 2$  °C) while complete mixing was accomplished using magnetic stirrers with a 5 cm long stir bar moving at 300 - 500 rpm.

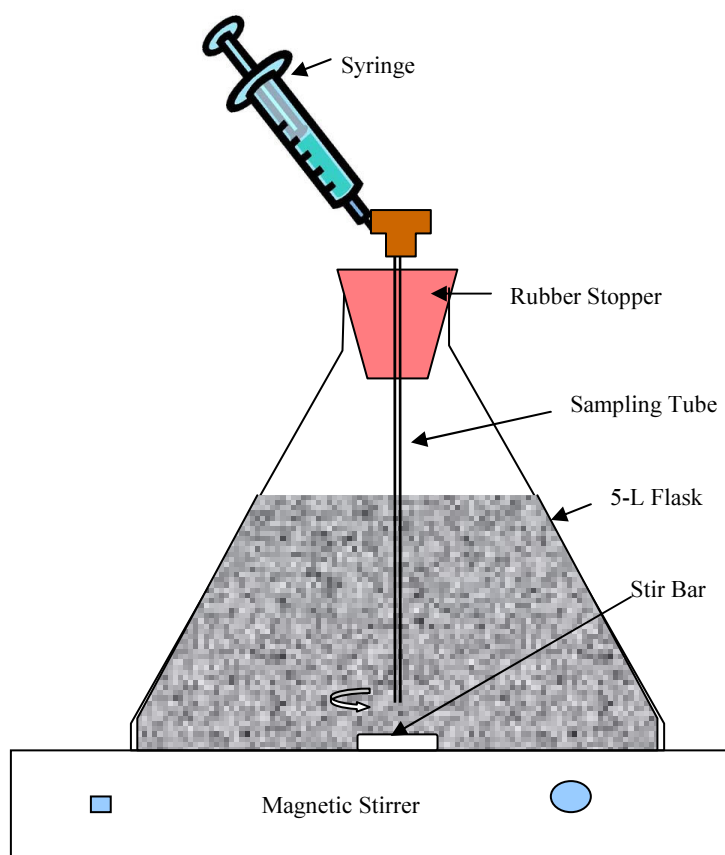


**Figure 3-6.** Schematic diagram of a denitrification batch test reactor

### **3.1.3.1 Preparation of Biomass**

Several preliminary track studies indicated a healthy presence of denitrifying bacteria in the sludge of the SBR as indicated by reduction of  $\text{NO}_3^-$ -N to  $\text{N}_2$  gas and removal of COD. Consequently, the sludge was used as a source of denitrifying biomass for all the experiments carried out during this study. In some cases, sludge was stored for 10-15 days at 4 °C with no apparent diminishing ability of the sludge to denitrify.

The residual COD and nitrogen present in the sludge would render the initial C: N ratio meaningless as well as mask the consumption of external carbon (i.e. the VFAs in the anaerobic digester effluent); thus sludge washing was required to minimize the initial concentration of COD and nitrogen. The biomass washing procedure involved stirring, settling and decanting with tap water. It was done in a 5 L flask by adding the tap-water to the top level of the flask, stirring for 30 min and allowing to settle for one hour. After the settlement, the supernatant was decanted without substantial loss of solids. This process was repeated until the COD level in the supernatant dropped to 5 mg/L or less. Finally the sludge was washed once more with deionized water. The concentration of MLSS was measured before use in the batch tests. Initially, a few tests on denitrification were done with different concentrations of MLSS, and a concentration of 1,200 mg/L was targeted to carry out all batch tests for the study on the effect of arsenic on denitrification. In addition, some extra tests were done using a lower concentration of MLSS (75-600 mg/L) to examine the arsenic removal isotherm caused by the biomass only.

### **3.1.3.2 Feeding Methodology**

As mentioned in Section 3.1.3.1 the denitrifying biomass obtained from the SBR was washed until very low concentrations of residual C and N were observed. After determining the concentration of the MLSS, an appropriate volume of the biomass was mixed with tap water and poured into the denitrifying batch reactors so that the final MLSS concentration in the 5 L reactor would be approximately 1,200 mg/L. An external carbon source was then prepared from the 2 L waste effluent obtained from the digester by centrifugation and filtration. That is, digester effluent was first

centrifuged (Eppendorf Centrifuge 5402) at 4,400 rpm (rotation per minute) for 15 minutes and then the supernatant was filtered through a 0.45  $\mu\text{m}$  nitrocellulose filter paper (millipore) under vacuum. An appropriate volume of this filtrate as well as the  $\text{NO}_3^-$  solution were added to the reactors to yield an optimum C: N ratio of approximately 3.0. In addition, other denitrifying reactors were spiked with different concentrations of arsenic before making up the final volume of the reactors to 5 L by adding additional tap water. Details of the volumes and concentrations of these reactants are given in Section 3.1.3.4.

### **3.1.3.3 Preparation of Stock Solutions**

For feeding purpose, stock solutions of  $\text{NO}_3^-$ -N, As (III) and As (V) were made. Each of these solutions was prepared in a volumetric flask (Pyrex Glass), cleaned with 0.3 M hydrochloric acid and rinsed with deionized water. A concentration of 1,000 mg As (III)/L was prepared by adding 1.32 g of arsenic tri-oxide ( $\text{As}_2\text{O}_3$  by BDH Chemical Ltd. England) in 1 L deionized water. For As (V), 4.17 g of sodium arsenate heptahydrate ( $\text{Na}_2\text{HAsO}_4 \cdot 7\text{H}_2\text{O}$  by BDH Chemical Ltd. England) was added to prepare 1,000 mg As (V)/L. Potassium nitrate ( $\text{KNO}_3$ ) from BDH Chemical Ltd. England was used to prepare  $\text{NO}_3^-$ -N solution (i.e. 16 g  $\text{KNO}_3$  was added in 1 L deionized water to prepare a stock solution of 2,200 mg  $\text{NO}_3^-$ -N /L). All stock solutions prepared were stored in a refrigerator (4 °C) for up to a period of 2 months.

### **3.1.3.4 Selection of Concentration of Various Parameters**

Several trial and error preliminary tests were done to choose the appropriate concentrations of MLSS, carbon,  $\text{NO}_3^-$ -N and arsenic to be added. Initial concentrations of these additives were selected according to the following rationale;

- 1) The MLSS concentration was selected on the basis of a practically reasonable denitrification time frame of 4-6 h. That is, two batch tests were done using two different concentrations of MLSS (i.e. 800 and 1,500 mg/L) and, after observing the denitrification times for both sets of data, a MLSS of



1,200 was selected to be a target concentration suitable to complete the denitrification process in a denitrification time of 4 hours.

- 2) Various concentrations of  $\text{NO}_3^-$  - N were added and 25 mg  $\text{NO}_3^-$  -N/L was fixed to target initial concentration as this was normally denitrified over a 4 hour period.
- 3) For the selected initial concentrations of MLSS (1,200 mg/L) and  $\text{NO}_3^-$  -N (25 mg/L), five different tests were run with five different volumes (0, 30, 60, 120 and 200 mL) of digester effluent (VFAs) resulting in C/ N ratios of 0.0 (no extra carbon added), 0.96, 1.92, 3.84 and 5.76. After evaluating the results obtained from these tests (Section 5.1.3), a C/N ratio of approximately 3.0 (VFA volume 100 mL), sufficient to complete the denitrification test without experiencing carbon limiting conditions, was selected for all the denitrification batch tests to yield an optimum specific rate of denitrification. While using carbon sources such as VFAs, a C/N ratio of  $\geq 2.0$  has been shown to be sufficient to ensure that no carbon-limiting condition exists during denitrification (Her and Huang, 1995; Elefsiniotis, et al., 2004).
- 4) After a few trials using randomly selected concentrations of As (III) it was envisaged that the effect of As (III) would be clearly seen in the range of 5 to 50 mg/L As (III). A total of five denitrification batch test runs (R1, R2, R3, R4 and R5) were carried out with each run consisting of four tests with different concentrations of As (III). In the similar manner, four denitrification batch test runs (R6, R7, R8, and R9) were executed using three different concentrations of As (V) in two of the runs and four different concentrations in the remaining two runs. Table 3-2 indicates the details of the concentrations of arsenic and other reactants added in the batch test runs carried out over the course of the denitrification research.

**Table 3-2:** Initial concentrations of arsenic and other reactants (as per added)

Run/Reactor	Arsenic added			Run/Reactor	Arsenic added	
	mg/L	Type			mg/L	Type
R1-1	0	As(III)		R6-1	0	As(V)
R1-2	5	As(III)		R6-2	50	As(V)
R1-3	10	As(III)		R6-3	500	As(V)
R1-4	18	As(III)				
R2-1	0	As(III)		R7-1	0	As(V)
R2-2	5	As(III)		R7-2	100	As(V)
R2-3	18	As(III)		R7-3	1000	As(V)
R2-4	25	As(III)		R7-4	2000	As(V)
R3-1	0	As(III)		R8-1	0	As(V)
R3-2	5	As(III)		R8-2	50	As(V)
R3-3	10	As(III)		R8-3	100	As(V)
R3-4	50	As(III)		R8-4	1000	As(V)
R4-1	0	As(III)		R9-1	0	As(V)
R4-2	18	As(III)		R9-2	500	As(V)
R4-3	25	As(III)		R9-3	2000	As(V)
R4-4	50	As(III)				
R5-1	0	As(III)		MLSS = 1,200 mg/L NO <sub>3</sub> <sup>-</sup> - N = 25 mg/L VFA = 100 mL C/N = 3:1		
R5-2	10	As(III)				
R5-3	25	As(III)				
R5-4	50	As(III)				

To observe the removal of arsenic by denitrifying biomass, some additional tests were also done with a lower concentration of arsenic (0.6 mg/L). A total of four such batch test runs (RA, RB, RC and RD) were carried out with each run consisting of five different tests with MLSS concentrations of 75, 185, 375, 560, and 750 mg/L. Table 3-3 lists the details of the MLSS concentrations and other reaction conditions of each of these batch tests.

**Table 3-3:** Arsenic removal tests with different concentrations of MLSS

<b>Run/Reactor</b>	<b>MLSS (mg/L)</b>	<b>C and N added</b>	<b>As Type</b>
RA-1	75	yes	As(III)
RA-2	185	yes	As(III)
RA-3	375	yes	As(III)
RA-4	560	yes	As(III)
RA-5	750	yes	As(III)
RB-1	75	no	As(III)
RB-2	185	no	As(III)
RB-3	375	no	As(III)
RB-4	560	no	As(III)
RB-5	750	no	As(III)
RC-1	75	yes	As(V)
RC-2	185	yes	As(V)
RC-3	375	yes	As(V)
RC-4	560	yes	As(V)
RC-5	750	yes	As(V)
RD-1	75	no	As(V)
RD-2	185	no	As(V)
RD-3	375	no	As(V)
RD-4	560	no	As(V)
RD-5	750	no	As(V)

The C/N ratio (3:1) was the same ratio as the previous denitrification batch tests; however, the reactors used in these tests were of smaller size (500 mL). These tests were run for a contact period of 24 h at room temperature ( $20 \pm 2$  °C). Finally, four more tests, one without biomass, one with normal biomass, and two with disrupted and dead) biomass were done to confirm whether the process of arsenic removal was due to biological uptake or just physical adsorption. The biomass was killed by boiling for 15 min while cell disruption was carried out by an ultrasonic processor (Converter Model CV33).

### 3.2 Sampling and Analytical Methods

Various chemical and physical parameters were analyzed over the course of this research. Some parameters were monitored solely to observe the system performance (both reactors and digester), while others were collected explicitly to be part of the research data. Table 3-4 indicates the parameters that were monitored during the research work.

**Table 3-4:** Physical / chemical parameters monitored during the experiments

Chemical Parameters			SBR	Digester	D. Batch Tests
Name	Symbol	Unit			
Dissolved Oxygen	DO	mg/L	Yes	No	Yes
Total Nitrogen	TN	mg/L	Yes	Yes	Yes
Nitrate Nitrogen	NO <sub>3</sub> <sup>-</sup> - N	mg/L	Yes	Yes	Yes
Nitrite Nitrogen	NO <sub>2</sub> <sup>-</sup> - N	mg/L	Yes	Yes	Yes
Ammonium Nitrogen	NH <sub>4</sub> <sup>+</sup> - N	mg/L	Yes	Yes	Yes
Chemical Oxygen Demand	COD	mg/L	Yes	Yes	Yes
Total Organic Carbon	TOC	mg/L	Yes	Yes	Yes
pH	-		Yes	Yes	Yes
Alkalinity	mg/L as CaCO <sub>3</sub>		Yes	Yes	Yes
Total Suspended Solids / Mixed Liquor Solids	TSS / MLSS	mg/L	Yes	Yes	Yes
Total Solids	TS	mg/L	No	Yes	No
Total Volatile Suspended Solids / Mixed Liquor Volatile Suspended Solids	TVSS / MLVSS	mg/L	Yes	Yes	Yes
Total Volatile Solids	TVS	mg/L	No	Yes	No
Volatile Fatty Acids	VFA	mg/L	No	Yes	Yes
Total Arsenic	As	mg/L	No	No	Yes
Sludge Volume Index	SVI	mL/g	Yes	No	No

With respect to all three systems, samples were first collected in a clean and dry plastic or glass bottle. Sampling bottles were cleaned with 0.3 M hydrochloride solution and rinsed with demineralised water; and in most cases, samples were taken while the reactor contents were fully mixed. Dissolved oxygen in the SBR was

monitored online using a DO probe. Most of the samples were prepared by vacuum filtering through a glass fibre filter followed by 0.45  $\mu\text{m}$  micromillipore gridded membrane filters made from nitrocellulose. Two-step filtration was essentially done to measure all soluble parameters such as  $\text{NH}_4^+\text{-N}$ ,  $\text{NO}_3^-\text{-N}$ , and sCOD as well as the parameters analyzed by sophisticated analyzers for such as TOC and VFAs. Analyses of VFAs and TOC were carried out on an HP 6890 Series Gas Chromatograph and an Apollo 9000 TOC Combustion Analyzer respectively. Arsenic, COD, alkalinity, MLSS and MLVSS were analysed in accordance with Standard Methods (APHA, 1992), while pH was measured using a standard probe. The details of the analyses of each parameter are described in the following section.

In the SBR, samples were taken at different phases of the cycle. MLSS and SVI were measured daily while the reactor was at the end (or close to the end) of an aerobic phase. For track studies of  $\text{NO}_3^-\text{-N}$ ,  $\text{NH}_4^+\text{-N}$  and COD, samples were taken at every 15 min during the anoxic phase, while at every 1 h during the aerobic phase. COD and  $\text{NH}_4^+\text{-N}$  were analysed for every supply of raw sewage from the treatment plant, while MLSS, COD and  $\text{NO}_3^-\text{-N}$  were normally checked in decanted effluent from the SBR. Once, the anaerobic digester was fully developed, the samples were analysed every week for TS, VS, TSS, COD and VFAs (acetic, propionic, n-butyric, iso-valeric and n-valeric acids); while, TOC, alkalinity,  $\text{NO}_3^-\text{-N}$ , and  $\text{NH}_4^+\text{-N}$  were measured only sporadically. From each denitrification batch test, samples were taken at 0, 30, 60, 90, 120, 150, 180, 210 and 240 min. intervals. All samples were taken by connecting a 40 mL plastic syringe to the top of the sampling tube of each reactor. Only the first sample (taken at 0 min) was used to measure MLSS and MLVSS, in addition to all other parameters. Soluble COD and  $\text{NO}_3^-\text{-N}$  were analysed for all samples of the denitrification batch tests. Alkalinity, total arsenic and VFAs were analysed for the first (0 min) and last (240 min) samples. In all the arsenic removal batch tests, the initial and final (after 24 h reaction) concentrations of the arsenic were analysed.

### 3.2.1 Arsenic

Arsenic was measured in the lab using silver diethyldithio carbamate (SDDC) spectrophotometric method (APHA, 1992; Ahmed, 2003b). The arsenic generator and absorber assembly was prepared as shown in Figure 3-7. In this method, arsenic-containing samples were decomposed by adding acids. Arsenic (V) is produced and together with inorganic arsenic originally present is subsequently reduced to arsenic (III) by potassium iodide and stannous chloride. By adding zinc to this solution, the arsenic is reduced further to arsine gas ( $\text{AsH}_3$ ).

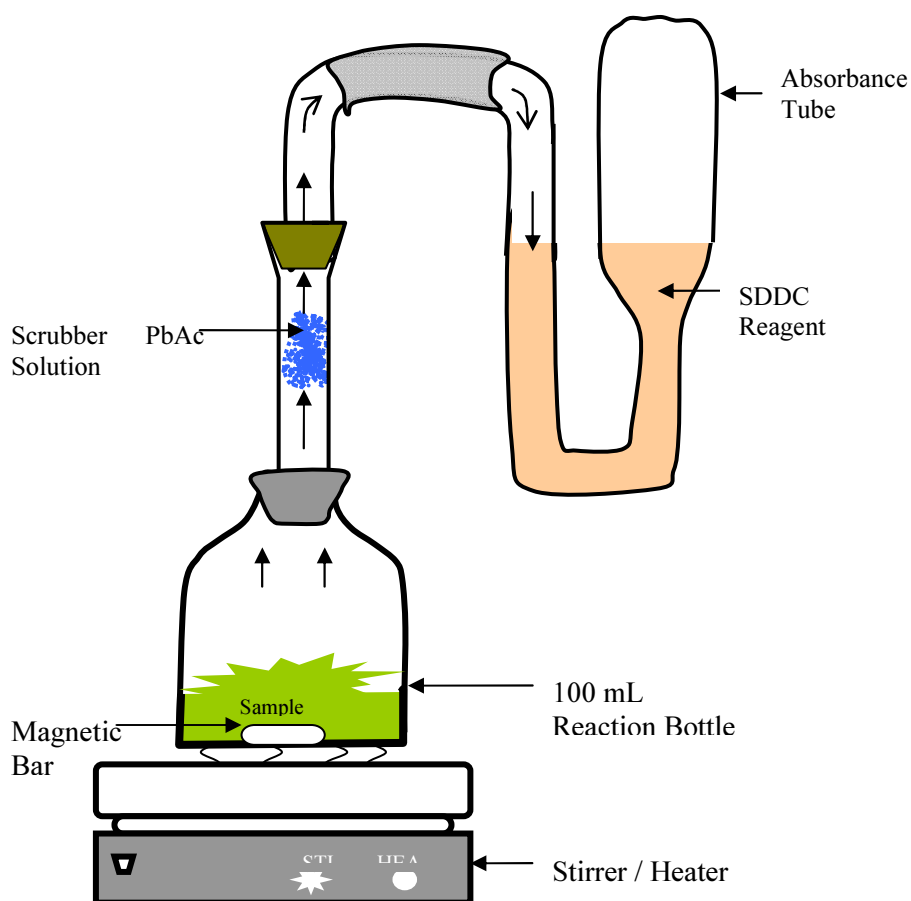


**Figure 3-7.** Arsenic generator and absorber assembly

Nascent hydrogen is produced by the reaction of hydrochloric acid on zinc and this reduces the arsenic to  $\text{AsH}_3$ . The resulting mixture of gases is passed through a scrubber containing wool impregnated with lead acetate ( $\text{PbAc}$ ) solution to remove

hydrogen sulphide and other sulphides which interfere with the results. The gases are then passed into an absorption tube containing a solution of SDDC in pyridine. Arsine gas reacts with the SDDC solution gave a red colour silver solution. Testing was performed in accordance with the procedure described in Standard Methods (APHA, 1992). After a reaction time of half an hour, the solution was then poured into a 1 cm quartz-cell and the absorbency of the solution was measured with the HACH DR/2500 spectrophotometer at 535 nm. For each new stock of SDDC solution a standard calibration curve (absorbance versus concentration of arsenic) was plotted for the total arsenic range of 0 to 12  $\mu\text{g}$  which was then used to determine total arsenic in the sample. A typical calibration curve is in Appendix A1.

### **3.2.2 Nitrate and Nitrogenous Parameters**

#### **3.2.2.1 Nitrate**

Nitrate was measured by the cadmium reduction method, which is a colorimetric method that involves contact of the  $\text{NO}_3^-$  in the sample with cadmium particles, which cause  $\text{NO}_3^-$  to be converted to  $\text{NO}_2^-$  (APHA, 1992; HACH, 1997). The  $\text{NO}_2^-$  produced is determined colorimetrically by diazotizing with sulphanilamide and coupling with N-(1-naphthyl) – ethylenediamine dihydrochloride (NED dihydrochloride) to form a red colour azo dye whose intensity is proportional to the original amount of  $\text{NO}_3^-$ -N. The red colour is measured by an electronic spectrophotometer that measures the amount of light absorbed by the treated sample at a 500-nanometer wavelength. The absorbance value is then converted to the equivalent concentration of  $\text{NO}_3^-$ -N by using a standard curve.

The reagents used for this method were purchased from the HACH Company in packages. Among the available reagents in different ranges, almost all of the  $\text{NO}_3^-$ -N values in this research were measured by using the high range (0 to 30 mg/L) reagent (Nitrover®5, for 25 mL sample volume). The spectrophotometer HACH DR/2000 was used to measure the absorbance and consequently the concentration of  $\text{NO}_3^-$ -N. Testing was performed in accordance with the procedure described in HACH method 8039 (HACH, 1997). The concentration measured with this method is very sensitive to the technique or the workmanship applied. Thus the technique

was initially appraised by practicing several times with different standard concentrations, and also several successive tests were done on known standard concentrations of  $\text{NO}_3^-$  - N during the entire period of the research. Samples were preserved at 4 °C and normally analysed within 24 hours. Prior to testing these samples were warmed to room temperature.

### **3.2.2.2 Ammonia**

Ammonia was measured using the salicylate colorimetric method. In this method,  $\text{NH}_4^+$  compounds combine with salicylate to form monochloramine, which reacts with salicylate and forms 5-aminosalicylate. Then in the presence of sodium nitroprusside catalyst, the 5-aminosalicylate is oxidized and forms a blue coloured compound. The blue colour is masked by the yellow colour from the excess reagent to give a final emerald-green complex (HACH, 2003). The emerald-green colour developed in the reaction is proportional to the presence of  $\text{NH}_4^+$  and measured at 655 nm.

Kits from different companies were available to measure the  $\text{NH}_4^+$  at different concentration ranges using this method. HACH Test N Tubes for high range  $\text{NH}_4^+$  (0.4 to 50 mg/L  $\text{NH}_4^+$  -N) were used for all the tests done during the research. The spectrophotometer HACH DR/2500 was used to measure the intensity of colour and consequently the concentration of  $\text{NH}_4^+$  present in the samples. Testing was performed by following the procedure steps described in HACH method 10031 (HACH, 2003). Since the sample size used in this method was very small (0.1 mL), extra attention was given to obtaining a representative sample by mixing the reactor contents thoroughly and replication. To check the sensitivity of the method, several tests were done on different concentrations of the  $\text{NH}_4^+$ - N standard solution. Normally samples were analysed immediately after sampling; however, a few samples were preserved at 4 °C and analysed within 24 hours. Immediately prior to testing, these preserved samples were warmed to room temperature. A stock  $\text{NH}_4^+$  solution of a concentration 100 mg/L  $\text{NH}_4^+$ - N was prepared by dissolving 3.819 anhydrous ammonium chloride ( $\text{NH}_4\text{Cl}$  by MandB, Australia), dried at 100 °C in deionized water and diluting to 1 L.



### **3.2.2.3 Nitrite**

Nitrite was measured using the ferrous sulphate colorimetric method. In this method, the reagent ferrous sulphate is used in an acidic medium to reduce the  $\text{NO}_2^-$  to  $\text{N}_2\text{O}$ . Ferrous ions combine with the  $\text{N}_2\text{O}$  to form a greenish-brown complex in direct proportion to the  $\text{NO}_2^-$  present. The procedure and the reagent (NitriVer®2) were used in accordance with HACH method 8153 (HACH, 2003). The intensity of the colour was measured by the HACH DR/2500 spectrophotometer at 585 nm. In the beginning, deionized water instead of a sample was analysed to obtain a blank sample value and this value was subtracted from the final result of all samples.

### **3.2.3 COD**

COD is used as a measurement of the oxygen equivalent of the organic matter content of a sample that is susceptible to oxidation by a strong chemical oxidant. The COD was measured by digesting the sample in a digester using potassium dichromate. A silver compound ( $\text{Ag}_2\text{SO}_4$ ) was used as a catalyst to promote oxidation and, a mercuric compound ( $\text{HgSO}_4$ ) to reduce interference from the oxidation of chloride ions from the dichromate. The oxidation process was carried out by mixing 2 mL of a sample in 5 mL of high range (0 to 1200 mg/L) digestion solution, prepared in the lab in HACH glass tubes with a screw cap (10 x 100 mm). This was allowed to digest in the HACH Digital Reactor Block 200 (DRB200) at 150 °C for 2 h. After the oxidation step was completed, the amount of dichromate consumed was determined colorimetrically. Four absorbance values were determined each for 300, 600, 900, and 1,200 mg/L COD standard solutions and the calibration curve (absorbance versus COD concentration) was prepared (Appendix A2). These absorbance values were loaded for the corresponding COD values in the DR/2000 spectrophotometer and a new program for a range of 0 to 1,200 mg/L COD (User entered method # 951) was created by following the procedure described in the DR/2000 spectrophotometer manual (HACH, 1995).

#### **3.2.3.1 Preparation of COD Reagents**

COD reagents were prepared following standard methods (APHA, 1992). Standard potassium dichromate solution (0.0417M) was prepared by dissolving 12.259 g

laboratory reagent grade potassium dichromate ( $K_2Cr_2O_7$  by M & B, Australia), previously dried at 105 °C for two hours in deionised water and diluted to 1 L. Then 33.3 g Mercuric Sulphate ( $HgSO_4$  by BDH Chemical, England) was added to the solution to reduce interference from the oxidation of chloride ions from the dichromate. Sulphuric acid reagent was prepared by adding 5.5 g laboratory grade silver sulphate ( $Ag_2SO_4$ ) per kg  $H_2SO_4$  (25.3 g extra pure  $Ag_2SO_4$  by Scharlau Chemie, Spain, in 2.5 L  $H_2SO_4$ ) and letting to stand for 48 h to dissolve. The high range digestion solution was prepared by adding 150 mL of standard potassium dichromate solution in 350 mL of sulphuric reagent. This mixing was done in a water bath with extra care. Each time, this digestion solution prepared was examined by the standard COD solution (Potassium hydrogen phthalate standard) and preserved at 4 °C. To prepare a 1,200 mg/L standard COD solution, 1.0213 g dried (at 120 °C for 1 h) analytical grade potassium hydrogen phthalate ( $HOOC-C_6H_4-COOK$  by Ajax Finechem Pty Ltd.) was dissolved in deionized water and diluted to 1 L.

### 3.2.4 VFAs

The concentration of major VFAs including acetic, propionic, n-butyric, iso-valeric and n-valeric acids were determined by a Hewlett-Packard Gas Chromatography unit equipped with an HP 19091N-133 column (HP INNOWax Polyethylene Glycol 30 m  $\times$  250  $\mu$ m  $\times$  0.25  $\mu$ m) and a flame ionization detector (FID). Samples were first centrifuged (Eppendorf Centrifuge 5402) at 4,400 rpm for 15 min and then the supernatant was filtered through 0.45  $\mu$ m nitrocellulose filter paper (Millipore) under a vacuum. Most samples were analysed within 2 - 4 hrs. On occasion, some samples were stored at 4 °C for more than 12 h until analyzed. Immediately before the analysis these samples were warmed back to room temperature and 2 mL were transferred to a gas chromatography vial. The injection volume for analysis was set at 1.0  $\mu$ L and the inlet temperature was 280 °C. The initial temperature in the oven was 120 °C, which was maintained for 1 min and then increased up to 250 °C at a rate of 10 °C per min. Once this temperature was reached, the temperature was held constant for 2 min, then decreased to 120 °C and held for 0.5 min. The flame ionization detector (FID) temperature was 300 °C. Each VFA present was identified

by comparing the travel time with that of known standards. The amount of each acid was quantified by comparing the area under the peak of the chromatograph to that of known standards from calibration curves (Appendix A3). For all standards, chemicals were of analytical grade supplied by established lab-chemical suppliers such as acetic acid from Biolab (Australia) Ltd, propionic acid and n-Butyric acid from BDH, England and iso-valeric and n-valeric acid from Sigma-Aldrich, Germany.

### **3.2.5 TOC**

Total organic carbon was analysed by using combustion – infrared method (APHA, 1992). In this method, acid is added to the sample to convert inorganic carbon (IC) to CO<sub>2</sub> gas that is stripped out of the liquid by a carrier gas. The remaining inorganic carbon-free sample is then oxidized and CO<sub>2</sub> is generated. The carrier gas then sweeps the derived CO<sub>2</sub> through a nondispersive infrared (INDIR) detector sensitive to the absorption frequency of CO<sub>2</sub>. The NDIR generates a non linear signal that is proportional to the instantaneous concentration of CO<sub>2</sub> in the carrier gas. That signal is then linearized and integrated over the sample analysis time. The resulting area is then compared to the area of standard calibration curve and a sample concentration is calculated (Tekmar, 2003).

Samples for TOC analysis were prepared as for VFAs analysis and about 30 mL of each prepared sample was transferred to a 40 mL screw thread volatile organic analysis (VOA) vial. The samples were then analysed by a TOC analyzer (Apollo 9000 Combustion TOC Analyser with STS 8000 autosampler, by Teledyne Tekmar), using a TOC Talk software. When the TOC talk software was started, a TOC Talk control screen appeared with setup options, run options, results and a status bar that depicted event list items in real time along with the mode status and the current NDIR mV output. A 1000 mg C/L of TOC standard stock solution was prepared by dissolving 2.948 g of citric acid monohydrate (C<sub>6</sub>H<sub>8</sub>O<sub>7</sub>·H<sub>2</sub>O, by Scharlau, Spain) in deionized water and diluting to 1 L. A typical COD calibration curve is shown in Appendix A4.

### 3.2.6 Alkalinity

Alkalinity was measured by the standard titration method (APHA, 1992). In this method the alkalinity of the sample is determined by the volume of standard acid required to titrate a known sample volume to an end point pH. The formula used to calculate the alkalinity is given as;

$$\text{Total Alkalinity in mg / L as CaCO}_3 = \frac{A \times N \times 50000}{\text{mL Sample}} \quad (3.1)$$

Where A = mL standard acid used in titration

B = normality of standard acid (0.02N H<sub>2</sub>SO<sub>4</sub>)

Titration was carried out until an end point of pH 4.5. A 100 mL sample was stirred in a 250 mL beaker during the titration using a magnetic stirrer. The stirring action was assumed to be vigorous enough to allow rapid equilibrium of CO<sub>2</sub> between the solution and the atmosphere.

### 3.2.7 pH

A pH electrode (RE357Tx Microprocessor pH Meter) was used to measure the pH. Normally a pH electrode is a tube that is small enough to put it sample jars and it tied to a pH-meter by means of a cable. A special type of fluid is located within the electrode; usually 3M potassium chloride (KCl). Some electrodes contain a gel that has the same properties as the 3M-fluid. In the fluid there are silver and platinum wires. The system is quite fragile, because it contains a small membrane. The H<sup>+</sup> and OH<sup>-</sup> ions will enter the electrode through this membrane. The ions will create a slightly positive charge and a slightly negative charge in each end of the electrode. The potential of the charges determines the number of H<sup>+</sup> and OH<sup>-</sup> ions and when this is determined the pH will appear digitally on the pH-meter. The potential is co-dependent on the temperature of the solution. Which is why the temperature is also presented on the pH-meter.

### **3.2.8 Dissolved Oxygen (DO)**

The DO concentration was measured using a DO probe and meter (YSI Model 57 Oxygen Meter). A DO probe contains a sensor which is dipped in KCl solution. A membrane separates the sensor from the solution being measured. Dissolved solution is free to pass from the solution into the probes in a KCl solution. A DO meter is able to take a reading by passing a polarizing voltage across the sensor, causing oxygen which has passed through the membrane to react at a cathode creating a flowing current (BIOLAB, 2003). The membrane is disposable and usually replaced every two-week or as required. The KCl solution was also changed while changing the membrane.

### **3.2.9 TSS and VSS**

TSS and VSS were measured by filtering the sample through glass fibre filter (Whatman glass fibre filter circles; grade GF/C; 90 mm  $\Phi$ ), that had been oven dried at 103 to 105 °C for at least 24 hrs prior to the test. For a rapid filtering process a vacuum was applied. First the filter paper was wetted with a small volume of distilled water to seat it on the filtering apparatus. Then a measured volume (normally between 75 – 90 mL) of well mixed sample was passed through the GF/C. About 10 ml of distilled water was passed three successive times through the filter system. Then the GF/C was taken carefully out and put in the oven (103 to 105 °C) for at least one hour to evaporate the whole water content from the filter paper. Before reading the weight of the GF/C with the suspended solids, it was stored in a desiccator to achieve a constant mass. The difference in the mass of GF/C before and after the filtration yielded the TSS. To obtain the VSS, the filter paper with the solid mass on it was ignited in a furnace at 550 °C.

### **3.2.10 Total Solids (TS) and Total Volatile Solids (TVS)**

Total solids (TS) and total volatile solids (TVS) were determined according to standard methods (APHA, 1992). According to this method a well mixed sample is evaporated in a weighed dish by drying to a constant weight in an oven at 103 to 105 °C. To obtain the TVS the sample is ignited to a constant weight at 500  $\pm$  50

°C. The increase in weight over that of the empty dish represents the TS, while, the weight lost per unit volume of sample on ignition is calculated as the TVS. The sample volume for TS is chosen so that it normally yields a residue of 10 to 200 mg. During this research, the TS and TVS were calculated only for the effluent of the anaerobic digester. Clean 90 mm  $\Phi$  porcelain evaporating dishes were first ignited at  $500 \pm 50$  °C for about 1 h in a furnace and stored and cooled in a desiccator until needed. A well mixed 50 mL sample then was poured into a pre-weighed dish. The sample was evaporated in an oven at 103 to 105 °C. The dish then was cooled in a desiccator to a constant temperature, and weighed in a very sensitive analytical balance (capable of weighing to 0.1 mg) to get the mass of the residue for TS. This residue was ignited to a constant weight at  $500 \pm 50$  °C in a furnace for 1 h or more according to the mass of residue present in the dish. After ignition, the dish was taken out and allowed to cool partially in air and then it was transferred to a desiccator. As soon as the dish reached a constant temperature it was weighed. The weight lost per unit volume of sample on ignition was calculated as the TVS.

### 3.2.11 Sludge Volume Index (SVI)

A sludge volume index (SVI) is the volume in mL occupied by 1 g of a mixed liquor after 30 min settling. SVI typically is used to monitor settling characteristics of activated sludge and other biological suspensions in a sewage system (Dick and Vesilind, 1969). During this study, the daily SVI was measured to monitor the settling characteristics of the sludge in the SBR. One litre of a well mixed sludge was taken in a 1-L graduated cylinder from the SBR during the aerobic phase (normally close to the end of the phase) and it was then allowed to settle for 30 min. In the meantime, a sample was taken for TSS from the SBR. The 30 min settled sludge volume was noted and the SVI was calculated according to the formula;

$$SVI(mL / g) = \frac{\text{settled sludge volume (mL / L)} \times 1000}{TSS(mg / L)} \quad (3.2)$$

## 4 MATERIAL AND METHODS FOR ADSORPTION TESTS

### 4.1 Adsorbents

#### 4.1.1 Physical Chemical Properties

Iron sand used in this study was supplied by Industrial Sands Ltd. Auckland New Zealand, a private supplier of high quality processed sands. Some of the physical-chemical properties of the sand were available from the supplier and some were analysed in the lab are shown in Table 4-1.

**Table 4-1: Common physical and chemical properties of NZIS**

Analysis/ properties		Units	Available from Supplier	Test results from lab
Silica		%	3.1	
Aluminium Oxide		%	3.9	
Ferric oxide		%	79.5	
Calcium oxide		%	1.1	
Magnesium Oxide		%	3.3	
Moisture		%	0.15	0.10
Loss on Ignition		%	6.3	
Tapped bulk density		g/mL	2.81	2.82
Particle density		g/mL	4.54	4.84
Porosity		%	38.0	41.5
Quantitative analysis of element	O	%		26.23
	Mg	%		1.36
	Al	%		3.27
	Si	%		4.98
	Ti	%		4.43
	Mn	%		-
	Fe	%		59.73
	Total	%		100.00

Iron sand was washed with deionised water to remove dust adhering to the surface of the particles and dried at 105°C for at least 24 hrs prior to adsorption experiments.

### 4.1.2 Sieve Analysis

The sieves analysis was done in the Geo-mechanics Laboratory of the University of Canterbury in accordance with Standard Methods. Five standard sieves were selected with opening dimensions of 600, 300, 150, 75 and 0  $\mu\text{m}$ . A mechanical shaker was used to perform the sieving action. The sieve analysis results (Figure 4-1) show that about 80 % of the sand particles had a size of 75 to 150  $\mu\text{m}$ , while the remaining 20 % were of a 150 to 300  $\mu\text{m}$  size.

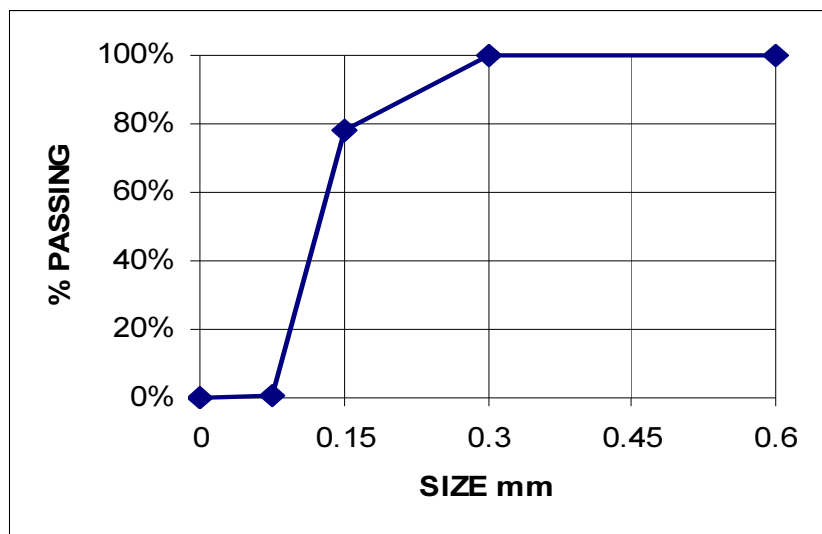


**Figure 4-1.** Sieve analysis result of New Zealand Iron Sand (NZIS).

## 4.2 Analytical Methods

All the reagents used were of analytical grade. Stock arsenic solutions (1000 mg/L) were prepared by dissolving arsenic tri-oxide and sodium arsenate heptahydrate (Section 3.1.3.3). The total arsenic concentration was analyzed by the SDDC photo-spectrometry method (Section 3.2.1). The absorbent solution of SDDC was prepared in Pyridine and a new calibration curve was made for every new stock of reagents. The solution pH was monitored by a Hach pH meter (Model # SensION3) and adjusted by addition of dilute HCl and NaOH solutions.



## 4.3 Adsorption Experiments

### 4.3.1 Batch Experiments

The batch experiments in this study were carried out by reacting 500 mL of arsenic solution in a 500 mL Erlenmeyer flask (Pyrex) with 10 g of iron-sand (20 g/L concentration). Since ionic strength effects have been reported in a study of ion adsorption at mineral water interfaces (Lutzenkirchen, 1997; Xu, 2009), NaCl was added to all arsenic solutions in this research to maintain a relatively constant ionic strength of 0.01 M NaCl as the background electrolyte. The experiments were conducted at room temperature ( $20 \pm 2^\circ\text{C}$ ) and each flask was stirred continuously in a magnetic stirrer. The speed of the stirrer was set so that the sand particles were well dispersed into the solution.

**Table 4-2:** Batch tests with different concentration of arsenic

Batch	Arsenic Added ( $\mu\text{g/L}$ )	Arsenic Type	Batch	Arsenic Added ( $\mu\text{g/L}$ )	Arsenic Type
B1-1	200	As(III)	R7-1	200	As(V)
B1-2	600	As(III)	R7-2	600	As(V)
B1-3	1000	As(III)	R7-3	1000	As(V)
B1-4	1500	As(III)	R7-4	1500	As(V)
B1-5	2000	As(III)	R8-1	2000	As(V)
B1-6	4000	As(III)	R8-2	4000	As(V)
B1-7	12000	As(III)	R8-3	12000	As(V)
B1-8	20000	As(III)	R8-4	20000	As(V)
Adsorbent (iron sand) = 20 g/L Reaction time = 72 h, pH = 7.5			Back ground ionic strength = 0.01 M NaCl		

To study the effect of pH (3 - 11) on arsenic removal, experiments were performed with initial arsenic concentrations of 4,000  $\mu\text{g/L}$  and an adsorbent dose of 20 g/L at a fixed contact time of 144 h. During these experiments, the effect of contact time was also studied by analysing the percent arsenic removed during the contact time of 3 to 144 h. Adsorption isotherm studies were conducted by varying the concentration of arsenic (200 to 20,000  $\mu\text{g/L}$ ), in a contact time of 72 h at a pH of 7.5 (Table 4-2). After a predetermined contact time of 72 h, the aqueous samples in each bottle were decanted and filtered through a 0.45  $\mu\text{m}$  microspore filter. The supernatant was analyzed for total arsenic.

### 4.3.2 Column Experiments

Iron sand for the column experiment was used after the preparation described for the batch tests (Section 4.3.1). The experiments were carried out using plastic volumetric flasks (500 mL) representing a column of 30 mm inner diameter and 150 mm height, with an empty bed volume of 600 mL with NZIS packed until the 450 mL level at a porosity of approximately 0.4. The water flowing through the column contained 400  $\mu\text{g/L}$  of As, in a 0.01 M NaCl solution. The water was pumped from a 5L container using a peristaltic pump (Masterflex model # 751800, Cole Parmer Instrument Co. USA) and supplied through the top of the column. The flow rate was kept at 1.0 mL/min, which yielded a contact time of approximately 180 min. The schematic diagram of the experimental column set of experiments is shown in Figure 4-2.

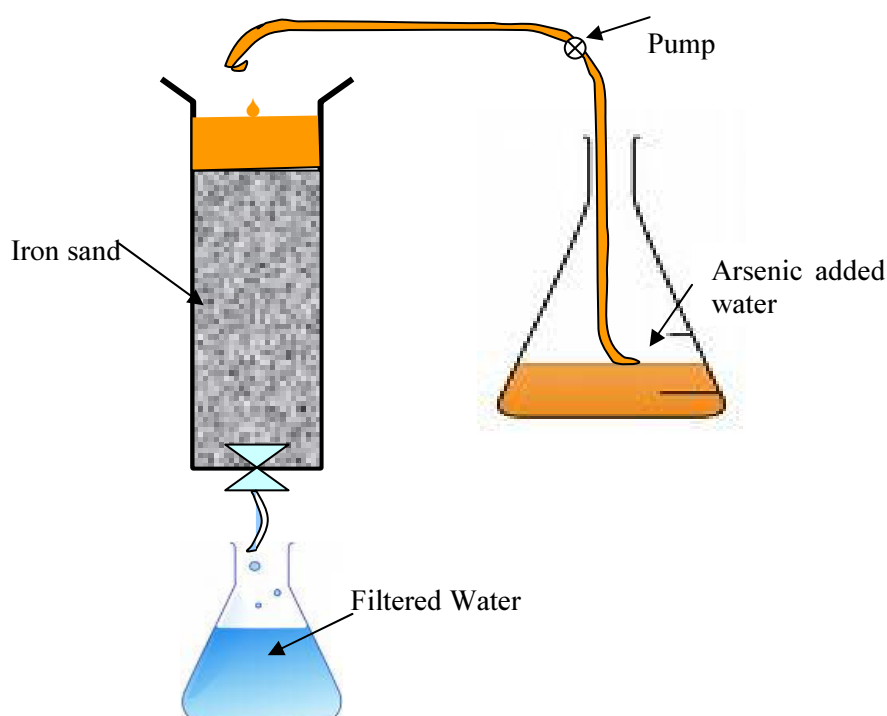


**Figure 4-2.** Schematic diagram of column experiments

Two parallel experiments were conducted, one for As (III) and another for As (V). The effluent was sampled at regular time intervals and was analyzed for residual total arsenic. The experiment was continued until breakthrough which occurred in about six months.

## 5 DENITRIFICATION STUDIES, RESULTS AND DISCUSSIONS

### 5.1 Start-up and Preliminary Operation

#### 5.1.1 SBR

##### 5.1.1.1 Dissolved Oxygen (DO) in SBR

A typical DO profile in an SBR-cycle is shown in Figure 5-1. The profile contains features that correspond to the change in the concentration of DO during one full cycle of the SBR. These features are of interest as they indicate when certain events have occurred and can provide insight into the treatment process. In the figure, the peak point “P” shows the DO level corresponding to the starting point of the cycle, which is just before the fill period.

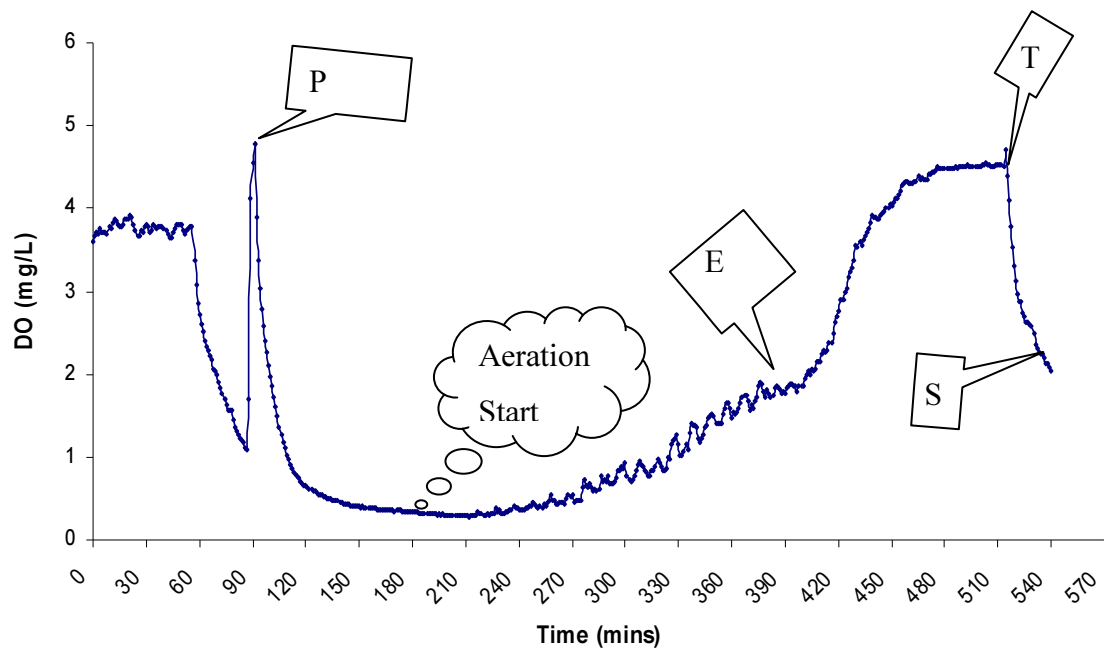


**Figure 5-1.** Typical DO profile in the SBR system

During filling, the air supply was cut off and the DO level fell rapidly to 1.0 mg/L or lower, thus an anoxic period was thought to start with the filling phase and continue for 1 h 30 min. Aeration would then be started by turning the air supply

valve on. However, as the Figure shows, the DO level started to rise only after approximately 90 min of aeration, hence, the anoxic period was not limited to the period when there was no air supply. In other words, Figure 5-1 indicates that the DO level dropped to less than 0.5 mg/L between the period 120 min to 240 min which should be considered as a major portion of the anoxic period. Eventually, the DO level rose to 4.0 mg/L by the end of the aerobic period. The speed with which the DO increased during the aerobic period was quite slow and during more than half of the period, its level remained below 2.0 mg/L.

Point “E” shown in the profile is thought to correlate to the point when  $\text{NH}_4^+\text{-N}$  is all converted to  $\text{NO}_3^-\text{-N}$ , a feature commonly known the “ammonia elbow”(Ra, et al., 2000; Holman and Wareham, 2003). DO breakthrough typically occurred at this ammonia elbow because oxygen was no longer required to act as an electron acceptor for oxidation of  $\text{NH}_4^+\text{-N}$ . This means that additional oxygen was available to accumulate, increasing the DO concentration to a peak value of usually around 4 mg/L. When aeration was terminated (at point “T”), the DO concentration fell rapidly because biological activity consumed the residual DO. The profile shows that the free available DO was fully depleted within 30 min from point “T”. After settling for 30 min, the DO probe was exposed to air (from point “S” to “P”) during the decanting phase and this accounts for the rapid rise in DO level.

#### **5.1.1.2 MLSS and SVI in SBR**

As mentioned, the concentration of the biomass expressed as MLSS and the settleability expressed as SVI were measured every day during the operating period of about 600 days. The profiles are shown in Figure 5-2 (a) and (b) respectively.

The MLSS profile indicates that during the majority of the operating period, the concentration of the MLSS varied between 2,000 to 5,000 mg/L. The first period of approximately four months was considered a start-up period of the SBR since the developed MLSS concentration was deemed to be not stable enough to use for further purposes. The MLSS concentration during the first month of the operation was at the lower end of the spectrum (about 2,000 mg/L) likely because the SBR was a new environment for the biomass. After a period of one month, the biomass

was thought to be acclimatized to the operating sequence and the MLSS concentration increased to a higher level (mostly > 3,000 mg/L). During the entire period of operation, the mean MLSS concentration was measured to be  $3,007 \pm 724$  mg/L. To maintain a targeted MLSS concentration of approximately 3,000 mg/L, about 1 L/day of sludge was wasted yielding an SRT of  $20.7 \pm 4.4$  d.

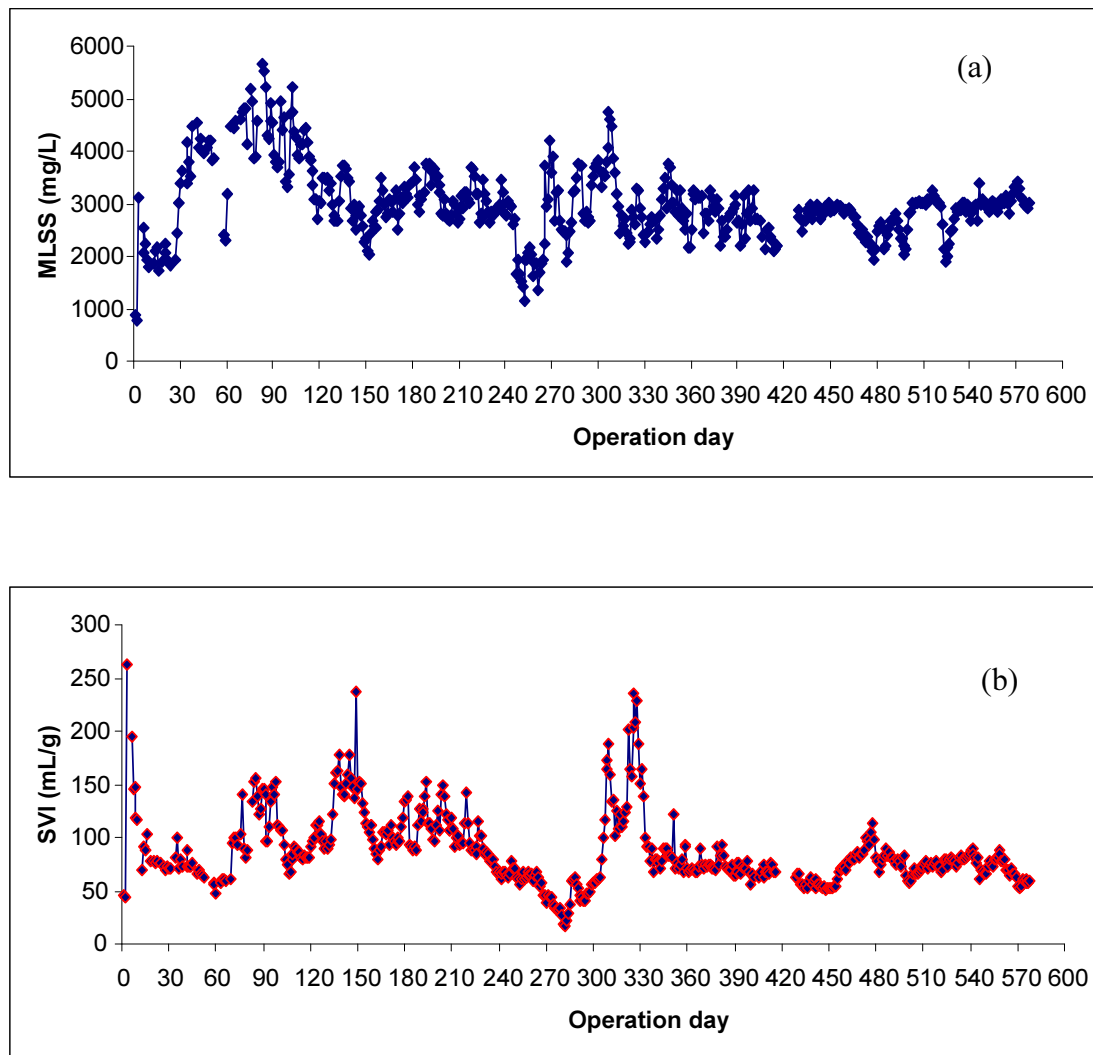


**Figure 5-2.** MLSS (a) and SVI (b) profile in the SBR

The MLSS was relatively stable after the 4 month period which suggests a healthy population of bacteria was established and maintained in the SBR. Wastage from the SBR was collected to use in the third system of the research i.e. the denitrification batch tests. During the operating period foaming was a major problem that affected the MLSS concentration although there were some other

operational problems such as power failures and irregularity in feed supply. These resulted in relatively high fluctuation in the MLSS, particularly between operating days 250 to 300. To minimise the impact of this on research, biomass wasted during that period was discarded.

The profile of the SVI shows excellent settleability throughout the period of the system operation. The SVI was measured between 50-120 mL/g resulting in a very low effluent solids concentration (in many cases less than 20 mg/L). The average value of SVI was calculated to be  $87 \pm 33$  mL/g. The large standard deviation was attributed to the operational problems described in previous paragraph; however, over the 600 days of the operating period, this impact was thought to be minimal.

#### **5.1.1.3 Track Studies**

Three key parameters, COD,  $\text{NO}_3^-$ -N, and  $\text{NH}_4^+$ -N were tracked over a complete operating-cycle of the SBR and five track studies were conducted to observe the change in these parameters. Figure 5-3 shows a representative plot of the average of five such tracks depicting the mean values for COD,  $\text{NO}_3^-$ -N and  $\text{NH}_4^+$ -N. The concentration of the  $\text{NH}_4^+$  - N in the feed solution ( $32.5 \pm 3.5$  mg/L) was diluted (1:1 ratio) by the bulk liquid concentrations carried over from the previous cycle ( $\text{NH}_4^+$  - N < 5.4 mg/L) yielding initial concentrations between 14.1 and 19.7 mg/L at the beginning of each track study. During the anoxic period (90 min) there was no change in the concentration of  $\text{NH}_4^+$  - N confirming no nitrification during the anoxic phase of each run; while nitrification occurred only during the aerobic phase of 5 h 30 min. During this latter phase,  $\text{NH}_4^+$  - N was reduced from a mean value of 16.38 to 2.30 mg/L with more than 85 % nitrogen changing from  $\text{NH}_4^+$  - N to  $\text{NO}_3^-$  - N (i.e. > 85 % nitrification). Over time, nitrification increased the concentration of  $\text{NO}_3^-$  - N to 14.4 to 18.2 mg/L in the bulk liquid which was subsequently diluted (1:1 ratio) to a relatively lower concentration from the feed solution during the feed phase. The denitrification process starting at the anoxic phase was so rapid, that the initial concentration of the  $\text{NO}_3^-$  - N was measured in the range of 5.6 to 7.2 mg/L only. This was reduced to gaseous nitrogen over the anoxic phase of 90 min.

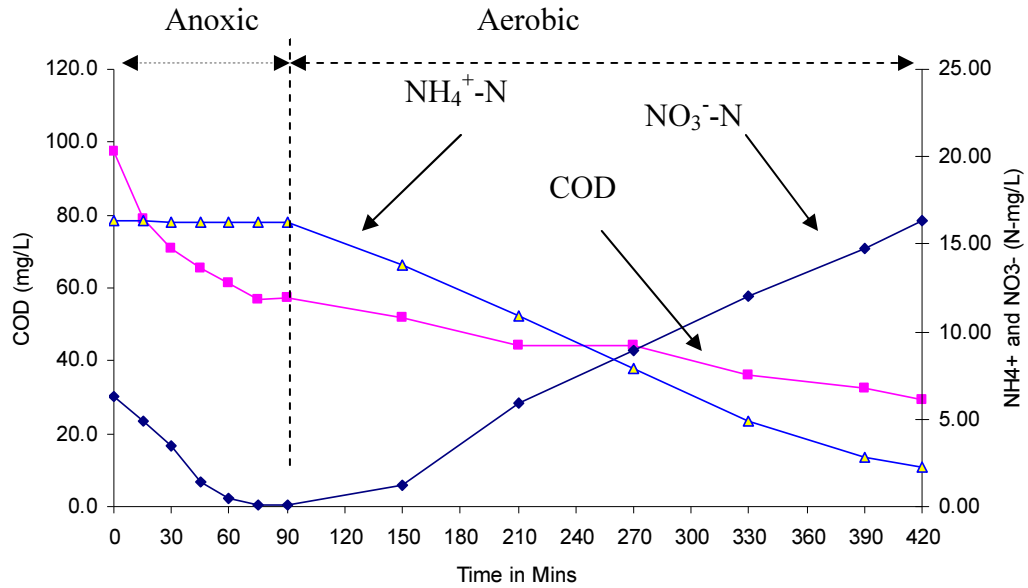


**Figure 5-3.** Typical track study of COD, NO<sub>3</sub><sup>-</sup>-N, and NH<sub>4</sub><sup>+</sup>-N in the SBR

Figure 5-3 also indicates COD consumption during the anoxic phase, as the carbon is used to support denitrification. The initial concentration of sCOD measured 75 to 150 mg/L and was obtained by mixing the feeding solution ( $285 \pm 45$  mg/L) and the residual bulk liquid concentration of 25 to 35 mg/L, carried over from the previous cycle. During the anoxic period, the COD dropped to a concentration range of 47 to 66 mg/L. Additional COD was utilized by facultative heterotrophs during the aerobic period eventually reaching a relatively low value of 25 to 35 mg/L. The complete track study data are shown in Appendix B1.

The MLVSS concentration in the SBR was measured for each track study and an average specific denitrification rate of 0.11 g NO<sub>3</sub><sup>-</sup>-N/gVSS per day was calculated. The rate is comparable to other research treating domestic wastewaters; (Munch, et al., 1996; Farabegoli, et al., 2004) and, clearly indicates that a healthy denitrifying biomass was developed in the SBR. The C/N ratio in the SBR was calculated to be 4:1; which was sufficient to ensure both complete removal of NO<sub>3</sub><sup>-</sup>-N, in addition to the majority of carbon found in the influent.

## 5.1.2 Anaerobic Digester

### 5.1.2.1 General Characterisation of Feed Solution and Effluent

The main objective of the anaerobic digester operating in this research was to produce a stable level of VFAs using soy flour as a synthetic feed. As mentioned earlier, the concentration of the soy flour used in the feed solution was 40 g/L. Table 5-1 shows the basic characteristics of the influent and effluent of the anaerobic digester. With respect to solubilisation of organic matter, the table indicates that the effluent from the digester experienced an 11.1 percentage points increase in the soluble fraction of the total COD (from 16.8 % in the influent to 27.9 % in the effluent). This was thought to be converted to predominantly VFAs, since the influent VFA concentration was effectively very low ( $300 \pm 85$  mg/L as HAc).

**Table 5-1:** Major parameters in the influent and effluent of the anaerobic digester

Parameters	Unit	Mean value	
		Influent	Effluent
COD <sub>Total</sub>	mg/L	56,200 $\pm$ 2500	53,000 $\pm$ 3000
sCOD	mg/L	9,450 $\pm$ 150	14,800 $\pm$ 450
COD soluble fraction	%	16.8	27.9
TOC	mg/L	2010 $\pm$ 277	3,600 $\pm$ 720
Total Nitrogen	mg/L	n/m	440 $\pm$ 85 *
pH		5.9 to 6.2	4.7 to 4.9
TS	mg/L	34,565 $\pm$ 1217	25,903 $\pm$ 1533
TVS	mg/L	32,569 $\pm$ 1056	24,824 $\pm$ 922
MLSS	mg/L	26,610 $\pm$ 1365	23,074 $\pm$ 1,040
MLVSS	mg/L	25,030 $\pm$ 1142	20,598 $\pm$ 778
Total VFAs (as HAc)	mg/L as HAc	300 $\pm$ 85	5,997 $\pm$ 538
Alkalinity (as CaCO <sub>3</sub> )	mg/L	n/m	1,100 $\pm$ 150
Temperature	°C	20 $\pm$ 2	31 $\pm$ 4

\* Total Nitrogen break-down

$NO_3^- - N$	4.6 $\pm$ 0.8 mg/L
$NO_2^- - N$	9.0 $\pm$ 2.5 mg/L
$NH_4^+ - N$	340 $\pm$ 76 mg/L
Organic Nitrogen	81.4 mg/L (by calculation)
Total Nitrogen	440 $\pm$ 85 mg/L

n/m – not measured



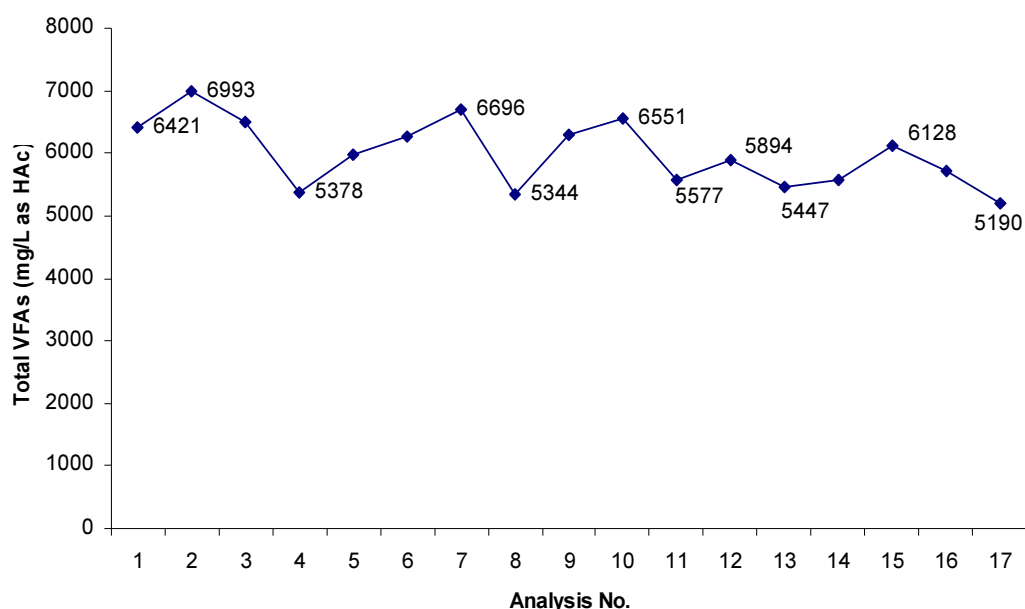
It was noted however that the total COD reduced between the influent and effluent; thus, some carbon was lost as gas. More details on the solubilisation, VFA generation and speciation and gas production are discussed in Sections 5.1.2.2 to 5.1.2.5.

The effluent pH of the anaerobic digester was measured almost every day and was noted to be between 4.7 and 4.9. Although, it has been reported that the optimum pH for hydrolysis and acidogenesis is between pH 5.5 and 6.5 (Penaud, et al., 1997; Kim, et al., 2003) hydrolytic and acidogenic bacteria can survive with a well maintained population (producing reasonably high concentration of VFAs) at a very low pH such as 4.8 (Liu, et al., 2006). Hence, no special treatment was applied to raise the pH to the reported optimal level. On the other hand, hydrogen-utilizing methanogenic bacteria are quite sensitive to pH and generally prefer a relatively narrow range over which growth will occur. For example, one species of methanogenic bacteria grow in a range from about pH 6.5 to 7.7 (Smith and Hungate, 1958). Other research on a mixed population of methanogenic bacteria (VandenBerg, et al., 1974) found that methanogenesis was optimum at pH around 7 and totally inhibited at a pH of 6.2 and lower. Normally the growth rate of methanogens is greatly reduced below pH 6.6 and lower than 5.0 it is suppressed completely (Mosey and Fernandes, 1989). Consequently, the pH inside the anaerobic digestion system (4.7 to 4.9) was considered to suppress methanogenic bacteria and enrich acidogenic bacteria.

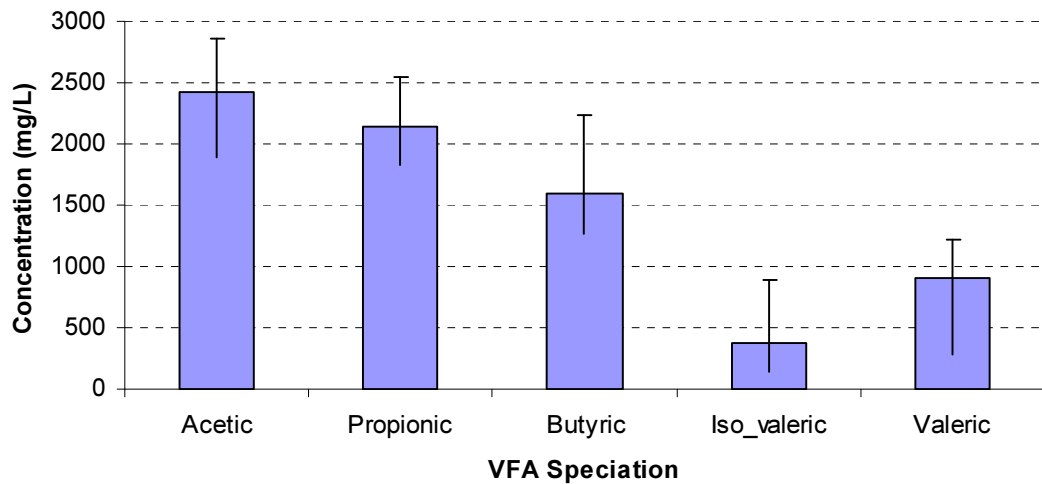
A significant amount of nitrogen in the effluent was in the form of  $\text{NH}_3/\text{NH}_4^+ - \text{N}$ ; however these compounds had little effect on the subsequent denitrification reactors because there was a comparatively low level of  $\text{NO}_3^- - \text{N}$  and  $\text{NO}_2^- - \text{N}$  in the effluent and no conversion of  $\text{NH}_4^+$  to these forms of nitrogen is possible in the denitrification reactors due to the anoxic conditions. The temperature of the digester was not controlled during the operating period but was recorded at  $31 \pm 4^\circ\text{C}$ , which is in the same range of most digesters treating municipal domestic waste, since they usually operate at  $(35\text{--}37^\circ\text{C})$  (Forster-Carneiro, 2008).

### 5.1.2.2 VFAs Production and Speciation

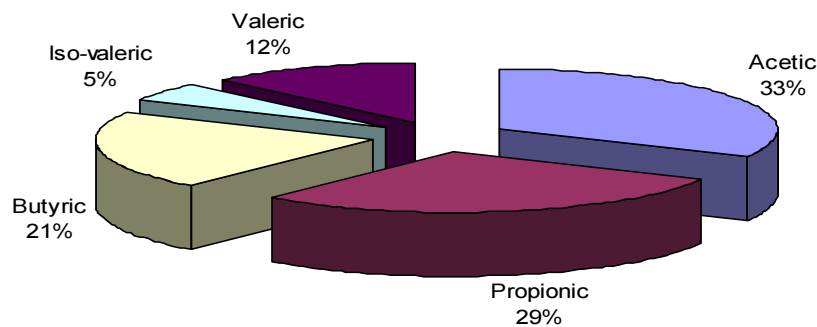
The total concentration of VFAs (expressed as HAc) as well as the speciation of acids expressed as a concentration and percent distribution in the digester are presented in Figure 5-4 (a), (b) and (c). As shown in Figure 5-4 (a), the total VFA level in the digester fluctuated more at the beginning of the research, becoming relatively stable later on, leading to a mean total value of  $5,997 \pm 538$  mg/L (expressed as HAc). Figure 5-4 (b) also indicates, acetic (HAc), propionic (HPr), n-butyric (n-HBu), iso-valeric (iso-HVa) and n-valeric (n-HVa) acids were all identified in the anaerobic digester effluent measured to have mean individual concentrations to be  $2,425 \pm 292$  mg/L HAc,  $2,140 \pm 201$  mg/L HPr,  $1,591 \pm 281$  mg/L HBu,  $369 \pm 243$  mg/L iso-HVa and  $911 \pm 223$  mg/L n-HVa respectively. The relative percentage of the individual acids are shown in Figure 5-4 (c) with 33 % HAc, 29 % HPr, 21 % HBu, 5 % iso-HVa and 12 % n-HVa. It was noted that the order of the three highest levels of concentration of the VFA species generated was the same as the preferential order of utilization for particular VFAs for denitrification (Elefsiniotis, et al., 2004). These were also the same carbon source eventually to be used in the subsequent denitrification batch tests.



(a)



(b)



(c)

**Figure 5-4.** Profiles of VFAs (a) total expressed as HAc, (b) speciation expressed in concentration and (c) speciation expressed in percentage.

Comparative data for the proportion of VFAs is given in Table 5-2. The proportions of VFA species produced were within the range of those found by other researchers (Pitman, et al., 1992; Raynal, et al., 1998; Lee, 2008) who observed levels between 28-48 % acetic, 20-36 % propionic, 16-29 % butyric and 10-18 % valeric acid respectively. A few other researchers (Table 5-2) found comparatively higher level of acetic acids (48-70 %) probably because of different feed sources or operational conditions such as pH, temperature, SRT, HRT and reactor configuration. In one

study (Elefsiniotis and Oldham, 1994a), it was reported that the major constituents of a substrate (carbohydrate, proteins and lipids) utilization pattern was significantly affected by variation in HRT and pH. While, Elefsiniotis and Oldham (1994b) observed a slight increase in VFAs production with a variation in SRT from 10 to 20 d at a constant HRT of 12 h. On the other hand, Elefsiniotis and Oldham (1994c) has indicated that VFAs production is not affected by changing the pH from 4.3 to 5.2, but the production is significantly lower (25–30%) at higher pH values of about 6.0.

**Table 5-2:** Typical VFAs composition distributions for fermentation effluents

<b>Acetic acid (%)</b>	<b>Propionic acid (%)</b>	<b>Butyric acid (%)</b>	<b>Valeric acid (%)</b>	<b>Reference</b>
56	30	7	-	(Rabinowitz, et al., 1997)
70	25	5	-	(Carlsson, et al., 1996)
38	36	16	10	(Pitman, et al., 1992)
48	30	10	-	(Elefsiniotis and Oldham, 1994b)
33	20	29	18	(Raynal, et al., 1998)
52	6	38	4	(Zhu, et al., 2008)
51	28	20	1	(He, 2006)
28	26	26	20	(SJ Lee, 2008)
33	29	21	17	This study

### 5.1.2.3 Particulate Organic Carbon Solubilization

The VSS/VS ratio in the feed soy solution was measured to be 0.768 (Table 5-1), indicating more than 75 % of the substrate was in the particulate form. Since particulate organic matter first needs to be hydrolyzed before being taken up by microorganisms, solubilization is a major step in acidogenic digestion and the sCOD is the parameter representing the extent of hydrolysis and solubilization. The degree of COD solubilisation can be calculated by calculating the change in percent sCOD between influent and effluent of the reactor; however, the rate of solubilization is expressed as a specific COD solubilization rate (i.e. the net amount of sCOD generated per day per unit mass of VSS in the digester (mg sCOD/mg VSS per day)). Table 5-3 shows the net solubilization and the specific COD solubilization rate for this study. In the effluent 27.9 % COD was soluble (sCOD =

14,800 mg/L), compared to 16.8 % (sCOD = 9,450 mg/L) in the influent of the digester. Thus, this increase of 11.1 percentage points of COD solubilisation in the anaerobic digestion system yielded a specific COD solubilization rate of 0.025 mg sCOD/mg VSS per day.

**Table 5-3:** Anaerobic digester particulate organic carbon solubilisation

Parameter		Unit	Mean Value
HRT		day	10
COD <sub>Total</sub>	Influent	mg/L	56,200 ± 2,500
	Effluent	mg/L	53,000 ± 3,000
sCOD	Influent	mg/L	9,450 ± 150
	Effluent	mg/L	14,800 ± 450
% of sCOD	Influent	%	16.8 ± 0.5
	Effluent	%	27.9 ± 0.8
TOC	Influent	mg/L	2,010 ± 277
	Effluent	mg/L	3,600 ± 720
TVSS	Influent	mg/L	25,030 ± 1533
	Effluent	mg/L	20,598 ± 778
TVS	Influent	mg/L	32,569 ± 1056
	Effluent	mg/L	24,824 ± 922
Net COD solubilisation		%	11.1 ± 0.3
Net sCOD		mg/L	5,350 ± 300
Specific COD Solubilization rate		mg sCOD/ mg VSS per day	0.025 ± 0.003
Net filtered TOC		mg/L	1,590 ± 443
Specific TOC Solubilization rate		mg TOC/mg VSS per day	0.008 ± 0.002
VSS reduction		%	17.7 ± 1.8
VS reduction		%	23.8 ± 2.3

As shown in Table 5-3, other parameters such as TOC and VSS destruction can also be used to indicate solubilization. For example, if a part of the substrate converts from particulate to soluble form, there should be an increase in the TOC concentration. Hence, the net increase in the TOC concentration (effluent TOC minus influent TOC) represents the degree of solubilization while the mg TOC/mg VSS per day represents the rate of solubilization. Note that the amount of gas

generated in the digester was minimal (from visual inspection), thus carbon loss through gas was not taken into account in the calculation of either the TOC or COD solubilization rate. A specific TOC solubilization rate of 0.008 mg TOC/mg VSS per day (net TOC filtered 1590 mg/L) was measured in the digester. These solubilization parameters are quite close to the values reported by other researchers (Maharaj and Elefsiniotis, 2001; He, 2006). In particular, He (2006) used the same feed soy solution under almost similar operational conditions and obtained a specific COD solubilization rate of 0.022 mg sCOD/mg VSS per day and an specific TOC solubilization rate of 0.007 mg TOC/mg VSS per day. Maharaj and Elefsiniotis (2001) on the other hand used a primary sludge as feed and obtained specific COD solubilization rate of 0.0154 to 0.0789 mg sCOD/mg VSS per day at different HRT conditions (30 to 60 h). A relatively higher specific COD solubilization rate of 0.124 mg sCOD/mg VSS per day (Elefsiniotis, et al., 2005) and specific TOC solubilization rate of 0.07 mg TOC/mg VSS per day (Elefsiniotis, et al., 2005) was reported using a mixture of starch-rich industrial wastewater with municipal wastewater and a primary sludge feed to an anaerobic digester.

Finally, the extent of organic carbon solubilization can be viewed from the perspective of the reduction in VSS, which provides additional evidence as to whether the particulate substrate in the feed is amenable to solubilization or not. Typically 40 to 65 % VSS reduction is expected (Vesilind, 2003). The percentages of VSS reduction were measured to be  $17.7 \pm 1.8$  % higher than the VSS reduction percentage of He (2006), which was reported to be 14 %. Other researchers (Elefsiniotis, et al., 1996; Maharaj and Elefsiniotis, 2001) have reported a very high range of VSS reduction (70 to 75 %).

An empirical equation from Metcalf and Eddy (1991),

$$V_d = 13.7 \times \ln(SRT) + 18.9 \quad (5.1)$$

where  $V_d$  is the volatile solids destruction (%) and SRT the time of digestion (d) allows an estimation of the amount of volatile solids destroyed. For this research, equation 5.1 estimates the volatile solids destruction should be around 50 % which is much higher than the 23.8 % destruction of volatile solids recorded in this

research. This was because the feed concentration chosen (TS = 34,565 mg/L or 3.42 %) matched the COD load to values typical of primary sludge (Table 5-1) but which is unfortunately well above the optimum range for solids loading to digesters of 0.5 to 2.0 % (Banister and Pretorius, 1998). In other words, the low percent VSS reduction is probably attributed to solids overloading of the digester. Nonetheless, the result indicates that the organic particulates in the soy solution were liquefied to soluble carbohydrates, lipids and proteins which would have been eventually converted into lower molecular weight organic compound such as VFAs and other metabolic intermediates.

#### 5.1.2.4 VFA Production Rate

The VFA concentration in the influent and effluent was measured to be  $300 \pm 85$  and  $5997 \pm 538$  mg/L as HAc respectively, indicating a net VFA of  $5,697 \pm 453$  mg/L as HAc was produced in the digester. The VFA production can also be expressed as a specific VFA production rate (i.e. the net amount of VFA produced per day per unit amount of VSS in the digester (mg VFA as HAc/mg VSS per day)). Table 5-4 shows the specific VFA production rate measured in this research and the rate of (0.028 mg VFA/mg VSS per day) is comparable to the values reported by other researchers (Elefsiniotis, et al., 2005; He, 2006; Lee, 2008). He (2006) obtained a comparatively lower specific VFA production rate of 0.014 mg VFA/mg VSS per day from a digester operated under similar operational conditions, while Elefsiniotis et al. (2005) reported a relatively higher specific VFA production rate of 0.07 mg VFA/mg VSS per day. Lee (2008) observed that the specific VFA production rate decreased linearly from 0.030 mg VFA/mg VSS per day at 5 d SRT to 0.013 mg VFA/mg VSS per day at 15 d SRT.

**Table 5-4:** Specific VFA production rate

HRT (day)	VSS (mg/L)	Net VFAs (mg/L as HAc)	Net VFAs (mg COD/L)	VFA-COD/ sCOD (%)	Specific VFA production rate (mg VFA as acetic acid/mg VSS per day)
10	20,598	5,697	11,328	76.5	0.028

In addition the total measured VFA (5,697 mg/L as HAc) can be expressed as sCOD (mg COD/L) as shown in Table 5-4. The fraction of sCOD in the form of VFAs was estimated by converting the VFA concentrations to COD equivalents using conversion factors: 1.067 for HAc, 1.514 for HPr, 1.818 for HBu, and 2.039 for iso-HVa and n- HVa. These conversion factors were worked out from the simple oxidation reactions of VFAs (Table 5-5). The VFAs converted to the equivalent COD (11,328 mg COD/L) accounted to 76.5 % of total sCOD (14,800 mg/L) measured in the digester. This value is with in the range of 70 % to 90 % suggested by Elefsiniotis et al. (2005).

**Table 5-5:** COD and VFA concentration conversion factors

VFAs	Oxidation reaction of VFAs	Conversion Factor (mg COD/mg VFA)
Acetic acid	$CH_3COOH + 2O_2 \rightarrow 2CO_2 + 2H_2O$	1.067
Propionic acid	$2CH_3CH_2COOH + 7O_2 \rightarrow 3CO_2 + 3H_2O$	1.514
Butyric acid	$CH_3CH_2CH_2COOH + 5O_2 \rightarrow 4CO_2 + 4H_2O$	1.818
Valeric acid	$2CH_3CH_2CH_2CH_2COOH + 13O_2 \rightarrow 5CO_2 + 5H_2O$	2.039

It is evident therefore that sCOD contributing compounds in the digester were not only the VFAs listed above but also some other unidentified substrates, mainly attributed to metabolic intermediates and unused soluble substrate (Elefsiniotis and Oldham, 1994b).

#### 5.1.2.5 Gas Production

In this study the digester gas was analyzed only once (by a Landfill Gas Analyser, Geotechnical Instruments, UK) and the gas composition was measured to be 16 % CH<sub>4</sub>, 82 % CO<sub>2</sub> and an extremely low level of H<sub>2</sub> and other gases (less than 2 %). These results are quite similar to those previously reported for acidogenic-phase digestion (Elefsiniotis and Oldham, 1994b; He, 2006; Lee, 2008). Ideally, the CH<sub>4</sub> content in the digester should be negligible; however, in practice, varying amounts (1-50 %) of CH<sub>4</sub> have been detected in acid-phase digesters (Chanakya, et al., 1992;

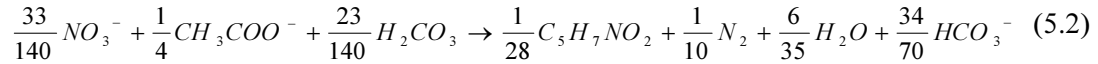


Cooney, et al., 2007). This may be due to either incomplete separation of the two phases which results in the coexistence of heterotrophic CH<sub>4</sub> producers and/or the presence of certain fast-growing autotrophic methanogenic microorganisms such as *Methanobacterium* (Novaes, 1986). As mentioned previously, the low pH value (4.7-5.0) encountered during this study generally resulted in little observable gas production, indicating successful suppression of methanogenesis. (Chanakya, et al., 1992; Cooney, et al., 2007)

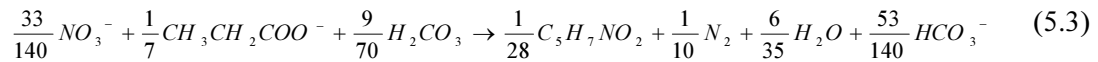
### 5.1.3 Selection of C/N Ratio for Denitrification Batch Tests

Since naturally produced VFAs were selected for use in the denitrification batch tests, acetic, propionic, butyric and valeric acids were the main carbon sources under consideration. Stoichiometric equations for a complete denitrification including cell synthesis using three different VFAs (i.e. acetic, propionic, and butyric acid) have been suggested by Elesfsiniotis et al. (2004) as

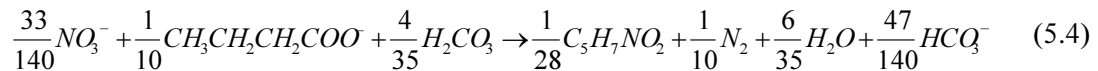
#### Acetic acid



#### Propionic acid

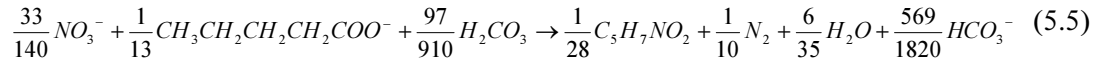


#### Butyric acid



In the similar way a balanced equation can be constructed for valeric acid as:

### Valeric acid



Based on Eq. (5.2), a reduction of 1 g  $NO_3^-$ -N theoretically consumes 4.55 g HAc, with a production of 0.29 g new cells. Hence the theoretical optimal C/N ratio for HAc is calculated to be 1.82, without any competition from other heterotrophs. In a similar way, Eq. (5.3 - 5.5) give the optimal theoretical C/N ratios for HPr, HBu and HVa as 1.56, 1.45 and 1.40 respectively. To work out the actual optimal C/N ratio, four batch tests (B1-B4) were carried out with initial VFA-C concentrations of 20, 40, 80 and 120 mg/L and  $NO_3^-$ -N of 25 mg/L (Table 5-6). In addition, one more test (B5) was done with no VFA addition.

Individual VFA-C concentrations in the digester effluent were calculated to be 970 mg HAc-C/L, 856 mg HPr-C/L, 636 mg HBu-C/L, 148 mg n-HVa- C/L and 364 mg iso-HVa-C/L giving a total sum of 2974 mg VFA-C/L. This VFA-C is about 83 % of the measured TOC (3600 mg/L), which was reasonably close to the percent sCOD corresponding to the VFAs (i.e. 76.5 %). From this it was deduced that approximately 20 % additional unknown soluble organic compounds in the digester were present. By considering the existence of these unknown compounds, an extra 20 % carbon was taken into account when calculating actual C/N ratios. In this way the combinations of anaerobic digester effluent and standard  $NO_3^-$  solution added, generated five different C/N ratios of 0, 0.96, 1.92, 3.84 and 5.76 respectively. After a denitrification reaction time of 3.5 h, the specific denitrification rates for these different C/N ratios were calculated and summarised in Table 5-6. The  $NO_3^-$ -N level was measured every 60 min during the denitrification process and the results are shown in Figure 5-5.

**Table 5-6:** Specific denitrification rate for different C/N ratios

Batch Test	NO <sub>3</sub> <sup>-</sup> -N added (mg/L)	VFAs-C added (mg/L)	C/N ratio (only VFA)	C/N ratio including 20 % additional C	Specific denitrification rate (g NO <sub>3</sub> <sup>-</sup> -N /g VSS per day)
B1	25	20	0.8	0.96	0.128
B2	25	40	1.6	1.92	0.179
B3	25	80	3.2	3.84	0.174
B4	25	120	4.8	5.76	0.071
B5	25	0	0	0	0.026

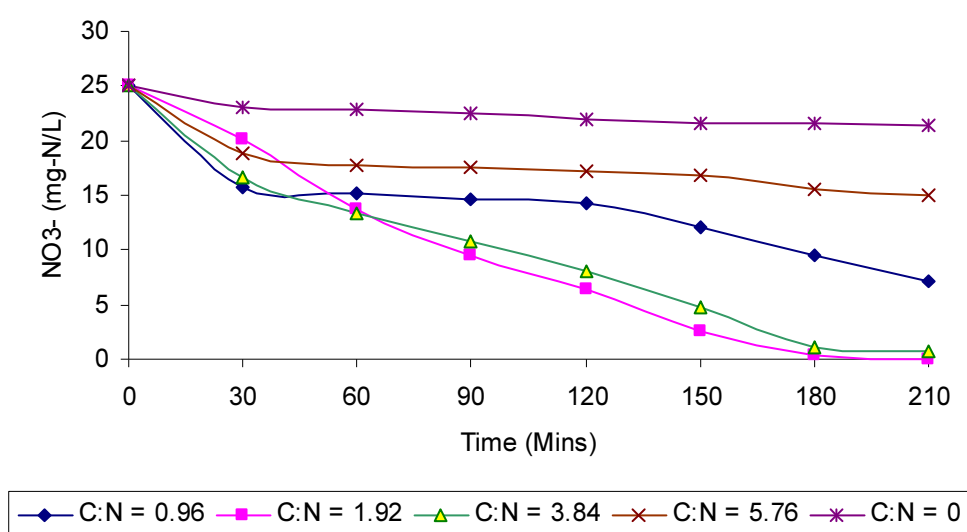


**Figure 5-5.** Track study of NO<sub>3</sub><sup>-</sup> - N during C/N optimisation test

From Figure 5-5, it can be deduced that the actual optimum C/N ratio lies between 2.0 and 4.0, somewhat higher than all the theoretical requirements using the four major VFAs. This range is very similar to the optimum C/N values reported by Her and Huang (1995) who suggested that a C/N ratio of approximately 2.0 is needed for complete denitrification, that is, if acetic acid or glucose are used as a C-source. In addition, they suggested that it should be a larger ratio for larger molecular weight carbon compounds.

In their preliminary experiments, the denitrification efficiency started to decrease with a C/N ratio of more than 4.0, particularly when benzoic acid was used. Carbon breakthrough occurred at a C/N ratio of approximately 15.0 and breakthrough also occurred at a similar C/N ratio when methanol was used as carbon source. On the

other hand, the denitrification process was found to perform well with a C/N ratio as high as 20, when glucose or acetic acid was used as the carbon source.

#### 5.1.4 Reaction of Nitrate with Arsenic

During this research, no reaction was observed between  $\text{NO}_3^-$ -N and As (V), but some  $\text{NO}_3^-$ -N was observed to be removed when reacting with As (III). This phenomena was reinforced by (Zingaro, 1994) who reported that one of the readily available forms of As (III) (arsenic trioxide ( $\text{As}_2\text{O}_3$ )) oxidizes to arsenic acid ( $\text{H}_2\text{AsO}_4^-$  (As (V))) in the presence of  $\text{NO}_3^-$ . The stoichiometric relationship is shown in equation 5.6.



In this study, the reaction was observed to be incomplete during a reaction time of 4 h and whatever amount of  $\text{As}_2\text{O}_3$  was going to be oxidized was oxidized instantaneously. It would be useful to fully evaluate the reaction rate and estimate the theoretical amount of  $\text{NO}_3^-$  - N consumed during the reaction, but that was decided to be outside the scope of this research. However, six reactions were performed with 10 mg As (III)/L at different  $\text{NO}_3^-$  - N concentrations (44.0, 41.8, 40.7, 39.6, 38.5 and 37.4 N- mg/L). On each occasion, the amount of  $\text{NO}_3^-$  -N consumed was observed and it was noted that the six  $\text{NO}_3^-$  - N concentrations immediately dropped to a lower value than that computed by straight addition. A graph was plotted (Figure 5-6) to get a factor (added / measured  $\text{NO}_3^-$  - N concentration) as a function of added  $\text{NO}_3^-$  - N concentration for that particular concentration (10 mg/L) of As (III). This graph was used in order to get an initial dose of  $\text{NO}_3^-$ -N to be added (as a function of the added As (V) concentration) so that the initial concentration fell as close as possible to the target value.

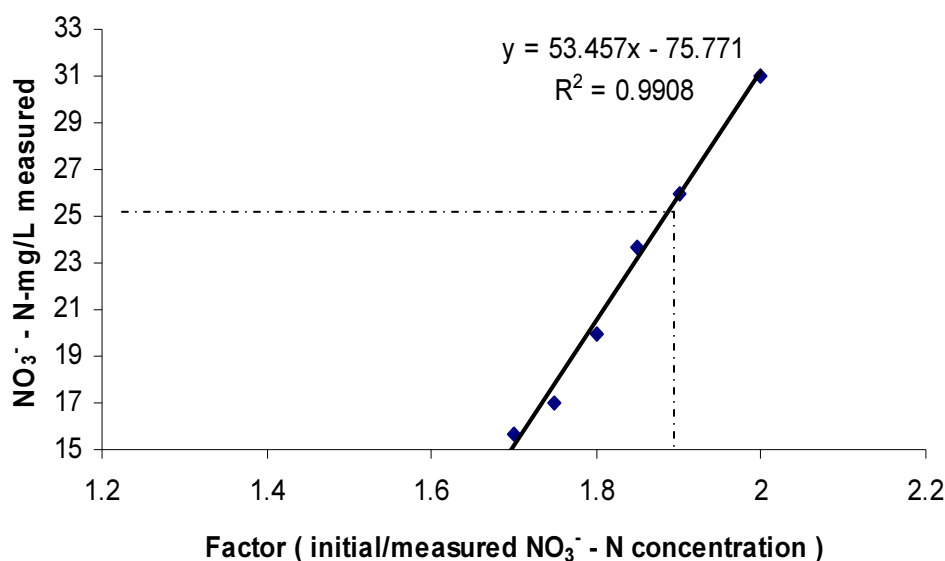


**Figure 5-6.** Nitrate consumption during the reaction with arsenite

For example, an initial target value of 25 mg/L of NO<sub>3</sub><sup>-</sup>-N was set and to get that initial value, roughly 47 (i.e.  $\sim 1.88 \times 25$ ) mg/L NO<sub>3</sub><sup>-</sup> - N needed to be added to account for the NO<sub>3</sub><sup>-</sup>-N that reacted with an arsenic concentration of 10 mg As (III)/L. In a similar way, during the study of the denitrification batch tests, other calculations were necessary to obtain the estimated initial concentration of NO<sub>3</sub><sup>-</sup> - N before reaction with different concentrations of As (III).

### 5.1.5 Alkalinity Production during Denitrification

As mentioned in Section 2.4.2, during the denitrification reaction some alkalinity is produced. Hence, for each carbon source there is a theoretical value of alkalinity supposed to be produced during denitrification. For example, the theoretical alkalinity production rate for ethanol is 3.57 mg alkalinity as CaCO<sub>3</sub> per mg NO<sub>3</sub><sup>-</sup>-N consumed (Table 2-3). In a similar way, values have been calculated for the four kinds of VFAs identified in the digester effluent (acetic, propionic, butyric and valeric acids) (Table 5-7). The concentrations of these four VFAs accounted for about 76.5 % of the total sCOD to be used in the denitrification tests and the rest (23.5 %) was assumed to be unidentified VFAs and/or other metabolic intermediates (Section 5.1.2.2). Assuming a theoretical alkalinity production rate of

3.6 mg alkalinity as  $\text{CaCO}_3$  per mg  $\text{NO}_3^-$ -N (close to the 3.57 value for ethanol), an average theoretical alkalinity production rate of 5.41 mg as  $\text{CaCO}_3$  per mg  $\text{NO}_3^-$  - N for the effluent of the digester was calculated (Table 5-7).

**Table 5-7:** Estimation of an average theoretical alkalinity production rate for the carbon used in the denitrification batch tests.

Substrate use	% In the digester effluent	Theoretical alkalinity production rate (mg alkalinity as $\text{CaCO}_3$ per mg $\text{NO}_3^-$ - N )
Acetic Acid	25.25	7.36
Propionic Acid	22.19	5.74
Butyric Acid	16.06	5.09
Valeric	13.00	4.74
Others (Unknown)	23.50	3.60 (assumed)
Average (Weighted)	100	5.41

Three separate denitrification batch tests, (0.6 mg/L of As (III), 0.6 mg/L of As (V), and 0.0 mg/L arsenic) were performed and the alkalinities before and after the reactions were calculated. The net gain in the alkalinity during the denitrification reaction was recognized as the practical alkalinity production rate; and, these values are shown in Table 5-8. Since the practical values are fairly comparable to the theoretical values, this provided additional evidence to support the process as being denitrification.

**Table 5-8:** Alkalinity production rate; a comparison between theoretical and practical values

Type of Arsenic and Concentration	Alkalinity produced (mg $\text{CaCO}_3$ per mg $\text{NO}_3^-$ - N )	
	Theoretical	Practical
No As	5.41	5.58
As (III) = 0.6 mg/L	5.41	5.60
As (V) = 0.6 mg/L	5.41	5.11

## **5.2 Effect of Arsenite (As (III)) on the Denitrification Rates**

### **5.2.1 Track Studies of Nitrate and COD**

As mentioned in Section 3.1.3.4 (Table 3-2), a total of 20 denitrification batch tests were carried out using As (III) over 5 different runs. That is, each run had four experimental reactors (using three different concentrations of As (III) and one reactor specified as a control reactor (i.e. no As)). A target  $\text{NO}_3^-$ -N concentration of 25 mg/L was set and the corresponding dose of standard  $\text{NO}_3^-$  solution was added to each of the control reactors in the five runs. Extra  $\text{NO}_3^-$ -N was added to all the experimental reactors to account for the  $\text{NO}_3^-$  that reacted with the As (III) added. The  $\text{NO}_3^-$ -N and COD in each reactor were measured every 30 min (starting from 0 min) during a reaction time of 4 h. The results are shown in Figure 5-7 to 5-11 (numerical data in Appendix B2).

In the controls, the  $\text{NO}_3^-$ -N concentration at  $t = 0$  min was measured to be between 20 and 24.6 mg/L (i.e. slightly less than the concentration added (25 mg/L)). This may have been due to the instantaneous start of the denitrification reaction causing some reduction of  $\text{NO}_3^-$ -N as the first sample was taken. For example, the control reactor for Run 1 had a measured concentration of 20 mg/L indicating that denitrification instantaneously removed 5 mg/L of  $\text{NO}_3^-$ -N. On the other hand, in the experimental reactors where As (III) was added, the  $\text{NO}_3^-$ -N concentration at  $t = 0$  min was found to deviate between 22.5 and 29.8 mg/L (i.e. more than the controls). The reason for such a wide deviation was assumed to be the estimation process for the amount of reacted  $\text{NO}_3^-$ -N with the initial As (III). In any case, since the main objective of the batch tests was to quantify the specific rates of denitrification, it was not of great concern that the initial concentration of the  $\text{NO}_3^-$ -N varied.

To observe reproducibility, at least three different tests were carried out for each concentration of As (III) (0, 5, 10, 18, 25 and 50 mg/L) and an average value was computed. The results obtained for each Run are shown and discussed separately as follows:

## Run 1

As shown in Figure 5-7 there were four tests in Run 1 (i.e. one control and three with As (III) concentrations of 5, 10, and 18 mg/L). When there was no As (III),  $\text{NO}_3^-$ -N was found to reduce from 20 to 0 mg/L in 60 min. At the 5 and 10 mg/L As (III) concentrations, the  $\text{NO}_3^-$ -N dropped from 29.5 to 0 mg/L and 29.0 to 0 mg/L in 180 and 240 min respectively.

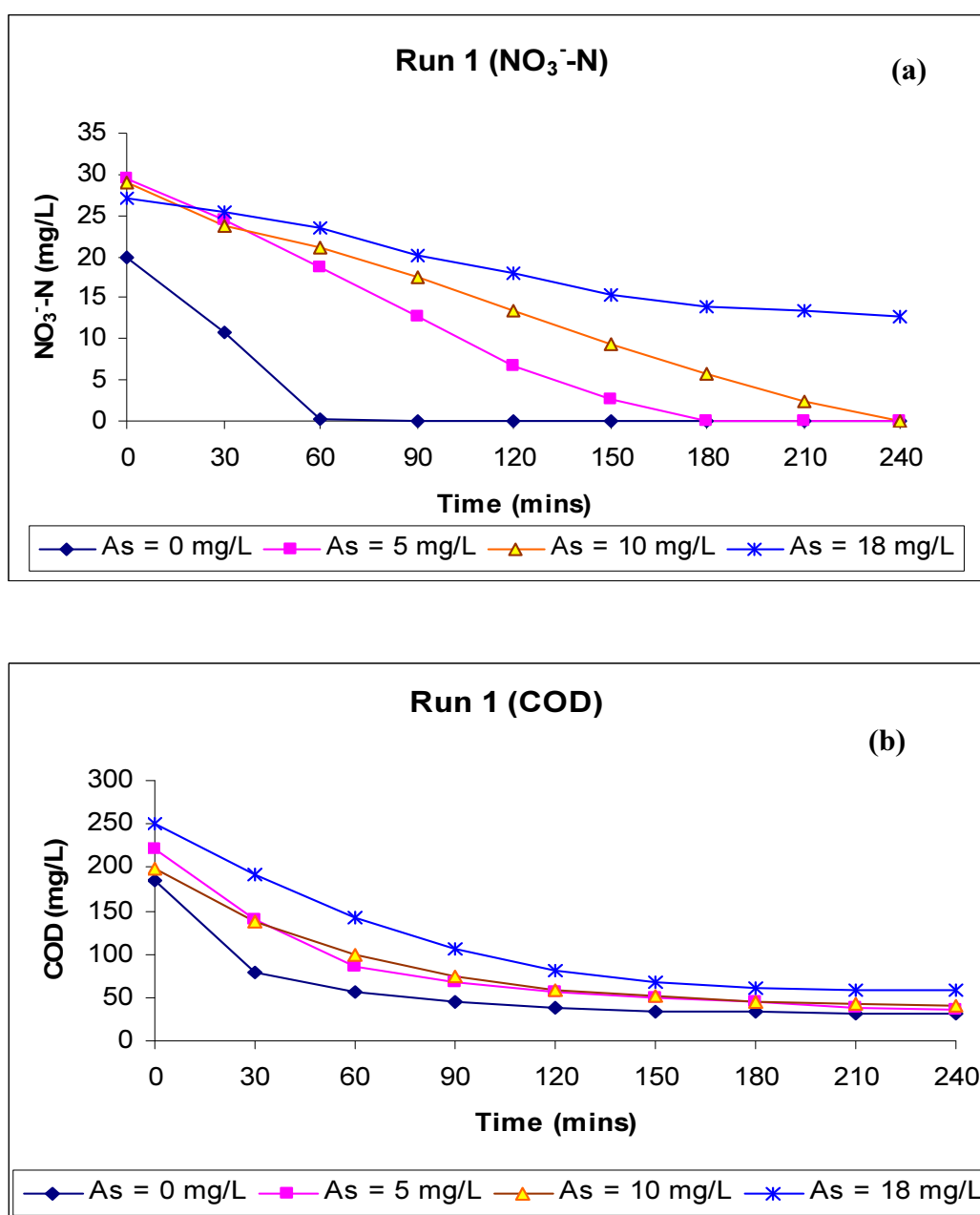


**Figure 5-7.** Track study of  $\text{NO}_3^-$ -N (a) and COD (b) in Run 1.



The results therefore clearly indicate that the biomass was able to completely denitrify the initial  $\text{NO}_3^-$ -N concentration; however, the As (III) made a distinct impact on the length of time it took the biomass to completely denitrify. This impact was further confirmed by the results from subsequent batch tests. That is, when the As (III) concentration was increased to 18 mg/L, in this instance the reactor failed to completely denitrify in the 4 hours allotted to the test and only 52.8 % denitrification was observed.

Additional evidence of denitrification was inferred by examining the COD removal pattern (Figure 5-7 (b)). It is reasonable to suppose that much of the carbon was being used to support denitrification, with the rate of consumption clearly slowing as the As (III) concentration increased. Note that the difference in the initial COD concentrations of 184 and 250 mg/L for the two cases of 0 and 18 mg/L of As (III) can be explained by a very fast denitrification of the control reactor removing about 5 mg/L  $\text{NO}_3^-$ -N and consuming about 66 mg/L COD at 0 min sampling. Since carbon removal occurred after all the  $\text{NO}_3^-$ -N were eliminated and the total amount of carbon removed was fairly similar in all 4 batch reactors, it is suspected that some carbon was also being removed by non-denitrifying heterotrophic activity.

## **Run 2**

For Run 2, four batch tests with As (III) concentrations of 0, 5, 18, and 25 mg/L were selected. The track study of  $\text{NO}_3^-$ -N is shown in Figure 5-8 (a) and, as shown, the  $\text{NO}_3^-$ -N in the control reactor dropped from 22.5 to 0 mg/L in 120 min which was twice as long as the 60 min required in Run 1. It is noted however that the initial  $\text{NO}_3^-$ -N concentration was slightly higher than the 20 mg/L in Run 1 in addition to the fact that the final  $\text{NO}_3^-$ -N concentration for Run 2 was very close to zero (i.e. 1.2 mg/L) at the 90 min mark. The graph pattern indicates that it likely experienced complete denitrification within 100 min; however, the sample was taken at 120 min only to find the  $\text{NO}_3^-$ -N level to be 0 mg/L. Because of this, to calculate the specific denitrification rate (Appendix B2) the last point of denitrification was considered to be at 90 min in spite of the 120 min for the final sample.

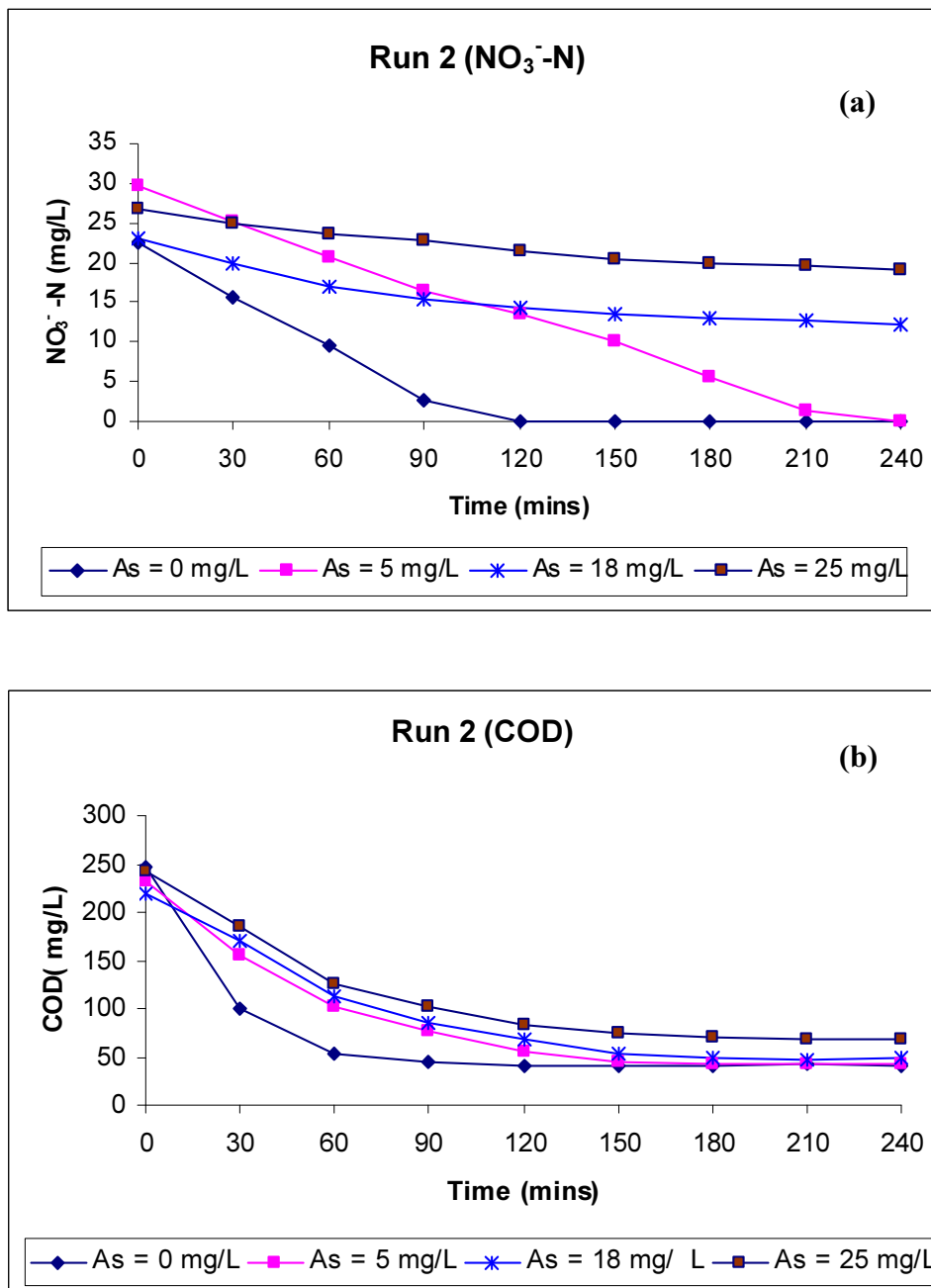


**Figure 5-8.** Track study of NO<sub>3</sub><sup>-</sup>-N (a) and COD (b) for Run 2.

When the As (III) concentration was 5 mg/L, the initial NO<sub>3</sub><sup>-</sup>-N concentration was 29.6 mg/L, which is almost identical to the 5 mg/L track associated with Run 1 (i.e. 29.5 mg/L). Comparing results, the initial NO<sub>3</sub><sup>-</sup>-N for 5 mg/L of As (III) completely denitrified in 180 min in Run 1 while in Run 2, the NO<sub>3</sub><sup>-</sup>-N was also completely denitrified, but there was a delay of 30 min. It can be concluded therefore that there was a distinct inhibition in denitrification for Run 2 compared to Run 1 and it could possibly be because of the deterioration in quality of biomass during storage. This

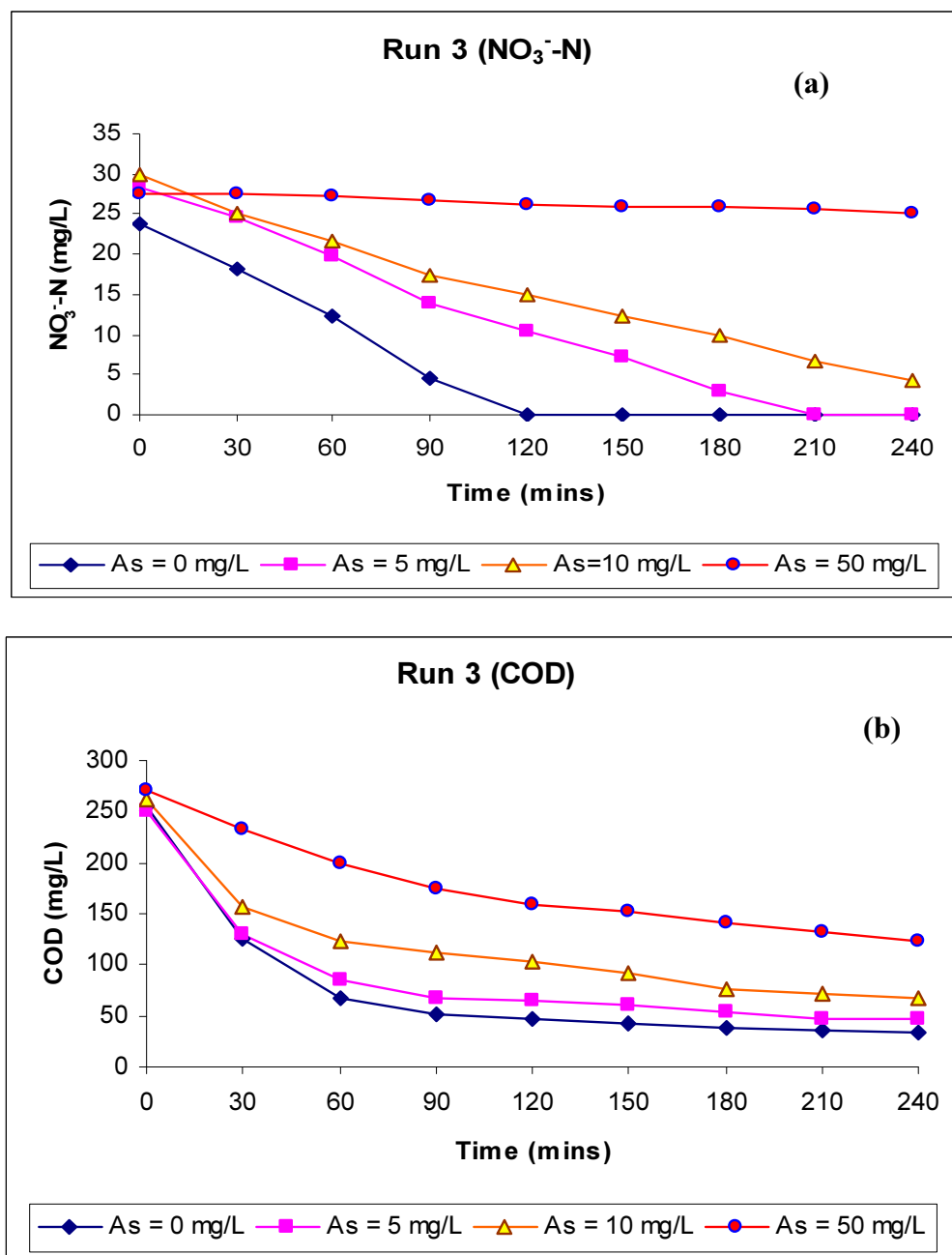
was further confirmed by the results from the batch test with an As (III) concentration of 18 mg/L. In this case, the observed percent of denitrification in the 4 h allotted to the test was 47.6 % which was somewhat less than the 52.8 % recorded for Run 1. Finally, the reactor spiked with an As (III) concentration of 25 mg/L only was able to denitrify 28.7 % of the initial  $\text{NO}_3^-$ -N concentration further confirming the impact of As (III) on denitrification.

Figure 5-8 (b) shows the COD track study measured in all 4 reactors. The COD pattern of consumption is very similar to that observed for Run 1, where the rate of COD consumption slowed as the As (III) concentration increased. In addition, a relatively similar amount of residual COD (40, 43, 48, and 68 mg/L) was observed in the batch reactors at the end of the reaction. As expected, the initial COD concentrations in all 4 reactors were measured to be very close to each other.

### **Run 3**

In Run 3, three As (III) concentrations (0, 5, and 10 mg/L) were repeated, while one concentration was further increased to 50 mg/L. The  $\text{NO}_3^-$ -N removal patterns in the three batch tests were observed to be very similar to those in previous runs. However, there was a minor delay in denitrification in the 0 and 10 mg/L As (III) reactors. This was an indication of the necessity of an additional time to acclimatize specially for the biomass which was under long storage. At the concentration of 50 mg/L, the  $\text{NO}_3^-$ -N removal graph was almost flat (Figure 5-9 (a)) indicating almost no denitrification. In fact the denitrification rate in this concentration was extremely slow and the  $\text{NO}_3^-$ -N was only removed from 27.4 to 25.2 mg/L in the allotted reaction time of 4 h (i.e. 8.0 % denitrification). Despite a reaction time of 4 h, this reactor was allowed to continue denitrifying until complete denitrification was achieved. At that point, 100 % of the initial  $\text{NO}_3^-$ -N (27.4 mg/L) was removed in approximately 48 h with almost a similar specific denitrification rate (i.e no acclimatization to the higher As (III) concentration). A conclusion was that the biomass was able to completely denitrify the initial concentration of  $\text{NO}_3^-$ -N while simultaneously exposed to a concentration of As (III) as high as 50 mg/L; however, the specific denitrification rate would not change but the reaction time extended substantially, in accordance with the amount of  $\text{NO}_3^-$ -N removed.

In Run 3, no change in the general pattern of COD consumption was observed (Figure 5-9 (b)). However, in the 50 mg/L As (III) reactor a comparatively higher residual COD (124 mg/L) was measured. This may mean that also the other non-denitrifying heterotrophic organisms were affected by the high dose of As (III) (i.e. 50 mg/L).



**Figure 5-9.** Track study of NO<sub>3</sub><sup>-</sup>-N (a) and COD (b) for Run 3.

## Run 4

In the previous run (Run 3) the  $\text{NO}_3^-$ -N track for 50 mg/L was observed to be almost flat, thus representing an effective upper bound for the batch tests during the allotted reaction time of 4 h. In addition, a concentration of more than 50 mg/L of As (III) was thought to be hazardous from a “student-handling” perspective. Thus Run 4 consisted of replicates of the As (III) concentrations of 0, 18, 25, and 50 mg/L.

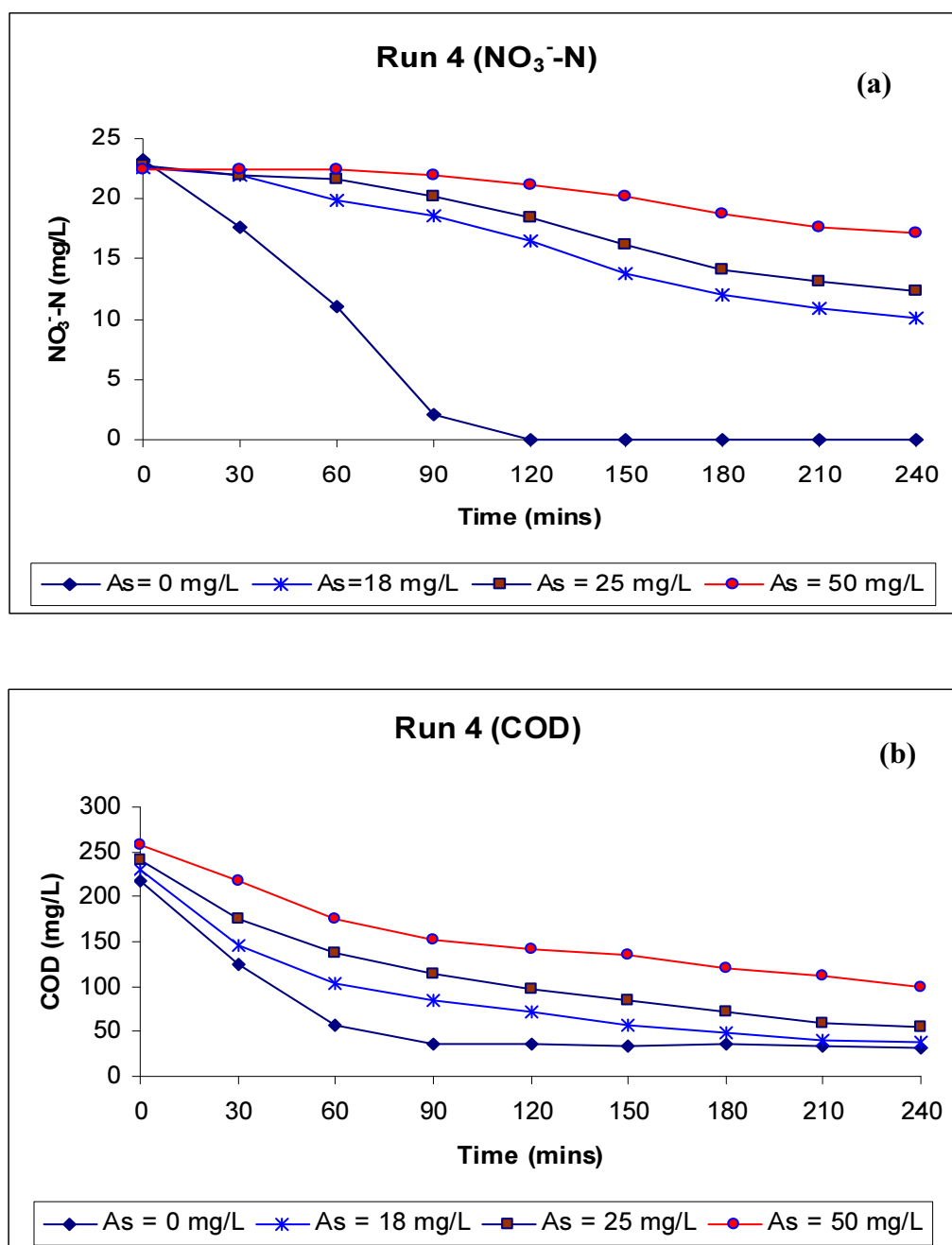


**Figure 5-10.** Track study of  $\text{NO}_3^-$ -N (a) and COD (b) for Run 4.

As shown in Figure 5-10 (a), the initial concentrations of  $\text{NO}_3^-$ -N in all of the four batch tests were measured to be very close to each other. Indeed, of all the runs, Run 4 showed the best ability to achieve a common starting point. It was noted however that all the points were slightly lower than the initial target concentration of 25 mg/L. The control track (As = 0 mg/L) of the  $\text{NO}_3^-$ -N was almost identical to the control track for Run 2; with both of these tracks showing approximately 90 % denitrification in 90 min of reaction time. The remaining three tracks following the normal pattern of showing a flatter slope as the As (III) concentration increased. The final denitrification occurring in the 18 mg/L As (III) reactor was measured to be 55.3 % which was very close to the 52.8 and 47.6 % recorded for Run 1 and 2 respectively. Particularly in this run, some indication of improvement in the denitrification efficiency was noticed in the reactor. For example, the percentage of denitrification at the end of the reaction observed in the 25 and 50 mg/L As (III) reactors were 45.6 and 23.5 % respectively which was substantially more than the 28.7 and 8.0 % recorded for previous runs with stored biomass. This increase was attributed to the fact that a substantial part of the biomass, which was used in Run 4 had been freshly obtained from the SBR, and therefore did not need extra time to be acclimatized.

A very smooth graph for COD consumption is shown in Figure 5-10 (b), and it was observed that a higher initial COD was measured with increased As (III) concentration. This pattern confirms that instantaneous denitrification was occurring in all the reactors and this lessens as the As (III) concentration increases.

### **Run 5**

Run 5 was the last run of the denitrification batch tests that considered As (III) concentrations of 0, 10, 25 and 50 mg/L. All the four As (III) concentrations were just replications selected from some of the previous runs. The results for this run are shown in Figure 5-11 (a) and (b).

The pattern for the reduction of  $\text{NO}_3^-$ -N is shown in Figure 5-11 (a). The track with no As (III) (As = 0 mg/L) well replicates the track of Runs 2 and 4, showing approximately the same percentage of denitrification (92 % denitrification in 90

min). In the 10 mg/L As (III) reactor, 100 % denitrification was observed in 240 min tallying with that observed in the corresponding reactor for Run 1. In the final two reactors (As = 25 and 50 mg/L), the percentages of denitrification observed were 44.8 and 14.0 % respectively which again were comparable to those observed in previous runs (Run 2,3 and 4).

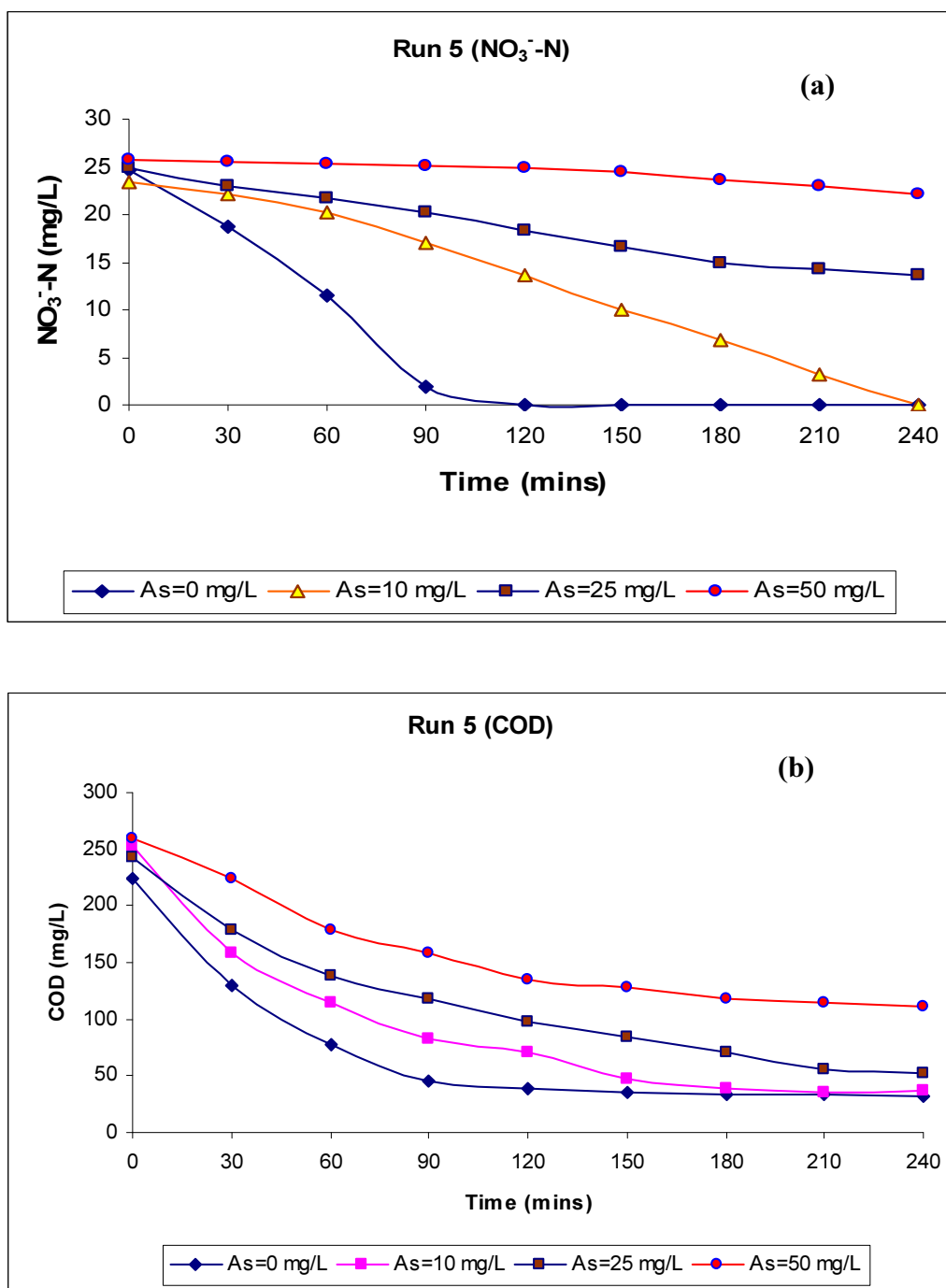


**Figure 5-11.** Track study of  $\text{NO}_3^-$ -N (a) and COD (b) for Run 5.

No special features were noticed in the COD track study shown in Figure 5-11 (b). The initial COD measured in the As (III) 10 mg/L reactor (252 mg/L) revealed a slightly higher value than in the reactor with As (III) 25 mg/L (243 mg/L), which seems slightly unusual. Additionally some COD points measured near to the end of the reaction ( $t = 180, 210$  and  $240$  min) were suspect since they were very close to the related points of control reactor. This however was not of great concern.

## 5.2.2 Computation of Denitrification Rates (Arsenite)

The specific denitrification rates obtained from the batch tests are shown in Table 5-9. In each of the five runs (R1, R2, R3, R4 and R5), four different denitrification rates were obtained for the different concentration of As (III) (including one for the control reactor). Thus, 5 denitrification rates were computed for the zero As (III) concentration ( $\text{As} = 0$  mg/L) and 3 for each As (III) concentration of 5, 10, 18, 25 and 50 mg/L respectively.

**Table 5-9:** Specific denitrification rate computed in the denitrification batch tests (with As (III))

As (III) (Mg/L)	Specific denitrification rate (g $\text{NO}_3^-$ -N/gVSS per day) in reactor					
	R1	R2	R3	R4	R5	Mean values $\pm$ $\sigma$
0	0.481	0.340	0.314	0.365	0.342	$0.368 \pm 0.065$
5	0.246	0.210	0.185	n/a	n/a	$0.214 \pm 0.031$
10	0.184	n/a	0.149	n/a	0.136	$0.156 \pm 0.025$
18	0.086	0.069	n/a	0.077	n/a	$0.077 \pm 0.008$
25	n/a	0.047	n/a	0.066	0.061	$0.058 \pm 0.010$
50	n/a	n/a	0.015	0.030	0.020	$0.022 \pm 0.007$

From the Table 5-9 it can be seen that the denitrification rate decreased considerably as the concentration of As (III) increased. In particular, the specific denitrification rate decreased from a high of 0.481 g  $\text{NO}_3^-$ -N/gVSS per day in one of the control reactors to a low of 0.015 g  $\text{NO}_3^-$ -N/gVSS per day at 50 mg/L As (III) for Run 3. It is noted that the control reactors experienced a comparatively higher mean specific



denitrification rate (ranging from 0.314 to 0.418 g NO<sub>3</sub><sup>-</sup>-N/gVSS per day) than the SBR (0.11 g NO<sub>3</sub><sup>-</sup>-N/gVSS per day). Since both systems were operated with favourable C/N ratios, the higher rate experienced in the denitrification reactor is attributed to VFAs being more amenable as a carbon source than the domestic sewage with negligible VFAs (Table 3-1) fed to the SBR.

The rates obtained in the control reactors are higher than the rate reported by He (2006) (0.028 g NO<sub>3</sub><sup>-</sup>-N/gVSS per day) even though both were done with same type of C-source and under almost identical operational conditions. Notwithstanding, the rates associated with the control reactors from this research are fairly comparable to most of the specific denitrification rates reported in other literature and appear to be at the middle of the spectrum (ranging from 0.008 to 0.754 g NO<sub>3</sub><sup>-</sup>-N/gVSS per day (Table 2-4)). In addition, some of the rates in Table 2-4 are associated with continuous, flow-through systems which generally have higher rates than those obtained from batch systems due to the non-steady state nature of batch systems and acclimation of bacteria to particular carbon sources in continuous flow through systems (Elefsiniotis, et al., 2004).

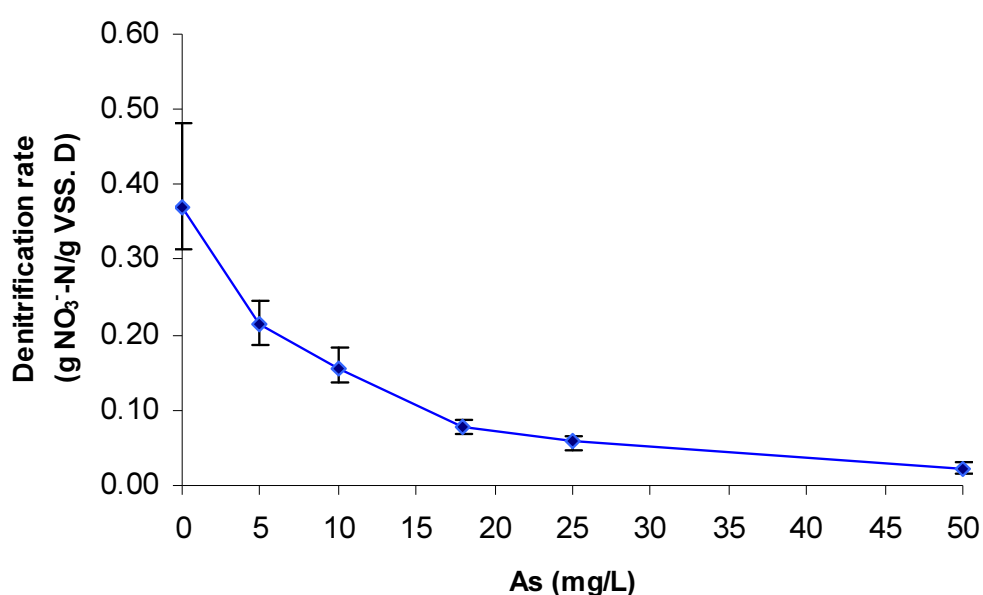


**Figure 5-12.** Decreasing denitrification rate with increasing arsenite concentration

The rates of denitrification obtained from the batch tests were also plotted against the concentrations of arsenic (Figure 5-12). Unambiguously evident is the effect of the As (III) on the denitrification rate, as the mean specific denitrification rate fell from 0.37 to 0.02 g NO<sub>3</sub><sup>-</sup>-N/g.VSS per day as the As (III) increased from 0 to 50 mg/L. Figure 5-12 also indicates that the height of the error bar (i.e. the standard deviation) is lowered as the As (III) concentration increases. This difference in the deviation is attributed to the dependency of the specific denitrification rate on other operational factors such as DO content, mixing, pH, redox potential etc.

### 5.2.3 Kinetic Equation of the Effect of Arsenite on Denitrification

The quantitative effect of the As (III) on the specific denitrification rate is shown in the Figure 5-12. Measuring the slope of the curve at a number of As (III) concentrations reveals the rate of change in the specific denitrification rate. Plotting this rate of change versus the corresponding specific denitrification rate for each data point yields a straight line indicating first order kinetics.

Correspondingly, if “R<sub>d</sub>” is denoted to be the specific denitrification rate and “C<sub>As</sub>” is the corresponding concentration of As (III) associated with that rate, the rate of change of specific denitrification rate (dR<sub>d</sub>/dC<sub>As</sub>) decreases as a first-order function with the specific denitrification rate (R<sub>d</sub>) obtained during the batch tests. It can be written as:

$$\frac{dR_d}{dC_{As}} = -kR_d \quad (5.7)$$

Where, “k” can be designated as a first-order constant (expressed as per unit time) reflecting the effect of the As (III) on the specific denitrification rate.

Rearrangement yields the following:

$$dR_d = -kR_d dC_{As} \quad (5.8)$$

Integrating the equation yields:

$$\ln R_d = -kC_{As} + C \quad (5.9)$$

Evaluating the value of “C” (the constant of integration) by using boundary conditions means that  $C_{As} = 0$ , “ $R_d$ ” = “ $R_{d0}$ ”, where “ $R_{d0}$ ” is the specific denitrification rate at As (III) concentration zero (i.e. “ $R_d$ ” at “ $C_{As} = 0$ ”).

Substituting into the equation, we obtain:

$$\ln R_d = -k \times (0) + C$$

$$\text{Therefore, } C = \ln R_{d0} \quad (5.10)$$

We now can write the integrated form for first-order kinetics, as follows:

$$\ln R_d = -kC_{As} + \ln R_{d0} \quad (5.11)$$

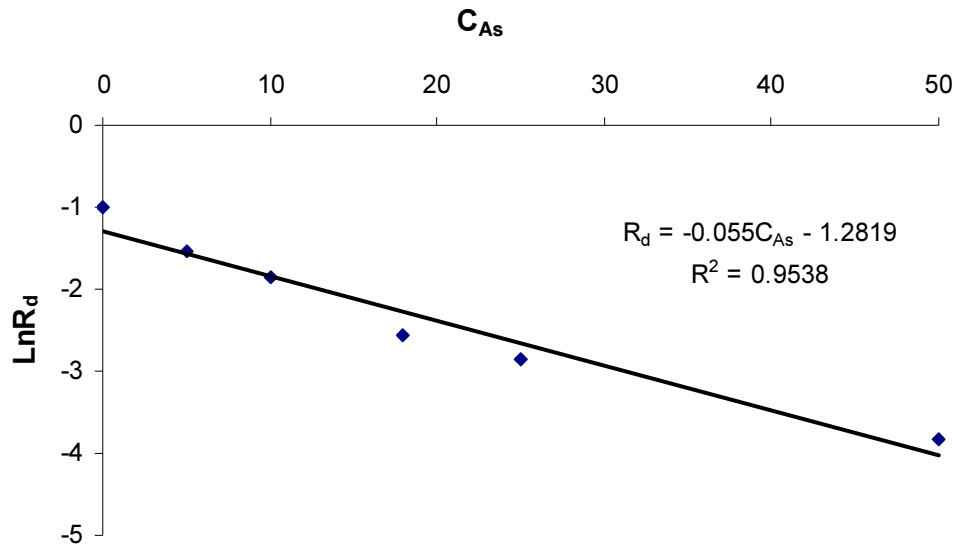


**Figure 5-13.** Model testing and evaluation of an equation

A graph of “ $\ln R_d$ ” versus “ $C_{As}$ ” was plotted (Figure 5-13) in order to calculate the constants “ $k$ ” and “ $R_{d0}$ ”, and a straight line was obtained with  $R^2$  value of 0.9538 indicating the model obeyed first order kinetics. The values for the constants “ $k$ ” and “ $R_{d0}$ ” are 0.055 and 0.278 respectively, which means the final equation is modelled to be:

$$R_d = 0.278e^{-0.055C_{As}} \quad (5.12)$$

Equation 5.12 models the specific denitrification rate curve and represents a quantitative effect of the As (III) on denitrification in the presence of naturally produced VFAs as carbon source. It can be seen therefore that the effect of the As (III) on the specific denitrification rate is an exponential one and valid for the particular range of As (III) concentration used during the batch tests. Other carbon sources may experience similar effects but with different values of “ $R_{d0}$ ” and “ $k$ ”.

## 5.3 Effect of Arsenate (As (V)) on the Denitrification Rate

### 5.3.1 Track Studies of Nitrate and COD

As shown previously in Table 3-2, a total of 14 denitrification batch tests with As (V) were carried out in 4 runs (R6, R7, R8 and R9). Run 7 and Run 8 had four experimental reactors each using three different concentrations of As (V) and one as a control reactor (i.e. no As (V)). In contrast, Runs 6 and 9 consisted of only three reactors (two with As (V) and one control). As opposed to the As (III) reactors which were set with a maximum concentration of 50 mg/L, the As (V) reactors had this value as the lowest level. As mentioned earlier (Section 3.1.3.4), any As (V) concentration was set only after having some idea of its effect on denitrification by observing some trials. Consequently, the As (V) concentration range selected for the batch tests (50 to 2,000 mg/L) was much higher than the concentration range set for As (III) (5 to 50 mg/L).

Once again, a target concentration of 25 mg/L  $\text{NO}_3^-$ -N was set, similar to the As (III) batch tests and the corresponding dose of standard  $\text{NO}_3^-$  solution was added to each of the fourteen reactors. The concentrations of  $\text{NO}_3^-$ -N and COD in each reactor were measured every 30 min (starting from 0) during the allotted reaction time of 4 h. The results are shown graphically in Figure 5-14 to 5-17 while numerical data has been relegated to Appendix B3.

As was the case for As (III) (Section 5.2.1), the  $\text{NO}_3^-$ -N concentration at  $t = 0$  min measured in all of the control reactors was slightly less than the concentration added (i.e. 25 mg/L). Furthermore, in the experimental reactors where As (V) was added, the  $\text{NO}_3^-$ -N concentration at  $t = 0$  min was measured to be very close to (and often less) than the added  $\text{NO}_3^-$ -N concentration (i.e. 23 to 25.8 mg/L). To observe reproducibility, at least two different tests were carried out for each concentration of As (V) (50, 100, 500, 1,000 and 2,000 mg/L) and mean values were computed. The results obtained for each run are shown and discussed in the following paragraphs.

## Run 6

For Run 6, as mentioned, three tests were carried out (i.e. one control and two with As (V) concentrations of 50 and 500 mg/L). As shown in Figure 5-14, when there was no As (V), the  $\text{NO}_3^-$ -N reduced from 22.9 to 0 mg/L indicating complete denitrification in 120 min.

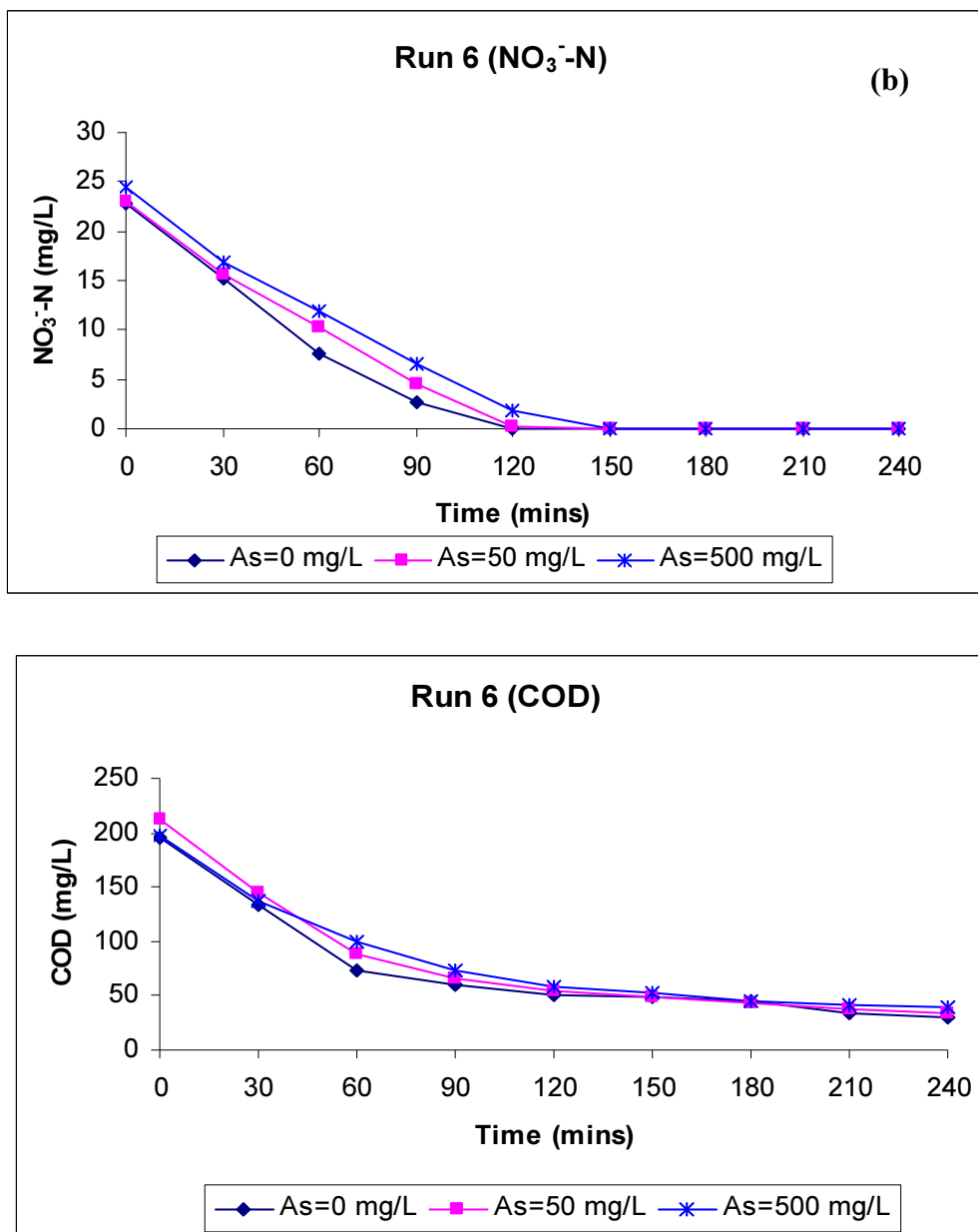


**Figure 5-14.** Track study of  $\text{NO}_3^-$ -N (a) and COD (b) for Run 6.

This time is similar to most of the control batch tests done with As (III) (controls for R2, R3, R4 and R5). In the 50 and 500 mg/L As (V) concentration reactors, the

initial  $\text{NO}_3^-$ -N concentrations were measured to be 23.0 and 24.5 mg/L respectively and both dropped to 0 mg/L in 150 min. These results indicate that the biomass in all 3 reactors was able to completely denitrify the initial  $\text{NO}_3^-$ -N concentration within the allotted reaction time of 4 h and indicate that there was no clear impact of As (V) on the length of time it took to denitrify.

A track study of the COD removal for Run 6 is shown in Figure 5-14 (b). Since, the carbon was presumably being used to support denitrification; the coincident pattern of COD removal for different concentrations of As (V) also indicates that there is no apparent effect of As (V) on denitrification at these concentrations.

### **Run 7**

For Run 7, four batch tests with As (III) concentrations of 0, 100, 1,000, and 2,000 mg/L were performed. The track study of  $\text{NO}_3^-$ -N is shown in Figure 5-15 (a) and as shown, the  $\text{NO}_3^-$ -N in the control reactor dropped from 23.4 to 0 mg/L in 120 min; the same time required to completely denitrify in the control reactors for most previous runs (Run 2 to 5 (As (III)) as well as Run 6 (As (V))).

In spite of some  $\text{NO}_3^-$ -N remaining in the 2,000 mg/L As (V) reactor, the  $\text{NO}_3^-$  elimination pattern in both the 1,000 and 2,000 mg/L reactors indicates that the majority of denitrification occurred within 120 min of reaction time (Figure 5-15 (a)). In the 2,000 mg/L As (V) reactor, 81.6 % denitrification occurred in first 120 min of reaction time while little  $\text{NO}_3^-$ -N removal was noticed in the remaining reaction time of 4 h (an increase of 81.6 to 84.3 % only in next 120 min). Because of this, to calculate the specific denitrification rate, the last point of denitrification was considered to be at 120 min in spite of the 240 min allotted.

In the two higher As (V) concentration reactors (As = 1,000 and 2,000 mg/L), it was also noted that the reaction rate was slower in the first half of the reaction time than in second half; while comparatively a constant reaction rate was seen in the two lower As (V) concentration reactors (As = 0 and 100 mg/L). This may be because the biomass in the higher As (V) concentration reactors needed some time to acclimatize to the quantity of As (V).

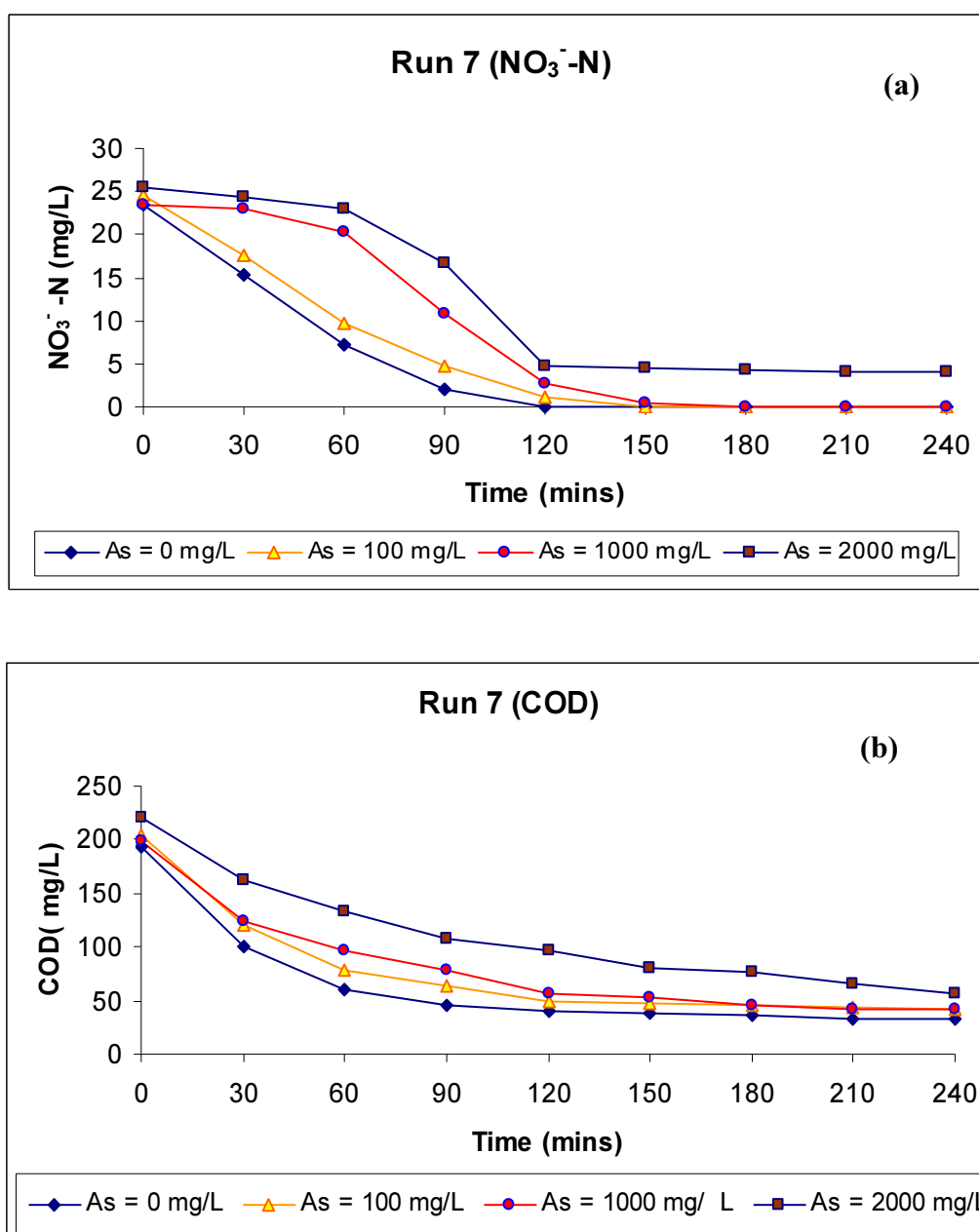


**Figure 5-15.** Track study of NO<sub>3</sub><sup>-</sup>-N (a) and COD (b) for Run 7.

Figure 5-15 (b) shows the COD track study results for all 4 reactors. Although there was not any sharp effect of the As (V) on denitrification, the COD pattern of consumption resembled the pattern observed for As (III) (Run 1 to 5); where the rate of COD consumption slowed as the As (III) concentration increased. Observing this pattern was only possible in this run because of the wide gap between the As (V) concentrations selected in the batch tests.



As in the As (III) reactors, carbon continued to be removed after all the  $\text{NO}_3^-$ -N were eliminated leaving a relatively similar amount of residual COD (32, 42, 42, and 56 mg/L). It is presumed that this is due to the activity of non-denitrifying heterotrophic activity tolerant of As (V).

### **Run 8**

As shown in Figure 5-16 (a), four batch tests with As (V) concentrations of 0, 50, 100 and 1,000 mg/L were undertaken as part of Run 8. The concentrations were just replications from some of the previous runs (i.e. R6 and R7). The time elapsed to remove the initial  $\text{NO}_3^-$ -N concentration in the four batch tests were very similar to that observed in previous runs. For example, the added  $\text{NO}_3^-$ -N in the 0, 50 and 100 mg/L As (V) batch reactors was completely denitrified in 120 min and for the 1000 mg/L concentration, the  $\text{NO}_3^-$ -N was removed in 150 min. These times corresponded to the times taken in the corresponding reactors in previous runs.

Comparing the  $\text{NO}_3^-$ -N elimination pattern for the three tracks for the As (V) concentration of 0, 50 and 100 mg/L with the associated tracks of Run 6 and 7, reveal that the profiles were similar; while in the 1,000 mg/L As (V) reactor, a more linear curve was obtained than in Run 7. As mentioned previously, the curve in Run 7 was flat in the first part of the reaction and relatively steep in the second portion. This indicates that Run 8's 1,000 mg/L As (V) concentration resulted in a quicker bio-acclimatization to the As (V) added, than achieved in Run 7. However, the exponential pattern observed in the reactors with low As (V) concentrations still suggests the necessity of an acclimatization period for the biomass to high As (V) concentrations.

Figure 5-16 (b) shows the track study results of the COD for Run 8, where no change was observed in the general pattern of COD consumption. However, it is noticed that the three COD tracks with comparatively lower As (V) concentrations (i.e. 0, 50, and 100 mg/L) are coincident with each other, while the higher concentration (1,000 mg/L) presents with a distinct track starting at a relatively higher initial COD (i.e. 254 mg/L) concentration and decreasing at a relatively

slower COD-removal rate. Notwithstanding, the final residual COD was measured to be similar in all four reactors (i.e. 38, 46, 45 and 52 mg/L).

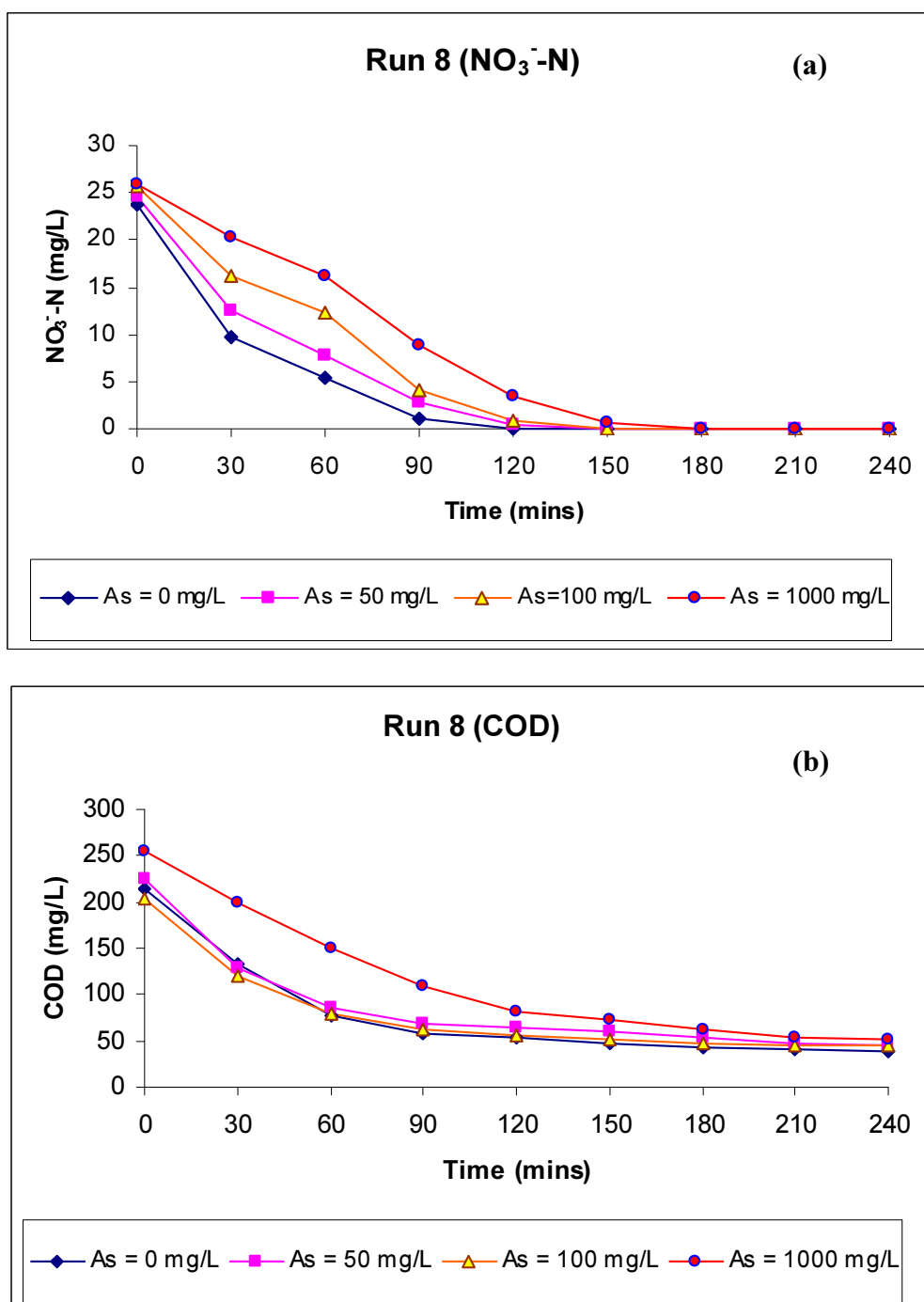


**Figure 5-16.** Track study of  $\text{NO}_3^-$ -N (a) and COD (b) for Run 8.

## **Run 9**

Run 9 was the last run designed to test the effect of arsenic (both As (III) and As (V)) on the denitrification in this research. In this run, as shown in Figure 5-17 (a), three tests with As (V) concentration 0, 500 and 2,000 mg/L were carried out. All three  $\text{NO}_3^-$ -N removal tracks are very similar to the tracks observed in previous runs associated with the same concentrations of As (V).

As observed in Run 7, during the period of addition of 2,000 mg/L As (V), the majority of the denitrification (76.6 %) occurred in the first 120 min of reaction time. In spite of the initial high denitrification rate, incomplete denitrification occurred with ultimately 91.1 %  $\text{NO}_3^-$ -N removed in the allotted reaction time of 4 h. One can suppose therefore that even with a high As (V) concentration (i.e. 2,000 mg/L) denitrifying biomass can remain active but only for a very short period (in this case < 2 h). As an aside, it should be noted that after a certain period exposed to such high concentrations, the denitrifying biomass die and COD is released. This was confirmed by allowing the two higher As (V) reactors (1,000 (from Run 8) and 2000 (from Run 9) mg/L) to continue for a period of 20 days. The resultant soluble CODs were measured to be 755 and 822 mg/L respectively. This substantial increase in soluble CODs (more than 1,300 % from the initial value of 52 and 58 mg/L respectively) is likely to cell lysis.

In addition, the  $\text{NO}_3^-$ -N removal rate was observed to slow in the first 30 min, confirming the necessity of allowing time to acclimatize the biomass to a higher As (V) amount added.

A very smooth graph for COD consumption is depicted in Figure 5-17 (b). The COD curves for all three As (V) concentrations (0, 500 and 2,000 mg/L) started at a common starting point and ended very close to each other. However, the graph follows the basic pattern of slowing the rate of COD consumption as the As (V) concentration increases. In addition, in the 2,000 mg/L As (V) reactor, the pattern of  $\text{NO}_3^-$ -N and COD removal do not seem to be alike, possibly indicating consumption of some COD by other heterotrophic biomass. Such differences in the patterns were also noticed in the 1,000 and 2,000 mg/L As (V) reactors for Run 7.

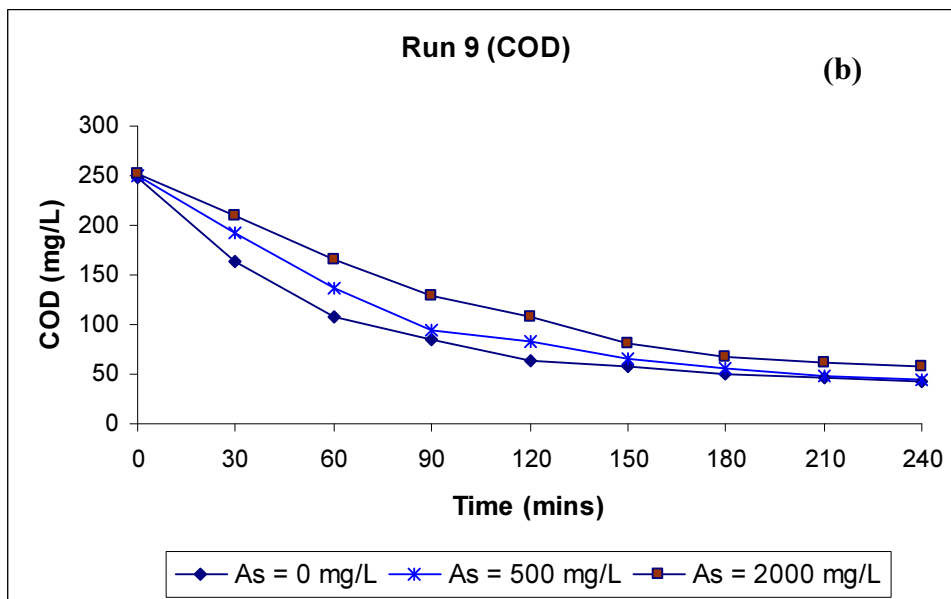
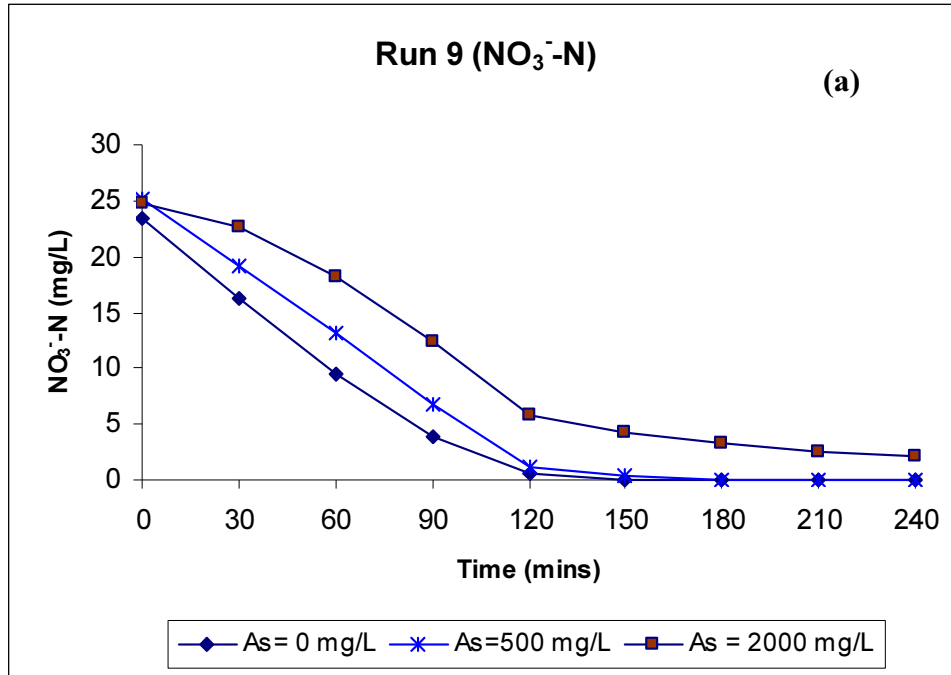


**Figure 5-17.** Track study of  $\text{NO}_3^-$ -N (a) and COD (b) for Run 9.

### 5.3.2 Computation of Denitrification Rates (Arsenate)

The specific denitrification rates obtained from the batch tests are shown in Table 5-10. Three denitrification rates were calculated for Runs 6 and 9 while four rates were calculated for Runs 7 and 8. The result was that 4 denitrification rates were

obtained for the zero arsenate concentration ( $\text{As} = 0 \text{ mg/L}$ ) while there were 2 rates for each As (V) concentration of 50, 100, 500, 1,000 and 2,000 mg/L respectively. From Table 5-10 it can be seen that the denitrification rate decreased as the concentration of As (V) increased; however, it was not as significant as was the case for As (III). In particular, the maximum decrease in the specific denitrification rate was only 37 % (a decrease from  $0.37 \text{ g NO}_3^- \text{-N/gVSS per day}$  in the control reactors of R8 to  $0.23 \text{ g NO}_3^- \text{-N/gVSS per day}$  with 2,000 mg/L As (V) (R9)). This is a negligible decrease in comparison to the 97 % decrease experienced at only a 50 mg/L As (III) concentration.

**Table 5-10:** Specific denitrification rate computed in the denitrification batch tests (with As (V))

As (V) (mg/L)	Specific denitrification rate ( $\text{g NO}_3^- \text{-N/gVSS per day}$ ) in reactor				
	R6	R7	R8	R9	Mean value $\pm \sigma$
0	0.30	0.36	0.37	0.34	$0.342 \pm 0.027$
50	0.28	n/a	0.34	n/a	$0.310 \pm 0.030$
100	n/a	0.26	0.32	n/a	$0.290 \pm 0.030$
500	0.26	n/a	n/a	0.30	$0.280 \pm 0.020$
1000	n/a	0.25	0.28	n/a	$0.265 \pm 0.015$
2000	n/a	0.24	n/a	0.23	$0.235 \pm 0.007$

n/a = not available

The mean specific - denitrification rates were then plotted against the concentrations of As (V) (Figure 5-18). It can be seen that the As (V) had little effect on the denitrification rate as overall the mean denitrification rate decreased from  $0.34$  to  $0.29 \text{ g NO}_3^- \text{-N/g.VSS per day}$  as the As (V) concentration increased from 0 to 100 mg/L. This effect became even less when the As (V) concentration increased from 100 to 2,000 mg/L.

It is also noted that the mean specific denitrification rate of 0.34 g NO<sub>3</sub><sup>-</sup>-N/gVSS per day obtained in the control reactors subjected to As (V) was very close to the mean value of 0.37 g NO<sub>3</sub><sup>-</sup>-N/gVSS per day obtained in the control reactors with As (III).

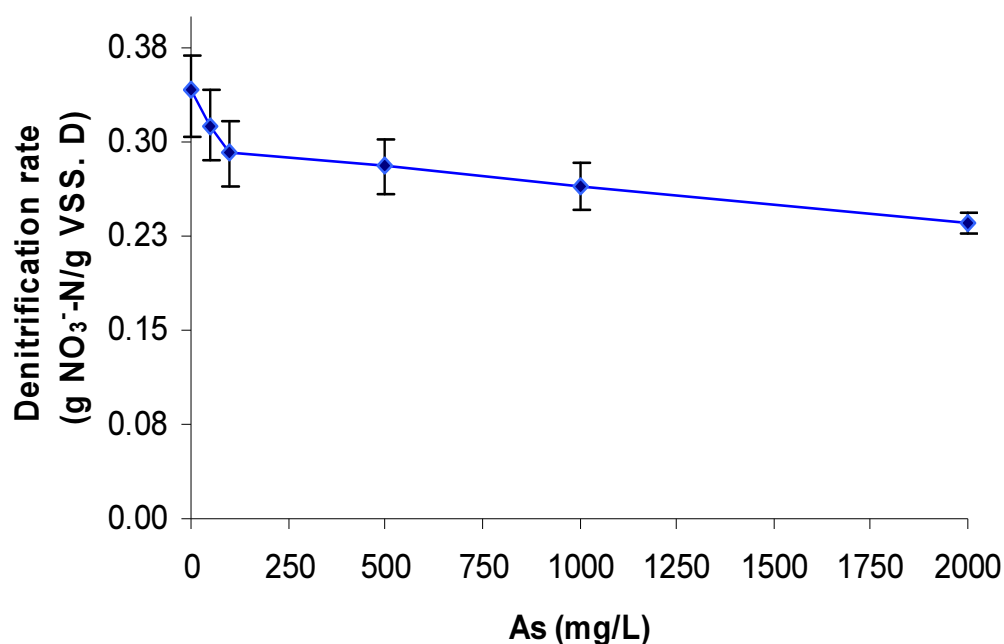


**Figure 5-18.** Decreasing denitrification rate with increasing arsenate concentration

### 5.3.3 Kinetic Equation of the Effect of Arsenate on Denitrification

The quantitative effect of the As (V) on the specific denitrification rate can be developed in a similar manner to As (III) (Section 5.2.3). That is, if  $R_d$  is denoted to be the specific denitrification rate, " $C_{As(V)}$ " is the corresponding concentration of As (V) associated with that rate and " $R_{d0}$ " is the specific denitrification rate at an As (V) concentration zero while " $k$ " is the first-order kinetic constant reflecting the effect of As (V) on the specific denitrification rate.

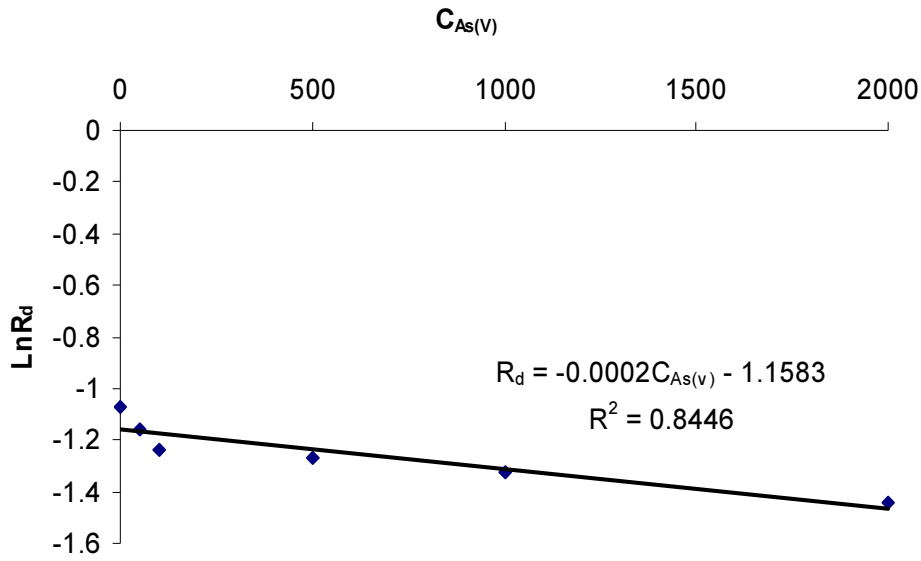


**Figure 5-19.** Model testing and evaluation of an equation on arsenate

To construct an equation for the effect of As (V) on the denitrification rate, it is assumed that the rate of change of the specific denitrification rate ( $dR_d/dC_{As(V)}$ ) decreased with the specific denitrification rate ( $R_d$ ) and followed a first-order function as was the case with As (III). Therefore, a graph of “ $\ln R_d$ ” versus “ $C_{As(V)}$ ” was plotted (Figure 5-19) by following the steps described in Section 5.2.3. A straight line was obtained with a  $R^2$  value of 0.8446 for this model using As (V). Evidently, it is not as good a model as for the As (III) model ( $R^2 = 0.9538$ ). From the graph nevertheless, the values obtained for the constants “ $k$ ” and “ $R_{d0}$ ” (i.e. 0.0002 and 0.314 respectively), suggested the final equation can be modelled as:

$$R_d = 0.314e^{-0.0002C_{As(V)}} \quad (5.13)$$

Equation 5.13 quantifies the effect of the As (V) on denitrification in the presence of naturally produced VFAs as carbon source and appears to be valid for a wide range of As (V) concentration (i.e. 0 to 2,000 mg/L).

The pattern shown in Figure 5-19 predicts that the plot can be fitted by two straight lines. That is, the test results can be divided into two parts, one for a range of 0 to 100 mg/L (i.e. 0, 50 and 100 mg/L) and another for the range of 100 to 2,000 mg/L (i.e. 100, 500, 1,000 and 2,000 mg/L) of As (V). Accordingly, as can be seen, two separate graphs of “Ln  $R_d$ ” versus “ $C_{As(V)}$ ” were plotted (Figure 5-20 (a) and (b)) in accordance with these ranges and two straight lines ( $R^2 = 0.9978$  and  $0.9977$  respectively) were obtained suggesting the model obeyed a first order function over the two different ranges. The effect of the As (V) on the specific denitrification rate is therefore different for the two specific ranges of the concentrations.

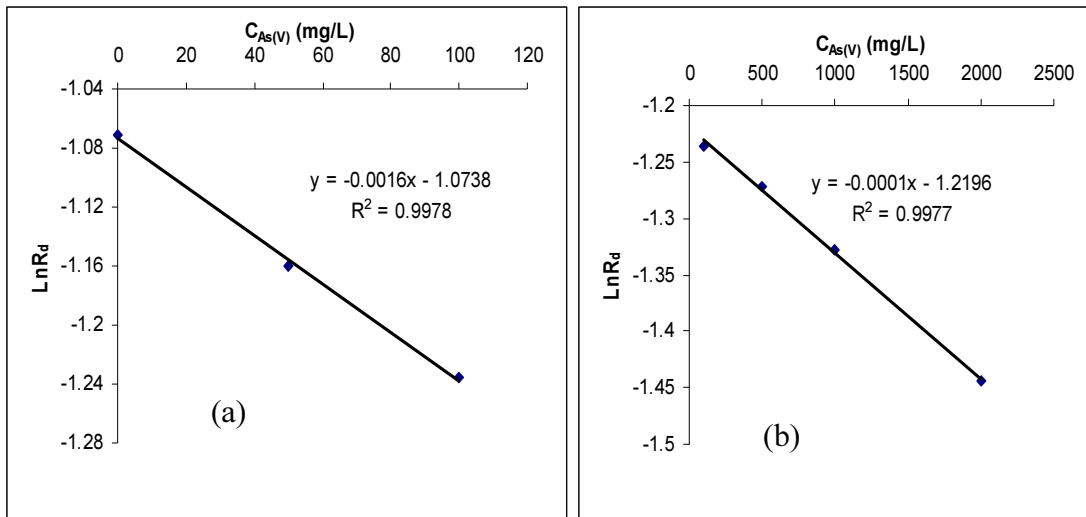


**Figure 5-20.** Model testing and evaluation of equation for two different ranges of arsenate concentrations (a) As (V) = 0 to 100 mg/L, (b) As (V) = 100 to 2,000 mg/L.

The first order constant “ $k$ ” of 0.0016 for the concentration range of 0 to 100 mg/L is greater than the value of 0.0001 for the range 100 to 2,000 mg/L. This means that for the first portion of the curve, there is a greater effect of As (V) on the rate of change in the denitrification rate. It is noted that the computed specific denitrification rates at As (V) = 0, “ $R_{d0}$ ”= 0.342 and 0.295 for the range 0 to 100 and 100 to 2,000 mg/L As (V) respectively are fairly comparable to the values obtained by the experiments (the controls for Runs R6 to R9).



Finally, with these constants, the two separate equations can be modelled as:  
For As (V) = 0 to 100 mg/L,

$$R_d = 0.295e^{-0.0002C_{As(V)}} \quad (5.14)$$

and for As (V) = 100 to 2,000 mg/L

$$R_d = 0.342e^{-0.0016C_{As(V)}} \quad (5.15)$$

## 5.4 Removal of Arsenite during the Denitrification Batch Tests

### 5.4.1 Removal Efficiency

At least one of each batch test containing As (III) concentrations of 5, 10, 18, 25 and 50 mg/L were run for an additional 2 h past the 4 h allotted reaction time and samples were analysed for As (III) every 2-h. The results for the removal of As (III) are shown in Figure 5-21.

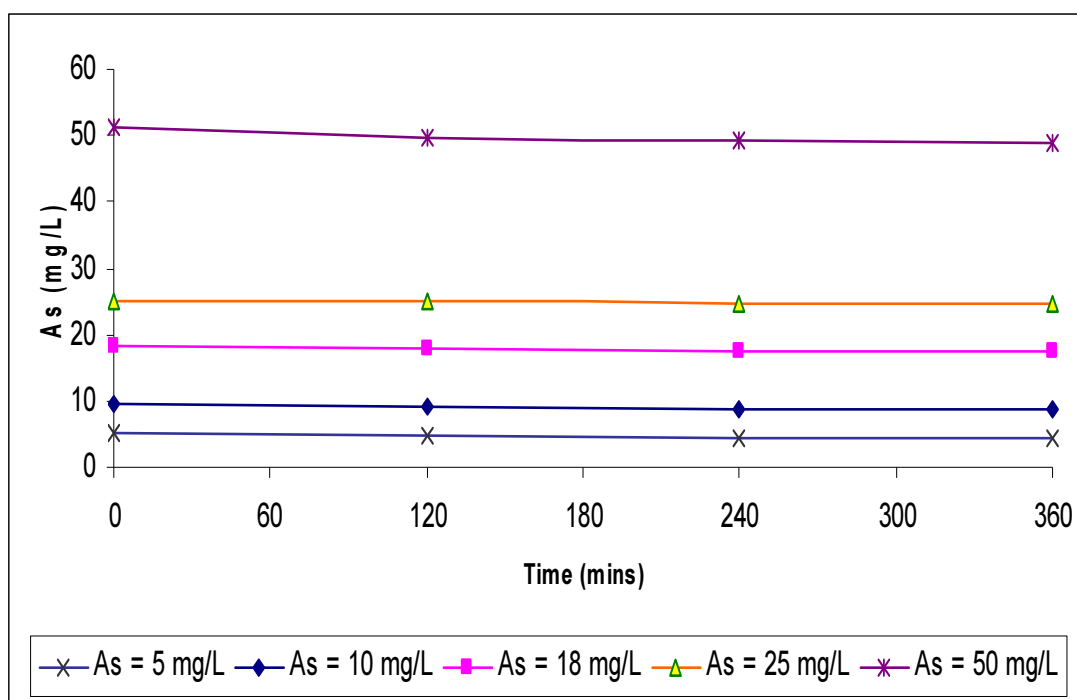


**Figure 5-21.** Track study of arsenite during the denitrification batch tests

It can be seen that there was no significant removal of As (III) during the conditions studied. Indeed, the percentages of As (III) removal ranged from 5.2 % when the As (III) concentration was 50 mg/L to 17.6 % when the As (III) concentration was 5 mg/L. Such a small removal rate meant that this removal of arsenic was not taken into account for the computation of the arsenic removal capacity of the biomass. However, as explained in Section 3.1.3.4 (Table 3-3), a total of 10 additional batch

tests were conducted to obtain the rate of arsenic removal by reacting 0.5 L of a solution containing 0.6 mg/L of As (III) with 5 different concentrations of denitrifying biomass (75, 185, 375, 560 and 750 mg/L). Five of the experiments were performed with an addition of 10 mL digester effluent (71.4 mg C/L) and  $\text{NO}_3^-$ -N (30 mg/L) while the final five had only biomass. After performing some preliminary tests, a contact time of 24 hrs was deemed to be sufficient to achieve the equilibrium point for maximum As (III) removal. Unless otherwise stated, a reaction time of 24 hrs was used and at that point the final concentration of As (III) was measured.

The effect of MLSS concentration (i.e. denitrifying biomass) on As (III) removal is illustrated in Figure 5-22, and reveals that when there was no extra C and N added, the As (III) removal efficiency was higher (78.1%) correlated to the higher concentrations of MLSS (750 mg/L). In addition, a gradual increase in the As (III) uptake was observed up to the maximum level of the MLSS concentration in this research (750 mg/L).

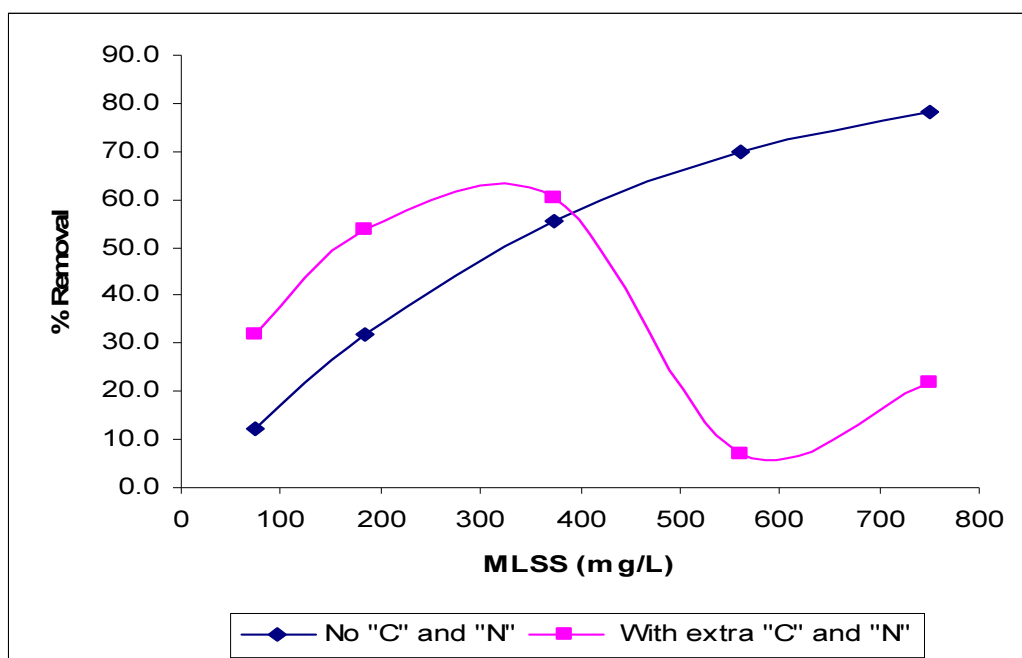


**Figure 5-22.** Effect of the concentration of MLSS on arsenite removal

The reason for As (III) removal by the MLSS appears to be bioaccumulation and this was confirmed by later tests (Section 5.6). In contrast, a wave-pattern was observed for arsenic uptake when extra C and N were added and further research would be needed to determine the exact cause of this undulating pattern.

### 5.4.2 Removal Isotherms

The experimental data obtained from the batch tests with no “C” and “N” addition were used to test the Langmuir Model (Eq. 5.16).

$$X = \frac{X_m b C_e}{1 + b C_e} \quad (5.16)$$

where, “X” is the amount of As (III) removed per unit weight of MLSS (µg/g) at pseudo-equilibrium,

“ $X_m$ ” is the maximum removal capacity (µg/g),

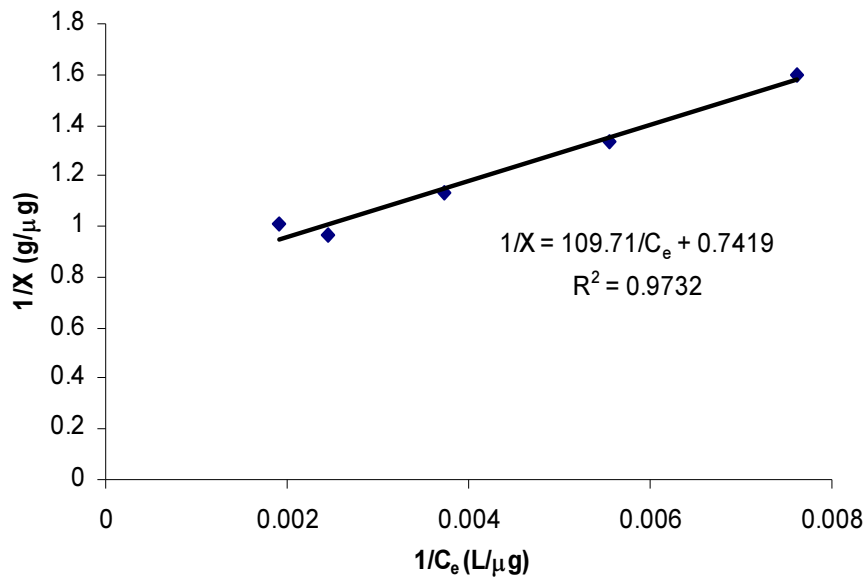
“ $C_e$ ” is the pseudo-equilibrium concentration (µg/L) in the solution; and

“ $b$ ” is constant related to the removal energy (L/µg).

The isotherm can be linearized and expressed as:

$$\frac{1}{X} = \frac{1}{b X_m C_e} + \frac{1}{X_m} \quad (5.17)$$

Equation (5.17) linearizes the experimental data by plotting “ $1/X$ ” against “ $1/C_e$ ” (Figure 5-23) and the curve performs well with an  $R^2$  value of 0.9732.



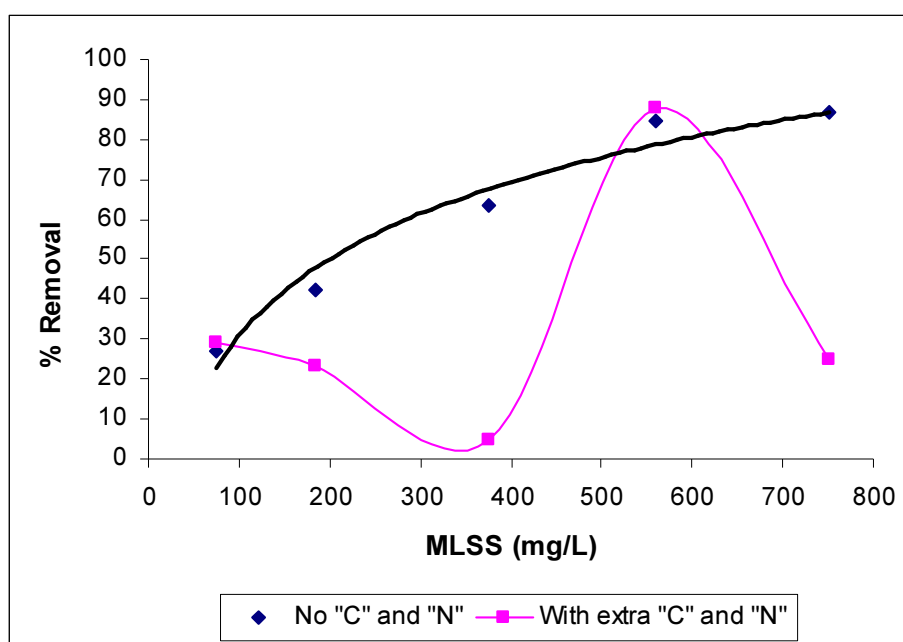
**Figure 5-23.** Langmuir plot for arsenite removal at different MLSS concentration

Figure 5-23 suggests that the maximum As (III) removal capacity of the denitrifying biomass is 1.35  $\mu$ g/g, which is in the same general order of magnitude to the As (III) removal by adsorption on normal sand (5.6  $\mu$ g/g) (Gupta, et al., 2005) and some types of wood char (1.2 to 7.4  $\mu$ g/g)(Mohan, et al., 2007). However, activated carbon and various commercial adsorbents have a far greater capacity to remove arsenic with substantially higher ranges of removal observed (28 - 428,000  $\mu$ g/g) (Mohan and Pittman, 2007). Since, most of the bacterial biomass have a negative surface charge they are poor at binding negatively charged or non-charged arsenic species. Some researchers however have tried to chemically modify bacteria and have succeeded in removing arsenic to a greater extent (up to 312  $\mu$ g As (V)/g) (Murugesan, et al., 2006; Halttunen, et al., 2007; Pokhrel and Viraraghavan, 2008); however, such experiments were beyond the scope of this research.

## 5.5 Removal of Arsenate during the Denitrification Batch Tests

### 5.5.1 Removal Efficiency

Since the concentration of As (V) was substantially higher than the As (III) and no significant removal of As (III) by the biomass was observed during the denitrification batch tests (Figure 5-21), no such tests for As (V) removal by biomass were performed during the normal denitrification batch studies (5 L solution with As (V) 50 to 2,000 mg/L). However, 10 additional batch tests (Table 3-3 (Section 3.1.3.4)) were performed to obtain the rate of As (V) removal by reacting 0.5 L of a solution containing 0.6 mg/L of As (V) with 5 different concentrations of denitrifying biomass (75, 185, 375, 560 and 750 mg/L).



**Figure 5-24.** Effect of the concentration of MLSS on arsenate removal

The effect of MLSS concentration (i.e. denitrifying biomass) on As (V) removal is shown in Figure 5-24. When no extra C and N were added, a gradual increase in the

As (V) uptake up to the maximum level of 750 mg/L MLSS was obtained with the highest uptake (86.7%) associated with a MLSS concentration of 750 mg/L. When extra C and N were added, a graph resembling a wave-pattern of As (V) uptake was obtained (similar to what occurred with As (III)) which again suggests the necessity for further research.

### 5.5.2 Removal Isotherms

As explained in Section 5.4.2, the experimental data obtained from the batch tests with no “C” and “N” addition were fitted to a Langmuir Model test (Eq. 5.16) by plotting a graph of “ $1/X$ ” against “ $1/C_e$ ” (Figure 5-25). Compared to the  $R^2$  value of 0.9732 with As (III), this value of 0.8248 was slightly lower indicating a lesser degree of fit with respect to the Langmuir Model for As (V) removal. The maximum capacity of the denitrifying biomass to remove As (V) was 2.10  $\mu\text{g/g}$ , which is slightly more than As (III), which was 1.35  $\mu\text{g/g}$ .

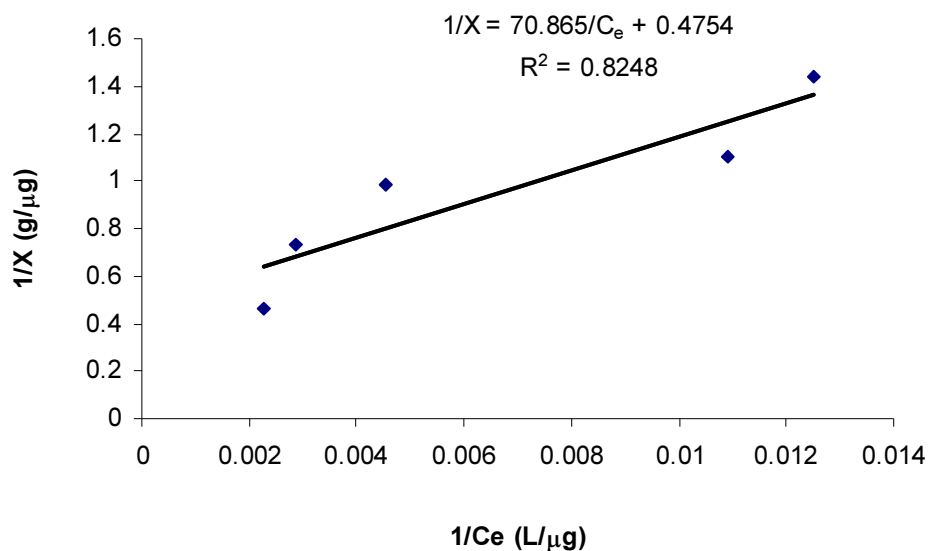


**Figure 5-25.** Langmuir plot for arsenate removal at different MLSS concentration

## 5.6 Removal Mechanism of Arsenic

As mentioned in Section 3.1.3.4, to investigate the arsenic removal mechanism, 4 batch tests were performed using three different types of biomass (i.e. active (normal), damaged by sound and dead (boiled)). The final test was a control without biomass. In all four tests, the initial concentration of arsenic was made up to be 600  $\mu\text{g/L}$  by adding an equivalent amount of a standard solution of As (III). After a contact time of 24 h, the arsenic remaining in each test-reactor was measured and the results are shown in Figure 5-26.

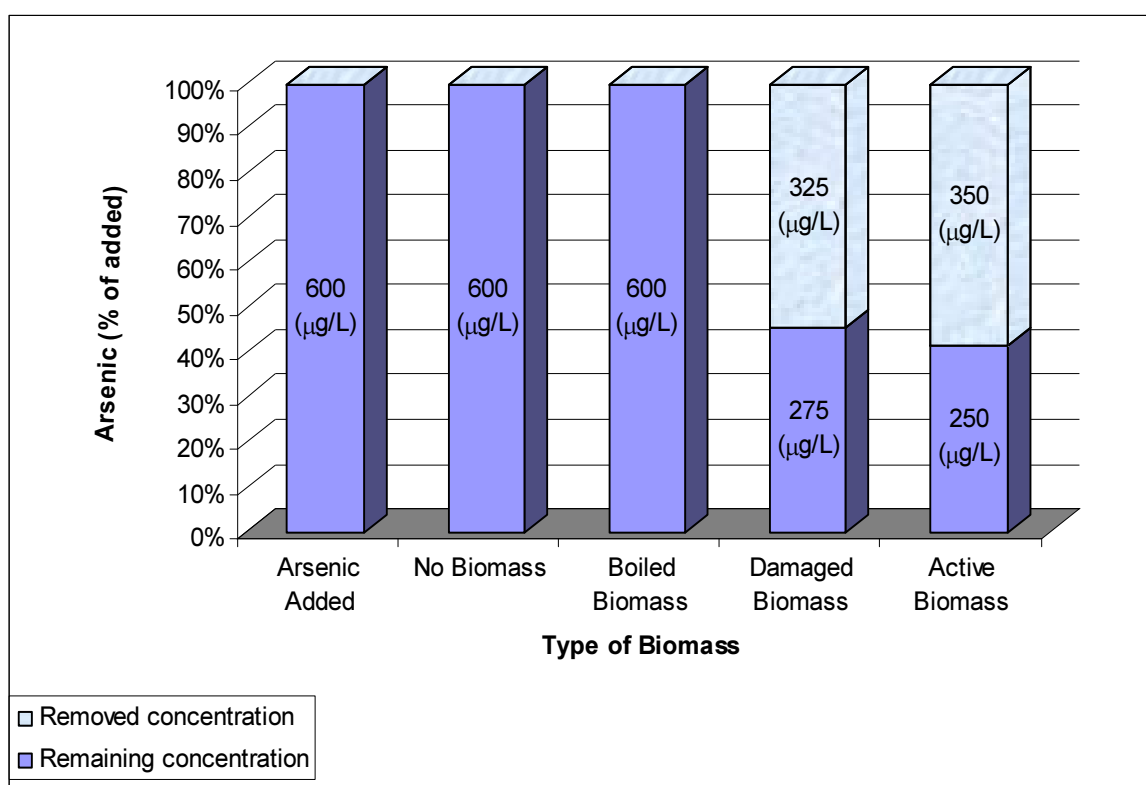


**Figure 5-26.** Concentrations of arsenite after a contact time of 24 h with different kinds of biomass.

As shown in Figure 5-26, when there was no biomass in the test-reactor the concentration of As (III) remained unchanged, which confirms that there was no abiotic uptake of As (III) during the test. Similarly, even when dead (boiled) biomass was used; there was no change in the As (III) concentration after a contact time of 24 h. In contrast, approximately 58.3 % of As (III) was removed when an active (i.e. normal) biomass was used. Additionally, the damaged biomass also



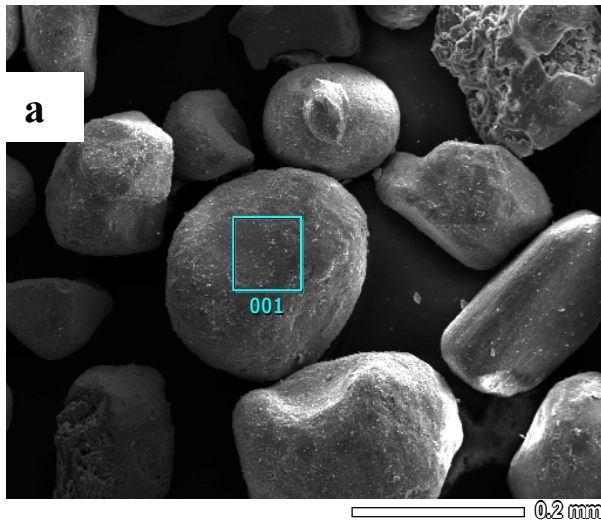
removed some As (III) (i.e. 54.2 %), which is slightly less than that the removed by normal biomass. This indicates a small fraction of the biomass was killed during the damaging treatment (using ultrasonic processor).

The above results clearly indicate that there was no physical-chemical adsorption of the As (III) on the dead biomass and less chance of adsorption on both normal and damaged biomass. It is reasonable to suppose that whatever amount of As (III) was removed was because of biological activity (i.e. biological uptake). Hence, a considerable fraction of bacteria in the biomass are able to survive the amount of As (III) added and eventually bioaccumulate the amount removed from the liquid.

The highest amount of arsenic accumulation reported in bacteria to date is 2,290 g As/ g dry weight of biomass for a marine bacteria, *M. Communis* (Takeuchi, et al., 2007). Other researchers (Silver, et al., 1981; Sauge-Merle, et al., 2003; Kostal, et al., 2004) report a comparatively a smaller range of bio-accumulation of arsenic (i.e. 110-765 g As/g) studying other strains of bacteria. Although no test was done in this research for bio-accumulation, the maximum capacity of the biomass to remove arsenic (i.e. 2.10 µg/g for As (V) and 1.35 µg/g for As (III)) gives a rough approximation of the accumulation. These values are much smaller than the mentioned research because the tests in this research were not performed with isolated bacteria whose specific focus was arsenic bio-accumulation. In addition, the tests were not done in a proper incubator as per the other studies.

## 6 ARSENIC ADSORPTION, RESULTS AND DISCUSSION

### 6.1 Scanning Electron Microscopy (SEM) Analysis



Scanning electron microscopy (SEM) was performed on the iron sand (NZIS) before and after the arsenic adsorption tests (Figure 6-1). Figure 6-1(a) shows the pristine NZIS (before the test), where there is no material spread on the surface or elsewhere. On the other hand some white material (possibly arsenic) was observed on

the surface of the sand particles after arsenic was added during the batch tests (Figure 6-1 (b) and (c)). Comparatively more adsorbed material was shown in Figure 6-1 (b<sub>1</sub>), corresponding to As (III).

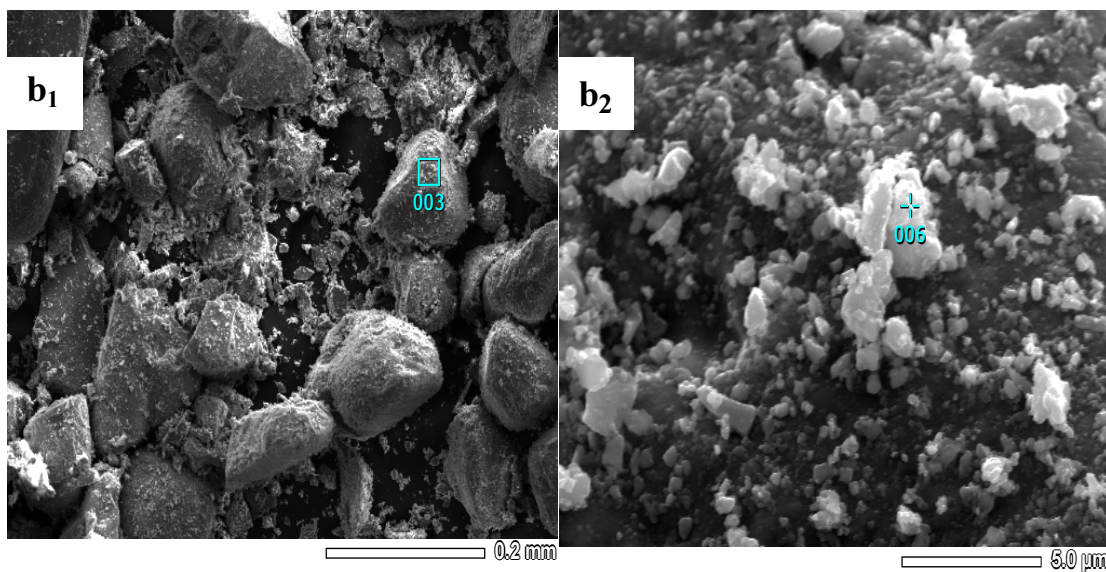
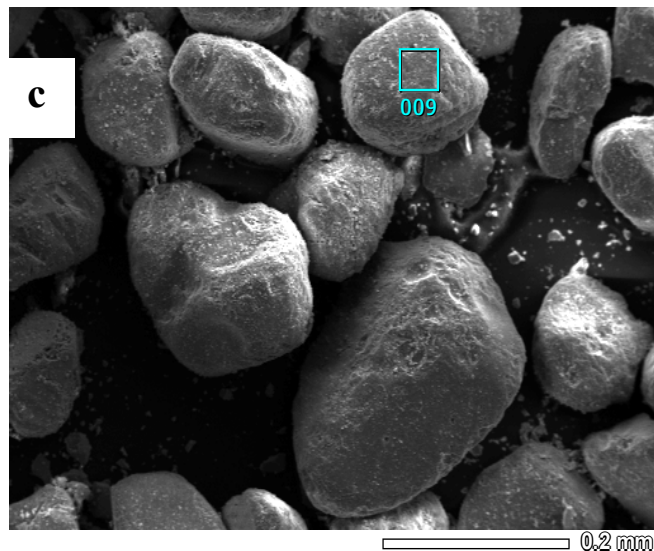


**Figure 6-1.** SEM Images of ISNZ (a) without adsorbed arsenic, (b<sub>1</sub>) and (b<sub>2</sub>) with As (III) (c) and As (V) adsorption during batch tests.

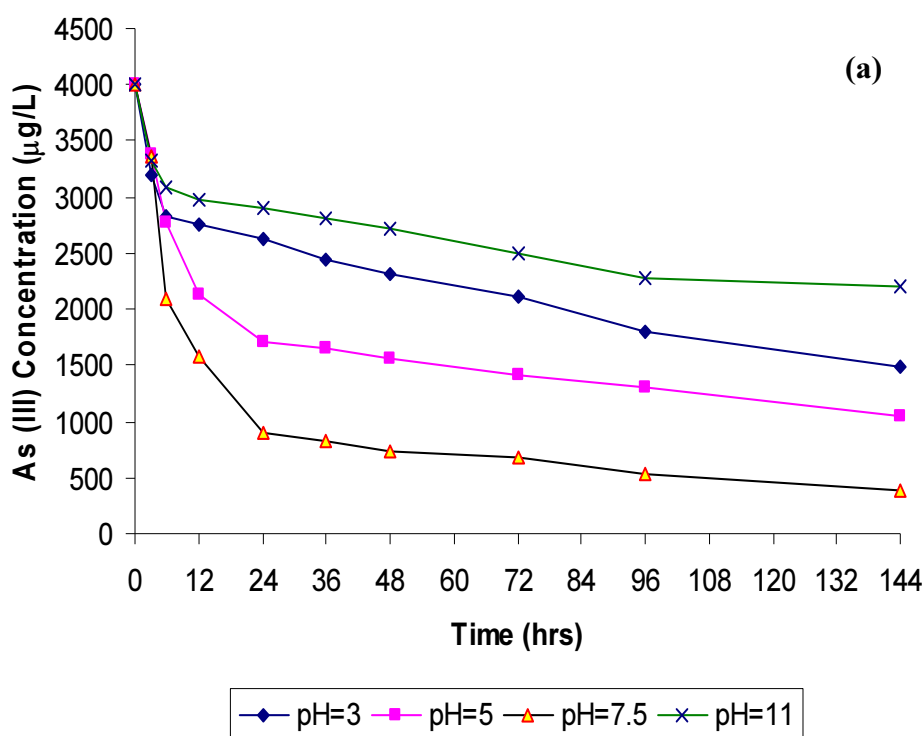


This image (Figure 6-1 (b<sub>1</sub>)) was further magnified (Figure 6-1 (b<sub>2</sub>)) and the material appeared in particulate form with a size of approximately 1  $\mu\text{m}$  and/or smaller. The maximum sizes of the sand particles appearing in Figure 6-1 are approximately 200  $\mu\text{m}$ , very similar to the size obtained from the sieve analysis (Section 4.1.2). During the SEM image analysis, some randomly selected sand particles were analysed for their composition (Table 4-1, Appendix C-1), and iron and oxygen were found to be the major elements with about 60 % and 30 % of total. These values support the percent of iron oxide (80 %) reported for NZIS (Techhistory, 2008). On the other hand the amount of arsenic adsorbed was negligible (<0.5 %) on the selected sites in comparison to the other constituents.

## 6.2 Batch Studies

### 6.2.1 Effect of pH

As mentioned (Section 4.3.1), the effect of pH on arsenic adsorption was studied in the pH range between 3 and 11 using a contact time of 144 h for both As (III) and As (V). Arsenic levels in the bulk liquid were sampled at different time intervals during the allotted contact time of 144 h and plotted as per Figure 6-2. The results from the adsorption experiments conducted at pH 7.5 (for both As (III) and As (V)) were used to observe the effect on adsorption of contact time (from 3 h to 144 h), while the different data at different pH conditions plotted in Figure 6-2 can be useful for a study of the effect of pH on kinetic studies on arsenic adsorption. Which is out of scope of this study; however, the results at pH 7.5 were used to determine the effect of contact time (kinetics) on the arsenic adsorption (Section 6.2.3).



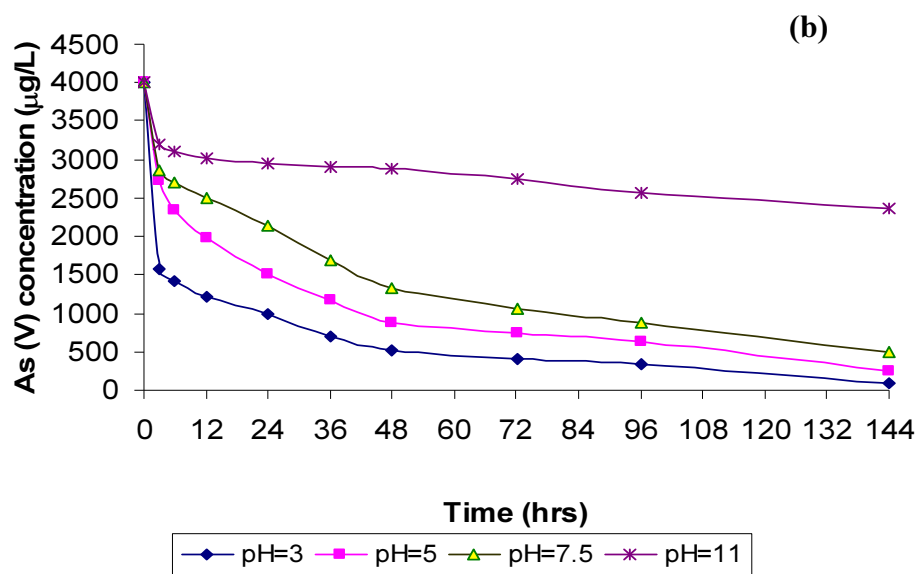


**Figure 6-2.** Effect of pH on (a) As (III) and (b) As (V) adsorption on NZIS as a function of contact time

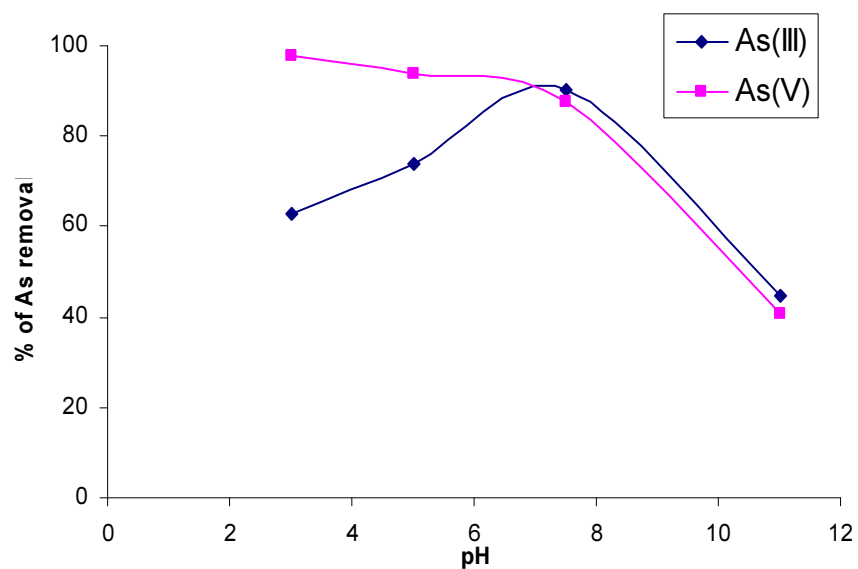


**Figure 6-3.** Effect of pH on As (III) and As (V) adsorption on NZIS at a contact time of 144 h.

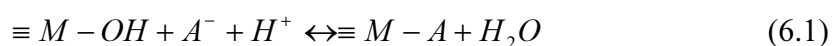
Figure 6-3 illustrates the effect of pH on arsenic (both As (III) and As (V)) adsorption on NZIS at a fixed contact time of 144 h. The results indicate that the initial pH of the solution had a substantial effect on adsorption of both the As (III) and As (V). That is, Figure 6-3 reveals that the maximum As (III) adsorption (approximately 90.0 %) on the NZIS occurred at an initial pH value of 7.5 while the As (V) adsorption reached its maximum (approximately 97.6 %) at the very low pH value of 3.

From Figure 6-3, it can be noted that the As (III) adsorption decreases at both lower and higher pH values than 7.5. When the initial pH was set at 5.0, only 74 % adsorption was observed. Further decreases in adsorption (63 %) was observed at a pH level of 3.0 and the pattern is of a decreasing nature for As (III) adsorption with decreasing pH (in the pH range 7.5 to 3.0). It is also noted that there was a sharp decrease in As (III) adsorption at a pH of 11 showing an adsorption of only 40.7 % in the allotted contact time of 144 h. Lenoble et al. (2002) reported a maximum As (III) adsorption (more than 80 %) at neutral pH values (6.0 to 8.0) using different type of iron oxides (amorphous iron hydroxide, goethite etc.), while Pattanayak et al. (2000) observed the maximum adsorption at a pH of 7.1, when using carbon-based adsorbents. As per these studies, in every case, adsorption of As (III) decreased at both lower and higher pHs than the optimum pH values reported.

Additionally, from Figure 6-3, it can be deduced that As (V) adsorption on NZIS is more favourable at an acidic pH. When the pH was in the acidic range (3.0 to 7.5) there was a slight decrease in As (V) adsorption with increasing pH, but the adsorption decreased sharply at a pH > 7.5. At a pH of 11, the adsorption of As (V) was low (40.7 %) and very close to the adsorbed amount of As (III) (44.8 %) at similar pH. Many other researchers have also noticed a similar pattern with respect to the pH effect on As (V) adsorption using various kind of adsorbents (Pattanayak, et al., 2000; Jeong, et al., 2007; Zhang, et al., 2008). For example, Jeong et al. (2007) reported a good adsorption in the pH range of 5.0 – 6.0 for As (V) adsorption when the test was done over a pH range of 5.0 to 9.0 on iron and aluminium oxide. Similarly, Pattanayak et al. (2000) and Zhang et al. (2008) observed maximum As (V) adsorption at a pH of 2.2 and 3.0 respectively when they were doing an

adsorption experiment on a carbon-based adsorbent (activated carbon and char-carbon) and modified “Red Mud” respectively.

The reason for acidic pH favouring As (V) adsorption may be the presence of more OH<sup>-</sup> ions at higher pH conditions that can compete with the As (V) anions for available sorption sites on the iron sand. NZIS contains different metal oxides in the structure and the hydroxylated surfaces of these oxides may develop charges on the surface in water. For example, the interaction between As (V) ion and metal oxide was modelled by assuming ligand exchange reactions as follows (Zhang, et al., 2008):



where “M–OH” is a surface hydroxyl group and “M–A” is the adsorbed species. Iron and aluminium oxides are the major constituent of NZIS and are also recognized as effective sites for the strong adsorption of As (V) (Deliyanni, et al., 2003; Pedersen, et al., 2006; Jeong, et al., 2007).

In contrast, the predominant species of As (III) are H<sub>3</sub>AsO<sub>3</sub> and H<sub>2</sub>AsO<sub>3</sub><sup>-</sup> in the pH range of 3.0 to 11.0 (Section 2.1.2). As the pH increases, the amount of negative arsenic species rises while the positively charged surface sites decrease up to the pH corresponding to zero potential charge of the adsorbent (pH<sub>zpc</sub>). In this connection, it can be stated that the arsenic can be adsorbed through an attraction of the neutral species to positively charged surface sites at lower pHs. However, the adsorption mechanism at higher pHs may be expressed by binding the negative species to partially positive surface (Altundogan, et al., 2002). Thus, the decrease in the adsorption yield at a pH of 11.0 may be attributed to an increase of negative surface sites as well as the amount of negative arsenic species.

Since the maximum As (III) uptake was observed at a pH of 7.5 and the As (V) uptake decreased substantially only above a pH of 7.5, all subsequent experiments were carried out at a pH of 7.5.

### 6.2.2 Effect of Contact Time (Kinetics of Arsenic Adsorption)

As mentioned (Section 4.3.1), the results from the adsorption experiments conducted at pH 7.5 (for both As (III) and As (V)) were used to observe the effect on adsorption of contact time (from 3 h to 144 h). In addition, the adsorption equilibrium time was noted. Figure 6-4 shows the percentage of arsenic removal against the contact time and it is clear that the arsenic adsorption increases rapidly with an increase in contact time up to 24 to 36 hours (depending on the As (III) or As (V) form) and then the adsorption increase slowly thereafter.

With respect to As (III), rapid adsorption was observed in the first 24 h revealing 77.3 % removal (Figure 6-4 (a)) while there was only a 12.8 % increase in the adsorption over the next 120 h. In a similar manner, 28.6 % of the As (V) adsorption occurred in the first 3 h followed by a slow adsorption in the next 33 h to reach 70 % adsorption in 36 h. Only 17.4 % adsorption of As (V) occurred in the following 108 h.

Figure 6-4 shows that adsorption equilibrium was not reached for either case at the end of the batch experiment of 6 days (144 hrs). Such a very long contact time needed to reach equilibrium suggests little chance of forming covalent bonds between the iron sand and the arsenic species. However, diffusion to the micropores in the adsorbent may have contributed to As removal (Guo, et al., 2007b).

The kinetic data indicates that the As removal (approximately 80 %) from the As (V) and As (III) solutions mainly occurred within 72 h and there was no significant change in residual As concentrations after this time up to 144 h. This means a pseudo-equilibrium of As adsorption was attained after 72 h, hence, adsorption isotherms could be conducted at a contact time of 72 h. A pseudo-equilibrium time of approximately 72 h was also observed when natural siderite was used as arsenic (both As(III) and As(V)) adsorbent (Guo, et al., 2007b). Figure 6-4 indicates that the adsorption of As (III) is better than As (V) on NZIS; however, details of the adsorption capacities are discussed in the next section (Section 6.2.3).



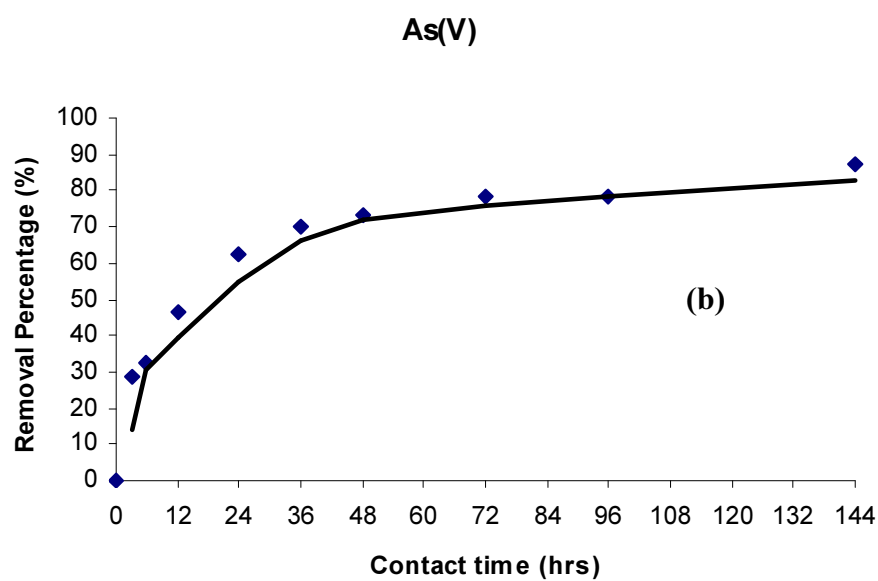
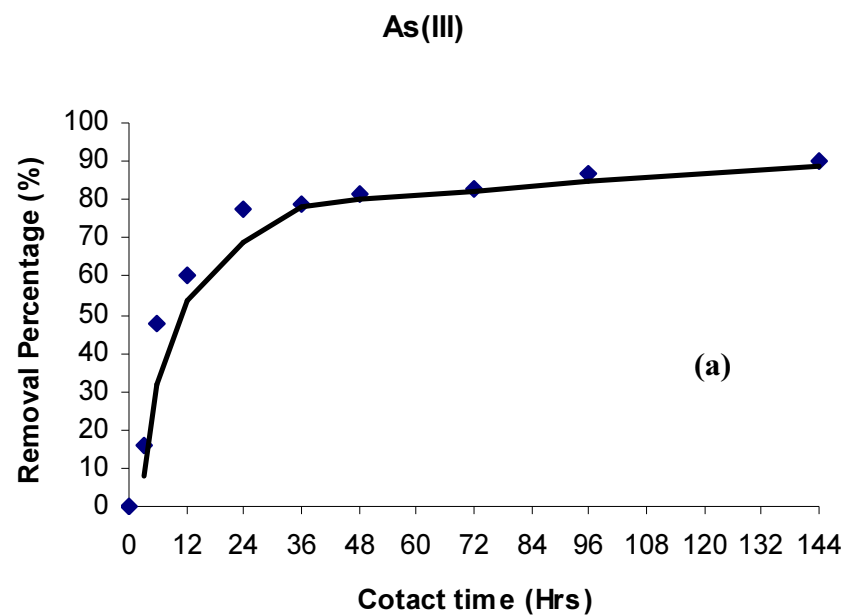


**Figure 6-4.** Effect of contact time on (a) As (III) and (b) As (V) adsorption  
(Initial As = 4000  $\mu\text{g/L}$ , NZIS dosage = 20 g/L, pH = 7.5)

### 6.2.3 Effect of Initial Arsenic Concentration (Adsorption Isotherms)

The As (III) and As (V) adsorption isotherms were conducted in batch tests with different concentrations of arsenic (concentration between 200 and 20,000 µg/L) and an adsorbent dose of 20g/L. During the batch tests, the adsorption capacities of the adsorbent were varied in the range of 9.1-623.8 and 9.6-190.8 µg/g for As (III) and As (V) respectively.

The experimental data obtained under these conditions were used to test two different adsorption models, the Langmuir and Freundlich models (Equations 6.2 and 6.3 respectively).

$$X = \frac{X_m b C_e}{1 + b C_e} \quad (\text{Langmuir}) \quad (6.2)$$

$$X = K C_e^{1/n} \quad (\text{Freundlich}) \quad (6.3)$$

Here, Equation (6.2) is the same equation mentioned in Section 5.4.2 (Equation 5.16) and the terms “b” and “X<sub>m</sub>” used in the equation have been already explained there. With respect to Equation 6.3,

“X” is the amount adsorbed (µg/g) at pseudo-equilibrium;

“C<sub>e</sub>” is the pseudo-equilibrium concentration (µg/L) in the solution;

“K” is the Freundlich constant denoting the adsorption capacity (µg/g) (L/µg)<sup>1/n</sup> of the adsorbent and;

“n” is the adsorption intensity parameter.

These isotherms can be further linearized and expressed as:

$$\frac{1}{X} = \frac{1}{b X_m C_e} + \frac{1}{X_m} \quad (6.4)$$

$$\text{Log}X = \text{Log}K + \frac{1}{n} \text{Log}C_e \quad (6.5)$$

Equation (6.4) linearizes the experimental data by plotting “1/X” against “1/C<sub>e</sub>” (Figure 6-5) and the curves perform well according to the Langmuir model with R<sup>2</sup> values of 0.9935 and 0.9992 for As(III) and As(V), respectively.

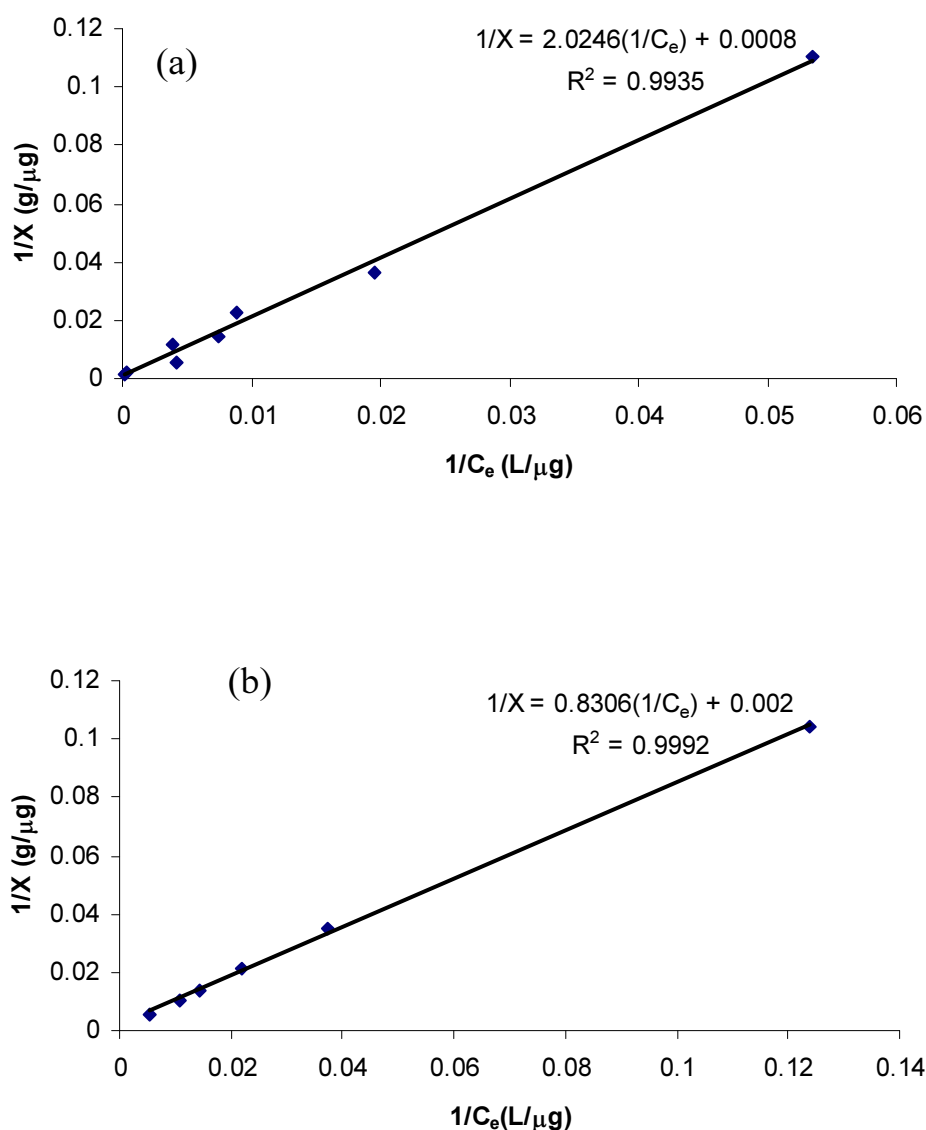


**Figure 6-5.** Linearized Langmuir plot for (a) As (III) and (b) As (V) at different initial As concentration (Background Ionic strength = 0.01 M NaCl; Adsorbent dose = 20 g/L; contact time = 72 h)

Similarly, Equation 6.5 is a linearized expression of the Freundlich isotherm. The plot of “Log(X)” and “Log (C<sub>e</sub>)” yields a straight line with a slope of “1/n” and an intercept of “Log (K)”. The logarithmic form of the Freundlich isotherms for removing both As (III) and As (V) are represented in Figure 6-6. This isotherm values also fitted well with R<sup>2</sup> values of 0.9225 and 0.9995 for As (III) and As (V), respectively.

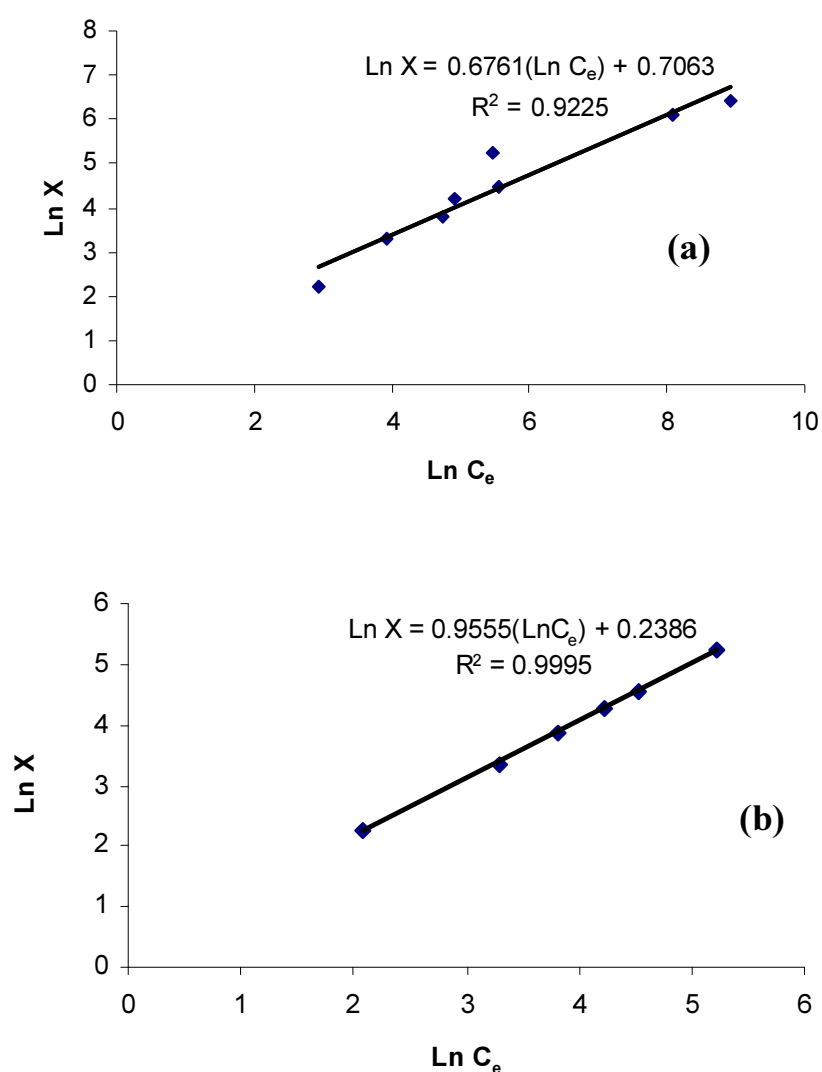


**Figure 6-6.** Linearized Freundlich plot for (a) As (III) and (b) As (V) at different initial As concentration (Background Ionic strength = 0.01 M NaCl; Adsorbent dose = 20 g/L; contact time = 72 h)

The comprehensive Langmuir and Freundlich Model results for both types of arsenic species are given in Table 6-1. The maximum arsenic adsorption capacity (known as the monolayer capacity “ $X_m$ ”) determined from the Langmuir isotherm defines the total capacity of adsorbent (NZIS) for the arsenic species. From the data, it is revealed that the theoretical adsorption capacity of the NZIS for As (III) (i.e 1,250  $\mu\text{g/g}$ ) is remarkably high (about three times) that for As(V) (500  $\mu\text{g/g}$ ). This seems to contradict the assumption of a better removal of As (V) versus As (III) (Section 2.1.4); however, some other materials containing iron oxides (e.g. hematite or goethite), hydrous ferric oxide (ferrihydrite) or hydrous ferric oxide (FeOOH) have also reported to have greater As (III) adsorption capacity than As (V) adsorption (Raven, et al., 1998; Guo, et al., 2007a, 2007b). Hence, the arsenic adsorption on these iron oxides may be due less to ionic bonds (the non-ionic form of As (III) is usually found in a normal pH range) but more to some other mechanism that need to be investigated. In addition, the iron mineral present in the NZIS (e.g. magnetite) has a high affinity for As (III).

**Table 6-1:** Correlation coefficients and adsorption isotherms parameters for both Langmuir and Freundlich Models.

As Type	Langmuir model			Freundlich model		
	$X_{\max}$ ( $\mu\text{g/g}$ )	b	$R^2$	K ( $\mu\text{g/g})(\text{L}/\mu\text{g})^{1/n}$	n	$R^2$
As (III)	1250.00	0.0004	0.9935	2.0265	1.48	0.9225
As (V)	500.00	0.0024	0.9992	1.2695	1.05	0.9995

Although some commercially-available synthetic adsorbents (for example Granular Ferric Hydroxide (a German product)) are better adsorbents (it has an arsenic removal capacity of 3,130  $\mu\text{g/g}$  for As(V) (Banerjee, et al., 2008)), few people could be expected to afford a commercial adsorbent. Many researchers thus have focused on naturally-available solid material for arsenic adsorption tests and their results are presented in Table 6-2 for comparative purposes.

From Table 6-2, it can be observed that NZIS is the best naturally-available solid material to remove both As (III) and As (V) by adsorption. Many researchers have

observed that the arsenic adsorption capacity of a normal sand can be increased by coating the sand with iron-oxide. For example, Gupta et al. (2005) reported an increase in As (III) adsorption from a value of 5.6 µg/g (i.e in uncoated sand) to 28.6 µg/g (in iron-oxide coated sand). A maximum arsenic adsorption value of 136 µg/g has been reported with iron-oxide coated sand when the test was performed with tap water containing 100 µg/L As (III) ((Thirunavukkarasu, et al., 2005).

**Table 6-2:** Comparison of maximum arsenic adsorption capacity on natural adsorbents

<b>Adsorbent</b>	<b>Arsenic species</b>	<b>Adsorption maxima (µg/g)</b>	<b>References</b>
Natural iron ores	As(V)	400	(Zhang, et al., 2004)
Ferruginous manganese ore	As(III)	537	(Chakravarty, et al., 2002)
Natural feldspar	As(V)	208	(Singh, et al., 1996)
Natural hematite	As(V)	219	(Singh, et al., 1996)
Natural manganese oxide	As(V)	200	(Ouvrard, et al., 2001)
Clinoptilolite-rich tuffs	As(V)	100	(Elizalde-Gonzalez, et al., 2001)
Normal Sand	As(III)	5.6	(Gupta, et al., 2005)
Red mud	As(III) As(V)	664 515	(Altundogan, et al., 2002)
Natural Siderite	As(III) As(V)	1,040 520	(Guo, et al., 2007b)
New Zealand Iron Sand (NZIS)	As(III) As(V)	1,250 500	This study

### 6.3 Column Study

As mentioned (Section 4.3.2) two parallel column-experiments, one for As (III) and another for As (V) were conducted to evaluate the feasibility of the New Zealand iron sand (NZIS) as a filter media for the removal of arsenic from contaminated water. In each case the influent solution was contaminated with an arsenic concentration of 400  $\mu\text{g/L}$ . The breakthrough curves for both As (III) and As (V) in the bed columns are displayed in Figure 6-7.

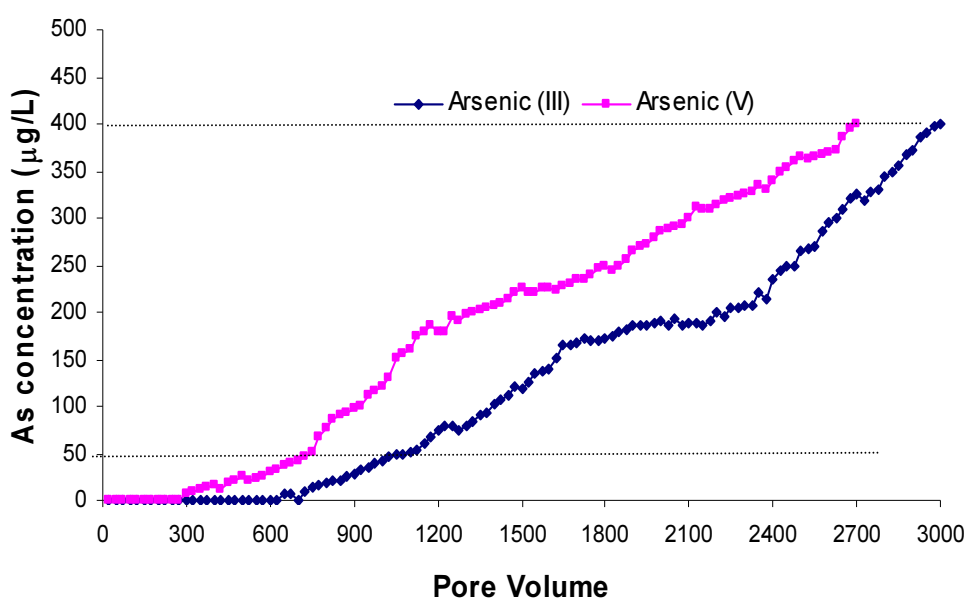


**Figure 6-7.** Development of As concentration in the effluent of the NZIS column-filter; influent concentration of solution = 400  $\mu\text{g As/L}$ , ionic strength = 0.01 M NaCl, flow rate = 1.0 mL/min.

In the case of As (III), the breakthrough was observed after a throughput of approximately 3,000 pore volumes, where a pore volume is defined as the volume of water required to replace water in the volume of a particular saturated porous media. In this case, for the NZIS bed columns, it was about 180 mL. Compared to As (III), the breakthrough for As (V) occurred slightly earlier (i.e. after a throughput of 2,700 pore volumes) which again confirmed that the removal of As (III) is easier than As (V) when NZIS is used as filter media to remove arsenic from water. Thus,

in comparison with many adsorbents being more effective in removing As (V) than As (III) (Chakraborti, et al., 2002; Mohan and Pittman, 2007; Sharma and Sohn, 2009), the NZIS studied can be used for remediating As-affected groundwater usually containing substantially As (III) without preoxidation of As (III) to As(V).

In the breakthrough curve associated with As (III) (Figure 6-7), the total arsenic in the effluent of the filter was below 10  $\mu\text{g/L}$  (a WHO Guideline value for total As) after a throughput of 700 pore volumes. A similar concentration for As (V) was observed after a throughput of pore volumes of only 300. Normally, such amounts could be used to estimate the amount of adsorbent for a filter facility as part of a feasibility study for use of the adsorbent as filter media. For example, if a family with 5 members live in an As contaminated area (As (III) = 400  $\mu\text{g/L}$ ) and it needs 25 L of treated water (5 L per capita) per day for drinking and/or cooking purposes, then in one year they need approximately 92 kg of NZIS to bring the arsenic level to a WHO standard of 10  $\mu\text{g/L}$ . Indeed, most of the arsenic contaminated countries (including Bangladesh and India) have set national standard for drinking water with a maximum total arsenic level of 50  $\mu\text{g/L}$ . This means that they would need less NZIS (approximately 60 kg) than the projected above for use as a filter media for the period of one year. It is noted that the filter media can be regenerated using several common methods; however this was not attempted during this research.



## 7 CONCLUSIONS AND RECOMMENDATIONS

### 7.1 Conclusions

The following conclusions can be drawn from this research:

#### 7.1.1 Conclusions from Denitrification Studies (Section 5)

##### SBR Conclusions

- An SBR operated with a 7 h 40 min cycle was able to remove approximately 56 % of the nitrogen via nitrification and denitrification. In this case, the influent total nitrogen was approximately 37 mg N/L ( $\text{NH}_4^+\text{-N} = 32.5 \pm 3.5$  mg-N/L,  $\text{NO}_3^-\text{-N} = 4.8 \pm 0.3$  mg-N/L) while the influent sCOD dropped from a mean value of  $285 \pm 45$  mg/L to  $29.4 \pm 4.04$  mg/L. Thus, the SBR was found to be a suitable technology for the removal of nutrients (carbon and nitrogen) from the wastewater studied.
- The SBR operated using a domestic wastewater at a C/N ratio of 4:1 was able to perform 100 % denitrification yielding a specific denitrification rate of 0.11 g  $\text{NO}_3^-\text{-N/gVSS}$  per day. Thus, the SBR provided a reliable source of denitrifying biomass for the remainder of the research.

##### Anaerobic Digester Conclusions

- The anaerobic digestion process operating at an SRT of 10 d produced a stable supply of VFAs using soy flour as a feed substrate. A favourable environment for acidogenesis was established and methanogenesis was operationally suppressed (evidenced by a low pH ranging from 4.7 to 4.9 and little gas production at 16 %  $\text{CH}_4$ ). The mean total VFAs generated in

the digester was  $5997 \pm 538$  mg/L as acetic acid with 33 % acetic, 29 % propionic, 21 % butyric, 5 % iso-valeric and 12 % valeric acid; while, the specific VFA production rate was calculated to be 0.028 mg VFA as acetic acid per mg VSS per day.

- The equivalent COD for the identified VFAs accounted for 76.5 % of the total sCOD in the digester indicating that a considerable amount of other unidentified carbon source in the digester existed in the digester effluent.
- The net sCOD produced in the digester was measured to be 5,350 mg/L with a net COD solubilization of 11.1 percentage points. This indicated that during the digestion process, particulate substrate was converted to the soluble form, and this conversion rate was expressed as the specific COD solubilization rate (0.025 mg sCOD/mg VSS per day), specific TOC solubilization rate (0.008 mg TOC/mg VSS per day), and VSS reduction (17.7 %).
- Total nitrogen in the anaerobic digestion effluent was measured to be  $440 \pm 85$  mg/L with the speciation of 1 %  $\text{NO}_3^-$ -N, 2 %  $\text{NO}_2^-$ -N, 77.3 %  $\text{NH}_4^+$ -N and 19.7 % organic nitrogen.

### Denitrification Batch Tests Conclusions

- When the specific denitrification rates were computed for different denitrification batch tests with different C/N ratios, an optimum C/N ratio was observed to be somewhere between 2 and 4. This value is somewhat higher than all the theoretical C/N ratios required for a complete denitrification using the four major VFAs identified in the digester effluent.
- It was observed that some  $\text{NO}_3^-$ -N was removed instantaneously while reacting with As (III) ( $\text{As}_2\text{O}_3$ ).

- For the denitrification batch tests, a theoretical value of alkalinity production of 5.41 mg alkalinity as CaCO<sub>3</sub> was fairly comparable to the practical value of 5.60 mg alkalinity as CaCO<sub>3</sub> produced per mg NO<sub>3</sub><sup>-</sup>-N reduction.
- Results from the series of denitrification batch tests show that the specific denitrification rate fell from 0.37 to 0.02 g NO<sub>3</sub><sup>-</sup>-N /g VSS per day as the concentration of As (III) increased from 0 to 50 mg/L. This provided a clear effect of As (III) on denitrification. This effect was further quantified with an exponential equation  $R_d = 0.278e^{-0.055C_{As}}$  ( $R^2$  value =0.9538); where, “ $R_d$ ” is the specific denitrification rate at the initial As (III) concentration of “ $C_{As}$ ”. This equation was deemed valid for an initial As (III) concentration range of 0 to 50 mg/L.
- Several initial trials showed that the effect of As (V) on denitrification was comparatively lower than that of As (III). The results from batch tests (initial concentrations of 0 to 2,000 mg As (V)/L)) indicated that the effect of As (V) was not as significant as was the case for As (III). That is, there was only a 37 % decrease in the specific denitrification rate when the initial arsenic concentration increased from 0 (specific denitrification rate was 0.34 g NO<sub>3</sub><sup>-</sup>-N /g VSS per day) to 2,000 mg/L (specific denitrification rate was 0.23 g NO<sub>3</sub><sup>-</sup>-N /g VSS per day). For the quantification of this effect of As (V), the range of the arsenic was divided into two parts, and equations were constructed; namely, for As (V) concentrations from 0 to 100 mg/L,  $R_d = 0.295e^{-0.0002C_{As(V)}}$  and for As (V) concentrations from 100 to 2,000 mg/L,  $R_d = 0.342e^{-0.0016C_{As(V)}}$  with  $R^2$  values of 0.9978 and 0.9977 respectively.
- It appeared that live denitrifying biomass was able to take up the arsenic biologically rather than physical adsorption on the surface. The calculated uptake rate for As (V), 2.10 µg/g dry biomass was slightly higher than for As (III) of 1.35 µg/g dry biomass.

### 7.1.2 Conclusion from Arsenic Adsorption (Section 6)

#### Batch Studies Conclusions

- It was confirmed that New Zealand Iron Sand (NZIS) is effective in removing both As (III) and As (V) from an arsenic contaminated water; however, the initial pH of the arsenic solution has a significant effect on the adsorption capability. When the adsorption tests were performed with an arsenic solution at an initial concentration of 4,000 µg/L and an adsorbent dose of 20 g/L at a fixed contact time of 144 h, a maximum adsorption of As (III) (approximately 90 %) occurred at pH of 7.5. In contrast, the As (V) adsorption reached its maximum value (approximately 97.6 %) at a very low pH value of 3. As (III) adsorption decreased at both lower and higher pH values than 7.5, while a slightly decreasing pattern of As (V) adsorption was observed with increasing pH until a pH value of 7.5 was reached. Following that, for As (V), adsorption sharply decreased at a pH more than 7.5.
- To reach adsorption equilibrium, a very long contact time was needed for both As (III) and As (V), showing no attainment of the ultimate adsorption until the end of batch experiment at 144 h. However, a major part of arsenic removal (approximately 80 %) occurred within a contact time of 72 h and no significant decrease in the residual arsenic concentration was observed. This suggests that a pseudo-equilibrium of As adsorption was achieved after 72 h.
- The pseudo-equilibrium adsorption values were fitted by both Langmuir and Freundlich Models (in all cases  $R^2 > 0.92$ ). From the Langmuir adsorption model, the estimated maximum adsorption capacity of the NZIS were 1,250 µg/g and 500 µg/g for As (III) and As (V) respectively. The results also indicated significantly higher (about three times) adsorption affinity towards As(III) than As(V). It was also noted that the arsenic removal capacities were many times higher than the arsenic removal capacity of 5.6 µg/g for normal sand.

## Column Studies Conclusions

- A NZIS column filter treated 700 pore volumes (PV) and 300 PV of water with 400 µg/L of As (III) and As (V) respectively to meet the WHO guideline value of 10 µg/L As. This shows that the adsorbent (i.e. NZIS) is a promising filter media to remove both As (III) and As (V) from arsenic contaminated drinking water. This particular study further supports that there is a better affinity of NZIS towards As (III) in comparison to As (V).
- The breakthrough of the arsenic solution occurred after a throughput of approximately 3,000 PV of As (III) and 2,700 PV of As (V) through the under-flow column filter with a bed height of 112 mm and a flow rate of approximately 1.0 mL/min.

## 7.2 Recommendations

- The effect of arsenic on denitrification vary depending on the carbon source using for denitrification and the presence of any other ionic substances (eg. phosphate, carbonate, calcium, magnesium etc) normally present in a domestic wastewater. Hence, further research on the effect of arsenic could be done by adding different doses of arsenic directly in a SBR (as used in this study) and monitoring the removal efficiency of nitrogen and carbon in the influent (wastewater) used.
- Normally a microbial community needs to be acclimatized to a new environment to prevent shock. Hence the effect of arsenic on an arsenic-acclimatized biomass may not be identical to the non-acclimatized biomass used in this study. Thus, a similar study can be done with a denitrifying biomass acclimatized in an arsenic contaminated (normally a very low dose in comparison to the dose to be studied for its effect) environment and the performance of the biomass can be compared.
- Naturally produced VFAs are an excellent external carbon source that may be used in a biological nutrient removal (BNR) wastewater treatment system. VFA generation in an anaerobic digester can perhaps be optimised by both changing the feed substrate (for example, rice flour, corn flour, wheat flour etc) or by adjusting the operational and environmental conditions such as loading rate, HRT/SRT, pH and temperature. From an economics point of view, it may be worthwhile to compare various waste materials (such as waste from a sugar factory, waste from a potato related food industry, waste from wheat-flour mill etc) as a feed substrate for the anaerobic digester producing the VFAs.
- It is recommended that all the unidentified carbon sources existing in the digester effluent (23.5 % of the total sCOD) be identified and the specific denitrification rate for each individual VFA be evaluated. Additionally, a

comparison of the denitrification rates between synthetic VFAs and naturally-produced VFAs could be investigated.

- To evaluate the reaction rate and to estimate the theoretical amount of  $\text{NO}_3^-$  - N consumed during the initial reaction with As (III) during its measurement, a comprehensive study could be performed which may include the thermodynamics of the chemical reaction.
- During the denitrification batch tests, the arsenic species (As (III) or As (V)) may actually have been oxidized or reduced; and the actual effect of the particular species on the denitrification rate needs more study via a species-wise analysis.
- The bio-uptake capability of arsenic might be dependant upon the species of microorganisms (e.g. bacteria, yeast or fungi) present in the wastewater, the type and initial concentration of the pollutant, the pH, and the biomass concentration and pre-treatment method. In order to make a more precise assessment of an organism's ability to uptake arsenic, some additional pre-treatment methods such as alkali or acid treatments, heat treatment etc could be investigated. Coupled with this objective, one could study the metabolism of organisms that have an ability to bio-uptake arsenic.
- Optimization of the removal of arsenic by NZIS in a column test can be performed by altering the flow rate, flow direction (up, down or horizontal), bed depth and the size of the iron sand particle. Also some kind of pre-treatment of the NZIS or mixing with other pre-tested adsorbents could be investigated to increase the arsenic removal capacity.
- One could study the adsorption mechanism of arsenic on the NZIS and the apparent effect of other competing anions present in the water.
- Since the applicability of an adsorbent depends on its desorption property and reusability, a study on the regeneration of the arsenic-saturated NZIS is also of

interest. Further research could select for a perfect regeneration agent as well as to study the effectiveness of regenerated materials on arsenic removal. In addition, a proper study on the management of the spent NZIS waste generated during the arsenic removal process is recommended.

- Further research could be done on the effect of other heavy metals on denitrification. One could also select many other types of materials as adsorbents for research into arsenic removal from water.



## REFERENCES

- Aesoy, A., and Odegaard, H. (1994). Denitrification in biofilms with biologically hydrolysed sludge as carbon source. *Water Science and Technology*, 29(10-11), 93-100.
- Ahmad, K. (2001). Report highlights widespread arsenic contamination in Bangladesh. *The Lancet*, 358 (9276), 133.
- Ahmed, M. F. (2003a). Arsenic Contamination: Regional and Global Scenario, in: *M Feroze Ahmed (Ed.), Arsenic Contamination: Bangladesh Perspective*. Centre for Water Supply and Waste Management, BUET, Dhaka, Bangladesh. pp 1-20.
- Ahmed, M. F. (2003b). Laboratory Methods for the Analysis of Arsenic in Drinking Water, in: *M Feroze Ahmed (Ed.), Arsenic Contamination: Bangladesh Perspective*. Centre for Water Supply and Waste Management, BUET, Dhaka, Bangladesh. pp 481-494.
- Ahmed, M. F. (2003c). Treatment of Arsenic Contaminated Water, in: *M Feroze Ahmed (Ed.), Arsenic Contamination: Bangladesh Perspective*. Centre for Water Supply and Waste Management, BUET, Dhaka, Bangladesh. pp 354-403.
- Akin, B. S., and Ugurlu, A. (2005). Monitoring and control of biological nutrient removal in a Sequencing Batch Reactor. *Process Biochemistry*, 40(8), 2873-2878.
- Akunna, J. C., Bizeau, C., and Moletta, R. (1993). Nitrate and nitrite reductions with anaerobic sludge using various carbon sources: glucose, glycerol, acetic acid, lactic acid and methanol. *Water Research*, 27(8), 1303-1312.

- Alexander A. T., Uli S., Stefan R., Eberhard R., Herbert M. Ambident Reactivity of the Nitrite Ion Revisited. *Angewandte Chemie International* , 44 (29), 4623-4626
- Altundogan, H. S., Altundogan, S., Tumen, F., and Bildik, M. (2002). Arsenic adsorption from aqueous solutions by activated red mud. *Waste Management*, 22(3), 357-363.
- An, D., He, Y. G., and Hu, Q. X. (1997). Poisoning by coal smoke containing arsenic and fluoride. *Fluoride*, 30, 29-32.
- Answer.com (2008). Retrieved on 25<sup>th</sup> June, 2008, from <http://www.answers.com/topic/soybean>
- APHA (1992). *Standards Methods for the Examination of Water and Wastewater*, 18<sup>th</sup> Edition, American Public Health Association / American Water Works Association/ Water Environment Federation, Washington DC.
- Aposhian, H. V., and Aposhian, M. M. (2006). Arsenic toxicology: Five questions. *Chemical Research in Toxicology*, 19(1), 1-15.
- Appelo, C. A. J., Drijver, B., Hekkenberg, R., and De Jonge, M. (1999). Modelling in situ iron removal from ground water. *Ground Water*, 37(6), 811-816.
- Appels, L., Baeyens, J., Degreve, J., and Dewil, R. (2008). Principles and potential of the anaerobic digestion of waste-activated sludge. *Progress in Energy and Combustion Science*, 34(6), 755-781.
- Arora, M. L., Barth, E. F., and Umphres, M. B. (1985). Technology evaluation of sequencing batch reactors. *Journal Water Pollution Control Federation*, 57, 867-874.

- Arslan-Alaton, I., Gursoy, B. H., and Schmidt, J.-E. (2008). Advanced oxidation of acid and reactive dyes: Effect of Fenton treatment on aerobic, anoxic and anaerobic processes. *Dyes and Pigments*, 78(2), 117-130.
- Arvin, E., and Kristensen, G. H. (1982). Effect of denitrification on the pH in biofilms. *Water Science and Technology*, 14(8), 833-848.
- ATSDR (2001). *Toxicological Profile for Arsenic, Hydrazines, Jet Fuels, Strontium and Trichloroethylene*. U.S. Department of Health and Human Services, Public Health Service, Agency for Toxic Substances and Disease Registry, Atlanta.
- AusAID (2004). *Managing arsenic in water supplies*. Interim AusAID Guidelines and Operating Procedures, Australian Government.
- Bacocchi, R., Chiavola, A., and Gavasci, R. (2005). Ion exchange equilibria of arsenic in the presence of high sulphate and nitrate concentrations. *Water Science and Technology: Water Supply*, 5(5), 67-74.
- Baeyens, W., Brauwere, A. d., Brion, N., Gieter, M. D., and Leermakers, M. (2007). Arsenic speciation in the River Zenne, Belgium. *Science of the Total Environment*, 384(1-3), 409-419.
- Bagla, P., and Kaiser, J. (1996). India's spreading health crisis draws global arsenic experts. *Science*, 274(174-175).
- Banerjee, A., Elefsiniotis, P., and Tuhtar, D. (1998). Effect of HRT and temperature on the acidogenesis of municipal primary sludge and industrial wastewater. *Water Science and Technology*, 38(8-9), 417-423.
- Banerjee, A., Elefsiniotis, P., and Tuhtar, D. (1999). The effect of addition of potato-processing wastewater on the acidogenesis of primary sludge under varied hydraulic retention time and temperature. *Journal of Biotechnology*, 72(3), 203-212.

- Banerjee, K., Amy, G. L., Prevost, M., Nour, S., Jekel, M., Gallagher, P. M., et al. (2008). Kinetic and thermodynamic aspects of adsorption of arsenic onto granular ferric hydroxide (GFH). *Water Research*, 42(13), 3371-3378.
- Banister, S. S., and Pretorius, W. A. (1998). Optimisation of primary sludge acidogenic fermentation for biological nutrient removal. *Water SA*, 24(1), 35-41.
- Baratoux, D. (2005). Origin and transport of volcanic sands in Iceland and implications for the evolution of volcanic material on Mars, in: *Proceedings of the 36<sup>th</sup> Annual Lunar and Planetary Science Conference, Houston*. pp 1603.
- Bardgett, R. D., Speir, T. W., Ross, D. J., Yeates, G. W., and Kettles, H. A. (1994). Impact of pasture contamination by copper chromium and arsenic timber preservative on soil microbial properties and nematodes. *Biology and Fertility of Soils*, 18, 71-79.
- Barker, H. A. (1981). Amino acid degradation by anaerobic bacteria. *Annual Review of Biochemistry*, 50, 23-40.
- Bell, L. C., Richardson, D. J., and Ferguson, S. J. (1990). Periplasmic and membrane-bound respiratory nitrate reductases in *Thiosphaera pantotropha*. The periplasmic enzyme catalyzes the first step in aerobic denitrification. *FEBS Letters*, 265(1-2), 85-87.
- Benjamin, M. M., Sletten, R. S., Bailey, R. P., and Bennett, T. (1996). Sorption and filtration of metals using iron-oxide-coated sand. *Water Research*, 30(11), 2609-2620.
- Berg, M., Stengel, C., Trang, P. T. K., Hung Viet, P., Sampson, M. L., Leng, M., et al. (2007). Magnitude of arsenic pollution in the Mekong and Red River Deltas - Cambodia and Vietnam. *Science of the Total Environment*, 372(2-3), 413-425.

- Bernet, N., Habouzit, F., and Moletta, R. (1996). Use of an industrial effluent as a carbon source for denitrification of a high-strength wastewater. *Applied Microbiology and Biotechnology*, 46, 92-97.
- Bhattacharya, S. K., Madura, R. L., Walling, D. A., and Farrell, J. B. (1996). Volatile solids reduction in two-phase and conventional anaerobic sludge digestion. *Water Research*, 30(5), 1041-1048.
- Bickers, P. O., and Oostrom, A. J. v. (2000). Availability for denitrification of organic carbon in meat-processing waste streams. *Bioresource Technology*, 73, 53-58.
- BIOLAB (2003). *Scientific product technical information*. Biolab, New Zealand.
- Bliss, P. J., and Barnes, D. (1986). Modelling nitrification in plant scale activated sludge. *Water Science and Technology*, 18(6), 139-148.
- Boon, B., Laudelout, H., and Barak, Y. (1962). Kinetics of nitrite oxidation by *Nitrobacter Winogradskyi*. *Biochemical Journal*, 85, 440-447.
- Borho, M., and Wilderer, P. (1996). Optimized removal of arsenic (III) by adaptation of oxidation and precipitation processes to the filtration step. *Water Science and Technology*, 34(9 pt 5), 25-31.
- Bouzas, A., Gabaldan, C., Marzal, P., Peña-roja, J. M., and Seco, A. (2002). Fermentation of municipal primary sludge: Effect of SRT and solids concentration on volatile fatty acid production. *Environmental Technology*, 23(8), 863-875.
- Bradley, P. M., and Chapelle, F. H. (1993). Arsenate inhibition of denitrification in nitrate contaminated sediments. *Soil Biology and Biochemistry*, 25(10), 1459-1462.

- Bull, M. A., Sterritt, R. M., and Lester, J. N. (1984). An evaluation of single- and separated-phase anaerobic industrial wastewater treatment in fluidized bed reactors. *Biotechnology and Bioengineering*, 26(9), 1054-1065.
- Bumbla, D. K., and Keefer, R. F. (1994). *Arsenic in the Environmen (Part 1), Cycling and Characterization*. John Wiley and Sons, Inc. Publishing, New York, U.S.A. pp 51-82.
- Bundschuh, J., Farias, B., Martin, R., Storniolo, A., Bhattacharya, P., Cortes, J., et al. (2004). Groundwater arsenic in the Chaco-Pampean Plain, Argentina: case study from Robles County, Santiago del Estero Province. *Applied Geochemistry*, 19(2), 231-243.
- Buschmann, J., Berg, M., Stengel, C., and Sampson, M. L. (2007). Arsenic and manganese contamination of drinking water resources in Cambodia: coincidence of risk areas with low relief topography. *Environment Science and Technology*, 41, 2146-2152.
- Caceres, D. D., Pino, P., Montesinos, N., Atalah, E., Amigo, H., and Loomis, D. (2005). Exposure to inorganic arsenic in drinking water and total urinary arsenic concentration in a Chilean population. *Environmental Research*, 98(2), 151-159.
- Carlsson, H., Aspegren, H., and Hilmer, A. (1996). Interactions between wastewater quality and phosphorus release in the anaerobic reactor of the EBPR process. *Water Research*, 30(6), 1517-1527.
- Carrera, J., Vicent, T., and Lafuente, F. (2003). Influence of temperature on denitrification of an industrial high-strength nitrogen wastewater in a two-sludge system. *Water SA*, 11-16.
- Chakraborti, D., Basu, G. K., Biswas, B. K., U.K. Chowdhury, Rahman, M. M., Paul, K., et al. (2001). Characterization of arsenic bearing sediments in Gangetic delta of West Bengal-India, in: *W.R. Chappell, C.O. Abernathy*,

*R.L. Calderon (Eds.), Proceedings of the 5<sup>th</sup> International Conference on Arsenic Exposure and Health Effects*, Elsevier Publishing. pp. 27-52.

Chakraborti, D., Rahman, M. M., Paul, K., Chowdhury, U. K., Sengupta, M. K., Lodh, D., et al. (2002). Arsenic calamity in the Indian subcontinent: What lessons have been learned? *Talanta*, 58(1), 3-22.

Chakravarty, S., Dureja, V., Bhattacharyya, G., Maity, S., and Bhattacharjee, S. (2002). Removal of arsenic from groundwater using low cost ferruginous manganese ore. *Water Research*, 36(3), 625-632.

Chanakya, H. N., Borgaonkar, S., Rajan, M. G. C., and Wahi, M. (1992). Two-phase anaerobic digestion of water hyacinth or urban garbage. *Bioresource Technology*, 42(2), 123-131.

Chang, K. N., Lee, T. C., Tam, M. F., Chen, Y. C., Lee, L. W., Lee, S. Y., et al. (2003). Identification of galectin I and thioredoxin peroxidase II as two arsenic-binding proteins in Chinese hamster ovary cells. *Biochemical Journal*, 371(2), 495-503.

Chen, W., Parette, R., Zou, J., Cannon, F. S., and Dempsey, B. A. (2007a). Arsenic removal by iron-modified activated carbon. *Water Research*, 41(9), 1851-1858.

Chen, Y., Jiang, S., Yuan, H., Zhou, Q., and Gu, G. (2007b). Hydrolysis and acidification of waste activated sludge at different pHs. *Water Research*, 41(3), 683-689.

Chiu, Y. C., Lee, L. L., Chang, C. N., and Chao, A. C. (2007). Control of carbon and ammonium ratio for simultaneous nitrification and denitrification in a sequencing batch bioreactor. *International Biodeterioration and Biodegradation*, 59(1), 1-7.

- Choong, T. S. Y., Chuah, T. G., Robiah, Y., Gregory Koay, F. L., and Azni, I. (2007). Arsenic toxicity, health hazards and removal techniques from water: an overview. *Desalination*, 217(1-3), 139-166.
- Chuang, C. L., Fan, M., Xu, M., Brown, R. C., Sung, S., Saha, B., et al. (2005). Adsorption of arsenic (V) by activated carbon prepared from oat hulls. *Chemosphere*, 61(4), 478-483.
- Cohen, A., Zoetemeyer, R. J., Van Deursen, A., and Van Andel, J. G. (1979). Anaerobic digestion of glucose with separated acid production and methane formation. *Water Research*, 13(7), 571-580.
- Constantin, H., and Fick, M. (1997). Influence of C-sources on the denitrification rate of a high-nitrate concentrated industrial wastewater. *Water Research*, 31(3), 583-589.
- Cooney, M., Maynard, N., Christopher, C., and Benemann, J. (2007). Two-phase anaerobic digestion for production of hydrogen-methane mixtures. *Bioresource Technology*, 98, 2641-2651.
- Craig, R. A., and Cook, G. M. (2004). Isolation and Characterization of Arsenate-Reducing bacteria from Arsenic-contaminated sites in New Zealand. *Current Microbiology*, 48(341-347).
- Cruz-Sanchez, E., Alvarez-Castro, J. F., Ramirez-Picado, J. A., and Matutes-Aquino, J. A. (2004). Study of titanomagnetite sands from Costa Rica. *Journal of Alloys and Compounds*, 369(1-2), 265-268.
- Cullen, W. R., Li, H., Pergantis, S. A., Eigendorf, G. K., and Harrison, L. G. (1994). The methylation of arsenate by a marine alga *Polyphysa Peniculus* in the presence of L-methionine-methyl-d<sub>3</sub>. *Chemosphere*, 28(5), 1009-1019.



- Danesh, S., and Oleszkiewicz, J. A. (1997). Volatile fatty acid production and uptake in biological nutrient removal systems with process separation. *Water Environment Research*, 69(6), 1106-1111.
- Deliyanni, E. A., Bakoyannakis, D. N., Zouboulis, A. I., and Matis, K. A. (2003). Sorption of As(V) ions by akaganeite-type nano-crystals. *Chemosphere*, 50(1), 155-163.
- Delwiche, C. C. (1956). Denitrification, in: *McElory and Glass (Eds.), A Symposium of Inorganic Nitrogen Metabolisms*. Johns Hopkins Press Publishing, Baltimore, U.S.A., pp 233.
- Dick, R. I., and Vesilind, P. A. (1969). The SVI - What is it? *Journal Water Pollution Control Federation*, 41, 1285.
- Dinopoulou, G., Rudd, P., and Lester, J. (1988). Anaerobic digestion of complex wastewater and the influence of operational parameters on reactor performance. *Biotechnology and Bioengineering*, 31, 958-968.
- Done, A. K., and Peart, A. J. (1971). Acute toxicities of arsenical herbicides. *Clinical Toxicology*, 4(3), 343-355.
- Driehaus, W., and Dupont, F. (2005). Arsenic removal - Solutions for a world wide health problem using iron based adsorbents. *Journal Europeen d'Hydrologie*, 36(2), 119-132.
- Driehaus, W., Seith, R., and Jekel, M. (1995). Oxidation of arsenate (III) with manganese oxides in water treatment. *Water Research*, 29(1), 297-305.
- Eastman, J., and Ferguson, J. (1981). Solubilisation of organic carbon during the acid phase anaerobic digestion. *Journal Water Pollution Control Federation*, 53, 352-366.

- Eckenfelder, W. W. J., and Santhanam, C. J. (1981). *Sludge Treatment*. Marcel Dekker, Inc. Publishing, New York, U.S.A.
- Elefsiniotis, P., & Li, D. (2006). The effect of temperature and carbon source on denitrification using volatile fatty acids. *Biochemical Engineering Journal*, 28(2), 148-155.
- Elefsiniotis, P., and Oldham, W. (1994a). Substrate degradation patterns in acid phase of anaerobic digestion of municipal primary sludge. *Environmental Technology*, 15, 741-751.
- Elefsiniotis, P., and Oldham, W. K. (1994b). Anaerobic acidogenesis of primary sludge: The role of solids retention time. *Biotechnology and Bioengineering*, 44(1), 7-13.
- Elefsiniotis, P., & Oldham, W. K. (1994c). Influence of pH on the acid-phase anaerobic digestion of primary sludge. *Journal of Chemical Technology and Biotechnology*, 60(1), 89-96.
- Elefsiniotis, P., Wareham, D. G., and Oldham, W. K. (1996). Particulate organic carbon stabilization in an acid-phase up-flow anaerobic sludge blanket system. *Environmental Science and Technology*, 30(5), 1508-1514.
- Elefsiniotis, P., Wareham, D. G., and Smith, M. O. (2004). Use of volatile fatty acids from an acid-phase digester for denitrification. *Journal of Biotechnology*, 114(3), 289-297.
- Elefsiniotis, P., Wareham, D. G., and Smith, M. O. (2005). Effect of a starch-rich industrial wastewater on the acid-phase anaerobic digestion process. *Water Environment Research*, 77(4), 366-371.
- Elizalde-Gonzalez, M. P., Mattusch, J., Wennrich, R., and Morgenstern, P. (2001). Uptake of arsenite and arsenate by clinoptilote-rich tuffs. *Microporous and Mesoporous Materials*, 46(2-3), 277-286.

- Fan, A. M., and Steinberg, V. E. (1996). Health Implications of Nitrate and Nitrite in Drinking Water: An Update on Methemoglobinemia Occurrence and Reproductive and Developmental Toxicity. *Regulatory Toxicology and Pharmacology*, 23(1), 35-43.
- Fang, H. H. P., and Liu, H. (2002). Effect of pH on hydrogen production from glucose by a mixed culture. *Bioresource Technology*, 82(1), 87-93.
- Farabegoli, G., Carucci, A., Majone, M., and Rolle, E. (2004). Biological treatment of tannery wastewater in the presence of chromium. *Journal of Environmental Management*, 71(4), 345-349.
- Fass, S., Ganaye, V., Urbain, V., Manem, J., and Block, J. C. (1994). Volatile fatty acids as organic carbon sources in denitrification. *Environmental Technology*, 15(5), 459-467.
- Feng, H., Hu, L., Mahmood, Q., Fang, C., Qiu, C., & Shen, D. (2009). Effects of temperature and feed strength on a carrier anaerobic baffled reactor treating dilute wastewater. *Desalination*, 238(1-3), 111-121.
- Ferguson, J. F., and Gavis, J. (1972). A review of the arsenic cycle in natural waters. *Water Research*, 6(11), 1259-1274.
- Flora, J. R. V., Suidan, M. T., Biswas, P., and Sayles, G. D. (1993). Modeling substrate transport into biofilms: Role of multiple ions and pH effects. *Journal of Environmental Engineering*, 119(5), 908-930.
- Follett, R. F. (Ed.). (1989). *Nitrogen management and ground water protection*: Elsevier Science Publishing Company Inc., New York, U.S.A.
- Fontenot, Q., Bonvillain, C., Kilgen, M., and Boopathy, R. (2007). Effects of temperature, salinity, and carbon: nitrogen ratio on sequencing batch reactor treating shrimp aquaculture wastewater. *Bioresource Technology*, 98(9), 1700-1703.

- Forster-Carneiro, T., Perez, M., Romero, L. I., (2008). Thermophilic anaerobic digestion of source-sorted organic fraction of municipal solid waste. *Bioresource Technology*, 99 (17), 6763–6770.
- Fraser, P., and Chilvers, C. (1980). Health aspects of nitrate in drinking water *Science of the Total Environment*, 18, 103-116.
- Gerardi, M. H. (2002). *Nitrification and denitrification in the activated sludge process*: John Wiley and Sons, Inc. Publishing, New York, U.S.A., pp 147-150.
- Ghafari, S., Hasan, M., and Aroua, M. K. (2009). Improvement of autohydrogenotrophic nitrite reduction rate through optimization of pH and sodium bicarbonate dose in batch experiments. *Journal of Bioscience and Bioengineering*, 107(3), 275-280.
- Ghosh, S. (1987). Improved sludge gasification by two-phase anaerobic digestion. *Journal of Environmental Engineering*, 116(6).
- Ghosh, S., and Pohland, F. G. (1974). Kinetics of substrate assimilation and product formation in anaerobic digestion. *Journal Water Pollution Control Federation*, 46(4), 748-759.
- Glass, C., and Silverstein, J. (1998). Denitrification kinetics of high nitrate concentration water: pH effect on inhibition and nitrite accumulation. *Water Research*, 32(2), 831-839.
- Goessler, W., and Kuehnelt, D. (2002). Analytical methods for the determination of arsenic and arsenic compounds in the environment, in: *W.T. Frankenberger Jr. (ed.) Environmental Chemistry of Arsenic*, Marcel Dekker Inc. Publishing, New York, U.S.A., pp 27-50.
- Goldberg, S. (2002). Competitive adsorption of arsenate and arsenite on oxides and clay minerals. *Soil Science Society of America Journal*, 66(2), 413-421.

- Goldberg, S., and Johnston, C. T. (2001). Mechanisms of arsenic adsorption on amorphous oxides evaluated using macroscopic measurements, vibrational spectroscopy, and surface complexation modeling. *Journal of Colloid and Interface Science*, 234(1), 204-216.
- Gomez, M. A., Gonzalez-Lopez, J., and Hontoria-Garcia, E. (2000). Influence of carbon source on nitrate removal of contaminated groundwater in a denitrifying submerged filter. *Journal of Hazardous Materials*, 80(1-3), 69-80.
- Grady, C. P. L., and Lim, H. C. (1980). *Anaerobic Digestion and Anaerobic Contact: Pollution Engineering and Technology. Biological Wastewater Treatment, Theory and Applications (Vol. 12)*. Marcel Dekker, Inc., Publishing, New York, U.S.A., pp 833-886.
- Gray, N. F. (2004). *Biology of wastewater treatment: Series of Environmental Science and management (2<sup>nd</sup> edition, Vol. 4)*. Imperial College Press, Publishing, London, UK., pp 743-777.
- Gu, Z., Fang, J., and Deng, B. (2005). Preparation and evaluation of GAC-based iron-containing adsorbents for arsenic removal. *Environmental Science and Technology*, 39(10), 3833-3843.
- Gumaelius, L., Smith, E. H., and Dalhammar, G. (1996). Potential biomarker for denitrification of wastewaters: Effects of process variables and cadmium toxicity. *Water Research*, 30(12), 3025-3031.
- Guo, H., Stuben, D., and Berner, Z. (2007a). Arsenic removal from water using natural iron mineral-quartz sand columns. *Science of the Total Environment*, 377(2-3), 142-151.
- Guo, H., Stuben, D., and Berner, Z. (2007b). Removal of arsenic from aqueous solution by natural siderite and hematite. *Applied Geochemistry*, 22(5), 1039-1051.

- Guo, H., Wang, Y., Shpeizer, G. M., and Yan, S. (2003). Natural occurrence of arsenic in shallow groundwater, Shanyin, Datong Basin, China. *Journal of Environmental Science and Health - Part A Toxic/Hazardous Substances and Environmental Engineering*, 38(11), 2565-2580.
- Guo, X. J., Fujino, Y., Kaneko, S., Wu, K. G., Xia, Y. J., and Yoshimura, T. (2001). Arsenic contamination of groundwater and prevalence of arsenical dermatosis in the Hetao plain area, Inner Mongolia, China. *Molecular and Cellular Biochemistry* 222(137-140).
- Gupta, V. K., Saini, V. K., and Jain, N. (2005). Adsorption of As(III) from aqueous solutions by iron oxide-coated sand. *Journal of Colloid and Interface Science*, 288(1), 55-60.
- HACH (1995). *DR/2000 Spectrophotometer Instrument Manual, for Use With Software Version 3*. Hach Company, Loveland Colorado, USA.
- HACH (1997). *Water Analysis Hand Book, 3<sup>rd</sup> Edition*. Hach Company, Loveland Colorado, USA.
- HACH (2003). *Water Analysis Hand Book, 4<sup>th</sup> Edition, Revision 2*. Hach Company, Loveland Colorado, USA.
- Halttunen, T., Finell, M., and Salminen, S. (2007). Arsenic removal by native and chemically modified lactic acid bacteria. *International Journal of Food Microbiology*, 120(1-2), 173-178.
- Hanaki, K., Matsuo, T., Nagase, M., and Tabata, Y. (1987). Evaluation of effectiveness of two-phase anaerobic digestion process degrading complex substrate. *Water Science and Technology*, 19, 311-322.
- Hatziconstantinou, G. J., Yannakopoulos, P., and Andreadakis, A. (1996). Primary sludge hydrolysis for biological nutrient removal. *Water Science and Technology*, 34(1-2 -2 pt 1), 417-423.

- Haug, R., Lebrun, T., and Totorici, L. (1983). Thermal pretreatment of sludges - a field demonstration. *Journal Water Pollution Control Federation*, 55(1), 23-34.
- Hawkes, D., Horton, R., and Stafford, D. A. (1978). The use of anaerobic digestion for the treatment and recycling of organic wastes. *Conservation and Recycling*, 2(2), 181-195.
- He, X. (2006). *The use of naturally generated volatile fatty acids for pesticide removal during the denitrification process*. Unpublished PhD Thesis, University of Canterbury, New Zealand, Christchurch.
- Her, J. J., and Huang, J. S. (1995). Influences of carbon source and C/N ratio on nitrate/nitrite denitrification and carbon breakthrough. *Bioresource Technology*, 54(1), 45-51.
- Holman, J. B. (2004). *The application of pH and ORP process control parameters within the aerobic denitrification process*. Unpublished PhD Thesis, University of Canterbury, New Zealand, Christchurch.
- Holman, J. B., and Wareham, D. G. (2003). Oxidation-reduction potential as a monitoring tool in a low dissolved oxygen wastewater treatment process. *Environmental Engineering*, 129(1), 52-58.
- Holman, J. B., & Wareham, D. G. (2005). COD, ammonia and dissolved oxygen time profiles in the simultaneous nitrification/denitrification process. *Biochemical Engineering Journal*, 22(2), 125-133.
- Holtan-Hartwig, L., Bechmann, M., Risnes Hoyas, T., Linjordet, R., and Reier Bakken, L. (2002). Heavy metals tolerance of soil denitrifying communities: N<sub>2</sub>O dynamics. *Soil Biology and Biochemistry*, 34(8), 1181-1190.

- Horan, N. J., Fletcher, L., Betmal, S. M., Wilks, S. A., and Keevil, C. W. (2004). Die-off of enteric bacterial pathogens during mesophilic anaerobic digestion. *Water Research*, 38(5), 1113-1120.
- Horiuchi, J., Shimizu, T., Tada, K., Kanno, T., and Kobayashi, M. (2002). Selective production of organic acids in anaerobic acid reactor by pH control. *Bioresource Technology*, 82, 209-213.
- Hug, S. J., Canonica, L., Wegelin, M., Gechter, D., and Von Gunten, U. (2001). Solar oxidation and removal of arsenic at circum-neutral pH in iron containing waters. *Environmental Science and Technology*, 35(10), 2114-2121.
- Hughes, M. F. (2002). Arsenic toxicity and potential mechanisms of action. *Toxicology Letters*, 133(1), 1-16.
- Hwang, M. H., Jang, N. J., Hyun, S. H., and Kim, I. S. (2004). Anaerobic bio-hydrogen production from ethanol fermentation: The role of pH. *Journal of Biotechnology*, 111(3), 297-309.
- IARC (1987). International Agency for Research on Cancer. Arsenic and arsenic compounds (Group 1). In: *IARC monographs on the evaluation of the carcinogenic risks to humans*. Retrieved on 6<sup>th</sup> February 2008 from <http://193.51.164.11/htdocs/monographs/suppl7/arsenic.html>.
- IETC (2008). *International Source Book on Environmentally Sound Technologies for Wastewater and Stormwater Management*. International Environmental Technology Centre, Newsletter and Technical Publications. United Nations Environment Programme (UNEP). Retrieved on 6<sup>th</sup> February, 2008 from [http://www.unep.or.jp/Ietc/Publications/TechPublications/TechPub-15/main\\_index.asp](http://www.unep.or.jp/Ietc/Publications/TechPublications/TechPub-15/main_index.asp)
- IPCS (2001). The International Programme on Chemical Safety (IPCS). *Environmental Health Criteria Series*, No. 224: *Arsenic and arsenic*



compounds (2<sup>nd</sup> edition), WHO, Geneva, Retrieved on 25<sup>th</sup> June, 2008, from [http://www.who.int/ipcs/publications/ehc/ehc\\_224/en/](http://www.who.int/ipcs/publications/ehc/ehc_224/en/)

- Irvine, R. L., and Busch, A. W. (1979). Sequencing batch biological reactors - an overview. *Journal Water Pollution Control Federation*, 51, 235-243.
- Irvine, R. L., Murthy, D. V. S., Arora, M. L., Copeman, J. L., and Heidman, J. A. (1987). Analysis of full-scale SBR operation at Grundy Center, Iowa. *Journal Water Pollution Control Federation*, 59, 132-138.
- IWA (2002). *Anaerobic Digestion Model No. 1(ADM1). Scientific and Technical Report No. 13*. Task group for mathematical modelling of Anaerobic Digestion Process, International Water Association (IWA).
- Jekel, M. R. (1994). Removal of arsenic in drinking water treatment, in: *J.O. Nriagu (Ed.) Arsenic in the Environment, Part 1: Cycling and Characterization*, John Wiley and Sons, Inc., Publishing, New York, U.S.A., pp 119-132.
- Jeong, Y., Fan, M., Singh, S., Chuang, C.-L., Saha, B., and Hans van Leeuwen, J. (2007). Evaluation of iron oxide and aluminium oxide as potential arsenic (V) adsorbents. *Chemical Engineering and Processing: Process Intensification*, 46(10), 1030-1039.
- Kartinen Jr, E. O., and Martin, C. J. (1995). Overview of arsenic removal processes. *Desalination*, 103(1-2), 79-88.
- Kiff, R. J. (1972). The ecology of nitrification - denitrification systems in activated sludge systems. *Journal Water Pollution Control Federation*, 71, 475-484.
- Kim, J. K., Oh, B. R., Chun, Y. N., and Kim, S. W. (2006). Effects of temperature and hydraulic retention time on anaerobic digestion of food waste. *Journal of Bioscience and Bioengineering*, 102(4), 328-332.

- Kim, M., Gomec, C. Y., Ahn, Y., and Speece, R. E. (2003). Hydrolysis and acidogenesis of particulate organic material in mesophilic and thermophilic anaerobic digestion. *Environmental Technology*, 24(9), 1183-1190.
- Kim, M. J., and Nriagu, J. (2000). Oxidation of arsenite in groundwater using ozone and oxygen. *Science of the Total Environment*, 247(1), 71-79.
- Kocar, B. D., and Inskeep, W. P. (2003). Photochemical oxidation of As (III) in ferrioxalate solutions. *Environmental Science and Technology*, 37(8), 1581-1588.
- Korte, N. E., and Fernando, Q. (1991). A review of arsenic (III) in groundwater. *Critical Reviews in Environmental Control*, 21(1), 1-39.
- Kostal, J., Yang, R., Wu, C. H., Mulchandani, A., and Chen, W. (2004). Enhanced arsenic accumulation in engineered bacterial cells expressing *ArsR*. *Applied and Environmental Microbiology*, 70(8), 4582-4587.
- Kwong, T. S., and Fang, H. H. P. (1997). Anaerobic degradation of cornstarch in waste water in two upflow reactors. *Journal of Environmental Engineering*, 122, 9-17.
- Labbe, N., Parent, S., and Villemur, R. (2003). Addition of trace metals increases denitrification rate in closed marine systems. *Water Research*, 37(4), 914-920.
- Lackovic, J. A., Nikolaidis, N. P., and Dobbs, G. M. (2000). Inorganic arsenic removal by zero-valent iron. *Environmental Engineering Science*, 17(1), 29-39.
- Lee, H., and Choi, W. (2002). Photocatalytic oxidation of arsenite in TiO<sub>2</sub> suspension: Kinetics and mechanisms. *Environmental Science and Technology*, 36(17), 3872-3878.

- Lee, S. J. (2008). *Relationship between oxidation reduction potential (ORP) and volatile fatty acid (VFA) production in the acid-phase anaerobic digestion process*. Unpublished Master Thesis, University of Canterbury, New Zealand, Christchurch.
- Lenoble, V., Bouras, O., Deluchat, V., Serpaud, B., and Bollinger, J.-C. (2002). Arsenic Adsorption onto Pillared Clays and Iron Oxides. *Journal of Colloid and Interface Science*, 255(1), 52-58.
- Li, B., and Irvin, S. (2007). The comparison of alkalinity and ORP as indicators for nitrification and denitrification in a sequencing batch reactor (SBR). *Biochemical Engineering Journal*, 34(3), 248-255.
- Li, D. (2001). Denitrification Using Volatile Fatty Acids (VFAs): *The Effects of Nitrate Concentrations, Types of VFAs, C/N Ratio and Temperature*. Unpublished Master Thesis, University of Auckland, New Zealand, Auckland.
- Li, D. H., and Ganczarczyk, J. J. (1986). Physical characteristics of activated sludge flocs. *Critical Reviews in Environmental Control*, 17(1), 53-87.
- Li, Y., and Noike, T. (1992). Upgrading of anaerobic digestion of waste activated sludge by thermal treatment. *Water Science and Technology*, 26(3-4), 857-866.
- Liao, B. Q., Droppo, I. G., Leppard, G. G., and Liss, S. N. (2006). Effect of solids retention time on structure and characteristics of sludge flocs in sequencing batch reactors. *Water Research*, 40(13), 2583-2591.
- Lin, S., Del Razo, L. M., Styblo, M., Wang, C., Cullen, W. R., and Thomas, D. J. (2001). Arsenicals inhibit thioredoxin reductase in cultured rat hepatocytes. *Chemical Research in Toxicology*, 14(3), 305-311.

- Lin, T. F., and Wu, J. K. (2001). Adsorption of arsenite and arsenate within activated alumina grains: equilibrium and kinetics. *Water Research*, 35(8), 2049-2057.
- Liu, D., Liu, D., Zeng, R. J., and Angelidaki, I. (2006). Hydrogen and methane production from household solid waste in the two-stage fermentation process. *Water Research*, 40(11), 2230-2236.
- Llabres, P., Pavan, P., Battistioni, P., Cecchi, F., and Mata-Alvarez, J. (1999). The use of organic fraction of municipal solid waste hydrolysis products for biological nutrient removal in wastewater treatment plants. *Water Research*, 33(1), 214-222.
- Lutzenkirchen, J. (1997). Ionic Strength Effects on Cation Sorption to Oxides: Macroscopic Observations and Their Significance in Microscopic Interpretation *Journal of Colloid and Interface Science*, 195 (1) 149-155
- MacDonald, R. S., Guo, J., Copeland, J., Browning Jr, J. D., Sleper, D., Rottinghaus, G. E., et al. (2005). Environmental influences on isoflavones and saponins in soybeans and their role in colon cancer. *Journal of Nutrition*, 135(5), 1239-1242.
- Maharaj, I., and Elefsiniotis, P. (2001). The role of HRT and low temperature on the acid-phase anaerobic digestion of municipal and industrial wastewaters. *Bioresource Technology*, 76, 191-197.
- Manning, B. A., Fendorf, S. E., Bostick, B., and Suarez, D. L. (2002). Arsenic (III) oxidation and arsenic(V) adsorption reactions on synthetic birnessite. *Environmental Science and Technology*, 36(5), 976-981.
- Manning, B. A., Fendorf, S. E., and Goldberg, S. (1998). Surface structures and stability of arsenic(III) on goethite: Spectroscopic evidence for inner-sphere complexes. *Environmental Science and Technology*, 32(16), 2383-2388.

- Manning, B. A., and Goldberg, S. (1997). Adsorption and stability of arsenic(III) at the clay mineral-water interface. *Environmental Science and Technology*, 31(7), 2005-2011.
- Marty, B. (1984). Microbiology of anaerobic digestion, in: A.M. Bruce, A. Kouzeli-Katsiri and P.J. Newman (Eds.), *Anaerobic Digestion of Sewage Sludge and Organic Agricultural Wastes*. Elsevier Applied Science Publishers, London, UK., pp 72-89.
- Meharg, A. A., and Hartley-Whitaker, J. (2002). Arsenic uptake and metabolism in arsenic resistant and non-resistant plant species. *New Phytologist*, 154(1), 29-43.
- Meng, X., Bang, S., and Korfiatis, G. P. (2000). Effects of silicate, sulfate, and carbonate on arsenic removal by ferric chloride. *Water Research*, 34(4), 1255-1261.
- Metcalf, and Eddy (1991). *Wastewater Engineering. Treatment, Disposal and Reuse*. McGraw-Hill, Publishing. New York, U.S.A.
- Moat, A. G., and Foster, J. W. (1988). *Microbial Physiology*(2<sup>nd</sup> Edition). John Wiley and Sons, Inc. Publishing, New York, U.S.A.
- Mohan, D., and Pittman, J. C. U. (2007). Arsenic removal from water/wastewater using adsorbents-A critical review. *Journal of Hazardous Materials*, 142(1-2), 1-53.
- Mohan, D., Pittman Jr, C. U., Bricka, M., Smith, F., Yancey, B., Mohammad, J., et al. (2007). Sorption of arsenic, cadmium, and lead by chars produced from fast pyrolysis of wood and bark during bio-oil production. *Journal of Colloid and Interface Science*, 310(1), 57-73.

- Mondal, P., Majumder, C. B., and Mohanty, B. (2006). Laboratory based approaches for arsenic remediation from contaminated water: Recent developments. *Journal of Hazardous Materials*, 137(1), 464-479.
- Monteith, H. D., Bridle, T. R., and Sutton, P. M. (1980). Industrial waste carbon sources for biological denitrification. *Progress in Water Technology*, 12(6), 127-141.
- Mosey, F. E., and Fernandes, X. A. (1989). Patterns of hydrogen in biogas from the anaerobic digestion of milk sugars. *Water Science and Technology*, 21(12), 1551.
- Moussa, M. S., Hooijmans, C. M., Lubberding, H. J., Gijzen, H. J., and Van Loosdrecht, M. C. M. (2005). Modelling nitrification, heterotrophic growth and predation in activated sludge. *Water Research*, 39(20), 5080-5098.
- Munch, E. V., Lant, P., and Keller, J. (1996). Simultaneous nitrification and denitrification in bench-scale sequencing batch reactors. *Water Research*, 30(2), 277-284.
- Muniz, G., Fierro, V., Celzard, A., Furdin, G., Gonzalez-Sanchez, G., and Ballinas, M. L. (2009). Synthesis, characterization and performance in arsenic removal of iron-doped activated carbons prepared by impregnation with Fe (III) and Fe (II). *Journal of Hazardous Materials*, 165(1-3), 893-902.
- Murcott, s. (2001). A Comprehensive Review of Low-Cost, Well Water Treatment Technologies for Arsenic Removal, in: *W.R. Chappell, C.O. Abernathy and R.L. Calderon (Eds.) Arsenic Exposure and Health Effects IV. Proceedings of the 4<sup>th</sup> International Conference on Arsenic Exposure and Health Effects*. Elsevier Science Ltd Publishing, pp 1-500.
- Murugesan, G. S., Sathishkumar, M., and Swaminathan, K. (2006). Arsenic removal from groundwater by pre-treated waste tea fungal biomass. *Bioresource Technology*, 97(3), 483-487.

- Ndon, U. J., and Dague, R. R. (1997). Effects of temperature and hydraulic retention time on anaerobic sequencing batch reactor treatment of low-strength wastewater. *Water Research*, 31(10), 2455-2466.
- Ng, J. C. (2005). Environmental contamination of arsenic and its toxicological impact on humans. *Environmental Chemistry*, 2(3), 146-160.
- Ng, J. C., Wang, J., and Shraim, A. (2003). A global health problem caused by arsenic from natural sources. *Chemosphere*, 52(9), 1353-1359.
- Novaes, R. F. V. (1986). Microbiology of anaerobic digestion. *Water Science and Technology*, 18(12), 1-14.
- NRC (1999). *Arsenic in Drinking Water*, National Research Council (NRC) Report. National Academy Press, Washington, DC, U.S.A.
- Nriagu, J. O. (2002). Arsenic poisoning through the ages, in: *Frankenberger Jr., W.T. (Ed.), Environmental Chemistry of Arsenic*. Marcel Dekker Publishing, New York, U.S.A., pp1-26.
- NZMIA (2008). Information from the website of New Zealand Minerals Industry Association. Retrieved on 1<sup>st</sup> June, 2008, from <http://www.minerals.co.nz/pdf/ironsand1.pdf>
- Obaja, D., Mace, S., and Mata-Alvarez, J. (2005). Biological nutrient removal by a sequencing batch reactor (SBR) using an internal organic carbon source in digested piggery wastewater. *Bioresource Technology*, 96, 7-14.
- Oremland, R. S., and Stolz, J. F. (2003). The ecology of arsenic. *Science*, 300(5621), 939-944.
- Oremland, R. S., Stolz, J. F., and Hollibaugh, J. T. (2004). The microbial arsenic cycle in Mono Lake, California. *FEMS Microbiology Ecology*, 48(1), 15-27.

- Ouvrard, S., Simonnot, M. O., and Sardin, M. (2001). Removal of arsenate from drinking water with a natural manganese oxide in the presence of competing anions. *Water Science and Technology: Water Supply*, 1(2), 167-173.
- Ozdemir, O., and Dunlop, D. J. (2003). Low-temperature behavior and memory of iron-rich titanomagnetites (Mt. Haruna, Japan and Mt. Pinatubo, Philippines). *Earth and Planetary Science Letters*, 216(1-2), 193-200.
- Panthi, S. R., Sharma, S., and Mishra, A. K. (2006). Recent status of arsenic contamination in groundwater of Nepal; a review. *Kathmandu University Journal of Science, Engineering and Technology*, 2(1).
- Pattanayak, J., Mondal, K., Mathew, S., and Lalvani, S. B. (2000). A parametric evaluation of the removal of As (V) and As (III) by carbon-based adsorbents. *Carbon*, 38(4), 589-596.
- Patureau, D., Davison, J., Bernet, N., and Moletta, R. (1994). Denitrification under various aeration conditions in *comamonas sp.*, strain SGLY2. *FEMS Microbiology Ecology*, 14(1), 71-78.
- Pavan, P., Battistoni, P., Traverso, P., Musacco, A., and Cecchi, F. (1998). Effect of addition of anaerobic fermented OFMSW (organic fraction of municipal solid waste) on biological nutrient removal (BNR) process: Preliminary results. *Water Science and Technology*, 38(1 pt 1), 327-334.
- Payne, W. J. (1973). Reduction of nitrogenous oxides by microorganisms. *Bacteriological Reviews*, 37(4), 409-452.
- Pedersen, H. D., Postma, D., and Jakobsen, R. (2006). Release of arsenic associated with the reduction and transformation of iron oxides. *Geochimica et Cosmochimica Acta*, 70(16), 4116-4129.
- Penaud, V., Delgenes, J. P., Torrijos, M., Moletta, R., Vanhoutte, B., and Cans, P. (1997). Definition of optimal conditions for the hydrolysis and acidogenesis



- of a pharmaceutical microbial biomass. *Process Biochemistry*, 32(6), 515-521.
- Pettine, M., Campanella, L., and Millero, F. J. (1999). Arsenite oxidation by H<sub>2</sub>O<sub>2</sub> in aqueous solutions. *Geochimica et Cosmochimica Acta*, 63(18), 2727-2735.
- Pichler, T., Veizer, J., and Hall, G. E. M. (1999). Natural input of arsenic into a coral-reef ecosystem by hydrothermal fluids and its removal by Fe (III) oxyhydroxides. *Environmental Science and Technology*, 33(9), 1373-1378.
- Pierce, M. L., and Moore, C. B. (1982). Adsorption of arsenite and arsenate on amorphous iron hydroxide. *Water Research*, 16(7), 1247-1253.
- Pitman, A. R., Lotter, L. H., Alexander, W. V., and Deacon, S. L. (1992). Fermentation of raw sludge and elutriation of resultant fatty acids to promote excess biological phosphorus removal. *Water Science and Technology*, 25(4-5), 185-194.
- Pokhrel, D., and Viraraghavan, T. (2008). Arsenic removal from an aqueous solution by modified *A. niger* biomass: Batch kinetic and isotherm studies. *Journal of Hazardous Materials*, 150(3), 818-825.
- Prakasam, T. B. S., and Loehr, R. C. (1972). Microbial nitrification and denitrification in concentrated wastes. *Water Research*, 6(7), 859-869.
- Qin, L., Liu, Y., and Tay, J. H. (2005). Denitrification on poly-b-hydroxybutyrate in microbial granular sludge sequencing batch reactor. *Water Research*, 39, 1503-1510.
- Ra, C. S., Lo, K. V., Shin, J. S., Oh, J. S., and Hong, B. J. (2000). Biological nutrient removal with an internal organic carbon source in piggery wastewater treatment. *Water Science and Technology*, 34(3), 965-973.

- Rabinowitz, B., Fries, M. K., Dawon, R. N., Keller, W., and Do, P. (1997). Biological Nutrient Removal at the Calgary Bonnybrook WWTP Replaces Costly Chemical Phosphorus Removal, in: *Proceedings of Water Environment Federation, 70<sup>th</sup> Annual Conference and Exposition*. Chicago, Illinois, pp 533.
- Randall, C. W., Barnard, J. L., and Stensel, H. D. (1992). *Design and retrofit of waste water treatment plants for biological removal*. Technomic Pub co. Publishing, Lancaster, PA, U.S.A.
- Raven, K. P., Jain, A., and Loeppert, R. H. (1998). Arsenite and arsenate adsorption on ferrihydrite: Kinetics, equilibrium, and adsorption envelopes. *Environmental Science and Technology*, 32(3), 344-349.
- Raynal, J., Delgenes, J. P., and Moletta, R. (1998). Two-phase anaerobic digestion of solid wastes by a multiple liquefaction reactors process. *Bioresource Technology*, 65(1-2), 97-103.
- Rene, E. R., Kim, S. J., and Park, H. S. (2008). Effect of COD/N ratio and salinity on the performance of sequencing batch reactors. *Bioresource Technology*, 99(4), 839-846.
- Rittmann, B. E., and Langeland, W. E. (1985). Simultaneous denitrification with nitrification in single-channel oxidation ditches. *Journal Water Pollution Control Federation*, 57(4), 300-308.
- Rittmann, B. E., and McCarty, P. L. (2001). *Environmental Biotechnology: Principles and Applications*. McGraw-Hill Publishing, New York, U.S.A.
- Robertson, L. A., and Kuenen, J. G. (1984). Aerobic denitrification: a controversy revived. *Archives of Microbiology*, 139(4), 351-354.
- Robertson, L. A., Van Niel, E. W. J., Torremans, R. A. M., and Kuenen, J. G. (1988). Simultaneous nitrification and denitrification in aerobic chemostat

cultures of *Thiosphaera pantotropha*. *Applied and Environmental Microbiology*, 54(11), 2812-2818.

Sadeq, M., Moe, C. L., Attarassi, B., Cherkaoui, I., ElAouad, R., and Idrissi, L. (2008). Drinking water nitrate and prevalence of methemoglobinemia among infants and children aged 1-7 years in Moroccan areas. *International Journal of Hygiene and Environmental Health*, 211(5-6), 546-554.

Sakadevan, K., Zheng, H., and Bavor, H. J. (1999). Impact of heavy metals on denitrification in surface wetland sediments receiving wastewater. *Water Science and Technology*, 40(3), 349-355.

Sancha, A. M., and Castro, M. L. (2001). Arsenic in Latin America: Occurrence exposure, health effects, and remediation, in: *Chappell, W.R., Abernathy, C.O., Calderon, R.L. (Eds.), Arsenic Exposure and Health Effects*, Elsevier Publishing, pp. 87-96.

Santini, J. M., Sly, L. I., Schnagl, R. D., and Macy, J. M. (2001). A new chemoautotrophic arsenite-oxidizing bacterium isolated from a gold mine: phylogenetic, physiological, and preliminary biochemical studies. *Applied Environmental Microbiology*, 66, 92-97.

Sauge-Merle, S., Cuina, S., Carrier, P., Lecomte-Pradines, C., Luu, D. T., and Peltier, G. (2003). Enhanced toxic metal accumulation in engineered bacterial cells expressing *Arabidopsis thaliana* phytochelatin synthase. *Applied and Environmental Microbiology*, 69(1), 490-494.

Schuliga, M., Chouchane, S., and Snow, E. T. (2002). Upregulation of glutathione-related genes and enzyme activities in cultured human cells by sub-lethal concentrations of inorganic arsenic. *Toxicological Sciences*, 70(2), 183-192.

Senn, D. B., and Hemond, H. F. (2002). Nitrate controls on iron and arsenic in an urban lake. *Science*, 296(2373-2376).

- Sharma, V. K., and Sohn, M. (2009). Aquatic arsenic: Toxicity, speciation, transformations, and remediation. *Environment International*, 35(4), 743-759.
- Shen, J., Wanibuchi, H., Waalkes, M. P., Salim, E. I., Kinoshita, A., Yoshida, K., et al. (2006). A comparative study of the sub-chronic toxic effects of three organic arsenical compounds on the urothelium in F344 rats; Gender-based differences in response. *Toxicology and Applied Pharmacology*, 210, 171-180.
- Shuval, H. I., and Gruener, N. (1977). Infant methemoglobinemia and other health effects of nitrates in drinking water. *Progress in Water Technology*, 8 (4/5), 183-193.
- Silver, S., Budd, K., and Leahy, K. M. (1981). Inducible plasmid-determined resistance to arsenate, arsenite, and antimony (III) in *Escherichia coli* and *Staphylococcus aureus*. *Journal of Bacteriology*, 146(3), 983-996.
- Silverstein, J., and Schroeder, E. D. (1983). Performance of SBR activated sludge processes with nitrification/denitrification. *Journal of Water Pollution Control Federation*, 55, 377-384.
- Singh, D. B., Prasad, G., and Rupainwar, D. C. (1996). Adsorption technique for the treatment of As(V)-rich effluents. *Colloids and Surfaces A: Physicochemical and Engineering Aspects*, 111(1-2), 49-56.
- Singh, T. S., and Pant, K. K. (2004). Equilibrium, kinetics and thermodynamic studies for adsorption of As(III) on activated alumina. *Separation and Purification Technology*, 36(2), 139-147.
- Skrinde, J. R., and Bhagat, S. K. (1982). Industrial wastes as carbon sources in biological denitrification. *Journal Water Pollution Control Federation*, 54(4), 370-377.

- Smith, A. H., Hopenhayn-Rich, C., Bates, M. N., Goeden, H. M., Hertz-Picciotto, I., Duggan, H. M., et al. (1992). Cancer risks from arsenic in drinking water. *Environmental Health Perspectives*, 97, 259-267.
- Smith, P. H., and Hungate, R. E. (1958). Isolation and characterization of *methanobacterium ruminantium* n. sp. *Journal of Bacteriology*, 75, 713-718.
- Smith, V. H., Tilman, G. D., and Nekola, J. C. (1999). Eutrophication: impacts of excess nutrient inputs on freshwater, marine, and terrestrial ecosystems. *Environmental Pollution*, 100(1-3), 179-196.
- Spallholz, J. E., Mallory Boylan, L., and Rhaman, M. M. (2004). Environmental hypothesis: is poor dietary selenium intake an underlying factor for arsenicosis and cancer in Bangladesh and West Bengal, India? *Science of the Total Environment*, 323(1-3), 21-32.
- Stouthamer, A. H. (1988). Dissimilatory reduction of oxidized nitrogen compounds, in: A.J.B. Zehnder (Ed.), *Biology of Anaerobic Microorganisms*, John Wiley and Sons, New York
- Stucky, D., and McCarty, P. (1978). Thermochemical treatment of nitrogenous materials to increase methane yield. *Biotechnology and Bioengineering*, 65, 97-103.
- Su, C., and Puls, R. W. (2001). Arsenate and arsenite removal by zerovalent iron: Kinetics, redox transformation, and implications for in situ groundwater remediation. *Environmental Science and Technology*, 35(7), 1487-1492.
- Subramanian, K. S., Viraraghavan, T., Phommavong, T., and Tanjore, S. (1997). Manganese greensand for removal of arsenic in drinking water. *Water Quality Research Journal of Canada*, 32(3), 551-561.
- Sun, G., Liu, J., Luong, T. V., Sun, D., and Wang, L. (2004). *Endemic arsenicosis: A clinical diagnostic with photo illustrations*. UNICEF East Asia and Pacific

Regional Office, Bangkok, Thailand, pp 1-63. Retrieved on 17<sup>th</sup> March, 2008 from [http://www.unicef.org/eapro/Endemic\\_arsenicosis.pdf](http://www.unicef.org/eapro/Endemic_arsenicosis.pdf)

Sun, X., and Doner, H. E. (1998). Adsorption and oxidation of arsenite on goethite. *Soil Science*, 163(4), 278-287.

Suzuki, N., Naranmandura, H., Hirano, S., and Suzuki, K. T. (2008). Theoretical calculations and reaction analysis on the interaction of pentavalent thioarsenicals with biorelevant thiol compounds. *Chemical Research in Toxicology*, 21(2), 550-553.

Takeuchi, M., Kawahata, H., Gupta, L. P., Kita, N., Morishita, Y., Ono, Y., et al. (2007). Arsenic resistance and removal by marine and non-marine bacteria. *Journal of Biotechnology*, 127(3), 434-442.

Teara (2008). *The Encyclopaedia of New Zealand*. Retrieved on 12<sup>th</sup> November, 2008, from <http://www.teara.govt.nz/EarthSeaAndSky/MineralResources/IronAndSteel>.

Techhistory (2008). *An History of Technological Innovation in New Zealand*. Retrieved on 15<sup>th</sup> January, 2009, from <http://www.techhistory.co.nz/IronSands/Titanium.htm>

Tekmar (2003). *Apollo 9000, TOC Combustion Analyzer User Manual*. Teledyne Tekmar, USA.

Thalasso, F., Vallecillo, A., Garcia-encina, P., and Fdz-polanco, F. (1997). The use of methane as a sole carbon source for wastewater denitrification. *Water Research*, 31(1), 55-60.

Thirunavukkarasu, O. S., Viraraghavan, T., Subramanian, K. S., Chaalal, O., and Islam, M. R. (2005). Arsenic removal in drinking water - Impacts and novel removal technologies. *Energy Sources, Part A: Recovery, Utilization and Environmental Effects*, 27(1-2), 209-219.

- Thirunavukkarasu, O. S., Viraraghavan, T., and Subramanlan, K. S. (2001). Removal of Arsenic in drinking water by iron oxide-coated sand and ferrihydrite-batch studies. *Water Quality Research Journal of Canada*, 36(1), 55-70.
- Thomas, K. L., Lloyd, D., and Boddy, L. (1994). Effects of oxygen, pH and nitrate concentration on denitrification by *Pseudomonas* species. *FEMS Microbiology Letters*, 118(1-2), 181-186.
- Tiedje, J.M., Sexstone A.L., Myrold, D.D. and Robinson, J.A. (1982). Denitrification: ecological niches, competition and survival. *Antonie van Leeuwenhoe*. 48(6),569-583.
- Tiedje, J. M. (1988). Ecology of denitrification and dissimilatory nitrate reduction to ammonium. In: Zehnder AJB (ed). *Biology of anaerobic microorganisms*. Wiley, New York , 179-244.
- Torpey, W. N., Andrews, J., and Basilico, J. V. (1984). Effects of multiple digestion on sludge. *Journal Water Pollution Control Federation*, 56(1), 62-68.
- Tournassat, C., Charlet, L., Bosbach, D., and Manceau, A. (2002). Arsenic(III) oxidation by birnessite and precipitation of manganese(II) arsenate. *Environmental Science and Technology*, 36(3), 493-500.
- Tseng, W. P. (1977). Effects and dose-response relationships of skin cancer and blackfoot disease with arsenic. *Environmental Health Perspectives* 19, 109-119.
- TTR (2008). *Trans-Tasman Resources Limited*. Retrieved on 12<sup>th</sup> November, 2008, from <http://www.ttrl.co.nz/default.aspx>
- Tyler, G. (1981). Heavy metals in soil biology and biochemistry, in: *Paul, E.A., Ladd, J.N. (Eds.), . Soil Biochemistry*. Marcel Dekker, New York. , 371-414.

- Umble, A. K., and Ketchum, A. L. (1997). A strategy for coupling municipal wastewater treatment using the sequencing batch reactor with effluent nutrient recovery through aquaculture. *Water Science and Technology*, 35, 177-184.
- USDA (2008). *National Nutrient Database for Standard Reference*, Retrieved on 8<sup>th</sup> September, 2007, from [http://www.nal.usda.gov/fnic/foodcomp/cgi-bin/list\\_nut\\_edit.pl](http://www.nal.usda.gov/fnic/foodcomp/cgi-bin/list_nut_edit.pl)
- USEPA (1973). *Nitrogenous compounds in the environment EPA/ASB-73/001*. Washington DC, USA.
- USEPA (1993). *Nitrogen Control Manual*, EPA-625/R-93/010; Office of Research and Development. Environmental Protection Agency, Washington, DC, USA.
- USEPA (2001). *Safe water; Arsenic*. Retrieved on 16<sup>th</sup> January, 2008, from [http://www.epa.gov/safewater/ars/arsenic\\_finalrule.html](http://www.epa.gov/safewater/ars/arsenic_finalrule.html).
- Van Den Berg, L., Lentz, C. P., Athey, R. J., and Rooke, E. A. (1974). Assessment of methanogenic activity in anaerobic digestion: apparatus and method. *Biotechnology and Bioengineering*, 16(11), 1459-1469.
- van Rijn, J., and Barak, Y. (1998). Denitrification in recirculating aquaculture systems; from biochemistry to biofilter. *The second International Conference on Re-circulating Aquaculture, Co-operative Extension/Sea Grant, Virginia Tech, Blacksburg, Virginia*, 179-187.
- Vasquez-Murrieta, M. S., Cruz-Mondragon, C., Trujillo-Tapia, N., Herrera-Arreola, G., Govaerts, B., Van Cleemput, O., et al. (2006). Nitrous oxide production of heavy metal contaminated soil. *Soil Biology and Biochemistry*, 38(5), 931-940.



- Vega, L., Styblo, M., Patterson, R., W, C. W., and Germolec, D. (2001). Differential effects of trivalent and pentavalent arsenicals on cell proliferation and cytokine secretion in normal human epidermal keratinocytes. *Toxicology and Applied Pharmacology*, 172, 225-232.
- Verrier, D., Roy, F., and Albagnac, G. (1987). Two-phase methanization of solid vegetable wastes. *Biological Wastes*, 22(3), 163-177.
- Wang, L. F., Liu, H. D., Lin, F. F., Su, M. Y., Xu, X. F., Sun, X. Z., et al. (1993). Endemic arsenism in a village of Xinjiang: epidemiology, clinical and preventive studies for 9 years. *Endemic Diseases Bulletin*, 8, 71-78.
- Wang, Q., Kuninobu, M., Ogawa, H. I., and Kato, Y. (1999). Degradation of volatile fatty acids in highly efficient anaerobic digestion. *Biomass and Bioenergy*, 16(6), 407-416.
- Wang, S., and Mulligan, C. N. (2006). Occurrence of arsenic contamination in Canada: Sources, behaviour and distribution. *Science of the Total Environment*, 366(2-3), 701-721.
- Watson, S. W., Bock, E., Harms, H., Koops, H.-P., and Hoper, A. B. (1989). Nitrifying bacteria, in: *Staley J.T., Bryant M.P., and Pfennig N. (Eds.), Bergey's Manual of Systematic Bacteriology*, Williams and Wilkins Publishing, Baltimore, U.S.A., pp 1808-1834.
- Welch, A. H., Lico, M. S., and Hughes, J. L. (1988). Arsenic in groundwater of the Western United States. *Ground Water* 26, 333-347.
- Welch, A. H., Stollenwerk, K. G., Paul, A. P., Maurer, D. K., and Halford, K. J. (2008). In situ arsenic removal in an alkaline clastic aquifer. *Applied Geochemistry*, 23(8), 2477-2495.

- WHO (2006). WHO Guidelines for drinking-water quality. 3<sup>rd</sup> edition incorporating first and second addenda. Vol (1), Recommendation. Retrieved on 28<sup>th</sup> February, 2008, from [http://www.who.int/water\\_sanitation\\_health/dwq/gdwq3rev/en/](http://www.who.int/water_sanitation_health/dwq/gdwq3rev/en/)
- Wikipedia (2008). *The free encyclopedia*. Retrieved on 28<sup>th</sup> November, 2008, from <http://en.wikipedia.org/wiki/Ironsand>
- Wilderer, P. A., Irvine, R. L., Goronszy, M. C., Artan, N., Demoulin, G., Keller, J., et al. (2001). *Sequencing Batch Reactor Technology*. International Water Association (IWA) Publishing, London, UK.
- Wilén, B. M., and Balmer, P. (1999). The effect of dissolved oxygen concentration on the structure, size and size distribution of activated sludge flocs. *Water Research*, 33(2), 391-400.
- Wilkie, J. A., and Hering, J. G. (1996). Adsorption of arsenic onto hydrous ferric oxide: effects of adsorbate/adsorbent ratios and co-occurring solutes. *Colloids and Surfaces A: Physicochemical and Engineering Aspects*, 107, 97-110.
- Wu, H., Yang, D., Zhou, Q., & Song, Z. (2009). The effect of pH on anaerobic fermentation of primary sludge at room temperature. *Journal of Hazardous Materials*, 172 (1), 196-201.
- Wylde, A. F., and Marshall, T. (1999). *The Saga of New Zealand Steel in "New Zealand is Different ". Chemical Milestones in new Zealand History*. Clerestory Press Publishing, Christchurch, New Zealand.
- Xu, R., Wang, Y., Tiwari, D., & Wang, H. (2009). Effect of ionic strength on adsorption of As (III) and As(V) on variable charge soils. *Journal of Environmental Sciences*, 21(7), 927-932.

- Xu, Y. (1996). Volatile fatty acids carbon source for biological denitrification. *Journal of Environmental Sciences*, 8(3), 257-268.
- Yang, H., Lin, W. Y., and Rajeshwar, K. (1999). Homogeneous and heterogeneous photocatalytic reactions involving As (III) and As (V) species in aqueous media. *Journal of Photochemistry and Photobiology A: Chemistry*, 123(1-3), 137-143.
- Yu, H. Q., and Fang, H. H. P. (2003). Acidogenesis of gelatin-rich wastewater in an upflow anaerobic reactor: Influence of pH and temperature. *Water Research*, 37(1), 55-66.
- Zeng, L. (2003). A method for preparing silica-containing iron (III) oxide adsorbents for arsenic removal. *Water Research*, 37(18), 4351-4358.
- Zhang, P., Chen, Y., & Zhou, Q. (2009). Waste activated sludge hydrolysis and short-chain fatty acids accumulation under mesophilic and thermophilic conditions: Effect of pH. *Water Research*, 43(15), 3735-3742.
- Zhang, Q. L., Lin, Y. C., Chen, X., and Gao, N. Y. (2007). A method for preparing ferric activated carbon composites adsorbents to remove arsenic from drinking water. *Journal of Hazardous Materials*, 148(3), 671-678.
- Zhang, S., Liu, C., Luan, Z., Peng, X., Ren, H., and Wang, J. (2008). Arsenate removal from aqueous solutions using modified red mud. *Journal of Hazardous Materials*, 152(2), 486-492.
- Zhang, W., Singh, P., Paling, E., and Delides, S. (2004). Arsenic removal from contaminated water by natural iron ores. *Minerals Engineering*, 17(4), 517-524.
- Zhu, H., Stadnyk, A., Beland, M., and Seto, P. (2008). Co-production of hydrogen and methane from potato waste using a two-stage anaerobic digestion process. *Bioresource Technology*, 99(11), 5078-5084.

Zingaro, R. A. (1994). Arsenic: Inorganic Chemistry, in: *R. Bruce King (Ed.) Encyclopaedia of Inorganic Chemistry*, John Wiley and Sons, Publishing Chichester, England. , Vol (1), 192-218.

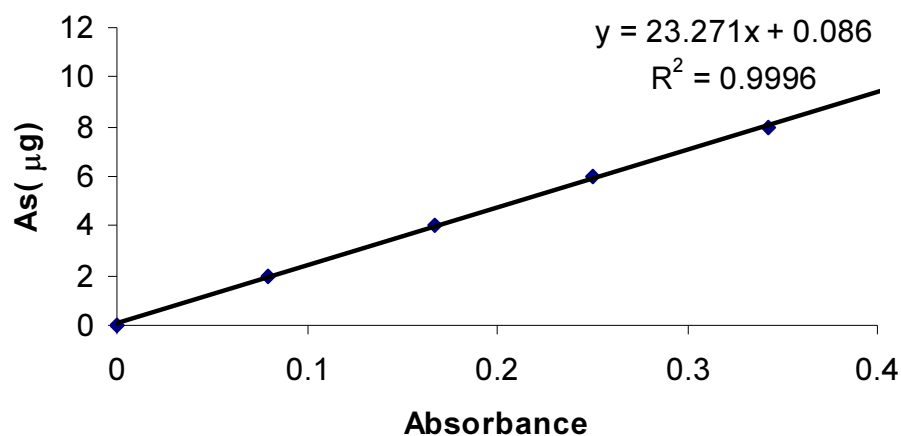
Zoetemeyer, R. J., van den Heuvel, J. C., and Cohen, A. (1982). pH influence on acidogenic dissimilation of glucose in an anaerobic digester. *Water Research*, 16(3), 303-311.

Zouboulis, A. I., and Katsoyiannis, I. A. (2002). Arsenic removal using iron oxide loaded alginate beads. *Industrial and Engineering Chemistry Research*, 41(24), 6149-6155.

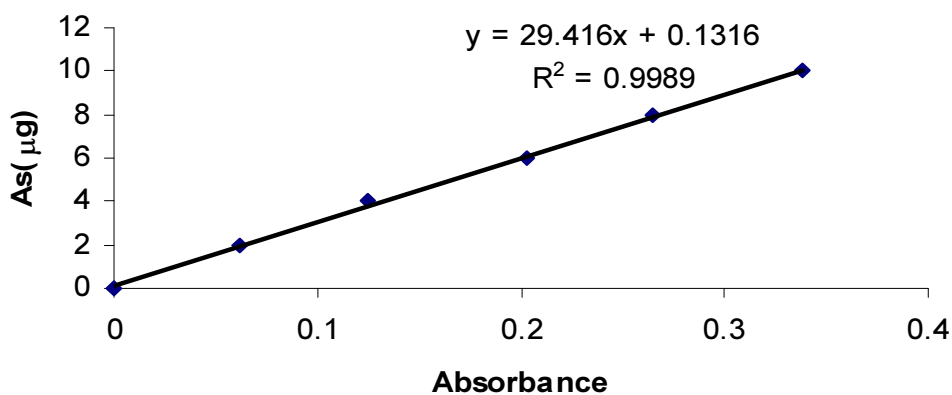
# Appendix

## Appendix A: Calibration Curves

### Appendix A1 ; Calibration curve for arsenic analysis (SDDC Method)

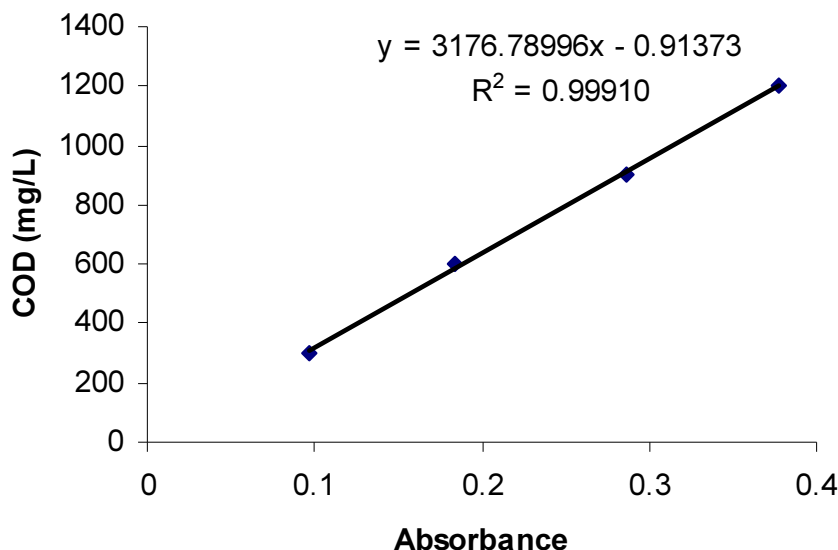


**As (III) standards**



**As (V) standards**

## **Appendix A2: Calibration curve and reagents for COD (DR/2000 (HACH) Spectrophotometer)**



---

### **Reagents**

#### **Reagent 1. Sulphuric acid reagent**

Sulphuric acid reagent was prepared by adding 25.3 g laboratory grade silver sulphate ( $\text{Ag}_2\text{SO}_4$ ) in 2.5 L  $\text{H}_2\text{SO}_4$  and letting to stand for 48 h to dissolve.

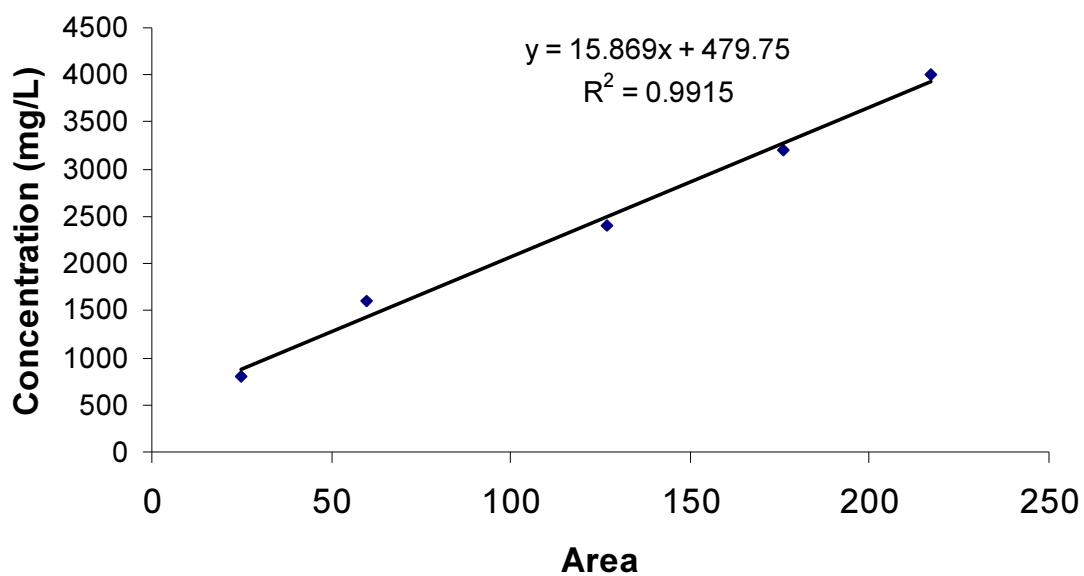
#### **Reagent 2. Standard potassium dichromate solution**

Standard potassium dichromate solution (0.0417M) was prepared by dissolving 12.26 g laboratory reagent grade potassium dichromate ( $\text{K}_2\text{Cr}_2\text{O}_7$ ), previously dried at 105 °C for two hours in deionised water with 167 mL  $\text{H}_2\text{SO}_4$  and diluted to 1 L. Then 33.3 g Mercuric Sulphate ( $\text{HgSO}_4$ ) was added to the solution to reduce interference from the oxidation of chloride ions from the dichromate.

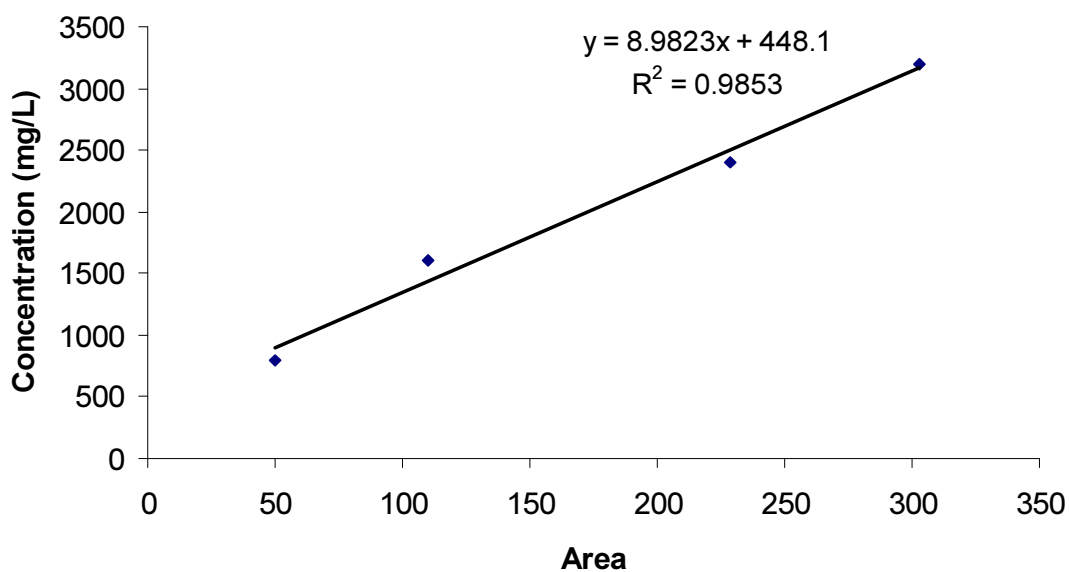
#### **Reagent 3. High range digestion solution**

The high range digestion solution was prepared by adding 150 mL of standard potassium dichromate solution in 350 mL of sulphuric reagent. This mixing was done in a water bath with extra care.

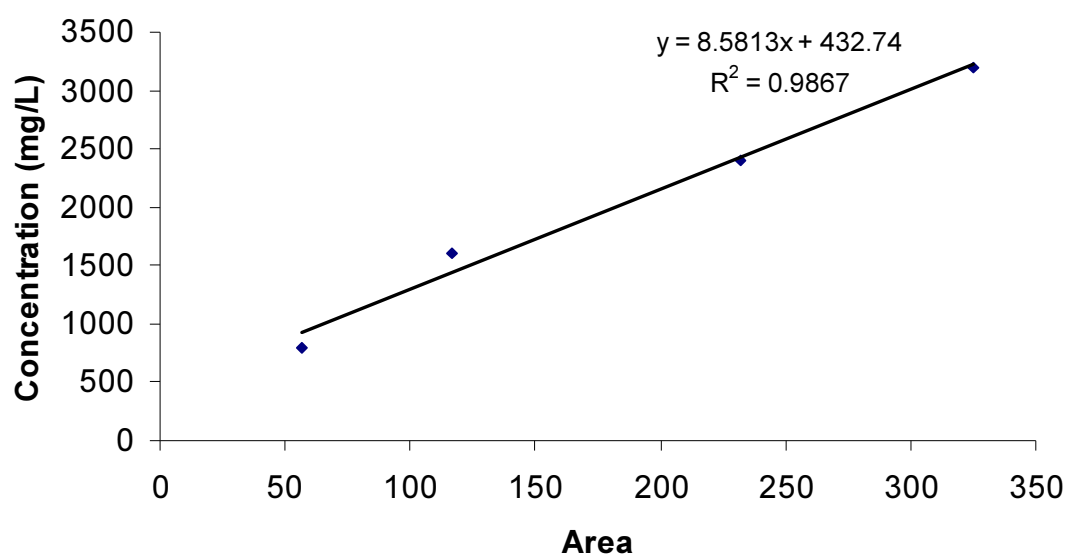
**Appendix A3: Calibration curves for VFAs**  
**(Hewlett-Packard Gas Chromatography)**



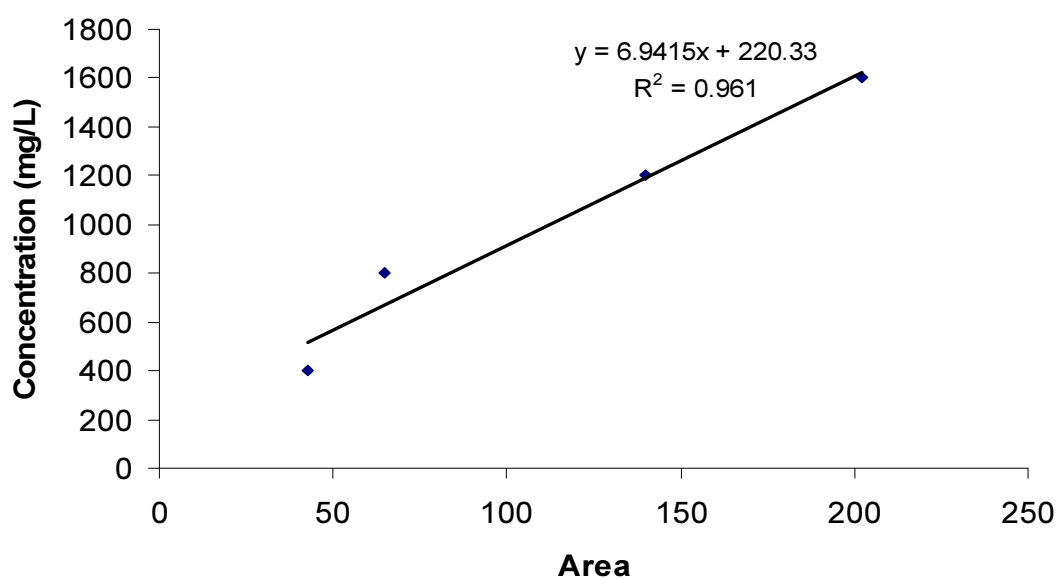
**Acetic acid standards**



**Propionic acid standards**



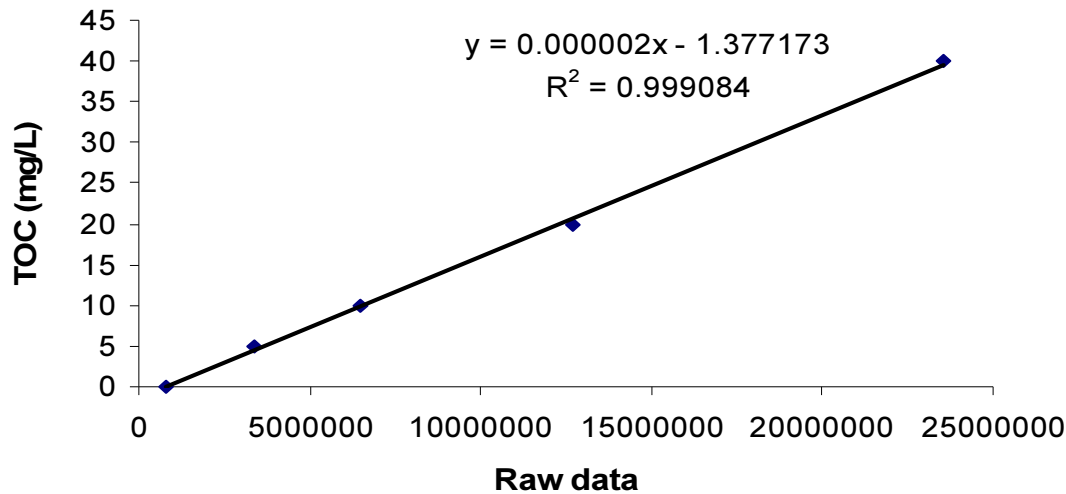
**Butyric acid standards**



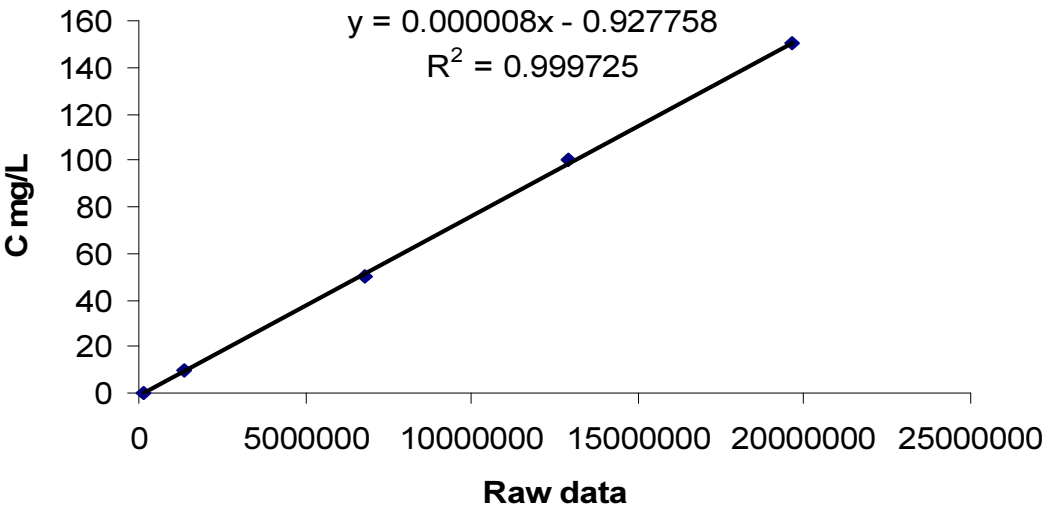
**Valeric acid standards**



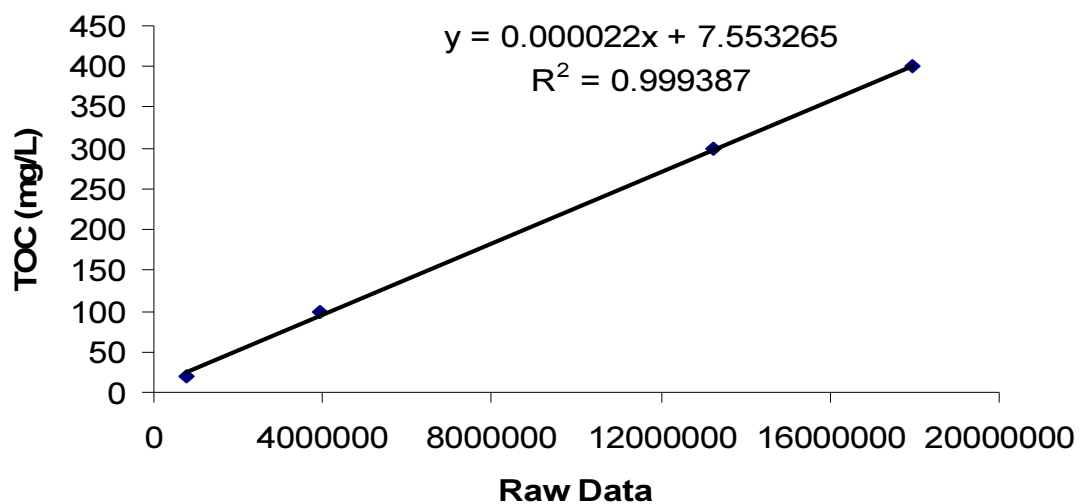
**Appendix A3: Calibration curve for TOC**  
**(Apollo 9000 Combustion TOC Analyser)**



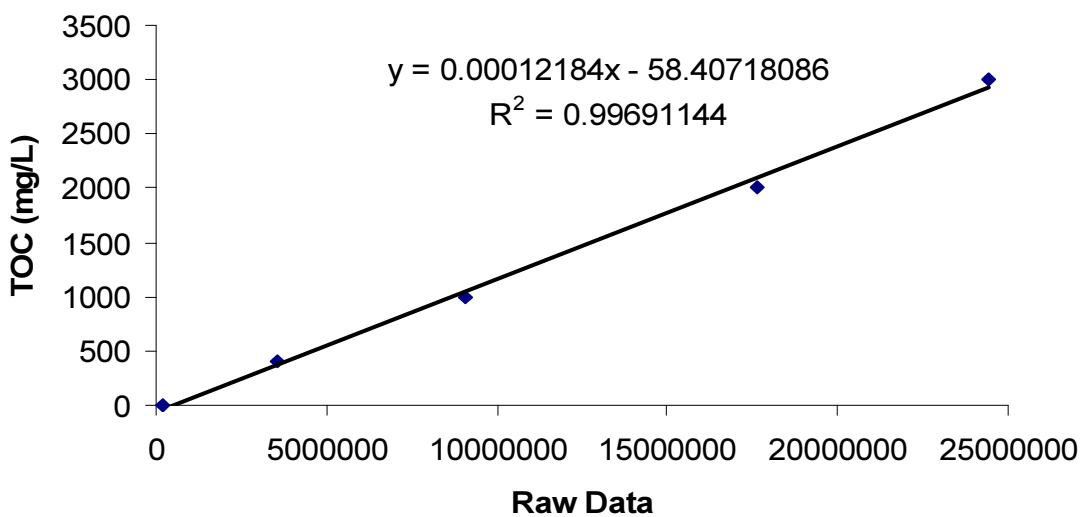
**Range (1-50 mg/L)**



**Range (5-200 mg/L)**



**Range (10-500 mg/L)**



**Range (100-4000 mg/L)**

## Appendix B: Experiment Data

### Appendix B1 : Track study data of $\text{NO}_3^-$ -N, COD and $\text{NH}_4^+$ -N in the SBR

Time (min)	$\text{NO}_3^-$ -N (mg/L)					Average
	N-1	N-2	N-3	N-4	N-5	
0	5.6	6.8	5.8	7.2	6.2	6.32
15	4.5	5.3	5	4.7	5	4.9
30	2.9	4.6	3.2	2.3	4.3	3.46
45	0.2	2.6	0.7	1.5	2.2	1.44
60	0.1	1.1	0.3	0.2	0.7	0.48
75	0	0.4	0.1	0	0.2	0.14
90	0	0.2	0	0	0.1	0.06
150	1.5	1	1.7	1.2	0.8	1.24
210	5.7	6.2	6.1	5.8	6	5.96
270	9.5	8.5	10	9.8	7	8.96
330	13	10.2	14.2	14.3	8.5	12.04
390	14.7	14.7	15.2	16.6	12.8	14.80
420	15.3	17.3	16.8	18.2	14.4	16.40
Time (min)	COD (mg/L)					Average
	COD1	COD2	COD3	COD4	COD5	
0	90	97	110	75	115	97.4
15	68	75	91	73	87	78.8
30	60	70	82	70	72	70.8
45	57	65	76	64	65	65.4
60	54	62	68	62	60	61.2
75	51	60	56	60	58	57.0
90	47	58	66	58	58	57.4
150	43	55	58	52	52	52.0
210	40	38	45	48	50	44.2
270	37	35	58	44	48	44.4
330	35	34	38	35	39	36.2
390	34	33	32	28	35	32.4
420	34	33	26	25	29	29.4
Time (min)	$\text{NH}_4^+$ -N (mg/L)					Average
	N_1	N_2	N_3	N_4	N_5	
0	19.7	18.4	14.1	15.6	14.1	16.38
15	19.7	17.8	14.2	15.7	14.2	16.32
30	19.7	17.7	14.2	15.4	14.2	16.24
45	19.5	17.9	14.1	15.5	14.3	16.26
60	19.7	17.5	14.2	15.6	14.1	16.22
75	19.7	17.6	14.1	15.5	14.6	16.30
90	19.3	17.4	14.2	15.5	15.1	16.30
150	16.2	14.3	13.2	12.3	13.2	13.84
210	13.5	10.2	11.8	9.8	9.2	10.90
270	10.5	6.5	9.6	7.2	5.5	7.86
330	7.5	2.9	7.8	3.8	2.5	4.90
390	6.3	0	5.2	2.1	0.5	2.82
420	5.4	0	4.5	1.6	0	2.30

**Appendix B2: Track study data of NO<sub>3</sub><sup>-</sup>-N and COD in the denitrification batch tests (As (III))**

Run 1								
Time	NO <sub>3</sub> <sup>-</sup> (N-mg/L)				COD (mg/L)			
	As = 0	As = 5	As = 10	As = 18	As = 0	As = 5	As = 10	As = 18
0	20	29.5	29	27.1	184	220	198	250
30	10.8	24.5	23.7	25.4	78	139	138	192
60	0.2	18.7	21	23.4	57	86	99	143
90	0	12.8	17.6	20.1	45	68	74	106
120	0	6.7	13.5	17.9	38	56	58	82
150	0	2.7	9.3	15.4	34	50	52	68
180	0	0	5.8	14	33	44	46	60
210	0	0	2.4	13.5	32	38	42	58
240	0	0	0	12.8	31	36	40	58
MLSS (mg/L)	1234	1200	1185	1240				
MLVSS (mg/L)	987.2	960	948	992				
Denitrification Rate (g NO <sub>3</sub> <sup>-</sup> -N / gVSS per day)	0.48	0.25	0.18	0.09				

Run 2								
Time	NO <sub>3</sub> <sup>-</sup> (N-mg/L)				COD (mg/L)			
	As = 0	As = 5	As = 18	As = 25	As = 0	As = 5	As = 18	As = 25
0	22.5	29.6	23.1	26.8	246	231	220	242
30	15.7	25.3	19.8	25	101	156	171	185
60	9.5	20.6	17	23.6	53	103	113	126
90	2.6	16.5	15.5	22.7	45	76	86	102
120	0	13.5	14.2	21.5	41	55	68	83
150	0	9.4	13.6	20.3	40	44	53	75
180	0	4.6	13	20	40	43	48	70
210	0	0	12.7	19.5	42	42	47	69
240	0	0	12.1	19.1	40	43	48	68
MLSS (mg/L)	1170	1213	1193	1228				
MLVSS (mg/L)	936.5	970.7	954.7	982.4				
Denitrification Rate (g NO <sub>3</sub> <sup>-</sup> -N / gVSS per day)	0.34	0.21	0.07	0.05				

Run 3								
Time	NO <sub>3</sub> <sup>-</sup> (N-mg/L)				COD (mg/L)			
	As=0	As=5	As=10	As=50	As=0	As=5	As=10	As=50
0	23.9	28.4	29.8	27.4	256	250	262	270
30	18.2	24.5	25.2	27.5	125	129	157	232
60	12.4	19.7	21.7	27.2	68	86	124	200
90	4.6	13.8	17.3	26.8	52	68	113	174
120	0	10.3	14.9	26.2	46	65	102	158
150	0	7.3	12.2	26	42	61	92	152
180	0	3	9.9	25.8	38	54	76	140
210	0	0	6.8	25.6	36	48	72	133
240	0	0	4.2	25.2	34	46	68	124
MLSS (mg/L)	1285	1370	1293	1113				
MLVSS (mg/L)	982.4	1096	1030	891				
Denitrification Rate (g NO <sub>3</sub> <sup>-</sup> -N / gVSS per day)	0.31	0.19	0.15	0.01				

Run 4								
Time	NO <sub>3</sub> <sup>-</sup> (N-mg/L)				COD (mg/L)			
	As=0	As = 18	As=25	As=50	As=0	As = 18	As=25	As=50
0	23.2	22.6	22.8	22.5	218	231	241	257
30	17.6	22	22	22.4	125	145	175	218
60	11	19.8	21.7	22.5	58	104	138	175
90	2.1	18.6	20.2	22	36	85	115	152
120	0	16.5	18.4	21.2	35	71	98	141
150	0	13.8	16.2	20.2	34	58	85	136
180	0	12	14.1	18.8	35	48	71	120
210	0	10.9	13.2	17.6	33	40	59	112
240	0	10.1	12.4	17.2	32	37	54	100
MLSS (mg/L)	1156	1230	1280	1333				
MLVSS (mg/L)	925	980	1020	1060				
Denitrification Rate (g NO <sub>3</sub> <sup>-</sup> -N / gVSS per day)	0.37	0.08	0.06	0.03				

Run 5								
Time	NO <sub>3</sub> <sup>-</sup> (N-mg/L)				COD (mg/L)			
	As=0	As = 10	As=25	As=50	As=0	As = 10	As=25	As=50
0	24.6	23.4	24.8	25.8	225	252	243	260
30	18.7	22.1	23	25.6	130	158	178	224
60	11.5	20.2	21.7	25.4	78	114	139	179
90	2	17	20.2	25.2	46	82	118	158
120	0	13.7	18.4	25.0	39	70	97	134
150	0	10.1	16.7	24.4	35	48	84	128
180	0	6.8	15	23.6	34	38	70	118
210	0	3.2	14.2	22.9	33	36	55	115
240	0	0	13.7	22.2	32	37	52	112
MLSS (mg/L)	1320	1293	1360	1333				
MLVSS (mg/L)	1056	1030	1088	1066				
Denitrification Rate (g NO <sub>3</sub> <sup>-</sup> -N / gVSS per day)	0.34	0.14	0.06	0.02				

**Appendix B3: Track study data of NO<sub>3</sub><sup>-</sup>-N and COD in the denitrification batch tests (As (V))**

Run 6								
Time	NO <sub>3</sub> <sup>-</sup>				COD			
	As = 0	As = 50	As = 500		As = 0	As = 50	As = 500	
0	22.9	23	24.5		195	212	198	
30	15.2	15.6	16.8		134	145	138	
60	7.6	10.2	12		73	88	99	
90	2.7	4.5	6.6		60	66	74	
120	0	0.3	1.8		51	54	58	
150	0	0	0		48	48	52	
180	0	0	0		46	43	46	
210	0	0	0		33	38	42	
240	0	0	0		31	34	40	
MLSS (mg/L)	1325	1300	1320					
MLVSS (mg/L)	1060	1040	1056					
Denitrification Rate (g NO <sub>3</sub> <sup>-</sup> -N / gVSS per day)	0.30	0.28	0.26					

Run 7								
Time	NO <sub>3</sub> <sup>-</sup>				COD			
	As=0	As=100	As=1000	As=2000	As=0	As=100	As=1000	As=2000
0	23.4	24.5	23.5	25.5	193	204	199	220
30	15.4	17.6	22.9	24.3	100	120	125	162
60	7.3	9.8	20.3	23.1	60	78	97	134
90	2.1	4.7	10.9	16.8	46	63	78	108
120	0	1.2	2.8	4.7	41	50	56	96
150	0	0	0.5	4.4	38	47	53	81
180	0	0	0	4.2	36	45	45	77
210	0	0	0	4	33	43	42	65
240	0	0	0	4	32	42	42	56
MLSS (mg/L)	1196	1320	1258	1280				
MLVSS (mg/L)	956.8	1056	1006.4	1024				
Denitrification Rate (g NO <sub>3</sub> <sup>-</sup> -N / gVSS per day)	0.36	0.26	0.25	0.24				

Run 8								
Time	NO <sub>3</sub> <sup>-</sup>				COD			
	As=0	As=50	As=100	As=1000	As=0	As=50	As=100	As=1000
0	23.8	24.6	25.7	25.8	214	225	204	254
30	9.8	12.5	16.2	20.2	133	129	120	200
60	5.3	7.8	12.2	16.1	78	86	79	150
90	1.1	2.7	4.2	8.8	57	68	63	110
120	0	0.4	0.8	3.4	53	65	56	82
150	0	0	0	0.6	47	61	52	72
180	0	0	0	0	42	54	48	62
210	0	0	0	0	40	48	46	54
240	0	0	0	0	38	46	45	52
MLSS (mg/L)	1320	1280	1180	1185				
MLVSS (mg/L)	982.4	1024	944	948				
Denitrification Rate (g NO <sub>3</sub> <sup>-</sup> -N / gVSS per day)	0.37	0.34	0.32	0.28				

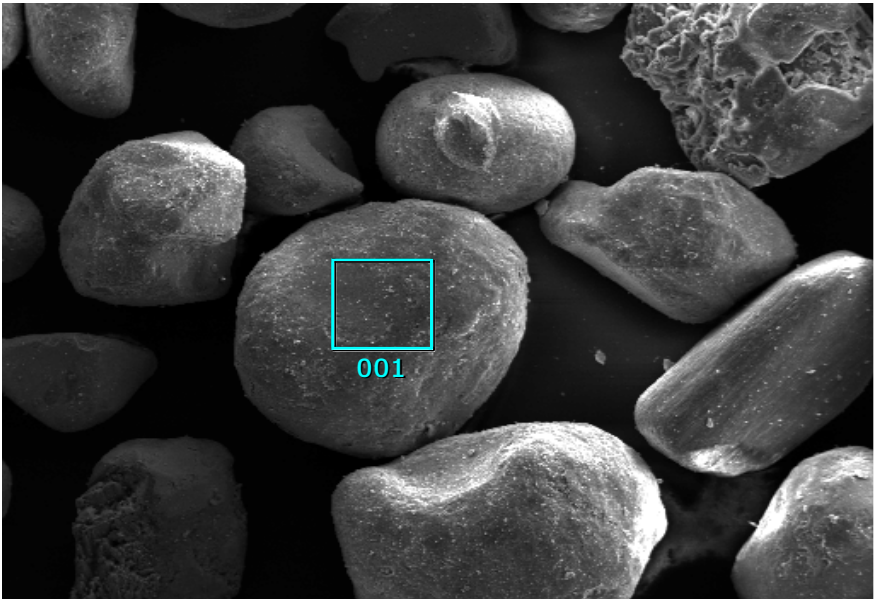
Run 9								
Time	NO <sub>3</sub> <sup>-</sup>				COD			
	As=0	As = 500	As=2000		As=0	As = 500	As=2000	
0	23.4	25.2	24.8		248	250	252	
30	16.2	19.1	22.7		164	192	210	
60	9.4	13.2	18.2		108	136	165	
90	3.8	6.8	12.4		84	95	129	
120	0.5	1.2	5.8		63	82	108	
150	0	0.3	4.3		58	65	81	
180	0	0	3.2		50	55	68	
210	0	0	2.5		46	49	62	
240	0	0	2.2		42	45	58	
MLSS (mg/L)	1156	1188	1250					
MLVSS (mg/L)	924.8	950.4	1000					
Denitrification Rate (g NO <sub>3</sub> <sup>-</sup> -N / gVSS per day)	0.34	0.30	0.23					



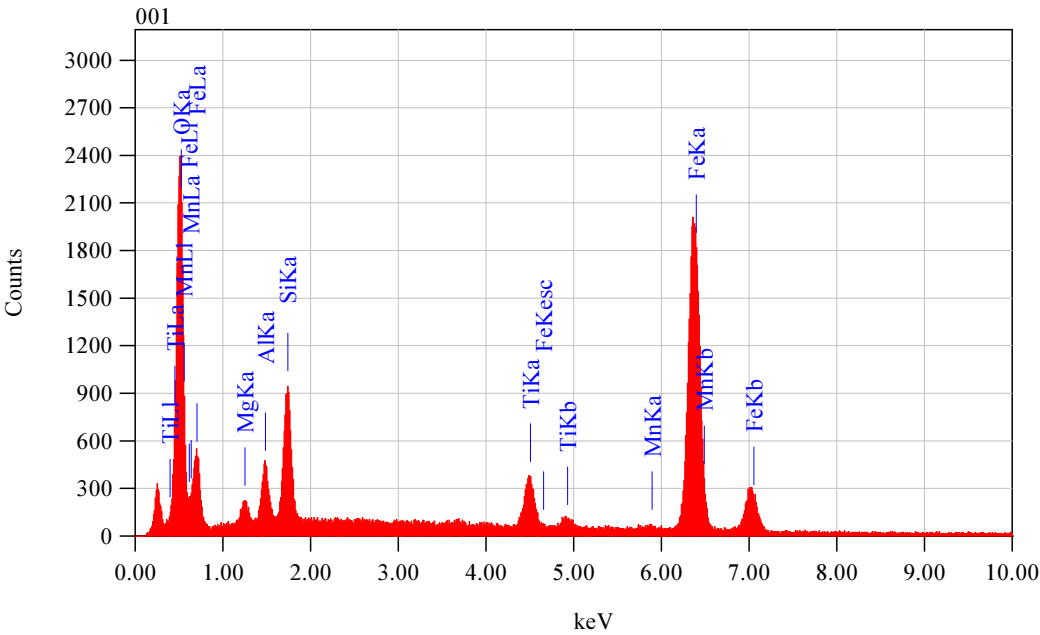
# Appendix C: Images & Photos

## Appendix C1: SEM image of NZIS (without arsenic)

Title : IMG1  
-----  
Instrument : 7000F  
Volt : 20.00 kV  
Mag : x 170  
Date : 2008/06/18  
Pixel : 512 x 384



0.2 mm



Acquisition Parameter  
Instrument : 7000F  
Acc. Voltage : 20.0 kV  
Probe Current: 0.59008 nA  
PHA mode : T3  
Real Time : 43.82 sec  
Live Time : 30.00 sec  
Dead Time : 30 %  
Counting Rate: 6660 cps  
Energy Range : 0 - 20 keV

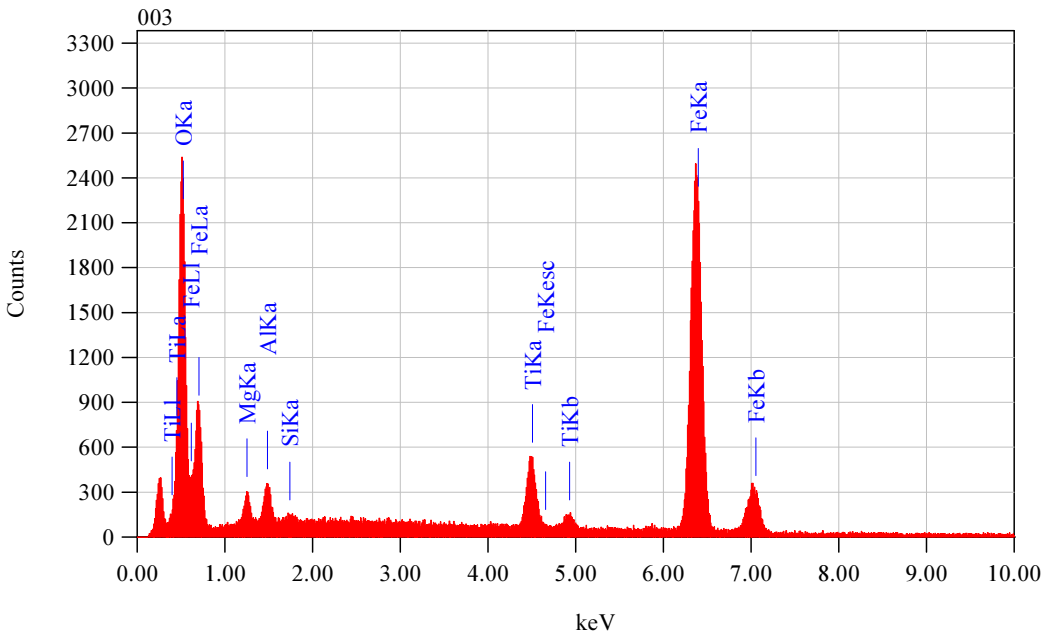
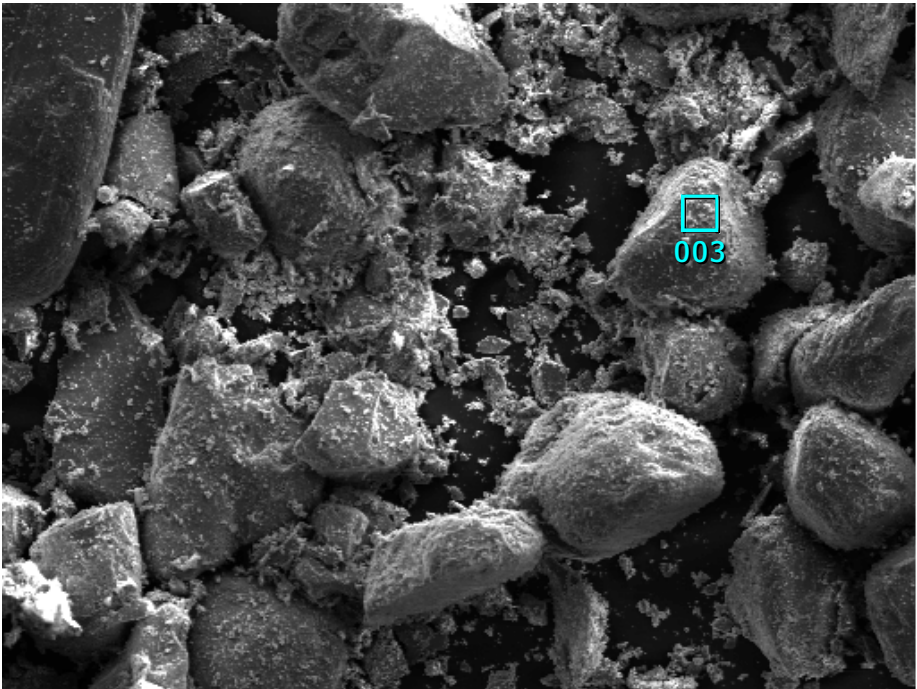
### ZAF Method Standardless Quantitative Analysis

Fitting Coefficient : 0.4155

Element	(keV)	mass%	Error%	At%	Compound	mass%	Cation	K
O K	0.525	32.08	0.28	58.05				37.2096
Mg K	1.253	1.63	0.39	1.94				0.6362
Al K	1.486	3.45	0.33	3.70				1.7489
Si K	1.739	6.62	0.30	6.82				4.2437
Ti K	4.508	4.08	0.37	2.47				4.1998
Mn K*								
Fe K	6.398	52.13	0.68	27.02				51.9618
Total		100.00		100.00				

Appendix C2: SEM image of NZIS (with As (III))

Title : IMG1  
-----  
Instrument : 7000F  
Volt : 20.00 kV  
Mag : x 170  
Date : 2008/06/18  
Pixel : 512 x 384



Acquisition Parameter  
Instrument : 7000F  
Acc. Voltage : 20.0 kV  
Probe Current: 0.59008 nA  
PHA mode : T3  
Real Time : 44.96 sec  
Live Time : 30.00 sec  
Dead Time : 32 %  
Counting Rate: 7038 cps  
Energy Range : 0 - 20 keV

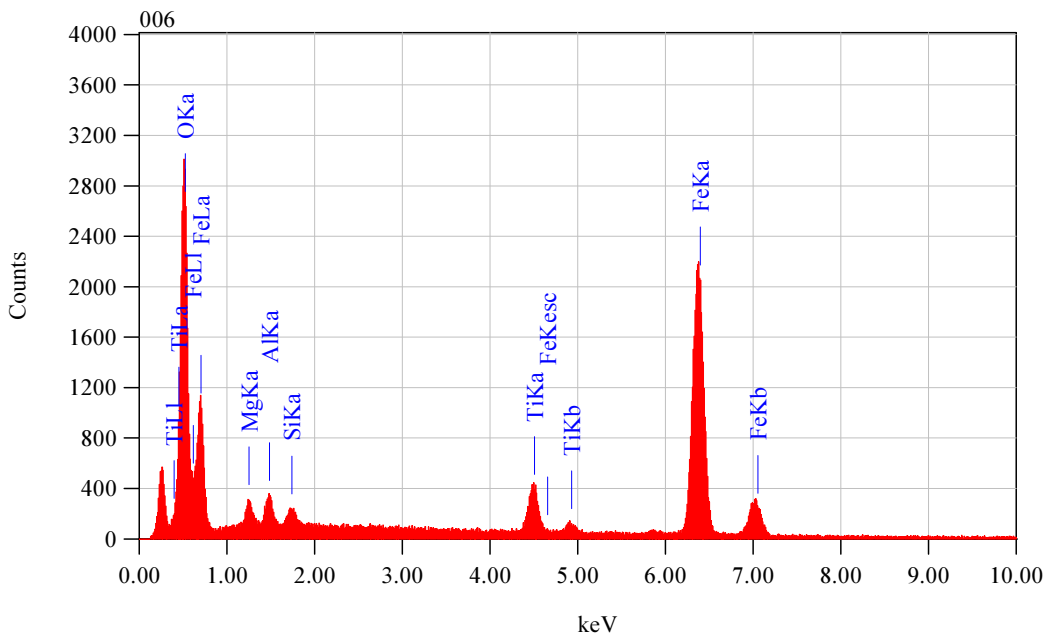
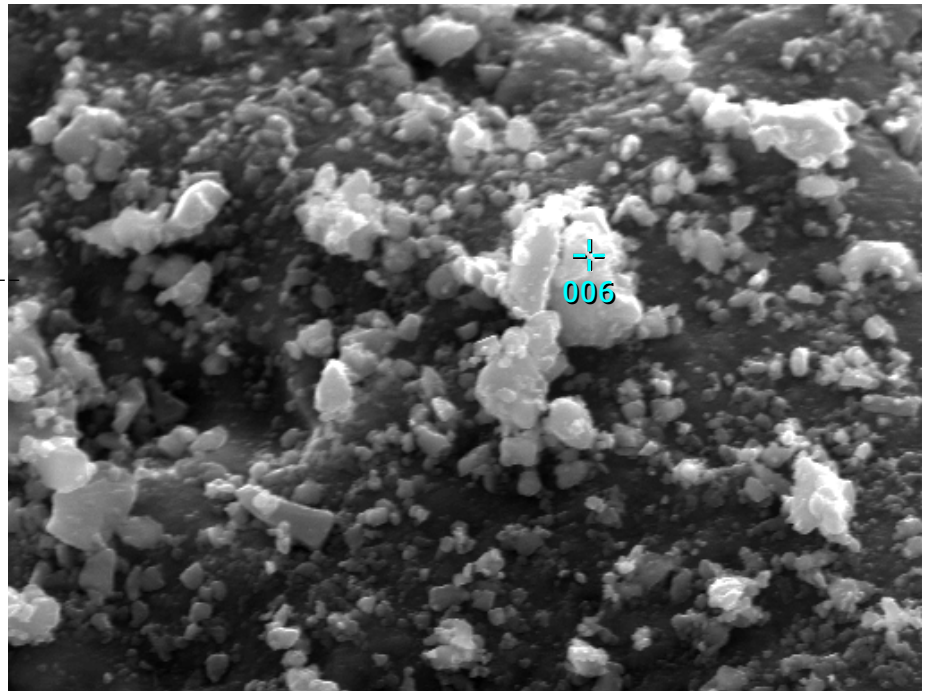
ZAF Method Standardless Quantitative Analysis  
Fitting Coefficient : 0.4229

Element	(keV)	mass%	Error%	At%	Compound	mass%	Cation	K
O K	0.525	30.74	0.36	58.45				34.8978
Mg K	1.253	2.54	0.44	3.18				0.9132
Al K	1.486	2.35	0.37	2.65				1.0954
Si K*	1.739	0.26	0.33	0.28				0.1546
Ti K	4.508	5.60	0.38	3.56				5.7216
Fe K	6.398	58.52	0.72	31.88				57.2175
Total		100.00		100.00				

Title : IMG1

---

Instrument : 7000F  
 Volt : 20.00 kV  
 Mag : x 6,000  
 Date : 2008/06/18  
 Pixel : 512 x 384



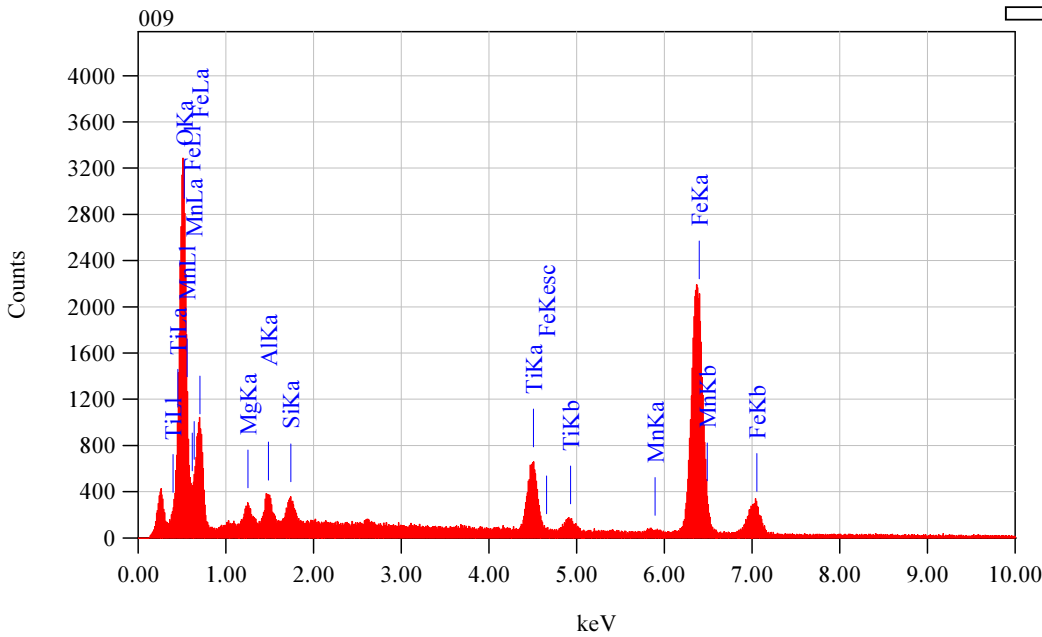
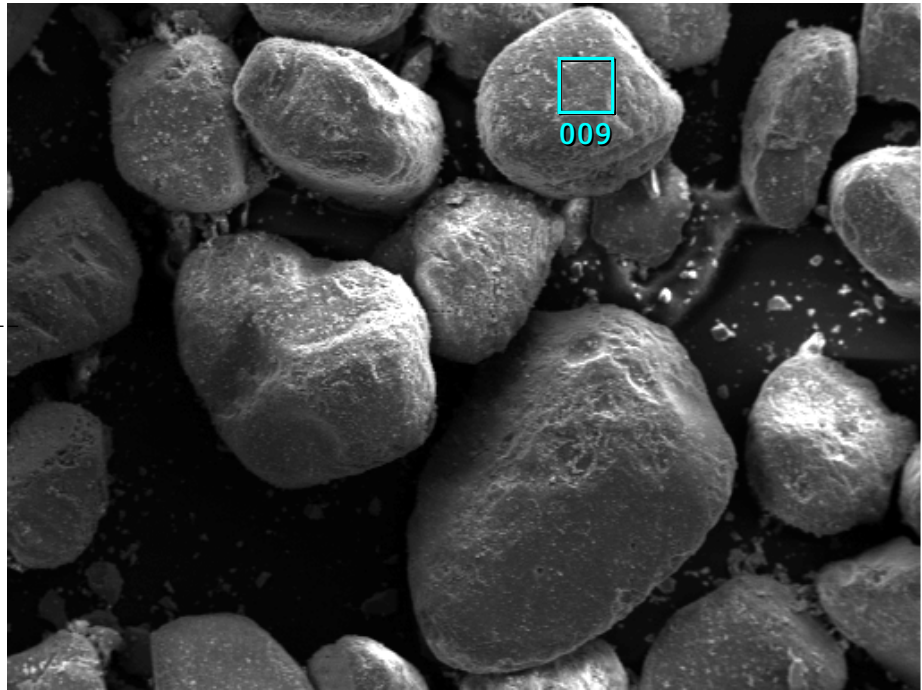
Acquisition Parameter  
 Instrument : 7000F  
 Acc. Voltage : 20.0 kV  
 Probe Current: 0.59008 nA  
 PHA mode : T3  
 Real Time : 44.85 sec  
 Live Time : 30.00 sec  
 Dead Time : 33 %  
 Counting Rate: 7358 cps  
 Energy Range : 0 - 20 keV

ZAF Method Standardless Quantitative Analysis  
 Fitting Coefficient : 0.4296

Element	(keV)	mass%	Error%	At%	Compound	mass%	Cation	K
O K	0.525	36.18	0.35	64.04				42.1483
Mg K	1.253	2.42	0.44	2.81				0.8603
Al K	1.486	2.16	0.37	2.27				0.9972
Si K*	1.739	0.90	0.33	0.91				0.5366
Ti K	4.508	4.63	0.39	2.74				4.5791
Fe K	6.398	53.71	0.74	27.23				50.8784
Total				100.00		100.00		

# Appendix C3: SEM image of NZIS (with As (V))

Title : IMG1  
 Instrument : 7000F  
 Volt : 20.00 kV  
 Mag : x 170  
 Date : 2008/06/18  
 Pixel : 512 x 384



Acquisition Parameter  
 Instrument : 7000F  
 Acc. Voltage : 20.0 kV  
 Probe Current : 0.59008 nA  
 PHA mode : T3  
 Real Time : 46.61 sec  
 Live Time : 30.00 sec  
 Dead Time : 34 %  
 Counting Rate : 7537 cps  
 Energy Range : 0 - 20 keV

## ZAF Method Standardless Quantitative Analysis

Element	(keV)	mass%	Error%	At%	Compound	mass%	Cation	K
O K	0.525	38.51	0.36	66.27				42.4015
Mg K	1.253	1.62	0.41	1.83				0.6042
Al K	1.486	2.18	0.34	2.22				1.0588
Si K	1.739	1.40	0.30	1.37				0.8766
Ti K	4.508	6.79	0.37	3.90				6.8933
Mn K*								
Fe K	6.398	49.51	0.69	24.41				48.1656
Total		100.00		100.00				



## Appendix C4: Some photographs from the experimental work



Figure C4-1: Anaerobic digester



Figure C4-2: Full set-up of the sequencing batch reactor system



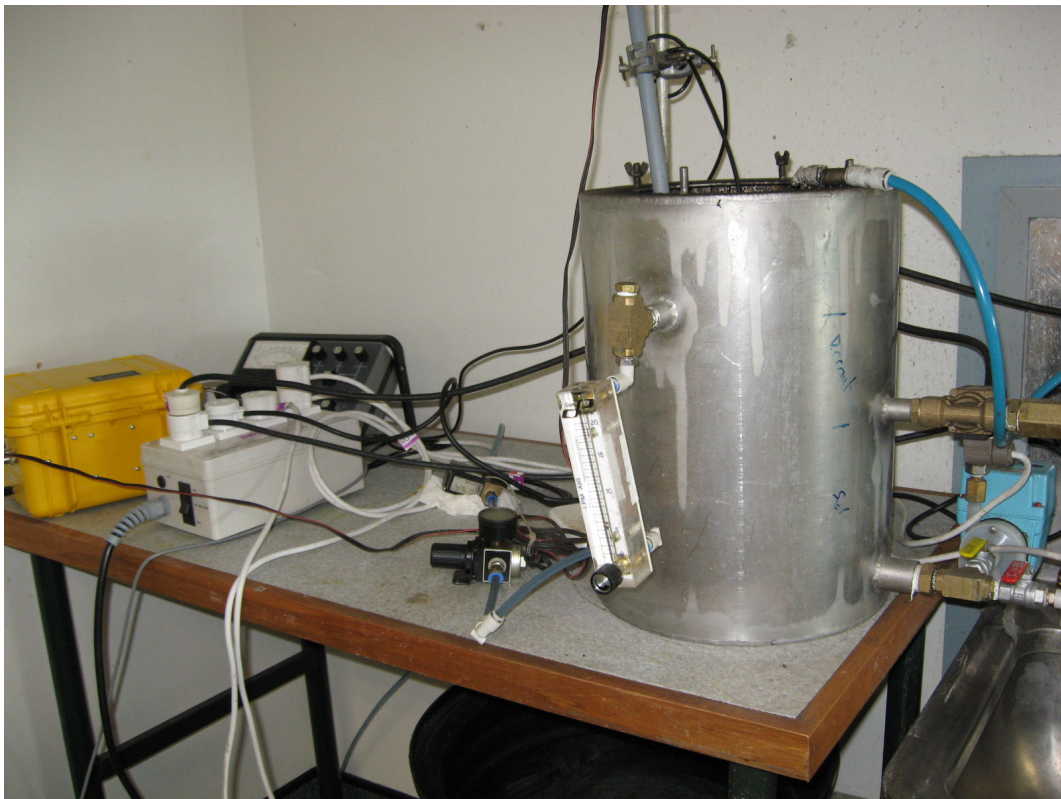


Figure C4-3: Reactor of the sequencing batch reactor system



Figure C4-4: Denitrification batch tests



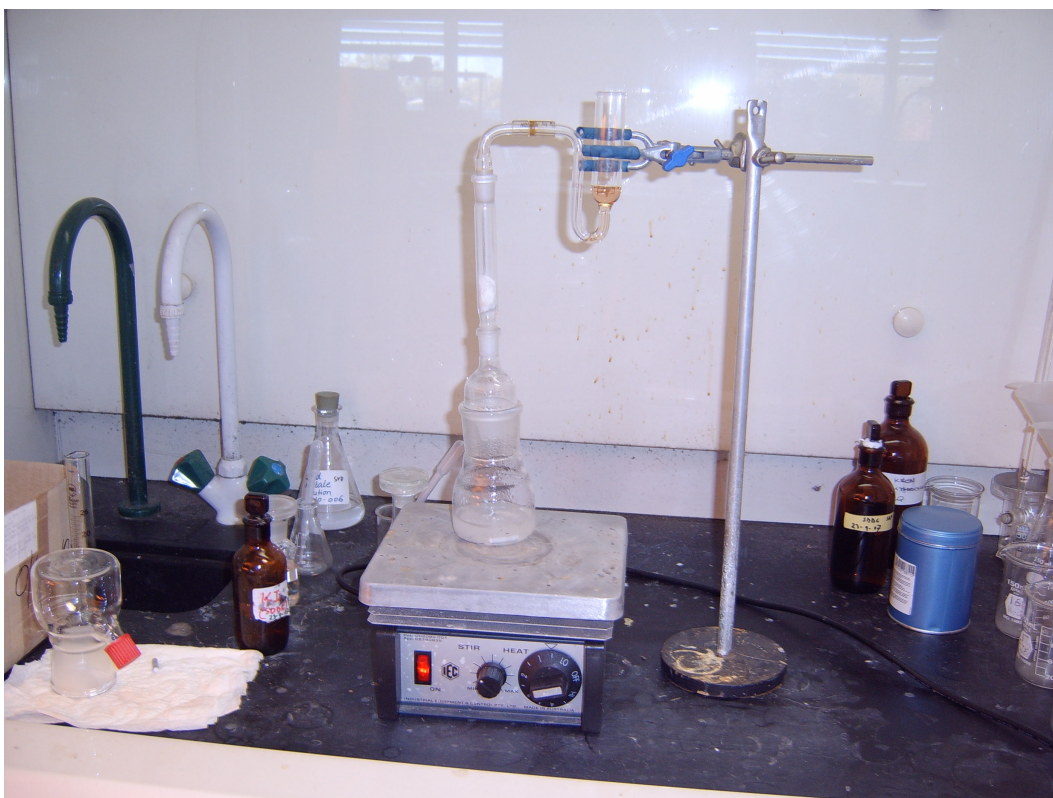


Figure C4-5: Full set-up of the arsenic testing system (SDDC Method) system



Figure C4-6: Close-up of the ongoing arsenic testing, pink colour is being developed in the SDDC solution because of the presence of arsenic in the sample